Beta secretase regulation and inflammation in pancreatic β-cells: the potential role of Rooibos.

Joleen Burger

Thesis presented in fulfilment of the requirements for the degree Master of Science in Medical Sciences in the Faculty of Medicine and Health Science at Stellenbosch University.

Supervisor: Dr Nireshni Chellan

Co-supervisors: Prof Christo Muller and Dr John Lopes

December 2018

Declaration

By submitting this thesis electronically, I declare that the entirety of the work contained therein is my own, original work, that I am the sole author thereof (save to the extent explicitly otherwise stated), that reproduction and publication thereof by Stellenbosch University will not infringe any third party rights and that I have not previously in its entirety or in part submitted it for obtaining any qualification.

_____

Signature   Date

ABSTRACT

Introduction

Chronic, low-grade inflammation is a hallmark of insulin resistance (IR) and underlies pancreatic β-cell failure and the development of type 2 diabetes (T2D), a disease characterized by a reduction in β-cell functional mass. However, therapeutics that directly protect β-cells from stressors, such as inflammation and oxidative stress, are limited. Amylin, a neuro-hormone, is co-secreted with insulin, therefore hyperinsulinemia often coincides with hyper secretion of amylin. Increased secretion of amylin is associated amyloid deposition which have detrimental effects on β-cell function. In pancreatic islets, β-secretase (BACE) modulates the deposition of cytotoxic islet amyloid, an initiator of intra-islet inflammation and oxidative stress, making BACE inhibition a therapeutic target. Insights into mechanisms involved in islet inflammation and the associated effect(s) of BACE, may reveal an opportunity to develop novel therapeutics to protect and preserve β-cells in T2D. In addition to their antidiabetic properties, aspalathin (Asp), Z-2-(β-D-glucopyranosyloxy)-3-phenylpropenoic acid (PPAG), and an unfermented Rooibos extract (GRT) may have anti-inflammatory effects in β-cells and may additionally modulate BACE activity.

Aim

To determine if GRT or two of its most bioactive polyphenols have BACE inhibition activity and can reduce pro-inflammatory effects in rat insulinoma (INS1) pancreatic β-cells.

Methods

A model of moderate inflammation was established in INS1 cells using a cytokine cocktail, containing tumor necrosis factor-α (TNF-α), interleukin-1β (IL-1β) and interferon-γ (IFN-γ). Rat insulinoma cell viability, function, and oxidative stress was measured in response to the cytokine cocktail and exposure to Asp, PPAG, and GRT by quantifying cellular adenosine triphosphate (ATP) production, cell death via apoptosis and necrosis, proliferation rate, insulin/amylin secretion and content, reactive oxygen species (ROS) production and nitrate (NO_2^-) generation. Beta secretase inhibition profiling of GRT, Asp, and PPAG was assessed using fluorescence resonance energy transfer (FRET) in a purified enzyme assay, followed by kinetically assessing BACE activity *in vitro*.

Results

The cytokine cocktail induced a state of moderate inflammation after 24 hours, mainly through IL-1β. High concentrations of Asp (1000 µM) and moreso, GRT (1 mg/ml), showed a trend

towards BACE inhibition compared to controls (56.20% ± 2.05, $p<0.0001$ and 39.80% ± 0.55, $p<0.0001$), but reduced mitochondrial dehydrogenase activity in inflamed INS1 cells (19.02% ± 2.98, $p<0.0001$; 36.88% ± 1.53, $p<0.0001$), while PPAG showed no measurable effect. Lower concentrations of Asp (0.1–10 µM), PPAG (0.1–10 µM), and GRT (0.0001-0.01 mg/ml) may have a protective effect on inflamed pancreatic β-cells as an increase, albeit not significant, in overall cell viability and function was observed, with a concomitant decrease in oxidative stress after 24 hours (97.66% ± 3.5, $p<0.66$; 95.54% ± 5.61, $p<0.52$; 96.80% ± 3.67, $p<0.55$).

Conclusion

Aspalathin and morseo, GRT, may potentially ameliorate inflammation-induced β-cell stress at low concentrations, while higher concentrations have some regulation of BACE activity in a dose dependent manner.

Key words: amylin, inflammation, BACE2, type 2 diabetes, Rooibos, polyphenols.

OPSOMMING

Inleiding

Kroniese, lae graad ontsteking is 'n kenmerk van insulienweerstandigheid (IR) en is onderliggend aan pankreatiese beta-sel wanfunksie en die ontwikkeling van tipe 2 diabetes (T2D), 'n siekte wat gekenmerk word deur 'n vermindering in β-sel funksionele massa. Terapeutiese middels, wat β-selle direk teen stressors soos inflammasie en oksidatiewe stres beskerm, is egter beperk. Amilien, 'n neuro-hormoon, en insulien word gesamentlik deur β-selle afgeskei; daarom word hipersekresie van insulien geassosieer met verhoogde sekresie van amilien. Die toename in amilien sekresie word geassosieer met die ophoping van amiloïed, wat 'n nadelige effek op β -sel funksie het. In die pankreaseilande moduleer beta-sekretase (BACE) die sitotoksiese ophoping van amiloïed, wat ontsteking en oksidatiewe stres aanstig; en maak dus BACE-inhibisie 'n terapeutiese teiken. Insig oor die onderliggende meganismes betrokke by pankreaseiland-inflammasie asook die geassosieerde effekte van BACE, kan moontlik 'n geleentheid onthul vir die ontwikkeling van nuwe terapieë om β-selle te beskerm en te bewaar tydens T2D. Benewens hul antidiabetiese eienskappe kan aspalatien (Asp), Z-2-(β-D-glukopiranoksieloksie)-3-fenielpropeniensuur (PPAG) en 'n ongefermenteerde Rooibosekstrak (GRT), anti-inflammatoriese effekte in β-selle hê, en moontlik β-selle beskerm deur BACE-aktiwiteit te moduleer.

Doelstelling

Om te bepaal of GRT, en twee van sy bioaktiewe polifenole, ontsteking in pankreatiese β-selle (INS1) kan verminder en ook BACE inhibisie eienskappe besit.

Metodes

'n Model van matige ontsteking is in INS1-selle gevestig met behulp van 'n sitokien-mengsel van tumornekrosefaktor-α (TNF-α), interleukien-1β (IL-1β) en interferon-γ (IFN-γ). Sel-lewensvatbaarheid, funksie, en oksidatiewe stres was bepaal in reaksie tot die sitokien mengsel na Asp, PPAG, en GRT behandeling, deur intrasellulêre adenosietrifosfaat (ATP), sel-dood via apoptose en nekrose, selproliferasie tempo, insulien/amiliensekresie en -inhoud, reaktiewe suurstofspesies (ROS) produksie en nitraat (NO_{2-}) generasie, te meet. Beta sekretase inhibisie deur GRT, Asp, en PPAG was bepaal met behulp van fluoressensie resonansie energie-oordrag (FRET) in 'n gesuiwerde ensiem-toets, gevolg deur kinetiese assessering van BACE aktiviteite *in vitro*.

Resultate

Die sitokien-mengsel het na 24 uur 'n toestand van matige ontsteking veroorsaak, hoofsaaklik deur IL-1β. 'n Neiging tot BACE inhibisie, vergeleke met die kontrole (56.20% ± 2.05, $p<0.0001$ en 39,80% ± 0.55, $p<0.0001$), is teen die hoër konsentrasies van Asp en GRT gesien. Hoë konsentrasies Asp (1000 µM) en tot 'n groter mate, GRT (1 mg/ml) het lewensvatbaarheid van ontsteekte INS1 selle verminder (19.02% ± 2.98, $p<0,0001$; 36,88% ± 1,53, $p<0,0001$), terwyl PPAG geen meetbare effek getoon het nie. Laer konsentrasies van Asp (0.1–10 µM), PPAG (0.1–10 µM), en GRT (0.0001-0.01 mg/ml) het sel-lewensvatbaarheid en funksie verbeter met gepaardgaande verlaging in oksidatiewe stress na 24 uur (97.66% ± 3.5, $p<0.66$; 95.54% ± 5.61, $p<0.52$; 96.80% ± 3.67, $p<0.55$).

Gevolgtrekking

Aspalathin, en veral GRT, het teen laer konsentrasies die β-sel in 'n mate teen sitokien-geïnduseerde ontsteking beskerm, terwyl hoër konsentrasies, op 'n dosis-afhanklike manier, BACE-aktiwiteit matig moduleer.

Sleutelwoorde: amilien, ontsteking, BACE2, tipe 2 diabetes, Rooibos, polifenole.

ACKNOWLEDGEMENTS

Without the assistance and support of the following people/institutions the completion of my master's degree would not have been possible:

- My supervisor, Dr N. Chellan for all her time and support in helping me to become the researcher I am today.

- My co-supervisors, Prof C.J.F. Muller and Dr J. Lopes for all their input and guidance in completing this thesis.

- The National Research Foundation (NRF) for their financial support (Thuthuka; Grant UID 106951).

- The South African Medical Research Council (SAMRC) for their financial support and the use of their facilities.

- Colleagues at the SAMRC, especially R. Van Aarde for technical assistance and Dr S. Bowles for moral support.

- Peers in the Department of Medical Physiology, who were always ready to have a conversation or two.

- My parents for all the sacrifices made and endless love, always supporting me.

- My friends for all their support.

CONTENT

LIST OF FIGURES

Chapter 4

Chapter 8

LIST OF TABLES

ABBREVIATIONS / ACRONYMS

Abbreviation / Acronym	
aa	Amino acids
ACE	Angiotensin-converting enzyme
AChE	Acetylcholinesterase
AD	Alzheimer's disease
AGE	Advanced glycation end-product
AKT	v-akt murine thymoma viral oncogene homologue 1 better known as protein kinase B
AMPK	5' AMP-activated protein kinase
ANOVA	One-way analysis of variance
AP-1	Activator protein 1
APP	Amyloid precursor protein
ARB	Angiotensin II receptor blockers
Asn	Asparagine
Asp	Aspalathin
ATP	Adenosine triphosphate
ATTR	Transthyretin-associated amyloidosis
AUC	Area under the curve
AV	Annexin-V
Aβ	Amyloid-beta
BACE 1/2	Beta-site amyloid precursor protein cleaving enzyme / beta-secretase 1/2
BCA	Bicinchoninic acid assay
BChE	Butyrylcholinesterase
Bcl2	B-cell lymphoma 2
BrdU	5-bromo-2'-deoxyuridine
BSA	Bovine serum albumin
Ca^{2+}	Calcium
cAMP	Cyclic adenosine monophosphate

CAT	Catalase
CD68	Cluster of Differentiation 68
CDK	Cyclin-dependent kinase
CNS	Central nervous system
CO_2	Carbon dioxide
COX2	Cyclooxygenase 2
CRP	C-reactive protein
Cu^+	Copper
DCF	Dichlorofluoroscein
DCFH	2'7'-dichlorofluoroscein
DEVD	Aspartic Acid - Glutamic Acid - Valine - Aspartic Acid
DMSO	Dimethyl sulfoxide
DNA	Deoxyribonucleic acid
DPBS	Dulbecco's phosphate buffered saline
ECL	Enhanced chemiluminescence
EGF	Epidermal growth factor
ELISA	Enzyme-linked immunosorbent assay
eNOS	Endothelial nitric oxide synthase
ER	Endoplasmic reticulum
ERK	Extracellular signal-regulated kinases
EtOH	Ethanol
FA	Fatty acids
fa/fa	Zucker obese rat
FAS	First apoptosis signal receptor gene
FBS	Fetal bovine serum
FFA	Free fatty acids
FITC	Fluorescein isothiocyanate
FRET	Fluorescence resonance energy transfer
G 1/2	Gap phase 1/2
G0	Resting phase

GF	Growth factor
GH	Growth hormone
GLUT 2/4	Glucose transporter 2/4
GRT	Aspalathin rich, unfermented Rooibos extract
GSH-Px	Glutathione peroxide
GSIS	Glucose stimulated insulin secretion
GSK3 α/β	Glycogen synthase kinase-3 alpha/beta
HCl	Hydrochloric acid
HEPES	4-(2-hydroxyethyl)-1-piperazineethanesulfonic acid
hIAPP	Human islet amyloid polypeptide
HIT	Hamster pancreatic beta cells
HPA	Hypothalamic-pituitary-adrenal
HPG	Hypothalamic-pituitary-thyroid and gonadal
HPLC	High-performance liquid chromatography
HRP	Horseradish peroxidase
Hz	Hertz
IAPP	Islet amyloid polypeptide
IC_{50}	Half of the maximal inhibitory concentration
IFN-γ	Interferon-gamma
IFN-т	Interferon-tau
Ig	Immunoglobulin
IGF-1	Insulin growth factor-1
IKK	Ikb kinases
IL-1β/2/6/8/10/12	Interleukin 1 beta/2/6/8/10/12
iNOS	Inducible nitric oxide synthase
INS1	Rat insulinoma pancreatic beta cells
IR	Insulin resistance
IRF-1	Interferon regulatory factor-1
IRS	Insulin receptor substrates
JNK	C-Jun terminal kinases

K^+	Potassium
KRBH	Krebs-Ringer bicarbonate-HEPES buffer
LDL	Low density lipoprotein
LY2886721	N-(3-((4aS,7aS)–2–amino-4a,5,7,7a–tetrahydro-4H-furo[3,4-d] [1,3] thiazine-7a-yl)–4-fluorophenyl)–5-fluoropicolinamide
M	Mitotic phase
MAPK	Mitogen-activated protein kinases
MCP-1	Monocyte chemoattractant protein-1
Mg^{2+}	Magnesium
MIN	Transgenic C57BL/6 mouse insulinoma cells
MIP-1α	Macrophage inflammatory protein-1 alpha
mRNA	Messenger ribonucleic acid
MTT	(3-(4,5-dimethylthiazol-2-yl)-2,5-diphenyltetrazolium bromide) tetrazolium
Na^+	Sodium
NED	*N*-1-napthylethylenediamine dihydrochloride
NF-κB	Nuclear factor kappa-B
NLRP3	NBD, LRR and PYD domains-containing protein 3
NO	Nitric oxide
NO_{2-}	Nitrite ion
Nrf2	Nuclear factor-like 2
ob/ob	B6.V-Lep^ob mice
OGTT	Oral glucose tolerance test
p75NRT	p75 Neurotrophin receptor
PAI-1	Plasminogen activator inhibitor-1
PARP	Poly (ADP-ribose) polymerase
PC 1/2/3	Pro-protein convertase 1/2/3
PDK1	Protein 3-phosphoinositide-dependent protein kinase-1
PDX-1	Pancreatic and duodenal homeobox 1
PI	Propidium iodide
PI3K/AKT	Phosphatidylinositol 3-kinase AKT

PIP	Phosphatidylinositol-3-phosphate
PIP2	Phosphatidylinositol-4,5-bisphosphate
PIP3	Phosphatidylinositol-3,4,5-triphosphate
PKC	Protein kinase C
PMSF	Phenylmethane sulfonyl fluoride
PPAG	Z-2-(β-D-glucopyranosyloxy)-3-phenylpropenoic acid
PPAR-γ	Peroxisome proliferator-activated receptor-gamma
PVDF	Polyvinylidene difluoride
RAGE	Receptor for advanced glycation end-products
RAS	Renin–angiotensin system
rIAPP	Rat islet amyloid polypeptide
RIN	Rat insulinoma cells
RIP	Regulated intermembrane proteolysis
RNS	Reactive nitrogen species
ROS	Reactive oxygen species
S	Synthesis
SB	Sample buffer
SDS-PAGE	Sodium dodecyl sulphate polyacrylamide gel electrophoresis
SEM	Standard error of mean
SFA	Saturated fatty acids
SNAPIN	Soluble NSF (N-ethylmaleimide-sensitive factor) Attachment Protein) Receptor (SNARE)-associated protein
SOCS-3	Suppressors of cytokine signalling-3
SOD	Superoxide dismutase
STAT-1	Signal transducer and activator of transcription-1
T1D	Type 1 diabetes
T2D	Type 2 diabetes
TAG	Triacylglycerol
TBS	Tris-buffered saline
TBST	Tris-buffered saline with tween

TF	Transcription factor
TGF-α	Transforming growth factor-alpha
Tlr-4	Toll-like receptor 4
TMB	3,3′,5,5′-tetramethylbenzidine
TMEM27	Transmembrane protein 27
TNF-α	Tumor necrosis factor-alpha
UPP	Ubiquitin-proteasome pathway
WAT	White adipose tissue
Zn^{2+}	Zinc
βTC	Beta-tumour cells

Units	
°C	Degree celsius
µg	Microgram
µl	Microliter
µM	Micromolar
cm^2	Square centimetre
Em	Emission
Ex	Excitation
FL-1/4	Fluorescence green (1) / red (4)
g	Gram
kDa	Kilodalton
l	Litre
mg	Milligram
ml	Millilitre
mM	Millimolar
mm	Millimetre
MW	Molecular weight
ng	Nanogram
nm	Nanometre
pg	Picogram
pH	Potential of hydrogen
pmol	Picomole
RLU	Relative light units
SS	Soluble solids
V	Volts
x *g*	Gravity

CHAPTER 1

Introduction

Type 2 diabetes is a disease characterised by IR of insulin responsive tissues such as muscle, liver, and adipose tissues which contributes to β-cell dysfunction and failure, ultimately resulting in reduced β-cell functional mass (Figure 1.1) (Abedini and Schmidt, 2013; Altirriba et al., 2010; Esterházy et al., 2011; Jeong and An, 2015; Sandovici et al., 2016). Underlying to the development of T2D are inflammatory as well as metabolic aberrations, that include chronic, low-grade inflammation, increased body mass, particularly white adipose tissue (WAT), and dysregulated glucose metabolism (Duncan et al., 2003; Saltiel, 2000).

Initially, in the pre-diabetic and early phases T2D, β-cells maintain euglycemia by increasing insulin secretion through compensatory hyperplasia/hypertrophy of the β-cell mass (Altirriba et al., 2010; Bourlier et al., 2008; Dludla et al., 2014; Donath, 2014; Esterházy et al., 2011; Henegar et al., 2008). In T2D, β-cell dysfunction leads to β-cell failure which is associated with: increased endoplasmic reticulum (ER) stress; mitochondrial dysfunction; and of particular interest to this study, inflammation and oxidative stress (Abedini and Schmidt, 2013; Harding and Ron, 2002; Hull et al., 2004; Prentki and Nolan, 2006; Robertson et al., 2004; Weir and Bonner-Weir, 2004). Immune cell infiltration, elevated pro-inflammatory cytokine levels, and activation of nuclear factor kappa-B (NF-κB); all associated with inflammation in the pancreatic islets, are pathological key features of T2D (Donath et al., 2008, 2005). Continuous exposure of β-cells to inflammation and hyperglycemia, leads to the production of reactive species, including ROS and reactive nitrogen species (RNS), which result in the oxidative damage of cellular machinery causing a loss in cell structure and function (Bansal and Bilaspuri, 2011; Pham-Huy et al., 2008).

Pancreatic β-cell failure leads to reduced β-cell functional mass due to an imbalance between β-cell growth (proliferation and/or neogenesis) and death (apoptosis and/or necrosis) (Akpinar et al., 2005). This imbalance as a result of increased cell death is due to the stimulation of several mechanisms; all associated with β-cell failure, and is enhanced by glucotoxicity and lipotoxicity (Figure 1.1) (Jeong and An, 2015; Sandovici et al., 2016).

Since amylin, a neuro-hormone, is co-secreted with insulin, hyperinsulinemia coincides with hyper secretion of amylin (Cooper et al., 1987; Westermark et al., 1986). Abnormalities in amylin folding, secretion, and function exacerbates β-cell dysfunction (Clark et al., 1996a, 1996b; Kahn et al., 1999a). The increased amylin secretion results in associated aggregation of amyloid deposits which can physically disrupt islet structure and induce inflammation,

perpetuating dysfunction. However, in the progression of T2D, amyloid predominantly exerts its toxic effect by activating multiple overlapping mechanisms and downstream signalling pathways (Abedini and Schmidt, 2013; Jeong and An, 2015). Amyloid induced toxicity is associated with increased oxidative stress responses as well as low density lipoprotein (LDL) uptake, suggesting that the underlying mechanisms of amylin toxicity involves changes in pathways associated with oxidative stress as well as lipid homeostasis (Janciauskiene and Ahrén, 2000). Amylin is also seen to interact with immune cells that activate inflammasomes, triggering signalling cascades that produce pro-inflammatory cytokines, such as IL-1β, by activating the NF-κB pathway, the inflammation master switch (Abedini and Schmidt, 2013; Masters et al., 2010; Tak and Firestein, 2001; Westwell-Roper et al., 2014).

A positive correlation is seen between amylin and BACE2 (Alcarraz-Vizán et al., 2017, 2015). Beta secretase 1 is a protease expressed in the brain where it contributes to the development of Alzheimer's disease (AD) (Southan and Hancock, 2013; Vassar, 2014; Venugopal et al., 2008). Beta secretase 2 is mainly expressed in the pancreas and although its function is not fully elucidated, it has several physiological functions (Vassar, 2014). Overexpression of amylin has been shown to block autophagy in β-cells, interfering with the degradation of BACE2 thus resulting in increased cleavage of transmembrane protein 27 (TMEM27) (Alcarraz-Vizán et al., 2017, 2015). Although TMEM27 plays a beneficial role in β-cell proliferation and insulin signalling, BACE2 cleavage of TMEM27 increases the deposition of amyloid and subsequent induction of inflammation and oxidative stress and thus presents as a therapeutic target (Esterházy et al., 2011; Southan and Hancock, 2013).

It is vital to elucidate the underlying mechanisms of β-cell dysfunction and failure to prevent or delay the onset and progression of T2D. Theoretically, β-cell protection can be accomplished through mechanisms preventing β-cell dysfunction induced by stressors such as oxidative stress and inflammation. Rooibos (*Aspalathus linearis*) is known as a rich source of polyphenols with antioxidant and anti-inflammatory properties (Beltrán-Debón et al., 2011; Joubert et al., 2008; Joubert and de Beer, 2011). Aspalathin and PPAG, both phenolic components of Rooibos, have been shown to directly stimulate insulin secretion from β-cells (Bramati et al., 2002; Kawano et al., 2009; Ku et al., 2015; McKay and Blumberg, 2007). Rooibos reduces oxidative stress through direct scavenging of free radicals and interfering with inducible nitric oxide synthase (iNOS), through interaction with several enzyme systems (Ayeleso et al., 2014; Kawano et al., 2009; Nijveldt et al., 2001). Furthermore, Asp may exert its effect via an insulin/insulin-like signalling pathway (Chen et al., 2013; Kawano et al., 2009). In addition to antioxidant properties, polyphenols, including flavonols and flavones, have a protective effect against Aβ formation and aggregation, by inhibiting BACE activity (Shimmyo et al., 2008).

It can be proposed that chronic, low-grade inflammation perpetuates the deleterious effects of amyloid and that BACE regulation might be a key therapeutic target through the modulation of amyloid deposition. We hypothesized that Rooibos may have anti-inflammatory effects in β-cells and may additionally modulate BACE activity, enhancing the anti-diabetic effect.
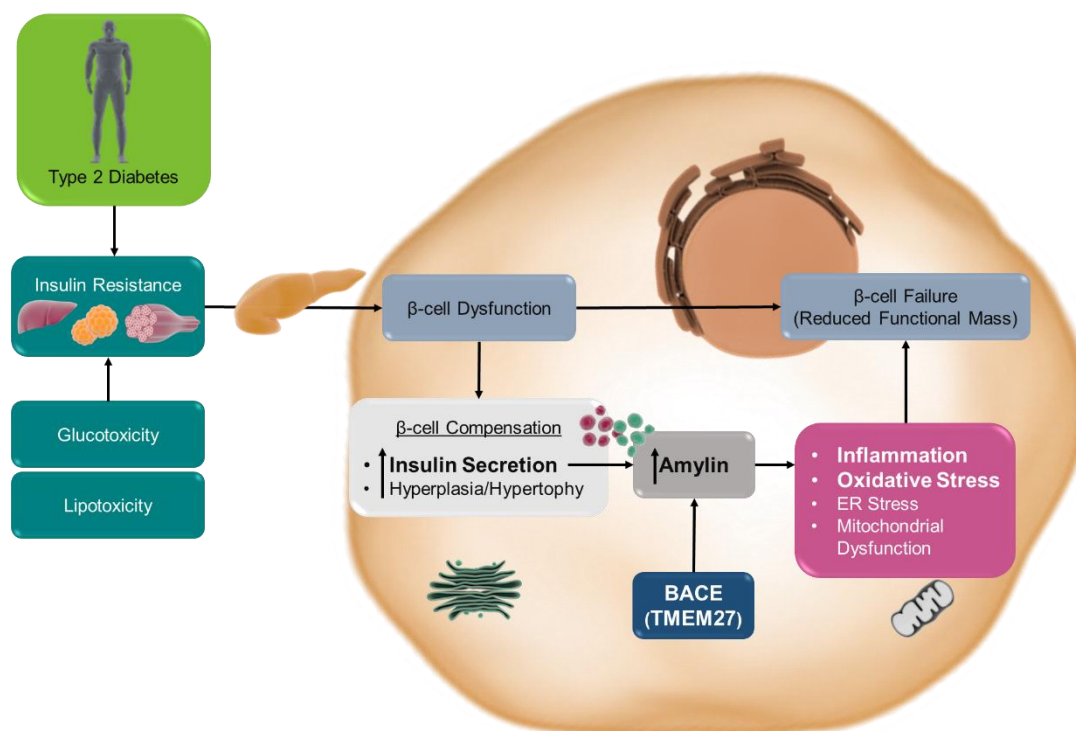
Figure 1.1: Diagrammatic presentation of mechanisms involved in type 2 diabetes. Type 2 diabetes is a disease characterised by IR in muscle, liver, and adipose tissues which leads to β-cell dysfunction and failure, ultimately resulting in reduced β-cell functional mass as a result of increased inflammation and oxidative stress. Several mechanisms are activated to compensate for cell dysfunction including increased insulin secretion; which then results in increased amylin secretion as it co-secreted with insulin. Beta secretase 2 correlates with amylin levels and is involved in TMEM27 cleavage, which influences β-cell proliferation and insulin signalling; making BACE inhibition a therapeutic target.

Literature Review

1.1. Progression of Type 2 Diabetes: Potential Role of Amyloid

1.1.1. Type 2 Diabetes

Type 2 diabetes is a complex disease associated with IR and subsequent hyperglycemia, which increases β-cell dysfunction leading to β-cell failure and ultimately results in reduced β-cell functional mass (Altirriba et al., 2010; Esterházy et al., 2011; Jeong and An, 2015). Insulin resistance can be defined as the inability of exogenous or endogenous insulin to increase glucose uptake and utilization; while in a physiologically normal subject insulin exerts this effect (Lebovitz, 2001). At the initial stage of T2D, the pancreatic β-cells adapt to IR by increasing its functional mass as well as insulin secretion to meet the elevated metabolic demands. However, the continuous state of hyperglycemia eventually exerts an adverse effect on the functionality of β-cells, resulting in impaired insulin secretion and a reduction in insulin gene expression, ultimately resulting in β-cell death (Altirriba et al., 2010; Dludla et al., 2014; Donath, 2014). Pancreatic β-cell mass is regulated by a balance of β-cell growth (replication) and by β-cell death (apoptosis/necrosis) (Akpinar et al., 2005). Apoptosis is a genetically programmed cell death, characterised by cell shrinkage, membrane blebbing, chromatin condensation, and deoxyribonucleic acid (DNA) fragmentation, followed by engulfment of the impaired cell by neighbouring cells (Kerr et al., 1972; Renehan et al., 2001). Necrosis on the other hand is an uncontrolled cell death that lacks the characteristics of apoptosis and occurs as a result of severe disease or injury (Golstein and Kroemer, 2007). Mechanisms leading to a decline in β-cell mass and function include: glucotoxicity, lipotoxicity, and the formation of amyloid deposits (section 1.1.2; subsection 1.1.2.3), which increase inflammation (section 1.2), oxidative stress (section 1.1.3), and ER stress as presented in Figure 1.2 (Abedini and Schmidt, 2013; Harding and Ron, 2002; Hull et al., 2004; Prentki and Nolan, 2006; Robertson et al., 2004; Weir and Bonner-Weir, 2004). Glucotoxicity occurs when cells are chronically exposed to excessive glucose levels that cause irreversible β-cell damage (Robertson et al., 2003). Lipotoxicity occurs when there is an over-accumulation of un-oxidized long-chain fatty acids (FA), which saturate the storage capacity of adipose tissue, resulting in the accumulation of lipids or intermediate lipid metabolites in non-adipose tissues such as the muscle, heart, liver, and pancreatic-islets (ectopic fat). Ectopic lipid deposition can have deleterious effects as these lipids are driven into alternative non-oxidative pathways, which lead to the formation of lipid moieties that promote cellular dysfunction (Kusminski et al., 2009).
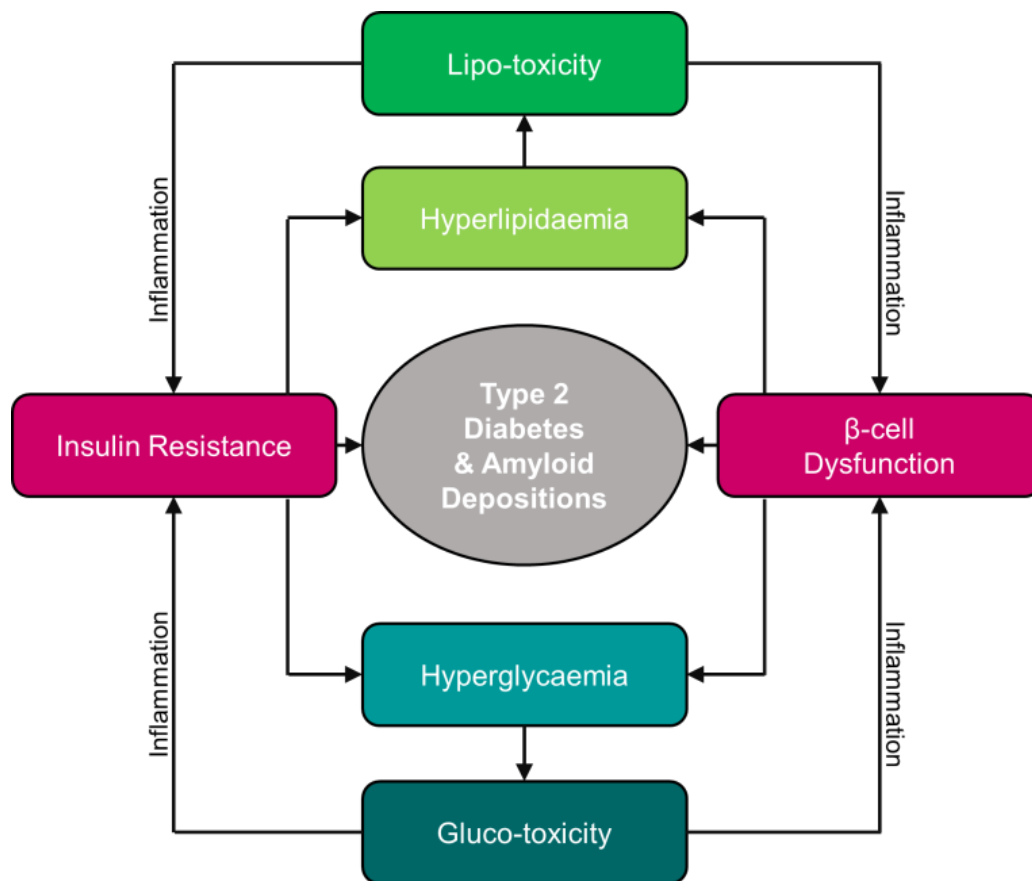
Figure 1.2: **Factors involved in amyloid depositions and subsequently in the progression of type 2 diabetes**. Schematic presentation of factors involved in IR and pancreatic β-cell dysfunction including hyperglycemia and hyperlipidemia, which result in glucotoxicity and lipotoxicity; with both leading to amyloid deposition and the progression of T2D by means of chronic low-grade inflammation (Adapted from Bonora, 2008).

Islet pathology in T2D is associated with elevated pro-inflammatory cytokine levels, and the activation of NF-κB (Donath et al., 2008, 2005). It is important to note, all the above mentioned mechanisms are linked with inflammatory responses (section 1.2) (Donath et al., 2003; Ehses et al., 2009; Hotamisligil and Erbay, 2008; Jourdan et al., 2013; Lerner et al., 2012; Masters et al., 2010; Oslowski et al., 2012; Pickup, 2004; Westwell-Roper et al., 2014). Therefore, it has been proposed that T2D is an inflammatory as well as a metabolic disease (Duncan et al., 2003).

Chronic, low-grade inflammation, a hallmark of several metabolic diseases, negatively influences the function of heart, liver, and pancreatic tissues (Abedini and Schmidt, 2013; Sandovici et al., 2016). The decline in pancreatic β-cell function with age, in the setting of IR, is a key factor in the progression of T2D (Sandovici et al., 2016) and is characterized by a

reduction in β-cell functional mass. This reduction in β-cell functional mass results in hyperglycemia due to insufficient insulin secretion relative to cellular metabolic demands, which is initially compensated for by hypersecretion of insulin (Altirriba et al., 2010; Esterházy et al., 2011). It is proposed that processes such as inflammation, increased oxidative stress, impaired β-cell proliferation, and increased apoptosis result in loss of pancreatic cell functional mass (Jeong and An, 2015; Sandovici et al., 2016). The above mentioned processes are also associated with increased formation and deposition of toxic islet amyloid polypeptide (IAPP) (Jeong and An, 2015), as described in section 1.1.2.

1.1.1.1. Insulin Signalling, Insulin Resistance, and Beta-cell Failure

The pancreas comprises of an exocrine and endocrine part, with the latter containing the islets of Langerhans crucial for glucose homeostasis. The main types of islet endocrine cells are: β-cells secreting insulin; α-cells secreting glucagon; and δ-cells responsible for somatostatin secretion (Elayat et al., 1995). Elevated blood glucose levels stimulate insulin production and secretion. Insulin's precursor protein carries a signal peptide which directs the peptide chain to the interior of the ER where pro-insulin is produced by the cleavage of the signal peptide and the formation of disulphide bonds, where after it passes through the Golgi apparatus to get packed into vesicles (Skelin et al., 2010).

Dean and Mathews (1970) described pancreatic β-cell electrical activity by showing that a glucose concentration higher than 7 mM results in depolarisation of the β-cell membrane. The depolarised cell membrane leads to the closing of the ATP sensitive K^+ channels which results in the excitation of a rhythmic electrical impulse. This impulse activates the voltage dependent Ca^{2+} channels and the subsequent hyperpolarised phase. The higher the glucose concentration the longer the duration of the active phase. At low levels of glucose, the ATP levels are too low to keep the ATP-sensitive K^+-channels closed. However, when the extracellular glucose concentration is elevated, glucose enters the cells through glucose transporter 2 (GLUT2). Glucose is then metabolically degraded and leads to increased ATP levels that are responsible for closing the K^+-channels in the plasma membrane. The closed K^+-channels cause depolarisation of the plasma membrane which results in the opening of the voltage gated Ca^{2+} channels and the subsequent influx of extracellular Ca^{2+} (Dean and Matthews, 1970; Guo et al., 2014). Electrical activity together with Ca^{2+} influx results in insulin release (Ashcroft and Rorsman, 1989).

After insulin release, insulin signalling is initiated when insulin binds with its specific receptor found mainly in muscle and fat tissues, inducing intracellular cascades. The insulin signalling pathway includes at least four distinct insulin receptor substrates (IRSs) which are key

regulatory proteins, with IRS-1 and IRS-2 considered the most relevant as they are linked to the actions of insulin as well as β-cell function (Greenberg and McDaniel, 2002; Kulkarni et al., 1999). Insulin receptor substrate-2 knockout mice are seen to result in IR and β-cell dysfunction with a 50% reduction in β-cell mass. However, IRS-1 knockout mice are seen to impede somatic growth while enhancing β-cell mass as these mice are 50% smaller in size compared to controls, while their β-cell mass is increased by two-fold. Insulin receptor substrate-1 knockout mice display mild IR and are hyperinsulinemic while IRS-2 knockout mice develop severe diabetes after 10 weeks. It can be postulated that a signalling balance between IRS-1 and IRS-2 may be required for normal β-cell function (Burks and White, 2001; Kahn, 1998a).

Insulin receptor-mediated tyrosine phosphorylation of IRS activates two major pathways; the phosphatidylinositol 3-kinase (PI3K)-protein kinase B (AKT) as well as the mitogen-activated protein kinase (MAPK) pathways, both regulated by negative feedback (Figure 1.3). The PI3K/AKT pathway gets activated downstream of the insulin receptor and is involved in insulin action on glucose uptake and gluconeogenesis suppression. The MAPK pathway is associated with gene expression and additionally cell growth regulation and differentiation by interacting with the PI3K/AKT pathway (Figure 1.3). The PI3K pathway catalyses the addition of a phosphate molecule to carbon-3 of the inositol ring of phosphoinositide, converting membrane phosphatidylinositol into phosphatidylinositol-3-phosphate (PIP), and generates phosphatidylinositol-3,4,5-triphosphate (PIP3) from phosphatidylinositol-4,5-bisphosphate (PIP2). Protein kinase B binds to PIP3 inducing AKT activation through the activation of kinases upstream. Protein kinase B is then released to translocate to the cytoplasm, nucleus, and even mitochondria to phosphorylate various substrates associated with gluconeogenesis, synthesis of glycogen, as well as glucose uptake (Schultze et al., 2012). Protein 3-phosphoinositide-dependent protein kinase-1 (PDK1), an AKT activating kinase, is seen to activate isoforms of protein kinase C (PKC), essential for GLUT-4 dependent regulation of glucose uptake (Figure 1.3).

Mitogen-activated protein kinases consist of subfamilies of serine/threonine kinases, including extracellular signal-regulated kinases (ERK1/2), p38, and c-Jun terminal kinases (JNK). The JNK and p38 kinases are activated by cellular stressors such as free fatty acids (FFA), interleukin-6 (IL-6), IL-1β, and TNF-α, and are therefore collectively known as stress-activated MAPKs. Cellular events in the cytoplasm are regulated by activated MAPKs, by phosphorylation of threonine and tyrosine. Activated MAPKs translocate to the nucleus where it plays a vital function in phosphorylation of transcription factors (TF) such as activator protein 1 (AP-1), controlling the expression of various pro-inflammatory genes downstream (Huang et

al., 2009).   Insulin signalling can be blocked by serine phosphorylation of IRS-1, which inactivates tyrosine phosphorylation of IRS.

Importantly, the NF-κB pathway is activated by AKT and MAPK, amplifying pro-inflammatory cytokine production, which contributes to IR and thus T2D. Insulin also activates other IRS serine kinases, which play a vital role in mediating inflammatory signalling pathways, suggesting a possible link between insulin signalling and inflammatory responses (Qatanani and Lazar, 2007). Increased PI3K levels are seen to stimulate the MAPK pathway through activation of SOS, Ras, C-Raf, GRB-10, and MEK, exacerbating the transcription of growth factors (GF) by ERK (Figure 1.3). Nitric oxide (NO), an endogenous signalling molecule, produced by iNOS, is able to degrade IRS. The activity of iNOS therefore leads to a decline in the activities of PI3K/AKT, consequently resulting in the reduction of insulin signalling and insulin activity (Zeyda and Stulnig, 2009).
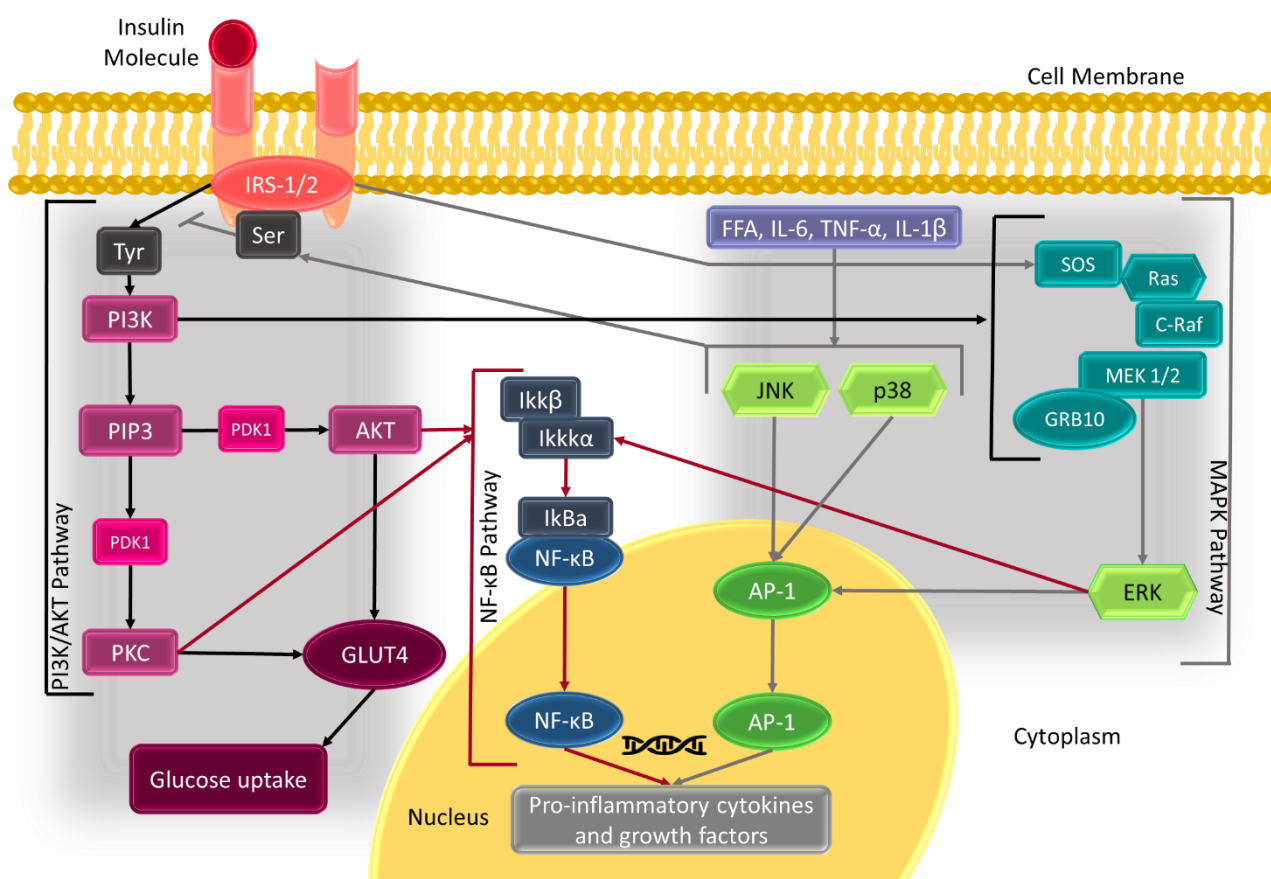
Figure 1.3: Downstream pathways stimulated by insulin secretion. Binding of insulin to its receptor leads to the activation of several downstream signalling pathways, including the PI3K/AKT (black arrows), MAPK (grey arrows), and NF-κB (red arrows) pathways; playing a vital role in glucose uptake as well as the transcription and expression of several pro-inflammatory cytokines and GFs (Adapted from Cruz et al. 2012).

As mentioned previously, T2D involves IR in mainly muscle, liver, and fat tissues, which is initially compensated for by increased insulin secretion. When insulin production becomes impaired (β-cell exhaustion), glucose intolerance or overt diabetes develop (Kahn et al., 1998; Larsson and Ahrén, 1996). Subjects with T2D present with increased insulin levels (Yalow and Berson, 1960) as well as high glucose levels during the fasting state, suggesting the presence of IR or decreased insulin sensitivity (Shen et al., 1970). Although insulin secretion in response to oral glucose in T2D individuals is increased, the first phase of insulin secretion is blunted (Ward et al., 1984), and the peak plasma insulin is delayed (Bonora et al., 1983). However, elevated levels of circulating insulin, in addition to normal glucose levels, results in impaired β-cell function (Perley and Kipnis, 1967; Polonsky et al., 1988). Decreased β-cell functional mass is seen as a triggering event in the progression of T2D (Weyer et al., 1999). Studies have shown that the volume of β-cells reduces by 40-60% in T2D individuals and an abnormality in the volume is already observed in individuals with increased fasting glucose levels (Butler et al., 2003). Studies also showed that the rate of β-cell replication is not impaired in T2D individuals, but rather an increased rate of apoptosis (Butler et al., 2003). Approximately 1% of β-cells enter the mitotic phases gap 1 (G1), synthesis (S), G2 and mitosis (M) from the resting (G0) phase, confirming a low turnover rate of β-cells. Various GFs such as: epidermal growth factor (EGF), transforming growth factor α (TGF-α), growth hormone (GH), and insulin growth factor-1 (IGF-1), are all vital in β-cell renewal and growth. Glucose also plays a role in maintaining an adequate amount of β-cells by stimulating proliferation at non-toxic concentrations, important for overall regulation of metabolism (Skelin et al., 2010).

1.1.2.   Amylin and Amyloid Deposition

A risk factor for the development of metabolic diseases, including T2D, is ageing; especially in individuals with genetic and epigenetic predispositions. Ageing leads to chronic, low-grade inflammation, which deleteriously influences the function of various tissues, including pancreatic islets (Abedini and Schmidt, 2013; Donath, 2014; Sandovici et al., 2016). Genes upregulated with age are significantly enriched for processes associated with immune and inflammatory responses as well as extracellular matrix organization (Sandovici et al., 2016). Prolonged exposure of human islets to high concentrations of glucose results in increased synthesis of IAPP, and therefore implies that prolonged hyperinsulinemia is associated with increased secretion of amylin (Gasa et al., 2001; Hou et al., 1999). As mentioned previously, the neuro-hormone amylin is co-secreted with insulin from pancreatic β-cells (Cooper et al., 1987; Westermark et al., 1986), and abnormalities in its folding, secretion, and function have detrimental effects on islet function and glucose regulation, leading to islet amyloidosis and β-cell dysfunction, and consequently T2D (Clark et al., 1996a, 1996b; Kahn et al., 1999).

1.1.2.1. Amylin Formation, Secretion, and Function

The precursor peptide of islet amyloid is amylin, a product of the pancreatic islet cells (Johnson et al., 1988; Westermark et al., 1987). The amylin gene, located on chromosome 12, leads to the formation of amylin peptides which fold to form α-helix monomers, oligomers, and cross β-sheet amyloid fibrils (Abedini and Schmidt, 2013; Cohen and Calkins, 1959). Protofibrils can be formed either by parallel stacking of molecules with parallel and antiparallel β-strands or antiparallel with parallel interaction between molecules as indicated by Figure 1.4 (Jaikaran and Clark, 2001). Initially, similar to insulin, amylin is synthesised as an 89-residue pre-prohormone (Sanke et al., 1988), followed by the removal of a 22-residue signal peptide, leading to the 67-residue pre-IAPP, then enzymatically cleaved by pro-protein convertase-1/3 (PC1/3) and PC2 in the Golgi apparatus forming a 37-residue mature hormone (Badman et al., 1996; Higham et al., 2000; Marzban et al., 2005); PIC1/3 and PIC2 also play a role in the conversion of pro-insulin to insulin (Bailyes et al., 1992). Additional post-translational alterations include the formation of a disulphide bridge between the 2nd and 7th residue, as well as amidation of the C-terminus tyrosine (Roberts et al., 1989). Mature amylin, together with insulin, is stored in the insulin secretory granule at a ratio of 1:50 to 1:100, and co-secreted in response to β-cell stimulation by glucose (Alcarraz-Vizán et al., 2015; Hanabusa et al., 1992; Jeong and An, 2015; Kahn et al., 1991, 1990; Thomaseth et al., 1996). Amylin levels are approximately 10-15% of insulin levels, during the fasting state (Hanabusa et al., 1992; Kautzky-Willer et al., 1994; Thomaseth et al., 1996); this may be due to the variation in clearance rates of amylin and insulin, as amylin clearance is slower than insulin (Leckström et al., 1997; Zhang et al., 2016).

The function of amylin is not fully elucidated; however, studies have demonstrated that amylin is involved in several physiological processes. Under normal physiological conditions, increased levels of blood glucose result in the release of amylin and insulin (Mulder et al., 1996). Insulin increases glucose uptake from the circulation into fat and muscle cells, while insulin and amylin inhibit glucose release from the liver. The latter is done by reducing glucagon secretion and thus decreasing postprandial glucose (Gedulin et al., 1997). However, amylin is seen to inhibit insulin-stimulated glycogen synthesis which may lead to IR (Leighton and Cooper, 1988; Sowa et al., 1990). Amylin and insulin also suppress postprandial secretion of glucagon from islet α-cells to regulate postprandial glycaemia (Akesson et al., 2003; Gedulin et al., 1997). However, in T2D individuals, plasma amylin and insulin decrease, implying that postprandial insulin: glucagon regulation is compromised and glucose levels are increased (Kahn et al., 1998).

Amylin also regulates carbohydrate storage to transfer triglycerides into muscle glycogen, (James et al., 1999) and satiety, by acting as a neurohormone and reducing food intake via receptors situated in the brainstem. High plasma levels of amylin, delay gastric emptying and subsequently improve postprandial glucose (Kong et al., 1997; Paulsson et al., 2014; Thompson et al., 1997; Woerle et al., 2008), while amylin deficiency do not delay gastric emptying in response to hyperglycemia (Woerle et al., 2008). Amylin also regulates blood pressure by vasodilation through the renin–angiotensin system (RAS) (Brain et al., 1990; Chin et al., 1994; Zhao et al., 2003), as well as renal filtration by regulating K^+ and Na^{2+} excretion (Harris et al., 1997; Wookey et al., 1998, 1996). Angiotensin-converting enzyme (ACE) inhibition is associated with a reduction of amylin binding in the renal cortex (Wookey et al., 1998). Reduced glomerular filtration correlates with the accumulation of amylin in circulation and is excreted in urine. Therefore, individuals with renal failure may have increased concentrations of circulating amylin (Ludvik et al., 1994). Amylin is also associated with Ca^{2+} homeostasis in bones (Alam et al., 1993; Gilbey et al., 1991). Taken together, it can be said that amylin is curtailed in several physiological processes and that any defect in amylin secretion or function might have detrimental consequences.
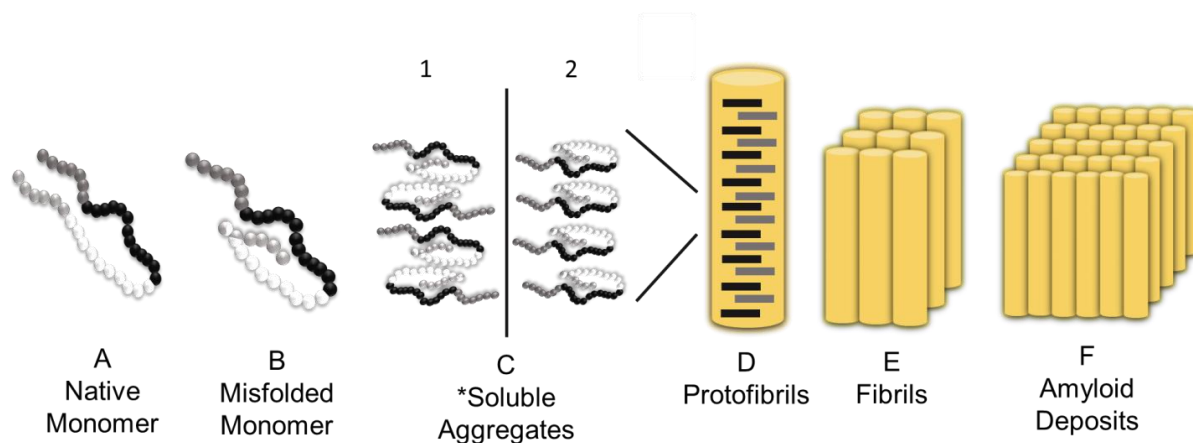
Figure 1.4: Amyloid formation in pancreatic islets. Diagrammatic presentation of amyloid formation from cytotoxic amylin aggregates to the deposition of amyloid. *Possible conformation of stacked hIAPP molecules within a protofilament: 1) antiparallel stacking of peptide molecules with parallel interaction between molecules; or 2) parallel stacking of molecules with parallel and antiparallel β-strands (Adapted from: Hull et al., 2004 and Jaikaran and Clark, 2001).

1.1.2.2.   Factors Causing Amylin Aggregation

Amylin is subjected to post-translational alterations that affect its function as well as its tendency to aggregate. Non-enzymatic alterations such as the deamination of the asparagine (Asn) residue in amylin results in a lowered net charge of amylin at a physiological potential of hydrogen (pH), suggesting decreased solubility and accelerated formation of amyloid (Abedini and Schmidt, 2013; Alcarraz-Vizán et al., 2015; Chargé et al., 1995; Jeong and An, 2015). Proteins folding to a compact tertiary structure, in their unaggregated state, lead to the formation of amyloid. Amyloid can also form when polypeptides are not ordered and fail to adopt a compact tertiary structure in their natural soluble state (Abedini and Schmidt, 2013).

Some amyloidogenic precursor proteins form small cytotoxic aggregates that adopt a mutual structure regardless of their amino acid (aa) sequence, and have characteristics associated with metabolic diseases (Kayed et al., 2003; Yao et al., 2013). These cytotoxic aggregates are soluble and appear to represent an early intermediate in the amyloid fibril formation pathway (Figure 1.4) (Porat et al., 2003; Shirahama and Cohen, 1967). Thus amyloid represents a continuous sequence of toxicity from early cytotoxic aggregates to mature amyloid fibrils, with the early small aggregates expressing the cytotoxicity associated with amyloid and the conventional amyloid deposits indicating the end stage of the process, being less cytotoxic (Hardy and Selkoe, 2002; Janson et al., 1999; Kayed et al., 2003; Li et al., 2011; Ludvik et al., 1994; Porat et al., 2003; Zhao et al., 2009).

Cellular environmental salt concentrations, chemical modifications, isomerization, natural ligands, deamination, oxidation, and glycation affect amylin stability. The amylin sequence can be altered genetically, where mutations have been seen to be associated with diabetes (Clark and Nilsson, 2004). A mutation in the S20G gene is indicated as an important amylin gene mutation, where a glycine for serine substitution occurs in mature amylin; resulting in increased hydrophobicity and amyloidogenic characteristics of IAPP, which may increase its fibrillogenic potential (Sakagashira et al., 2000). Other factors contributing to amylin aggregation include the prevention of the disulphide bond formation, deamination, and the absence of PC2 during amylin processing. Ions, such as Ca^{2+} and Zn^{2+}, have been shown to play a role in maintaining the structure of amylin by inhibiting aggregation of amyloid while Cu^{2+} ions are thought to play a role in the pathological mechanisms of amyloidosis in diabetes. Copper-promoted ROS production and the mitochondrial disruption affect the degeneration of pancreatic islets, which leads to the production of caspase-3 and poly (ADP-ribose) polymerase (PARP), which in turn promote apoptosis (Jeong and An, 2015; Taylor et al., 2008).

1.1.2.3. Proposed Mechanisms of Amylin Toxicity

Amyloid deposits may physically disrupt tissue structure, resulting in organ dysfunction. However, under most circumstances activation of multiple overlapping mechanisms and downstream signalling pathways are proposed to lead to the pathogenesis of T2D (Abedini and Schmidt, 2013; Jeong and An, 2015). Non-receptor based mechanisms include the disruption and permeabilization of cell membranes by amyloid fibrils and soluble oligomers, leading to increased intracellular Ca^{2+} which activates several pathogenic pathways, including ROS production, altered signalling pathways, mitochondrial dysfunction, cytochrome C release, and apoptosis (Abedini and Schmidt, 2013; Wang and Youle, 2009). Receptor mediated amyloid toxicity include FAS, p75NRT, and the receptor for advanced glycation end-products (RAGEs). Originally, RAGE was investigated for its ability to bind advanced glycation end-products (AGEs) but is now recognised as a multi-ligand pattern receptor with various classes of ligands including amyloid forming polypeptides. The receptor for advanced glycation end-products not only elicits signalling pathways leading to inflammatory responses and apoptosis, but it also plays a role in the internalization of bound amyloidogenic ligands (Abedini and Schmidt, 2013; Vlassara, 1997). In order to compensate for the increased amylin levels, autophagy is upregulated as a protective response to toxic aggregate accumulation in disease state (Abedini and Schmidt, 2013). Investigation of the exact mechanism of amyloid formation and its subsequent toxicity is highly relevant for the development of therapeutic agents for the treatment of T2D.
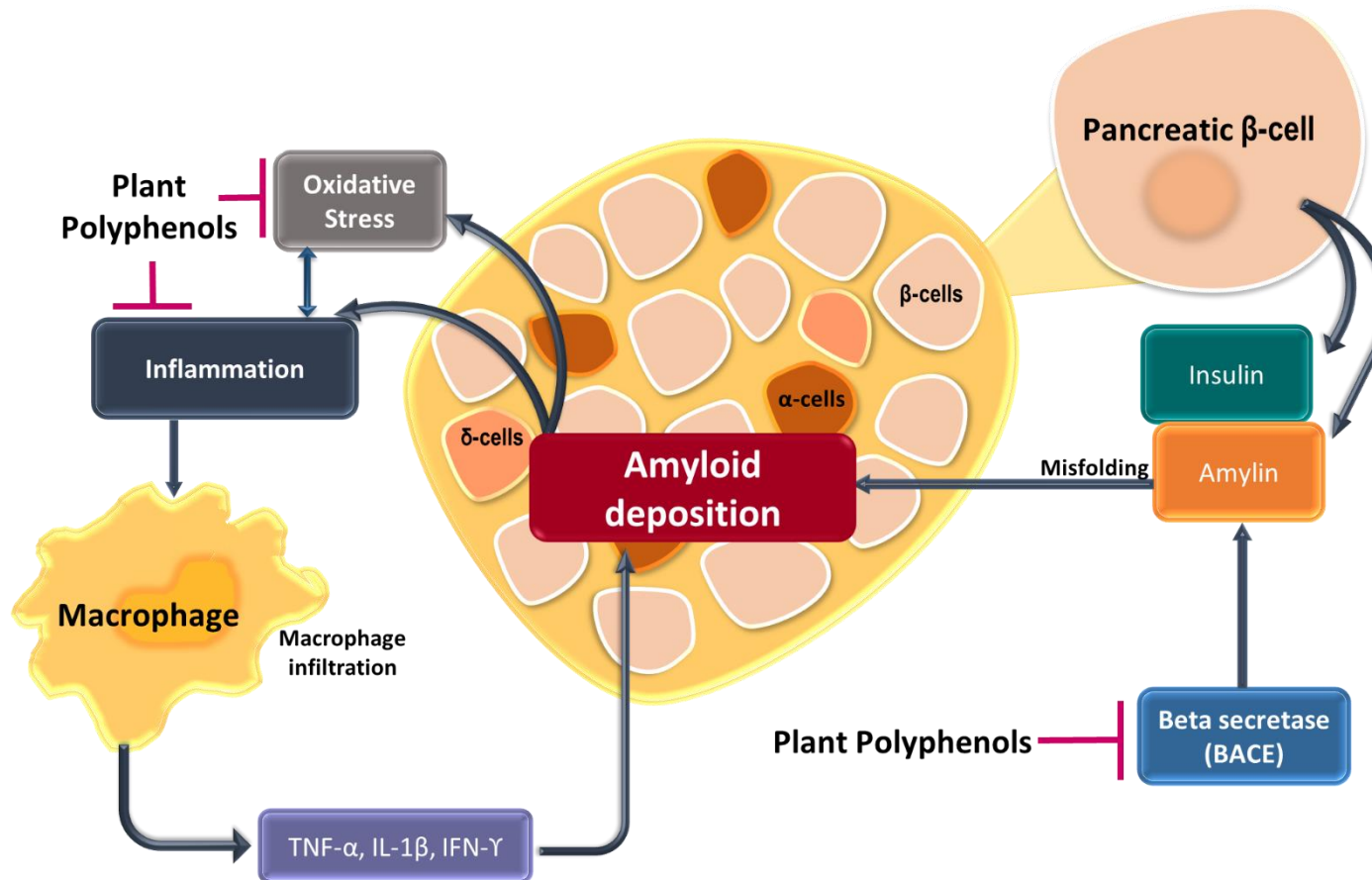
Figure 1.5: Pancreatic islet amyloid deposition. Diagrammatic presentation of the intracellular mechanisms of pancreatic islet amyloid deposition. Inflammation and oxidative stress play a profound role in β-cell pathophysiology, with amyloid deposition being a key contributor to the pro-inflammatory pathway via macrophage recruitment and the secretion of pro-inflammatory cytokines. Amyloid deposits are formed as a result of the polymerisation of amylin, a polypeptide co-secreted with insulin. Beta secretase enzymatic action is crucial in the cleavage of amylin and amyloid formation.

1.1.3. Oxidative Stress

Cells are continuously exposed to different types of stressors, such as inflammation and/or aging, that lead to the over production of reactive species called free radicals, including ROS and RNS, which by the transfer of their free unpaired electron result in the oxidation of cellular machinery causing healthy cells to lose their function and structure (Bansal and Bilaspuri, 2011; Pham-Huy et al., 2008). Free radicals play a role in the activation of different signalling pathways such as MAPK and ERK (section 1.1.1.1), pathways involved in gene expression (Cho and Wolkenhauer, 2003). Toxicity associated with amylin in pancreatic β-cells correlates with increased oxidative stress responses, as well as LDL uptake. This suggests that the underlying mechanisms of amylin toxicity involves changes in pathways associated with oxidative stress as well as lipid homeostasis (Janciauskiene and Ahrén, 2000). Oxidative stress plays a significant role in the development of several pathological diseases including T2D (Pham-Huy et al., 2008). The apo-lipoprotein component of LDL forms insoluble aggregates through oxidation, due to hydroxyl radical-induced cross-linkage between the apo-B monomers that are responsible for oxidative damage in diabetic complications (Pham-Huy et al., 2008). Free radical formation in T2D by non-enzymatic glycation of proteins, glucose oxidation, and increased lipid peroxidation damages enzymes, cellular machinery, and also leads to IR (Maritim et al., 2003). Insulin signalling is modulated by reactive species in two ways; firstly, in response to insulin secretion, the reactive species are produced to exert its full physiological function, while in contrast, excess levels of reactive species have a negative regulation on insulin signalling, leading to the development of IR, glucotoxicity, β-cell dysfunction and ultimately β-cell death (Evans et al., 2003). Inflammatory responses are associated with ROS production via several pathways. Evidence has shown that hyperglycemia triggers the excessive production of free radicals and causes oxidative stress. Excessive ROS are seen to damage the tertiary structure of antioxidant enzymes (Ku et al., 2015; März et al., 1996) and are considered to be mediators of various biological responses, such as cell proliferation and extracellular matrix deposition if not in excess (Ku et al., 2015). Reactive oxygen species also promote the activation of the nucleotide-binding oligomerization domain (NBD), leucine-rich repeat-containing receptors (LRR), and pyrin domain (PYD)-protein 3 inflammasome (NLRP3) and caspase 1, leading to the generation of mature IL-1β (Maedler et al., 2002; Zhou et al., 2010). Inflammasomes are also activated by elevated insulin demand and ER stress (Oslowski et al., 2012). Therefore, it can be suggested that oxidative stress leads to increased inflammation and vice versa.

In order to counteract the deleterious effects of these free radical species, the body has an endogenous antioxidant system and can also obtain exogenous antioxidants through diet.

These antioxidants neutralize the reactive species in order to maintain homeostasis to protect the cell from free radical-induced toxicity (Pham-Huy et al., 2008). However, an imbalance between the reactive species and the intrinsic antioxidant defence system leads to the phenomenon known as oxidative stress (Sies, 1997). When antioxidant levels are limited free radical-induced damage can become debilitating and cumulative. The elevation in the levels of ROS seen in T2D may be due to the decrease in destruction or increase in the production by catalase (CAT), superoxide dismutase (SOD), and glutathione peroxide (GSH-Px) antioxidants (Lipinski, 2001). The mitochondrion is a major source of oxidative stress, as remaining oxygen molecules are transformed to oxygen free radicals during oxidative metabolism (Mousa, 2008).

1.2. Inflammation in Type 2 Diabetes

Protective mechanisms induced by inflammation are vital for the health of an organism and dysregulation of the inflammatory responses can damage tissue, which leads to the onset of chronic diseases such as T2D. Initially, inflammation promotes β-cell proliferation and insulin production in order to compensate for IR, thus exerting a beneficial role (Maedler et al., 2002). However, chronic inflammation is detrimental to pancreatic β-cell function. As indicated earlier, inflammation in pancreatic β-cells arises because of several mechanisms, including over stimulation of pro-inflammatory pathways; of particular interest to this study is the association with ageing and amyloid deposition (Figure 1.5). Inflammatory markers such as TNF-α, C-reactive protein (CRP), IL-1β, and IL-6, positively correlate with characteristics of IR and the development of T2D (Ford, 2003; Pradhan et al., 2001; Vozarova et al., 2002; Yudkin et al., 1999). These markers and the main contributors to inflammation in T2D will be discussed in this section.

1.2.1. Adipose-derived Inflammation

Type 2 diabetes is associated with an increase in body mass, particularly WAT, and is important in lipid and glucose metabolism (Saltiel, 2000). White adipose tissue secretes factors with paracrine, endocrine, as well as autocrine effects. Moreover, WAT stores triacylglycerol (TAG), to regulate energy levels, protects other organs from ectopic fat and thus, from lipotoxicity (Torres-Leal et al., 2012). In addition to adipocytes, WAT comprises of pre-adipocytes, fibroblasts, connective tissue matrix, stromovascular cells, nerve fibers, lymph nodes, and immune cells (e.g., macrophages) which secrete bio-active substrates (Fain et al., 2004; Kershaw and Flier, 2004). Proteins known as adipokines are also produced by adipocytes which allow interaction between adipocytes and other tissues (section 1.2.1.4) and

affect physiological processes (Torres-Leal et al., 2012). In addition to adipokines, pro- and anti-inflammatory factors, such as chemokines, cytokines and acute-phase proteins are secreted (section 1.2.1.3). Pro- (e.g. TNF-α, IL-6, and monocyte chemoattractant protein-1(MCP-1)) and anti-inflammatory (e.g. IL-10) proteins secreted by adipocytes are proposed to promote T2D progression by chronic, low-grade systemic inflammation, leading to IR in obese subjects (Kang et al., 2016; Weisberg et al., 2003; Xu et al., 2004).

1.2.1.1.   Proposed Mechanisms of Adipose-derived Inflammation

Hyperplasia, increasing the number of cells, and/or hypertrophy, increasing the size of adipocytes are features associated with obesity and are associated with the production of increased extracellular matrix, increased angiogenesis, endothelial cell activation, macrophage infiltration, and secretion of inflammatory cytokines (Bourlier et al., 2008; Henegar et al., 2008). Hypertrophic adipocytes cause an imbalance between increased tissue mass and blood flow, causing hypoxia, macrophage infiltration, and inflammation (Goossens, 2008). Hypertrophic adipocytes are also seen to increase the expression and release of pro-inflammatory adipokines in humans (Skurk et al., 2007). Very large adipocytes can become lipolytic, resulting in elevated levels of FFA in plasma leading to lipotoxicity through impairment of non-adipose organs function (DeFronzo, 2004). It has been observed that TNF-α and IL-6 have stimulatory effects on lipolysis (Petersen et al., 2005; Trujillo et al., 2004; van Hall et al., 2003). The former increases the levels of cyclic adenosine monophosphate (cAMP) and increases the function of lipase, along with downregulation of perilipin by activating MAPK (Souza et al., 2003). In the liver, TNF-α downregulates expression of genes involved in FA oxidation as well as glucose uptake and metabolism (Guilherme et al., 2008). Therefore, TNF-α impairs lipid metabolism, resulting in excess FFA in plasma that promote the development of IR. It is also seen that increased levels of IL-6 promotes FFA elevation in circulation and increases oxidation of body fat in humans (Lyngsø et al., 2002; van Hall et al., 2003). Apart from ATP synthesis, the mitochondria remove circulating FFA via β-oxidation. The latter occurs in tissues where glucose homeostasis is relevant, such as the liver, muscle and adipose tissue (Maassen et al., 2007). Impaired mitochondrial β-oxidation of FA, in addition to increased glucose uptake, results in the accumulation of TAG, (Vankoningsloo et al., 2005), lipotoxicity in β-cells (Maassen et al., 2007), and hepatic IR (Zhang et al., 2007). Free fatty acids available are associated with lipotoxicity that leads to β-cell death. Prolonged exposure of β-cells to FFAs has cytostatic and pro-apoptotic effects. The cytostatic action is likely as a result of the FFA-induced reduction of intra islet glucose metabolism, while the pro-apoptotic effects are mostly caspase mediated, partially dependent on the ceramide pathway, and is possibly B-cell lymphoma 2 (Bcl-2) regulated (Briaud et al., 2001; Lupi et al., 2002). Interaction

between lipotoxicity and glucotoxicity is seen to be deleterious on β-cell function as it alters glucose homeostasis (Poitout and Robertson, 2002).

1.2.1.2. Macrophage Infiltration and Inflammation

It can be said that obesity co-exists with inflammation in adipocytes. Some pro-inflammatory cytokines are secreted by adipocytes, while the majority are primarily generated from infiltrated macrophages in the adipocytes (Maury et al., 2009). The imbalance between anti-inflammatory and pro-inflammatory cytokines leads to chronic, low-grade inflammation promoting metabolic diseases linked to obesity (Dandona et al., 2004; Ghanim et al., 2004; Johnson et al., 2012; Lumeng and Saltiel, 2011; Roche, 2004). Pro-inflammatory cytokines produced in adipose tissue, as a result of macrophage infiltration, cause IR in tissues and impair multiple tissue functions (Weisberg et al., 2006). It is been seen that both diet-induced obese mice as well as genetically modified obese mice have a significant increase in infiltrated macrophages (Davis et al., 2008; Lumeng et al., 2008; Murano et al., 2008).

Increased expression of macrophage-specific inflammatory-genes in the WAT of obese mice, such as macrophage inflammatory protein-1α (MIP-1α) and MCP-1 correlate positively with the production of insulin (Xu et al., 2003). Although, several obesity models have shown that adipocytes and macrophages localized in adipose tissue produce pro-inflammatory mediators, mechanisms on adipocyte hypertrophy, inflammation, and macrophage recruitment and activation are not fully elucidated. Direct regulation of toll-like-receptor (Tlr)-4 by certain saturated fatty acids (SFAs) is proposed to play a role in the process, because palmitate and other SFAs directly stimulate pro-inflammatory cytokine expression and NF-κB activation in adipocytes and macrophages (Song et al., 2006; Suganami et al., 2007). Suganami *et al.* indicated that FFA released from hypertrophic adipocytes signal macrophages through Tlr-4 and stimulate release of TNF-α. It is also seen that C3H / HeJ mice, which are Tlr-4 deficient mice, are less susceptible to fat-induced inflammation and IR, and are protected against hyperglycemia and inflammation in adipose tissue (Poggi et al., 2007; Suganami et al., 2007). Proteins associated with macrophages positively correlate with increased body mass. Furthermore, immunohistochemical analysis revealed that adipocytes expressing F4/80 (F4/80+), a macrophage marker, positively correlates with increased adipocyte size and body mass. Human adipose tissue stained for cluster of differentiation 68 (CD68), a macrophage antigen, showed similar correlations (Weisberg et al., 2003).

The link between obesity, impaired insulin activity, and inflammation involving pro-inflammatory cytokines was first demonstrated by Hotamisligil and co-workers (1993), with increased expression of TNF-α messenger ribonucleic acid (mRNA) in adipose tissue of obese

mice (fa/fa rat and ob/ob mouse). The study also indicated improved insulin action on glucose uptake when TNF-α was neutralized in these obese fa/fa mice (Hotamisligil et al., 1993).

1.2.1.3. Cytokines, Chemokines, and Acute-phase Proteins Associated with Adipose-derived Inflammation

Interleukin-6 can be categorized as both anti- and pro-inflammatory; acting as a defence mechanism in an early state of inflammation, while during chronic inflammation is damaging (Kamimura et al., 2003). Interleukin-6 decreases inflammatory responses by stimulating the synthesis of anti-inflammatory cytokines (Starkie et al., 2003; Steensberg et al., 2003; Z Xing et al., 1998). Visceral adipocytes, contribute to approximately 10-35% of IL-6 in circulation at basal levels (Mohamed-Ali et al., 1997).   Furthermore, the expression of IL-6 mRNA is elevated in adipose tissue and hypertrophy of adipocytes increases the secretion of IL-6 (Bastard et al., 2000; Fried et al., 1998; Kern et al., 2001; Sopasakis et al., 2004). It has been demonstrated that IL-6 mRNA increases in IR obese individuals (Bastard et al., 2000; Fried et al., 1998; Kern et al., 2001; Rotter et al., 2003), correlating with decreased rates of glucose stimulated insulin secretion (GSIS) (Bastard et al., 2002). Hepatic insulin dependent glycogen synthesis (Klover et al., 2003; Senn et al., 2002) and glucose uptake are also downregulated by IL-6 in adipocytes (Rotter et al., 2003), mediated by increased expression of suppressor of cytokine signalling (SOCS)-3. The latter inhibits the insulin receptor and targets IRS for proteosomal degradation and downregulate transcription of IRS-1 (Rotter et al., 2003; Sabio et al., 2008).

Monocyte chemoattractant protein-1 is also secreted by adipocytes (Christiansen et al., 2005; Skurk et al., 2007), and correlates positively with adipocyte size (Skurk et al., 2007). Animal models of obesity (Sartipy and Loskutoff, 2003; Takahashi et al., 2012) as well as obese individuals (Bruun et al., 2005; Christiansen et al., 2005; Kim et al., 2006) show increased levels of circulating MCP-1. Furthermore, it has been observed that MCP-1 levels are elevated in T2D individuals compared to non-diabetic individuals (Ezenwaka et al., 2009; Herder et al., 2006; Nomura et al., 2000).   Expression of MCP-1 mRNA increases in adipocytes (Christiansen et al., 2005; Dahlman et al., 2005). Studies have shown the IR-inducing effects of MCP-1 and attempted to elucidate the underlying mechanisms by which MCP-1 impairs insulin action. Adipocytes treated with exogenous MCP-1 showed a decrease in insulin-stimulated glucose uptake as well as decreased expression of genes such as PPAR-γ, GLUT-4, and lipoprotein lipase (Sartipy and Loskutoff, 2003). In cultured skeletal muscle cells from humans, increased MCP-1 levels reduced insulin-stimulated phosphorylation of AKT, glycogen synthase kinase-3α (GSK3α) and GSK3β proteins. Altered GSK3 leads to impaired

insulin signalling and reduced glucose uptake (Sell et al., 2006). Mice overexpressing MCP-1 have normal adiposity, impaired insulin sensitivity and increased adipose macrophage infiltration (Kamei et al., 2006).   Furthermore, it is seen that MCP-1 overexpression downregulates insulin-stimulated tyrosine phosphorylation of the insulin receptors and IRS proteins, and decreases AKT phosphorylation leading to IR in the liver and muscle of mice (Kamei et al., 2006). The above-mentioned studies suggest MCP-1 as an inflammatory link between IR and obesity.

Cytokines released from adipocytes (Wieser et al., 2013) also alter the pituitary-adrenal axis (Jones and Kennedy, 1993) accelerating pancreatic β-cell impairment (Oh et al., 2011). Cytokines have the ability affect the secretion of hormones from the anterior pituitary by acting on the hypothalamus, the pituitary gland or both. Cytokines involved include TNF-α, IL-1, IL-2, IL-6, and interferon-tau (IFN-т). Cytokines stimulate the hypothalamic-pituitary-adrenal (HPA) axis, suppressing the hypothalamic-pituitary-thyroid and gonadal (HPG) axis, as well as GH secretion (Jones and Kennedy, 1993). Cytokines stimulate the HPA axis to secrete glucocorticoids and catecholamines.   Catecholamines in turn increase IL-6 production (Papanicolaou et al., 1998). Interleukin-6 stimulates β-cell death, via signal transducers and activators of transcription-3-mediated production of NO (Oh et al., 2011). Glucocorticoids result in hepatic Zn^{2+} accumulation, gluconeogenesis, inhibit insulin secretion and decrease 5' AMP-activated protein kinase (AMPK) activity (Delaunay et al., 1997; Tsigos et al., 1997).

1.2.1.4. Adipokines

Adipokines secreted by adipocytes include the following; (1) adiponectin, an adipocyte-secretory protein, which is decreased in obese and diabetic states, negatively correlated with IR, and have a beneficial effect on postprandial glucose and lipid metabolism, increasing insulin sensitivity (Arita et al., 1999; Berg and Scherer, 2005; Weyer et al., 2001). Adiponectin exerts its protective effect via the AMPK pathway, against glucose metabolism impairment, reducing the risk for T2D (Hug et al., 2004). (2) Resistin, an inflammatory bio-marker and potential mediator of metabolic diseases associated with obesity, competes with lipopolysaccharides for Tlr-4 binding and leads to altered signalling mechanisms, including NF-κB and MAPK signalling pathways (Bokarewa et al., 2005; Tarkowski et al., 2010). The NF-κB pathway may be activated upon activation of the Akt/PI3K pathway via resistin binding to Tlr-4 (Sánchez-Solana et al., 2012). Resistin increases the secretion of pro-inflammatory cytokines via MAPK and increases ROS, thereby inhibiting endothelial nitric oxide synthase (eNOS) (Nagaev et al., 2006; Sánchez-Solana et al., 2012). Resistin downregulates various steps involved in insulin signalling in adipocytes and stimulate the expression of SOCS-3

(Steppan et al., 2005). Downstream, resistin inhibits the AMPK pathway and hepatic gluconeogenesis, and stimulates skeletal muscle uptake of glucose (Barnes and Miner, 2009). (3) Leptin, an appetite-supressing hormone, has systemic metabolic actions, indicating energy reserves to the central nervous system (CNS) (Bates and Myers, 2003). Leptin also reduces triglyceride accumulation in liver and skeletal muscle through the direct activation of AMPK and indirect actions mediated through the CNS, thereby improving insulin sensitivity (Minokoshi et al., 2002). Furthermore, leptin regulates pancreatic β-cell function through direct actions such as; leptin resistance in pancreatic β-cells which is one factor that contributes to the hyperinsulinemia, β-cell failure, and consequent glucose intolerance in the obese state (Morioka et al., 2007), and indirectly through the CNS as sustained hypothalamic leptin signalling in the hypothalamus restrain pancreatic insulin release and IR (Boghossian et al., 2006). (4) Adipocytes produce angiotensinogen, renin, ACE, and cathepsin D & G (non-RAAS) (Cassis, 2000). Angiotensin is involved in the regulation of blood pressure (Bestermann et al., 2005). Locally angiotensin plays a role in growth and development by stimulating prostacyclin (conversion of pre-adipocytes to adipocytes) and increasing the synthesis and storage of lipids in adipocytes (Ailhaud et al., 2000). (5) Plasminogen activator inhibitor-1 (PAI-1) promotes a pro-thrombotic state. Activation of coagulation induces PAI-1 expression by adipocytes and indirectly increases macrophage infiltration, IL-6, and TNF-α secretion with FFA and triglycerides exacerbate the process (Berg and Scherer, 2005).

1.2.2.   Amyloid-derived Inflammation

The deposition of amyloid fibrils in tissue is known as amyloidosis. Systemic amyloidosis occurs when a circulating amyloidogenic precursor protein deposits in various organs. Primary systemic amyloidosis occurs when there is deposition of a monoclonal immunoglobulin (Ig) light chain and may take place in almost all disorders of B lymphocyte lineage, while secondary amyloidosis is associated with chronic low grade inflammation which occurs by the accumulation of a N-terminal fragment of acute phase protein serum amyloid A (Benditt et al., 1971; Hull et al., 2004). Localized amyloidosis includes diseases characterized by the deposition of amyloid in one specific target organ (Hull et al., 2004). Senile amyloidosis, familial, and transthyretin-associated amyloidosis (ATTR), arise from deposition, in the target tissue (e.g. nerve or pancreatic tissue), of wild-type or one or more than 50 mutated forms of transthyretin, the most common being the point mutation Val30Met (Saraiva et al., 1984; P Westermark et al., 1990).

Islet inflammation, induced by amyloid toxicity as previously described (section 1.1.2.3), is involved in pancreatic β-cell dysfunction and apoptosis by activating pro-inflammatory responses (Figure 1.5). Evidence has shown that amylin interacts with immune cells, resulting

in the activation of inflammasomes, which trigger signalling cascades, producing pro-inflammatory cytokines, such as IL-1β, and by activating the NF-κB pathway as seen in Figure 1.6 (Abedini and Schmidt, 2013; Masters et al., 2010; Tak and Firestein, 2001; Westwell-Roper et al., 2014). At cellular and molecular levels, NF-κB is the inflammation master switch that regulates protein synthesis, which is vital for the activation and maintenance of inflammation. At tissue level, cellular stresses can modulate phosphorylation as well as transcriptional events by activating JNK and NF-κB, respectively, to control enzymatic functions and concentrations of receptors, chemokines, and cytokines (Figure 1.6) (Shoelson et al., 2006). Pro-inflammatory cytokines, IL-1β and IFN-γ, promote iNOS expression, thus increasing the production of NO locally (Arnush et al., 1998; Corbett et al., 1993, 1992; Russell et al., 2013). Evidence has indicated that pro-inflammatory cytokines can promote β-cell apoptosis, providing one mechanism of β-cell death (Eizirik and Mandrup-Poulsen, 2001; Marselli et al., 2001).

Aging of islet cells is associated with inflammation, with macrophage infiltration seen in old islet cells as seen in Figure 1.6 (Sandovici et al., 2016). It has also been shown that pancreatic islet macrophage infiltration increased in patients with T2D (Ehses et al., 2007). However, it is possible that early macrophage infiltration may be beneficial to islet functionality as well as its plasticity through cellular fusion (Ehses et al., 2007; Hess et al., 2003), while during disease progression, activated macrophages accelerate the dysfunction and death of pancreatic islet cells. Death occurs either through apoptosis or necrosis, as a result of increased levels of IL-1β and IFN-γ (Figure 1.6) (Collier et al., 2006; Grunnet et al., 2009; Gurzov et al., 2010; Steer et al., 2005; Weksler-Zangen et al., 2008).

As indicated in Figure 1.6, metabolic stressors, such as hyperglycemia, induces production of IL-1β by pancreatic β-cells. Interleukin-1β then perpetuates its own production and induces the production of several inflammatory factors, including TNF-α, IL-6, IL-8, and MCP-1, which attract macrophages as well as other immune cells; this is dependent on the levels of stress and the duration of IL-1β exposure (Butcher et al., 2014; Ehses et al., 2007; Richardson et al., 2009). Interleukin-8 attracts macrophages which in turn, exacerbates production of IL-1β (Ehses et al., 2008). Interleukin-1β activates the interleukin receptor type I, inducing recruitment of receptor adaptor proteins and signalling by several kinases, such as IκB kinases (IKKs). The IKKs phosphorylate IκB proteins promoting their degradation and stimulate NF-κB proteins, which translocate to the nucleus from the cytoplasm. Once in the nucleus, the different NF-κB subunits transactivate various genes (eg. iNOS) involved in inflammation (Baldwin, 1996; Corbett et al., 1992). Research proposes that the IKK/NF-κB axis serves as the link between inflammation and IR (de Luca and Olefsky, 2008; Shoelson et al., 2006).

Tumour necrosis factor-α is seen to influence glucose metabolism, inhibit insulin action and blunt pancreatic β-cell function via inflammatory processes (Pickup, 2004). As mentioned in adipose inflammation earlier (section 1.2.1), it can be suggested that TNF-α has an important function in the insulin signalling pathway by inhibiting tyrosine kinase activity of the insulin receptor, thus reducing the phosphorylation and activation of IRS-1, which in turn reduces the cells response to insulin (Figure 1.6). Reduction of gene expression, which encodes for proteins that form the insulin receptor substrates, has also been attributed to TNF-α (Stephens and Pekala, 1991). Tumour necrosis factor-α stimulates the transcription of the IL-6 gene (Vanden Berghe et al., 2000; Z Xing et al., 1998) and induces the generation of its receptor (März et al., 1996).

Pro-inflammatory cytokines have been linked with β-cell dysfunction and might lead to increased sensitivity to β-cell toxicity, through increased production of the free radical NO, which down-regulates cellular metabolism by mitochondrial function inhibition (Figure 1.6) (Greenberg and McDaniel, 2002). Maedler et al. (2002) proposed that that intra-islet expression of pro-inflammatory cytokines, particularly IL-1β, contributes to β-cell glucotoxicity in the pathogenesis of T2D (Maedler et al., 2002). Thus, it appears that IL-1β might be a master regulator of inflammation in the pancreatic islets in T2D. Although it has been shown that IL-1β can inhibit GSIS in β-cells, the impact of anti-inflammatory cytokines on β-cell function is not fully understood (Russell and Morgan, 2014). A few studies have indicated that anti-inflammatory cytokines reverse the inhibitory effects of pro-inflammatory cytokines on insulin secretion from β-cells (Marselli et al., 2001). It can be argued that anti-inflammatory cytokines are likely to inhibit IL-1β induced NO production in β-cells; by modulating NF-kB activation (Russell and Morgan, 2014).
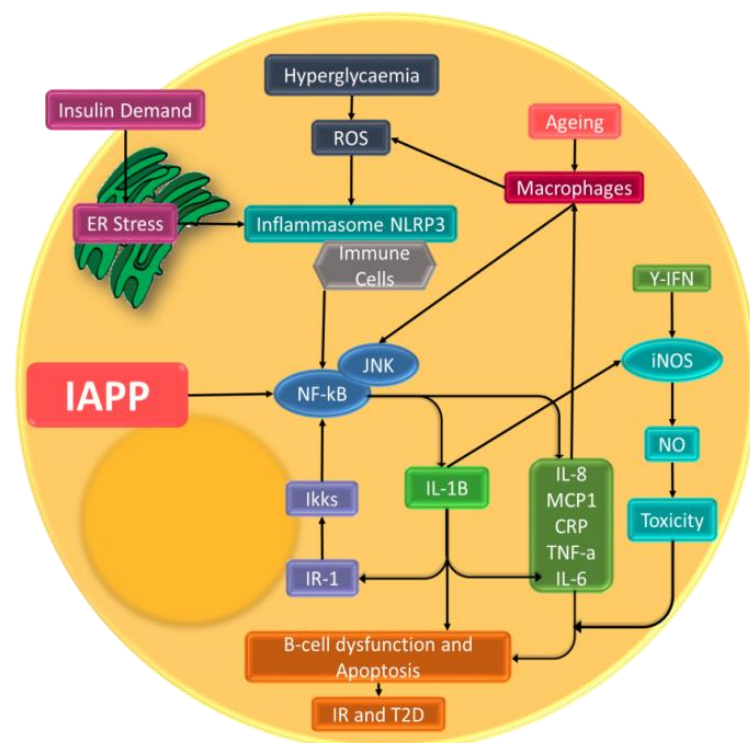
Figure 1.6: Pancreatic beta-cell inflammation. Diagrammatic presentation of the underlying mechanisms involved in pancreatic β-cell inflammation involved in β-cell dysfunction, IR, and subsequently T2D (Adapted from Donath et. al. 2014).

1.3.   Beta Secretase Regulation on Beta-cell Inflammation

The role of BACE in disease progression is controversial and has led to many conjectures of whether BACE has a beneficial or detrimental effect in the development of T2D. Two analogues exist, namely BACE1 and BACE2, and while both are type I aspartyl transmembrane proteins and 50-68% similar in homology, these proteases target different protein substrates (Alcarraz-Vizán et al., 2015; Mirsafian et al., 2014; Southan and Hancock, 2013; Vassar, 2014; Venugopal et al., 2008). The latter can be attributed to the fact that BACE1 and BACE2 share no similarity in their promotor regions, suggesting that these proteases are distinct in their regulation of gene transcription and thus function (Alcarraz-Vizán et al., 2015; Casas et al., 2010). The overall structure of BACEs follow the general structure of the aspartyl protease family; comprising a C-terminal domain, a N-terminal domain, and a connecting inter-domain (Mirsafian et al., 2014). The polypeptide, BACE1, consists of 501 aa (Lajtha et al., 2008), while BACE2 consists of 518 aa (Bennett et al., 2000). Polygenetic

analysis has shown that BACE1 and BACE2 are similar to cathepsins and pepsins, both these proteases are involved in protein cleavage (Southan and Hancock, 2013; Turk et al., 2012), suggesting a role for BACE in protein cleavage. Beta secretase proteases are synthesised in the ER as pro-BACE proteins, followed by maturation in the Golgi apparatus. Beta secretase proteins were previously described to cycle between different compartments of the secretory pathway in varying proportions in the trans-Golgi, plasma membrane, and endosomes. Beta secretase 1 is mostly found in the secretory pathway of the Golgi apparatus, while BACE2 is found in the endocytic pathway, supporting the hypothesis that these proteases differ in function (Casas et al., 2010). Proteins on the cell surface play a role in cell-to-cell communication and many of these plasma membrane proteins are involved in insulin secretion and pancreatic β-cell mass expansion (Casas et al., 2010; Stützer et al., 2013). These plasma membrane proteins are controlled through cleavage by proteases, including BACE (Stützer et al., 2013). Proteases control the amount, localization, and activities of its substrate targets; and are therefore important in mechanisms involved in pancreatic β-cells, to maintain homeostasis. Interfering with the levels of these proteases will not only alter the abundance of its substrate proteins but may alter the expression and activities of various other downstream proteins indirectly.

Beta secretase 1 is mostly expressed in the brain and, to a lesser extent, in the pancreas and is involved in the cleavage of the amyloid precursor protein (APP), forming amyloid-beta (Aβ), a hallmark of AD (Southan and Hancock, 2013; Vassar, 2014; Venugopal et al., 2008). Beta secretase 1 knock-out mice fail to produce Aβ (Southan and Hancock, 2013a; Venugopal et al., 2008), whereas overexpression of BACE1 led to elevated levels of Aβ formation (Vassar, 2014). Although it is known that BACE1 in the brain plays a significant role in the pathogenesis of AD, the role of BACE1 in pancreatic islet cells remains unclear despite its high abundance (Stützer et al., 2013). The high levels of BACE1 expressed in healthy pancreatic islets, therefore it can be suggested that BACE1 might be involved in the progression of T2D if homeostasis is altered. Similarly, high levels of BACE2 are expressed in the pancreas, more specifically pancreatic β-cells, suggesting that BACE2 might also be involved in the progression of T2D (Vassar, 2014). This suggestion is supported by data that has shown that BACE2 is one of only a few proteases reported to play a role in the regulation of pancreatic β-cell mass and function (Esterházy et al., 2011).

Aggregation of IAPP directly contributes to β-cell dysfunction, therefore exacerbating deleterious effect of T2D (Abedini and Schmidt, 2013; Alcarraz-Vizán et al., 2015a; Jeong and An, 2015). Overexpression of IAPP has been shown to block autophagy in β-cells, interfering with the degradation of BACE2 and resulting in increased cleavage of TMEM27. A positive correlation is seen between BACE2 and IAPP. The latter can be explained by the strong

correlation seen between the process of amyloidogenesis and the loss of pancreatic β-cell mass and insulin secretion deficiency. It can further be explained by BACE2 inhibition counteracting hIAPP-induced insulin secretory defects by increasing insulin secretion (Alcarraz-Vizán et al., 2017, 2015). Understanding how β-cells respond to amyloidosis is thus essential for novel therapeutic approaches.

Transmembrane protein 27 is expressed in pancreatic β-cells where it plays a functional role in β-cell proliferation, β-cell mass, as well as GSIS (Esterházy et al., 2011; Southan and Hancock, 2013). Transmembrane protein 27 is regulated by ectodomain shedding, resulting in a N-terminal fragment released into the extracellular space and a C-terminal fragment which remains in the membrane and is further processed through regulated intermembrane proteolysis (RIP). The shedding process is known to inactivate TMEM27 (Esterházy et al., 2011; Stützer et al., 2013). Transmembrane protein 27 levels are reduced in diabetic animals, with associated decreased islet mass, whereas increased expression of TMEM27 increases islet mass as well as cellular insulin content (Akpinar et al., 2005; Altirriba et al., 2010). Reduced levels of TMEM27 correlate negatively with BACE2 expression (Alcarraz-Vizán et al., 2015). The expression of TMEM27 and its role in β-cell mass, as well as insulin-stimulatory activity led to the hypothesis that β-cell growth and function can be improved by targeting the proteases involved in TMEM27 cleavage, in particular BACE2 (Esterházy et al., 2011; Stützer et al., 2013). Beta secretase 2 knockout in mice resulted in higher β-cell mass, proliferation, and glucose homeostasis supporting the above mentioned hypothesis (Alcarraz-Vizán et al., 2015; Vassar, 2014). The provided evidence thus suggests contradicting roles of BACE2 in the progression T2D, suggesting BACE2 may have both beneficial and detrimental effects on pancreatic β-cells. Inhibition of the enzymatic activity of proteases of pancreatic β-cells affects intracellular trafficking of the insulin receptor, the expression of the insulin gene, and insulin content proposing that BACE is involved in maintaining β-cell function. Moreover, BACE2 inhibition has shown to reduce toxic amyloid depositions in pancreatic islets (Alcarraz-Vizán et al., 2015; Casas et al., 2010), therefore BACE2 can be suggested as a therapeutic target. It has been proposed that BACE2 operates exclusively at intracellular sites, therefore its expression could be readily restricted to the site of administration (Abdul-Hay et al., 2012). The double drug target status of BACE's, with the incomplete functional picture of both BACE1 and BACE2, thus needs further investigation into the effect of its inhibition (Southan and Hancock, 2013).

1.4. Current Anti-diabetic Therapies: Implications for Beta-cells

It is important to elucidate the underlying mechanisms of β-cell dysfunction to prevent or delay the onset and progression of T2D in individuals at risk. To date, treatments attempting to protect β-cells focus mainly on pathogenic targets of T2D, such as IR and β-cell dysfunction. Theoretically, β-cell protection can be accomplished through mechanisms preventing β-cell dysfunction induced by stressors such as glucotoxicity, lipotoxicity, IR, oxidative stress, and inflammation.

Lifestyle changes, such as regular exercise and a healthy diet, are shown to improve insulin sensitivity and reduce β-cell insulin demand, as well as improve the immediate environment of islets through improved blood flow and a reduction in stressors. Lifestyle changes also decrease FFA and thus lipotoxicity (Eriksson and Lindgärde, 1991; Laaksonen et al., 2005; Pan et al., 1997; Tuomilehto et al., 2001).

1.4.1. Pharmaceutical Therapies

1.4.1.1. Glucotoxicity

Conventional T2D drugs including biguanides (i.e.Metformin), sulphonylureas (i.e. Glyburide, Glipizide, and Glimepiride), alpha-glucosidase inhibitors (i.e. Acarbose and Miglitol), and thiazolidinediones, PPAR-γ agonists (i.e. Rosiglitazone and Pioglitazone) are seen to protect β-cells by decreasing glucose levels and consequently glucotoxicity (Figure 1.7), as seen in clinical trials attempting to prevent or delay the onset of T2D. It seems that thiazolidinediones are more effective due to its agonists' antioxidant, anti-inflammatory, and anti-apoptotic properties (Parulkar et al., 2001). Rossetti and co-workers showed that stabilization of glucose levels with phlorizin, a glycosuric agent, restores insulin secretion, and subsequently reduces the risk of glucotoxicity (Rossetti et al., 1990).

1.4.1.2. Insulin Resistance

Impaired insulin secretion can also be targeted via mechanisms involved in IR. Islets that have the IRS-1 polymorphism show a reduction in mature insulin granules and impaired glucose responses (Marchetti et al., 2002). It's seen that thiazolidinediones stimulate insulin signalling pathways (Marchetti et al., 2002). It can be postulated that amendment of insulin sensitivity of islets should lead to (1) improved insulin secretion, as an elevation in insulin response to oral glucose tolerance test (OGTT) is seen by using PPAR-γ agonists, and (2) improved survival of β-cells as using Rosiglitazone (a thiazolidinedione part of PPAR-γ

agonists) is seen to maintain islets in a better condition than treatment with Metformin (a biguanide) or Glibenclamide (a sulphonylurea) (Miyazaki et al., 2002). The deficiency of protection by Metformin is surprising as it has both anti-apoptotic (Marchetti et al., 2004) and anti-inflammatory (Hattori et al., 2006) properties; whereas the deficiency of protection by Glibenclamide is coherent with the finding that Glibenclamide has a pro-apoptotic effect on β-cells (Maedler et al., 2005). These findings indicate that IR plays a crucial role in β-cell impairment and that insulin sensitizing agents may improve insulin secretion by reducing hyperglycemia and consequently β-cell stress.

1.4.1.3. Lipotoxicity

Beneficial effects of decreased body mass on β-cells can be improved further by anti-obesity drugs such as lipase inhibitors (i.e. Orlistat) (Torgerson et al., 2004) which reduce the accumulation of excessive adipose. The deleterious effects of FFA are seen to be prevented by pre-incubation with Rosiglitazone (Lupi et al., 2004), acting via its anti-inflammatory properties, as elevated FFA levels is seen to stimulate the NF-κB pathway. Thus, β-cell protection against lipotoxicity may be utilised through this mechanism. It has been observed that thiazolidinediones are able to decrease circulating FFA (Balfour and Plosker, 1999). As mentioned before (section 1.2.1.3; 1.2.1.4), adipose tissue secretes damaging molecules (Unger and Zhou, 2001), and therefore damaging effects may not only be as a result of FFA but also cytokines. Furthermore, statins (i.e. Pravastatin), are seen to reduce lipotoxicity, especially a reduction in triglycerides (Freeman et al., 2001), mediated by its antioxidant and anti-inflammatory properties (Liao and Laufs, 2005), reducing oxidative stress and inflammation. However, statins are also implicated in perpetuating T2D by perpetuating IR as reviewed by (Cybulska and Kłosiewicz-Latoszek, 2018).

1.4.1.4. Oxidative Stress and Inflammation

Treatment with antioxidant agents, such as aminoguanidine and *N*-acetylcysteine, decreases abnormalities in insulin gene expression and the deficit of transcription factors (e.g. PDX-1) due to hyperglycemia (Tanaka et al., 1999). Protection of β-cells from oxidation might be due to Gliclazide, a sulphonylurea which has the ability to scavenge free radicals (Kimoto et al., 2003). Protection of β-cells might also be accomplished by RAS inhibitors and statins, both seen to have pleiotropic effects, decreasing endothelial dysfunction, oxidative stress, and inflammation. Proposed mechanisms of RAS inhibitors on β-cell function include increased levels of K^+, improved insulin secretion, increased blood flow and β-cell perfusion (Carlsson et al., 1998) as well as anti-apoptotic properties (Tikellis et al., 2004). Additionally, RAS

inhibitors prevent glucotoxicity in β-cells (Lupi et al., 2006), by decreasing oxidative stress (Nakayama et al., 2005). Angiotensin II impairs insulin signalling pathways, while RAS inhibitors are seen to improve these pathways (Andreozzi et al., 2004; Shiuchi et al., 2004). Protection by RAS inhibitors, seen with improved glucose metabolism can be explained by the additional use of ACE inhibitors, which increase bradykinin, exerting its function on signalling and glucose transport (Henriksen et al., 1999). Moreover, a reduction in angiotensin II promotes proliferation of pre-adipocytes into mature adipocytes (Sharma et al., 2002), reducing FFA and increasing adiponectin, consequently improving glucose consumption in skeletal muscles, glucose production in the liver and β-cell insulin secretion. Furthermore, some angiotensin II receptor blockers (ARBs), such as Telmisartan, bind to PPAR-γ amplifying its effect on glucose metabolism (Benson et al., 2004).

Taken together, protection of pancreatic β-cells by an insulin sensitizing effect, in addition to reduced glucotoxicity, lipotoxicity, oxidant stress, and inflammation by thiazolidinediones may be used to explain glucose responses exerted by monotherapy with, for example, Rosiglitazone when compared to monotherapy with Glibenclamide (sulphonylurea) or Metformin (biguanide), as seen in the ADOPT Study (Kahn et al., 2006).

It is important to note that these drugs do not just exert its protective effect on one of the stressors directly but might indirectly have an effect on another stressor(s), exerting its functions through several shared mechanisms.
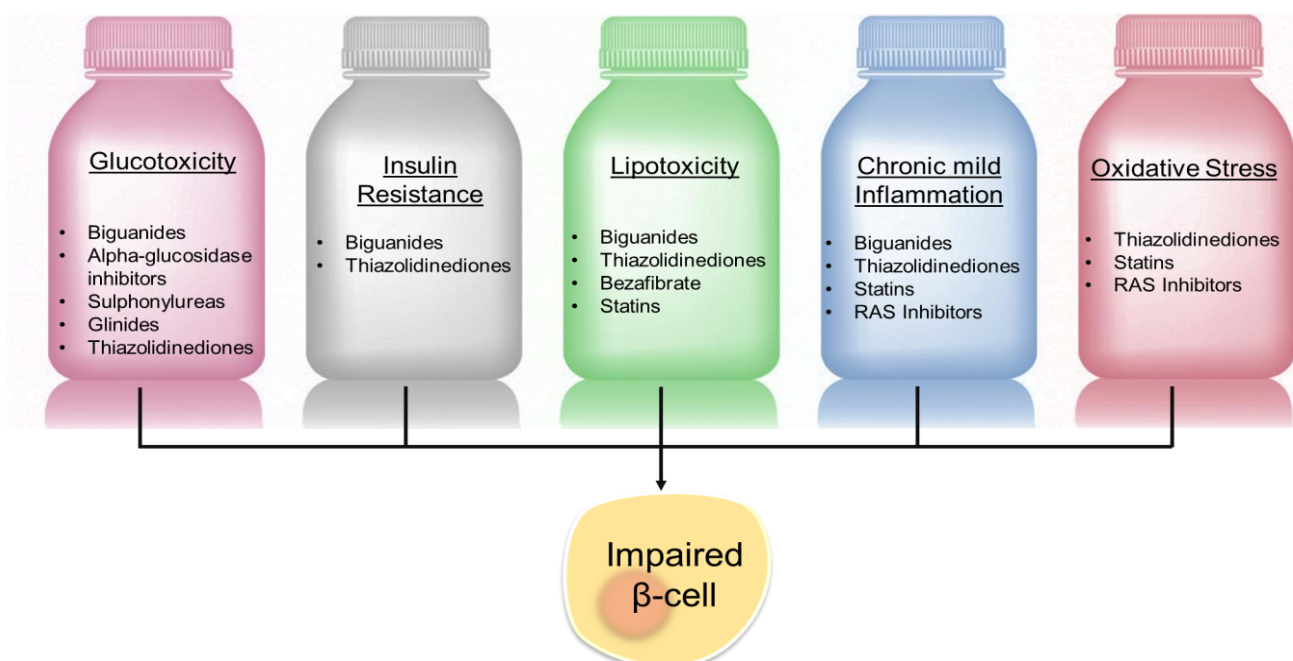
Figure 1.7: Current anti-diabetic therapies. Schematic presentation of therapies used to target pathophysiological factors such as; glucotoxicity, IR, lipotoxicty, chronic low-grade inflammation, and oxidative stress to prevent, delay, or treat T2D (Bonora, 2008).

1.4.2.   Potential Role of Rooibos in Beta-cell Inflammation

Therapeutics available for treatment of T2D are limited in their ability to treat the disease state due to issues with patient compliance, a lack of systemic efficacy, and adverse side effects (Ku et al., 2015). As a result of the latter, traditional medicine, such as plant-derived products, are studied for the beneficial properties they possess (Waisundara and Hoon, 2015). Plant polyphenols have long been of interest due to their strong antioxidant properties and ability to ameliorate diabetic complications (Chen et al., 2013; Kawano et al., 2009; Kumarappan and Mandal, 2008; Zang et al., 2006). Rooibos (*Aspalathus linearis*), an indigenous South-African plant, is well known as a rich source of polyphenols with antioxidant and anti-inflammatory properties (Beltrán-Debón et al., 2011; Joubert et al., 2008; Joubert and de Beer, 2011). It has been shown that plasma antioxidant status improves as a result of polyphenol exposure, also decreasing oxidative stress (Dludla et al., 2014; Villaño et al., 2010). Aspalathin, unique to Rooibos, and PPAG, both phenolic components of Rooibos, have been shown to increase glucose uptake in muscle cells and insulin secretion from β-cells (Bramati et al., 2002; Kawano et al., 2009; Ku et al., 2015; McKay and Blumberg, 2007). Additionally, the improved uptake of glucose as a result of PPAG can be attributed to PPAG's improved FA oxidation in IR rats (Muller et al., 2013). It has been seen that Rooibos exerts hypolipidemic activity in hyperlipidemic mice but the effect was strictly diet dependent (Beltrán-Debón et al., 2011). Cardiomyocytes that were pre-treated with fermented Rooibos extract showed reduced ROS formation as well as apoptosis (Dludla et al., 2014). Possible mechanisms by which Rooibos flavonoids reduce oxidative stress are through direct or indirect scavenging of free radicals, interfering with inducible iNOS, inhibition of xanthine oxidase, immobilization as well as adhesion of leukocytes to the endothelial wall through interaction with several enzyme systems (Ayeleso et al., 2014; Kawano et al., 2009; Nijveldt et al., 2001). The previously reported anti-inflammatory effects of Rooibos might be as a result of a decline in macrophage recruitment observed in studies (Beltrán-Debón et al., 2011). Also, it has been proposed that Asp might exert its effect via an insulin/insulin-like signalling pathway (Chen et al., 2013; Kawano et al., 2009).

1.4.3.   Potential Role of Rooibos on Amyloid Formation

In addition to antioxidant properties, several studies have indicated that polyphenols, including flavonols and flavones, have a protective effect against Aβ formation and aggregation (Shimmyo et al., 2008). Secondary metabolites of plants have a relatively low molecular weight and lipophilicity and are thus good candidates as BACE1 inhibitors (Jeon et al., 2003). A study performed by Jeon et al. (2003) showed that the methanolic extract of commercial

green tea has high inhibitory activity of BACE1. Catechin, a type of polyphenol commonly found in green tea, has also been seen to inhibit BACE1 in a dose dependent and non-competitive manner. Similarly, a study performed by Shimmyo et al. (2008) showed that four flavonols; quercetin, kaempherol, myricetin, and morin, and one flavone, apigenin, directly inhibited BACE1 activity in both a cell-free system and neuronal cells (Shimmyo et al., 2008). However, therapeutic BACE1 inhibition to block Aβ production and associated toxicity needs to be balanced as negative effects might arise from diminishing other physiologic functions of BACE1, in particular processing of substrates involved in neuronal function of the brain and periphery (Koelsch, 2017).

Luteolin and its two derivatives, orientin and isoorientin have been reported to have antioxidant (Ko et al., 1998), anti-inflammatory, and anti-diabetic effects (Alonso-Castro et al., 2012; Fu et al., 2010; López-Lázaro, 2009). In addition, Choi et al. (2014) showed inhibition of acetylcholinesterase (AChE), butyrylcholinesterase (BChE), and BACE1 by luteolin, orientin, and isoorientin, found at 0.007 g, 0.263 g, and 0.450 g per 100 g soluble solids (SS), respectively (Joubert and de Beer, 2011). In the same study by Choi et al (2014), apigenin, and its derivatives vitexin and isovitexin also showed inhibitory activity against AChE and BChE, while only vitexin showed inhibitory activity against BACE1 (Choi et al., 2014). It is proposed that the BACE1 promoter contains NF-κB binding elements (Bourne et al., 2007) and therefore elevated BACE1 expression elevates Aβ levels via NF-κB-dependent pathways (Buggia-Prevot et al., 2008). Moreover, research has suggested that luteolin suppresses signal transducer and activator of transcription-1 (STAT-1), interferon regulatory factor-1 (IRF-1), and NF-κB signalling pathways, thus attenuating inflammatory response of microglial cells (Kao et al., 2011). Chronic treatment with luteolin is seen to inhibit BACE1 activity and reduce Aβ levels in the brain (Zheng et al., 2015). The underlying protective mechanism of luteolin might thus be mediated by the inhibition of NF-κB (Fu et al., 2014).

Quercetin and rutin, both flavonoids found respectively at 0.001 g and 0.245 g per 100 g SS in unfermented Rooibos (Domitrović et al., 2012; Joubert and de Beer, 2011; Kang et al., 2013; Pan et al., 2014; Shi et al., 2013), enhanced the transcription of nuclear factor-like 2 (Nrf2), which upregulates the expression of the proteasome catalytic subunits. It is seen that both quercetin and rutin reduce the activation of caspase-3 in APP695-transfected SH-SY5Y bone marrow derived cells, where the reduction correlates with the reduction of proteasome activity (Martín-Aragón et al., 2016). Interestingly, degradation of BACE proteins is regulated by the ubiquitin-proteasome pathway (UPP) (Qing et al., 2004) as a lowering of BACE and an enhancement of its processing is seen in APP695-transfected SH-SY5Y bone marrow derived cells treated with rutin (Martín-Aragón et al., 2016). In the case of BACE inhibition studies for

flavonoid derivatives, many controversial results have been reported and might be as a result of the difference in concentrations used.

Diabetes is a chronic, systemic, and slow progressing disease. Insights into the mechanisms involved in inflammation, including that of BACE, and resultant dysfunction of pancreatic β-cells in the pathogenesis of T2D, may reveal an opportunity for the development of novel therapeutics that directly protect and preserve β-cells. The protective role of antioxidants, such as plant polyphenols, against inflammation is increasingly under investigation. Taking into consideration all of these aforementioned anti-diabetic properties of Rooibos, as well as the possible BACE inhibitory properties of specific phenolic compounds, we postulate that Rooibos may have acute anti-inflammatory effects in pancreatic β-cells and additionally may have the ability to modulate BACE, thus further enhancing the anti-diabetic effect.

Thus, the question that arises is whether chronic, low-grade inflammation perpetuates the deleterious effects of amyloid and what the implications for BACE regulation are?

1.5. Models to Study Beta-cell Inflammation

1.5.1. Cellular Mechanistic Studies

Living organisms are not the sum of their components, but rather the interaction between cellular components and their environment that determines functionality. Failure of these interactions to maintain homeostasis leads to pathophysiology and thus progression of complex and often chronic diseases. Despite the indication of numerous physiological processes such as insulin secretion, inflammation, and amyloid formation, some of the exact molecular mechanisms underpinning T2D still need to be elucidated. Therefore, it is vital to perform research on these exact mechanisms, integrate the mechanisms by which they are beneficial or deleterious on tissues and organ systems, and find ways to identify signals mediating the processes. Understanding the link between these pathological mechanisms and the consequent health outcomes may lead to potentially novel molecular and cellular therapeutic targets for disease prevention or delay. However, challenges such as knowing exactly what to measure, when to take a measurement, and linking specific measurements to a disease/health outcome remain. Identification of proteins involved in physiological processes of interest and quantifying their content as well as function are pre-requisites to overcome these challenges. The lack of appropriate animal models needs to be considered, since animal models used don't always reveal the full effect of a protein or substance. Animal models could be used to test novel molecules previously identified in cell culture studies, bearing in mind that interspecies translation needs to be negotiated.

1.5.2.   Pancreatic Beta-cell Lines vs. Rodent Models

1.5.2.1.   Pancreatic Beta-cell Lines

Research using β-cells is limited by the availability of pancreatic tissue and cellular and hormonal heterogeneity amongst donors. The isolation, purification of β-cells and the maintenance of their *in situ* properties remain challenging. *In vitro* cell culture studies provide an opportunity to assess physiological and pathophysiological processes before translating the findings to animal models. Additionally, cell lines allow researchers to determine the effects of treatments, under different conditions, subsequently leading to the potential development of therapeutics (MacDonald, 1990; Skelin et al., 2010). Cell structure, behaviour, and functional preservation is vital in ensuring that responses observed represent responses in the human body. Furthermore, it is important that there is consistency amongst experiments, and that the experiments are reproducible. Immortal cell lines are populations of cells that continuously undergo division and are not limited by the "Hayflick" limit proposed by Leonard Hayflick*,* who discovered that cultured human cells have limited capacity to divide, after which the cells become senescent. Therefore, these cells can be grown for continuous periods *in vitro* and are used to determine protein functions and to assess effects of exogenous protein expression on signalling of transcriptional processes (Shay and Wright, 2000). Since the majority of cells used have a tumourogenic origin, allowing continuous growth, they may have genetic mutations, altered chromosomal content and protein expressions, and thus modified metabolism profiles (MacDonald, 1990). These changes over a period of continuous growth indicate that cell lines also have disadvantages; however, with these shortcomings taken into consideration, invaluable information is gathered without the use of sentient animals. Furthermore, by using a single cell line heterogenous cell to cell interaction is absent, which influences other cellular mechanisms and cell functions. The latter may explain why some pancreatic β-cell lines present with impaired secretory properties and are unable to respond to glucose under normal physiological conditions (Skelin et al., 2010). To date, no β-cell line mimics human β-cell physiology entirely, but they are important in investigating molecular mechanisms underlying β-cell function as well as dysfunction (Skelin et al., 2010). Insulin-secreting cell lines that are widely used include rat insulinoma cells (RIN), hamster pancreatic beta cells (HIT), transgenic C57BL/6 mouse insulinoma cells (MIN), insulinoma cells (INS1) and beta-tumour cells (βTC). However, RIN cells have abnormal properties of glucose transport and/or phosphorylation and exhibit abnormal glucose sensitivity which fail to stimulate insulin release (Halban et al., 1983). Hamster pancreatic beta cells have low insulin content, about 2.5 - 20 times lower than in normal hamster islets, which contain about 56 µg of insulin per mg protein (Santerre et al., 1981). Transgenic C57BL/6 mouse insulinoma

cells sometimes show a sudden loss of glucose-induced insulin secretion as the passage number increases, possibly due to an outgrowth of cells with a poor response to glucose or a reduced gene expression responsible for glucose-induced insulin secretion (Miyazaki et al., 1990). Beta-tumour cells are seen to have increased hexokinase activity after several passages and thus influencing glucose sensitivity (Efrat, 2004; Efrat et al., 1988). The INS1 insulinoma cell line is derived from rat insulinomas, induced by X-ray irradiation, and possesses important properties of β-cells, such as good responses to glucose and moderate levels of insulin content (Asfari et al., 1992). Thus, although, β-cell lines are associated with some limitations, they provide valuable information about physiological and pathophysiological processes.

1.5.2.2.   Rodent Models

The alternative to cell lines is the use of animal models, in the case of amyloid studies, transgenic animal models such as rodents do not develop islet amyloid deposits, even though the IAPP sequence are present; making it difficult to study the effect of amyloid deposits in the progression of T2D (Gilead and Gazit, 2008). The IAPP sequence of rats (rIAPP) differ from human IAPP (hIAPP) in 6 of the 37 aa as indicated in Figure 1.8, and contains 3 proline residues in this region known to not favour β-sheet structures. Non-transgenic rodent models used to study T2D thus limit the investigation of amyloid and its effect on the associated physiological processes (P. Westermark et al., 1990). These models are seen to result in maintained elevated levels of plasma insulin in addition to increased levels of glucose, indicating that IR rather than insulin insufficiency is a factor in diabetic models. Therefore, mimicking islet amyloid-related impairment of β-cells, as observed during development of T2D, incorporation of hIAPP into rodent models may be used to investigate the disease state (Höppener et al., 1999). It is seen that transgenic mice overexpressing hIAPP are not effective in inducing islet amyloid formation and deposition (Höppener et al., 1993). In overcoming this limitation Hoppener et al (1999) crossed hIAPP transgenic mice with 'ob' mice. The homozygous mice (ob/ob) developed IR and subsequently diabetes as a result of a mutation in the leptin gene (Zhang et al., 1994).

Taking all the above-mentioned advantages and disadvantages of pancreatic β-cell lines and transgenic rodent models into consideration, using the INS1 cell line for the purpose of this specific study seems suitable.

| | | 20 | 29 | 37 |

human IAPP   KCNTATCATQRLANFLVHS SNNFGAILSS TNVGSNTY
rat IAPP   KCNTATCATQRLANFLVRS SNNLGPVLPP TNVGSNTY

Figure 1.8: Human amylin vs. rat amylin. Primary sequence of human and rat IAPP. Amino acid residues in pink indicate the six differences between human and rat IAPP (Lopes et al, 2007). The IAPP sequence of rats differ from hIAPP in 6 of the 37 aa, 5 of the aa are found between the 20th and 29th residue, hIAPP (20-29) is SNNFGAILSS and rIAPP (20-29) is SNNLGPVLPP (Betsholtz et al., 1989; Glenner et al., 1988; P. Westermark et al., 1990).

1.6. Summary

In T2D pancreatic β-cells are subject to damage as a consequence of inflammation and the formation of amyloid. With the incidence of T2D increasing globally therapeutic protection of β-cells remains a health care priority. In order to complete the picture of T2D progression, mechanisms involved in inflammation and subsequent amyloid depositions and vice versa, needs further investigation. Investigating these mechanisms may provide insights into the role of inflammation and BACE regulation in pancreatic β-cell impairment and may thus reveal an opportunity for the development of novel therapeutics to protect and preserve pancreatic β-cells, in this case by targeting the activities of BACE. The protective effect of antioxidants, from plant polyphenols, against inflammation is increasingly under investigation. Rooibos extract, rich in Asp and PPAG, may provide novel therapeutics by directly targeting BACE to regulate this enzyme's activities, consequently decreasing inflammation and the progression of T2D. Thus far, neither the BACE inhibitory effect, nor the anti-inflammatory effect of Rooibos in β-cells has been reported on.

Study Aim and Objectives

Aim

To determine if GRT or two of its most bioactive polyphenols have BACE2 inhibition activity and can reduce pro-inflammatory effects in INS1 pancreatic β-cells.

Objectives

1. To test drug targets in pancreatic beta-cells with induced inflammation.

Establish a model of inflammation in INS1 cells by the preliminary screening of individual cytokines as well as a cytokine cocktail to induce moderate inflammation, representative of the disease state; T2D. Assess the effect(s) on β-cell function (i.e. GSIS, proliferation rate, and amylin secretion), viability (i.e. cellular ATP production and cell death), and oxidative stress (ROS and NO production).

2. To screen GRT extract, as well as two of its most bioactive polyphenols, Asp and PPAG, for beta secretase inhibition activity.

In achieving this objective, a purified enzyme assay will be used to screen potential drug targets (derived from and including Rooibos) for BACE2 inhibition activity. Following these concentration response studies, the effective concentration(s) of the potential targets will be used to screen *in vitro*, using pancreatic β-cells with experimentally induced inflammation.

3. Determine the association between beta secretase 2 regulation and beta-cell inflammation.

Changes in BACE enzyme activity will be measured in the INS1 cells with induced inflammation (objective 2). Possible correlations between BACE2 activity and inflammation will be investigated.

CHAPTER 2

Materials and Methods

A complete list indicating the suppliers and catalogue numbers of consumeables, assays, and equipment are found in Addendum F.

The protective effect of Asp, PPAG, and Afriplex GRT extract on pancreatic β-cells with experimentally induced inflammation, was assessed. Rat insulinoma cells were used to assess cell viability, function, and oxidative stress, all measured in several experimental techniques to verify findings. Furthermore, BACE inhibition activity of Asp, PPAG, and GRT was assessed in a purified BACE enzyme assay as well as kinetically *in vitro* (Figure 2.2). The GRT extract (Afriplex (Pty) Ltd., Paarl, South Africa) contains 12.78% of Asp (Figure 2.1 A) and 0.42% of PPAG (Figure 2.1 B) (Patel et al., 2016). Aspalathin (batch: SZ1-356-54) has a purity of ± 99% and was produced synthetically based on a method described by Han et al. (2014). Synthetic PPAG has a purity of >99% (high-performance liquid chromatography (HPLC)) and was produced based on a method described by Marais et al. (1996). Both Asp and PPAG were produced by High Force Research Ltd. (Durham, England).
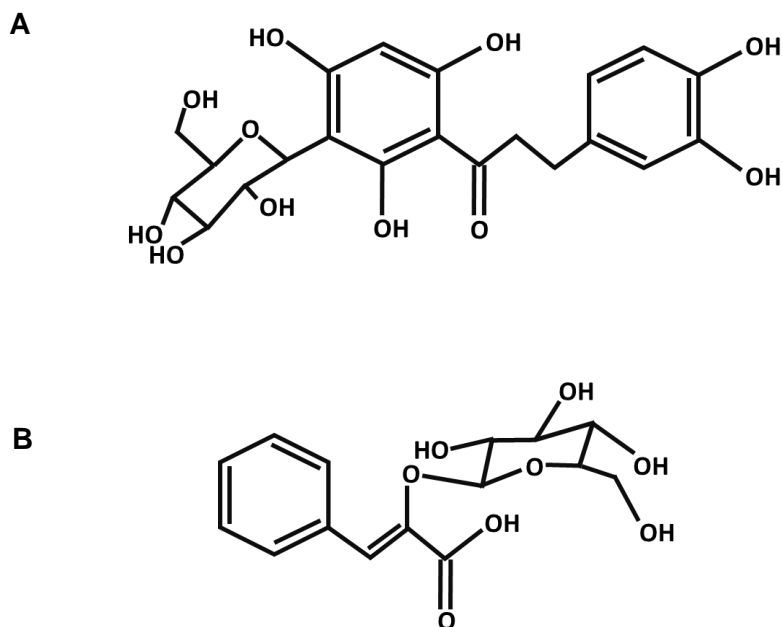
Figure 2.1: Chemical structure of Asp and PPAG. Chemical structure of Asp (A) and PPAG (B) (From: Muller et al. 2012;2013).
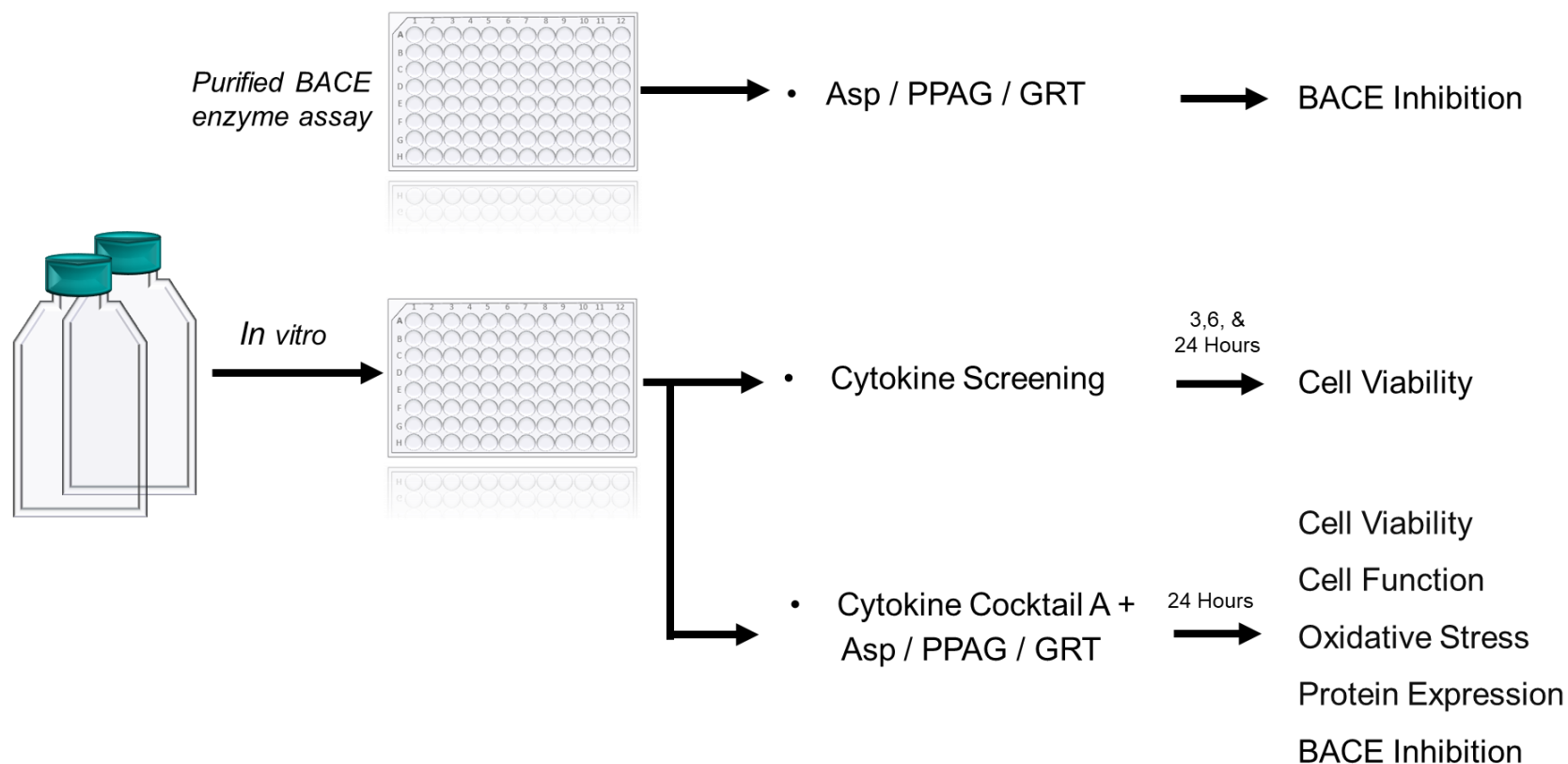
Figure 2.2: Experimental design. The protective effect of Asp, PPAG, and Afriplex GRT extract on INS1 pancreatic β-cells with induced inflammation was assessed. Cytokine cocktail A contains: 1.1 ng/ml of TNF-α, 1.0 ng/ml of IFN-γ, and 0.1 ng/ml of IL-1β. The dosages of Asp and PPAG were: 0.1, 1, 10, 100, and 1000 μM, while GRT dosages were: 0.0001, 0.001, 0.01, 0.1, and 1.0 mg/ml. Cell viability, function, oxidative stress, and protein expression was assessed. Beta secretase inhibition activity of Asp, PPAG, and GRT was also assessed in a purified BACE enzyme assay and kinetically, compared to a known BACE inhibitor (LY2886721).

2.1. Purified Beta Secretase Enzyme Assay

Beta secretase inhibition was assessed using a BACE activity detection kit. The assay is based on the FRET method. This assay is useful as it measures the fraction, or efficiency, of transferred energy from a donor (fluorophore) to an acceptor (chromophore) (Jares-Erijman and Jovin, 2003). Initially, the donor absorbs the energy due to the excitation of incident light and transfers this energy to a nearby acceptor. The emitted light is at wavelengths centred near the emission maximum of the acceptor. Energy transfer manifests itself by decreasing or quenching of the fluorescence signal of the donor accompanied by an increase in acceptor fluorescence intensity (Masters, 2014). Thus, by attaching fluorophores, referred to as probes, to known sites within molecules (i.e. BACE), the efficiency of energy transfer can be measured. In this assay the fluorescence signal is enhanced when BACE cleaves the substrate. The BACE inhibition activity of various concentrations of Asp, PPAG, and GRT was measured after 2 hours incubation at room temperature. Thereafter, the fluorescence signal was measured at Ex320 nm / Em405 nm, by using a SpectraMax i3 multimode plate reader. Beta secretase inhibition by Asp, PPAG, and GRT was compared to a known BACE inhibitor, N - (3 - ((4aS, 7aS) – 2 – amino - 4a, 5, 7, 7a – tetrahydro - 4H – furo [3, 4-d] [1, 3] thiazine - 7a - yl) – 4 - fluorophenyl) – 5 - fluoropicolinamide (LY2886721). This inhibitor is a potent and selective BACE inhibitor with an IC_{50} of 20 nM for recombinant hBACE. The inhibitor does not inhibit other aspartyl proteases such as cathepsin D, pepsin, and renin (End et al., 2001; Lubet et al., 2006). Fluorescence values used were extrapolated from the standard curve generated. Values used for the standard curve were: 100, 200, 300, and 500 pmol. Concentrations of Asp, PPAG, and GRT were as follows:

Table 2.1: Concentrations of Asp, PPAG, and GRT. Concentrations of Asp, PPAG, and GRT used for experiments.

Treatment	Concentrations				
LY2886721 (µM)	0.0039	0.039	0.39	3.9	39
GRT (mg/ml)	0.0001	0.001	0.01	0.1	1.0
PPAG (µM)	0.1	1.0	10	100	1000
Asp (µM)	0.1	1.0	10	100	1000

2.2. Cell Maintenance

All cell culture procedures were performed by applying aseptic techniques (Addendum A).

2.2.1. Thawing of Rat Insulinoma Cells

A cryogenic vial containing 1.9×10^6 INS1 cells (passage number 22; which was the same passage number consistently used for this study), stored in liquid nitrogen, was thawed in a pre-warmed water bath at 37°C. Thereafter, the cell suspension was transferred into a 15 ml falcon tube containing 10 ml pre-warmed complete growth medium (RPMI 1640 supplemented with 200 mM L-glutamine, 25 mM 4-(2-hydroxyethyl)-1-piperazineethanesulfonic acid (HEPES) and 10% fetal bovine serum (FBS). The 15 ml falcon tube was centrifuged at 800 x g for 5 minutes. The complete growth medium was aspirated, and the pellet resuspended into 10 ml of pre-warmed complete growth medium. The 10 ml of cell suspension was then divided into two 75 cm^2 cell culture flasks with the addition of 10 ml pre-warmed complete growth medium (total volume of 15 ml). Following one day of incubation under standard cell culture conditions (37°C in humidified air containing 5% CO_2) the complete growth medium was refreshed. The cells were then incubated under standard cell culture conditions for another three days, before sub-culturing (section 2.2.2).

2.2.2. Sub-culture

Sub-cultures of INS1 cells were created by scraping the adhered cells in the 75 cm^2 cell culture flasks when a confluency of 80-90% was reached after 4 days. Thereafter, the cells in the growth medium were mixed and a small volume (± 500 µl) of the cell suspension was collected for cell counting and viability assessment. A volume of 10 µl, containing both cell suspension and trypan blue in a 1:1 ratio, was added to one of the haemocytometer chambers. Subsequently, the viability of the cells was determined by counting the viable (unstained) and non-viable (blue stained) cells (Figure 2.3 A). Cells were counted in four of the nine 1.0 x 1.0 mm blocks (Figure 2.3 B). If the % cell viability was below 90% the cells were discarded. The viable cells, (Figure 2.3 A and C), were then seeded at 8×10^5 cells per 75 cm^2 culture flasks and at 7.9×10^5 cells per 25cm^2 culture flasks, in a total volume of 15 ml and 3 ml of pre-warmed complete growth medium, respectively. For the experiments, cells were seeded at 1×10^4 cells per well into a 96-well plate and at 3×10^5 cell per well into a 6-well plate, in a total volume of 200 µl per well and 3 ml complete growth medium, respectively, and plates were then incubated under standard cell culture conditions (Figure 2.3 C). After three days of incubation the 96-well plates were used for assays.

A

$$\text{Cell Viability (\%)} = \frac{\text{Viable cells}}{\text{Total number of cells (Viable + Non-viable)}} \times 100$$

B

C

(Number of Viable cells / Number of blocks counted (i.e. 4)) X2 (Dilution factor)

= X Amount of cells (x10^4) per ml

	75cm^2	25cm^2	96 well plate	6 well plate
=	8x10^5 / X cells (x10^5)	7.9 x10^5 / X cells (x10^5)	(1x10^4) (75 wells) / X cells (x10^5)	(3x10^5) (6 wells) / X cells (x10^5)
=	Y ml of cells			
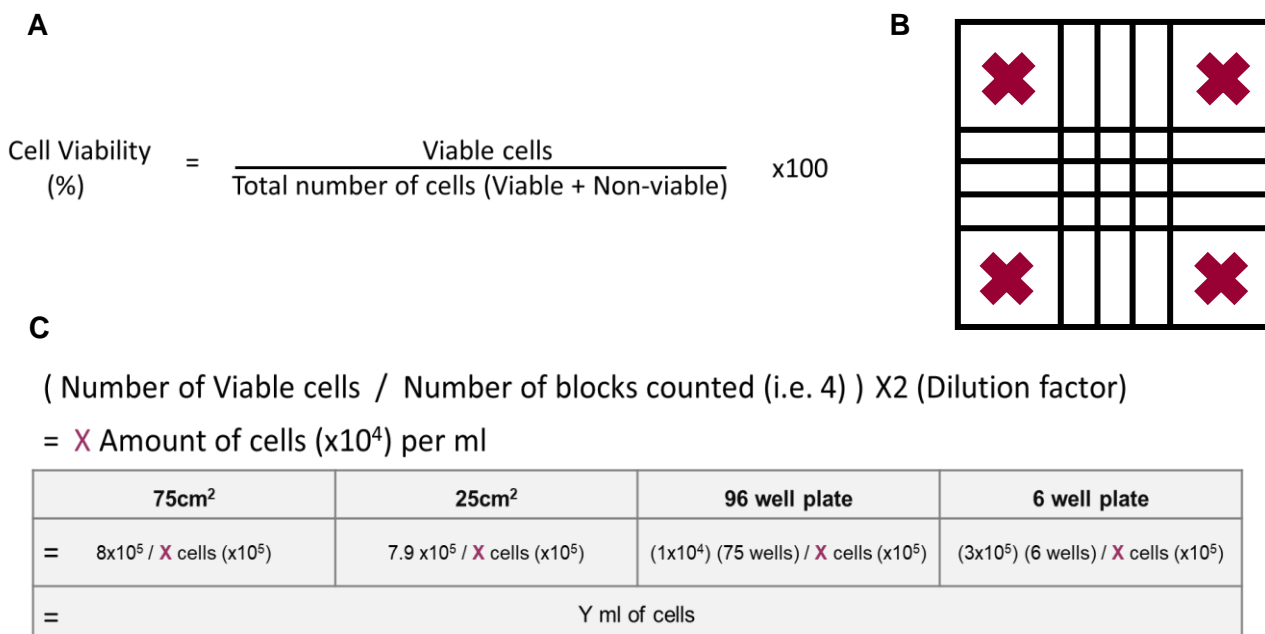
Figure 2.3: Cell viability. Equation for cell viability (A); blocks (1.0 x 1.0 mm) counted on haemocytometer to calculate the cell number and relative viability (B); equation for calculating the volume of cell suspension (ml) needed for seeding (C).

2.3. Treatment

Although the study aimed to mimic a T2D scenario in INS1 cells, co-exposure to high glucose levels, in addition to inducing an inflammatory state, was excluded for the preliminary screening of GRT, Asp, and PPAG. Glucotoxicity induce inflammation and therefore inflammation was directly induced with cytokines.

2.3.1. Inflammation Model – Rat Insulinoma Cells

In order to assess the putative protective effect of Asp, PPAG, and GRT against the damaging effects of T2D on pancreatic β-cells, a model of moderate inflammation was developed. The model was developed by exposing INS1 cells to inflammatory stressors such as; TNF-α, IFN-γ, IL-1β, as well as two cytokine cocktails containing different concentrations of all three cytokines for periods of 3, 6, and 24 hours. The concentrations of TNF-α assessed were 100; 25; 10; and 1.1 ng/ml. The concentrations of IFN-γ assessed included 100; 50; 10; and 1 ng/ml and for IL-1β 10; 1; 0.1; and 0.01 ng/ml. Cytokine cocktail A contained: 1.1 ng/ml of TNF-α, 1 ng/ml of IFN-γ, and 0.1 ng/ml of IL-1β (Chellan, 2014). The second cytokine cocktail, B, contained: 25 ng/ml of TNF-α, 10 ng/ml of IFN-γ, and 10 ng/ml of IL-1β (Yang et al., 2015). After each time point, a 3-(4,5-dimethylthiazol-2-yl)-2,5-diphenyltetrazolium bromide

tetrazolium (MTT) assay (section 2.4.1) was performed to assess cell viability, measured by mitochondrial dehydrogenase tetrazolium activity. The efficacy of Asp, PPAG, and GRT at various dosages against moderate inflammation induced in pancreatic β-cells by these cytokines was the assessed. The stressors were made up in complete growth medium; the latter on its own without cytokines served as negative control or vehicle control. Cytokine cocktail A was most effective in inducing a moderate state of inflammation in β-cells and was thus used for co-treatment in the experiments.

2.3.2.   Exposure to Asp, PPAG, and GRT

The protective effect of Asp, PPAG, and GRT on moderate inflammation in INS1 pancreatic β-cells was assessed by exposing the INS1 cells to various dosages of Asp, PPAG, and GRT for 24 hours. Concentrations of Asp, PPAG, and GRT were the same concentrations as indicated in Table 2.1. A MTT assay was used to assess cell viability at all concentrations. For the co-treatment with cytokine cocktail A, and either Asp, PPAG, or GRT, a MTT assay was performed after 24 hours to assess cell viability. All the treatments were made up in complete growth medium, the latter served as negative control, while cytokine cocktail A served as positive control.

2.4. Cell Viability

2.4.1.   MTT Assay

The MTT assay is a quantitative colorimetric assay that measures cell survival and proliferation by detecting mitochondrial dehydrogenase activity in living cells, as the tetrazolium ring is only cleaved in active mitochondria. The signal generated is dependent on the degree of mitochondrial dehydrogenase activity in the cells (Mosmann, 1983). Tetrazolium salt is used in this colorimetric assay as it measures the activity of various dehydrogenase enzymes (Slater et al., 1963). The conversion of the yellow tetrazolium solution to purple formazan crystals indicates the rate of mitochondrial dehydrogenase activity (Riss et al., 2004). After exposing the INS1 cells to stressors (cytokines) and/or either Asp, PPAG, or GRT, the growth medium was aspirated, and the cells washed with pre-warmed Dulbecco's phosphate buffered saline with Ca^{2+} and Mg^{2+} (DPBS). Afterwards, 50 µl of pre-warmed MTT solution (2 mg MTT / ml DPBS) was added into each well followed by incubation under standard cell culture conditions for 30 minutes. After incubation 200 µl dimethyl sulfoxide (DMSO) and 25 µl Sorensen's glycine buffer (pH 10.5) were added to each well to dissolve

the purple formazan crystals produced in the cells and the absorbance was then measured on a plate reader at 570 nm (Riss et al., 2004).

2.4.2. The ATP Assay

The ability of cells to synthesize ATP and maintain intracellular ATP levels is essential for cell survival. In dead cells synthesis of ATP ceases and endogenous ATPases rapidly deplete the remaining ATP from the cytoplasm (Riss et al., 2004). Cellular ATP levels were measured using the CellTiter-Glo® Luminescent Cell Viability Assay. The ATP assay was performed to verify the MTT results as it is known that plant polyphenols can interact with MTTs. Luminescence relies on luciferase which generates the signal, where mono-oxygenation of luciferin is catalysed by luciferase in the presence of Mg^{2+}, ATP, and molecular oxygen. Luminescent signals are proportional to the amount of ATP (Crouch et al., 1993; Riss et al., 2004). The INS1 cells were exposed to the co-treatment of cytokine cocktail A with the different dosages of either Asp, PPAG, or GRT as indicated in Table 2.1. After 24 hours, 25 µl of the media was transferred to a clean 96-well plate and frozen (-20˚C) for later assessment of oxidative stress (section 2.6.3). Thereafter, 75 µl of the CellTitter-Glo® reagent was added to each well of the white walled 96-well plate and incubated under standard cell culture conditions for 30 minutes, shaken attentively every 10 minutes to lyse the cells. Following incubation, a 5 µl sample of the lysate was transferred to a clean 96-well plate to measure the protein concentrations, using the Bradford protein assay according to the manufacturer's instructions. Luminescence of the cellular ATP in the remaining lysates was measured using the SpectraMax i3 multimode plate reader. Cellular ATP was normalised to the protein content of each well determined by the Bradford protein quantification assay (section 2.5.4).

2.4.3. Apoptosis/Necrosis

2.4.3.1. Kinetic Assay

2.4.3.1.1. Annexin-V and Propidium Iodide

To assess whether Asp, PPAG, or GRT have a toxic effect on INS1 cells with induced moderate inflammation, annexin-V (AV) and propidium iodide (PI) fluorescence was measured kinetically. Annexins are ubiquitous homologous proteins which bind phospholipids in the presence of Ca^{2+}. The apoptotic process includes loss of phospholipid asymmetry during early stages, resulting in translocation of phosphatidylserine from the inside of the lipid bilayer to the external surface of the cell membrane by the Mg^{2+}/ATP dependent enzyme, aminophospholipid translocase (Binder et al., 2000; Hoekstra et al., 1993). Allowing the

fluorescein isothiocyanate (FITC) conjugated anti-AV antibody to bind with phosphatidylserine, indicating early apoptosis. Propidium iodide intercalates with DNA in dead cells, where broken membranes have permitted entry of PI; indicative of late apoptosis and necrosis (Nicoletti et al., 1991; Suzuki et al., 1997; Vermes et al., 1995). Following the co-treatment of cytokine cocktail A with the different dosages of either Asp, PPAG, or GRT (Table 2.1), anti-AV (1.5 µl / 100 µl) and PI (1 mg/ml) was added to each well of a black wall 96-well plate. The plate was placed into the SpectraMax i3 multimode plate reader to measure the fluorescence every hour for 24 hours. Temperature was maintained at 37°C with 5% CO_2. The fluorescence signal of AV was read at Ex485 nm/Em535 nm; while PI was read at Ex535 nm/Em617 nm. Fluorescent readings were normalised by a MTT assay to ensure that the fluorescence signals obtained are representative of and correlated with the number of live cells.

2.4.3.1.2. *Caspase-3/7 Activation*

To assess the effect of Asp, PPAG, and GRT on the induction of apoptosis in cytokine-exposed INS1 cells caspase-3/7 fluorescence was measured. Activation of caspase-3 and -7 are known to play a role in the execution-phase of the apoptosis pathways (both intrinsic (mitochondrial) and extrinsic (receptor mediated)) (Salvesen, 2002). Caspase-3/7 Green Detection Reagent was used as a fluorogenic substrate for activated caspases-3/7. Activation of caspase-3/7 in apoptotic cells, results in a DEVD (Asp-Glu-Val-Asp) peptide that is cleaved enabling the fluorescent dye to bind to DNA resulting in fluorescence (Chang and Yang, 2000). The assay is indicative of caspase-3/7 activation and the associated cellular plasma membrane permeabilization, and thus cell death. Cells were co-treated with cytokine cocktail A and the different dosages of either Asp, PPAG, or GRT (Table 2.1), as well as caspase-3/7 (10 µM/well) in a black wall 96-well plate. Fluorescence was measured every hour for 24 hours at Ex485 nm / Em535 nm using the SpectraMax i3 multimode plate reader. Temperature was maintained at 37°C with 5% CO_2. Fluorescent readings were normalised by performing a MTT assay.

2.4.3.2. Flow Cytometry

To obtain samples to perform the flow cytometry assays described below, INS1 cells were cultured in clear 6-well cell culture plates. Cells were seeded at a cell density of $3x10^5$ cells/well followed by 4 days of incubation under standard cell culture conditions. Three 6-well plates were seeded on the same day to serve as replicates. Cells were then co-treated and incubated for a period of 24 hours. Concentrations used for flow cytometry samples were

chosen based on results seen in previous experiments. The cytokine cocktail was the same, while only one concentration (100 µM Asp, 100 µM PPAG, 0.1 mg/ml GRT, as well as 39 µM of the LY2886721 BACE inhibitor, A) per treatment was chosen due to results observed in section 3.4.2. The BACE inhibitor was used to see if it influences cell viability on its own. After 24 hours of exposure to co-treatment, the cells were scraped into 2 ml Eppendorf tubes. Thereafter, the samples were centrifuged at 600 x g for 5 minutes, followed by aspirating the supernatant. The pellet of INS1 cells was resuspended to 1 x 10^6/ml and stained with an anti-AV antibody (1.5 µl /100 µl) and PI (1 mg/ml) at 37˚C for 30 minutes. Samples were then centrifuged at 600 x g for 5 minutes, the stain aspirated, and the cells washed with DPBS. Thereafter, fresh DPBS (100 µl) was added, the cells resuspended and put on ice. Flow cytometry was performed on the samples using a BD Accuri ™ C6. The start-up of the flow cytometer was done according to the start-up procedures of the flow cytometer, this included running of the 6 and 8 bead standards to ensure that the flow cytometer is performing optimally. A threshold was set for samples using unstained and individually stained (one fluorescent probe only) of untreated cells using the pre-set AV/PI template. The untreated cell population was located in the lower left quadrant on the FL-1 vs FL-4 plot. Increased FL-1 fluorescence (FITC) intensity (green) indicates a shift to early apoptosis measured by the FITC conjugated anti-AV antibody, while a shift in the FL-4 fluorescence colour (red) indicates late apoptosis or necrosis measured by PI. The samples were run on a medium flow rate, with a collection limit based on the gated population of interest.

2.4.3.3.   Fluorescent Imaging – Caspase-3/7 Activation

To verify INS1 cell viability results seen in the kinetic measuring of caspase-3/7 activation, fluorescent images were taken of the 96-well plates after the 24 hours of readings (section 2.4.3.1.2) using the Nikon inverted microscope. Images were taken using the 20X objective, resulting in a 200X magnification. Dimethyl sulfoxide (0.1%) was used as a control of cell death. Fluorescent images were taken as well as phase microscopy images.

2.5.   Cell Function

2.5.1.   Sample Collection

Cell function of INS1 cells was assessed by their insulin response to glucose stimulation. Following 24 hour of exposure to cytokine cocktail A and the different concentrations of either Asp, PPAG, or GRT (Table 2.1), the treatments were aspirated from the 96-well plate. Thereafter, 100 µl of Krebs-Ringer bicarbonate-HEPES buffer (KRBH) containing 2.8 mM of

glucose was added to each well and the plate incubated under standard cell culture conditions for 30 minutes. This served as a washing step. To assess basal insulin secretion of the INS1 cells, the KRBH was aspirated and 100 µl of KRBH containing 2.8 mM of glucose was added to each well, followed by 90 minutes of incubation under standard cell culture conditions. To determine GSIS, 100 µl of KRBH containing 16.7 mM of glucose was added to each well, followed by 90 minutes of incubation under standard cell culture conditions. After incubation, taking care not to disturb the cells, the KRBH from the basal insulin secretion and the GSIS plates were transferred to clean 96-well plates and frozen at -20°C (Llanos et al., 2015; Malmgren et al., 2009; Pereverzev et al., 2002).

To assess the insulin content of the cells, 100 µl of EtOH-HCl (≥99.8% EtOH; 37% HCl) was added to each well to lyse the remaining INS1 cells. The 96-well plate containing the cells and EtOH-HCl solution was frozen at -20˚C.

Above mentioned cell culture plates were stored at -20˚C and used for later enzyme-linked immunosorbent assay (ELISA) analysis.

2.5.2.   Insulin ELISA

2.5.2.1.   Insulin Secretion

Insulin secreted into the KRBH media by INS1 cells, at both basal and stimulated glucose levels, was measured by using a rat/mouse insulin ELISA kit. Previously stored samples (at -20˚C) were brought to room temperature. Basal samples were diluted 16x, while the glucose stimulated samples were diluted 32x. The diluted samples were added to the pre-coated ELISA kit as described by the kit protocol. The absorbence of the bound substrates was read at Ex450 nm / Em570 & 630 nm using the SpectraMax i3 multimode plate reader. Concentrations of insulin secreted were extrapolated from the standard curve provided with the ELISA kit, using the following insulin concentrations: 0.2, 0.5, 1.0, 2.0, 5.0, and 10 ng/ml. In order to ensure the ELISA was successful a positive and negative quality control was used in addition to the standards listed above.

2.5.2.2.   Insulin Content

Insulin content in INS1 cells was measured using the same rat/mouse insulin ELISA kit used to assess insulin secretion. Previously stored samples (at -20˚C) were brought to room temperature. The plate containing the cells with the EtOH-HCl was sonicated followed by centrifuging the plate for 5 minutes at 5000 x g. The supernatant containing insulin was

transferred to a clean 96-well plate and the insulin content measured by an ELISA. To normalise for cell numbers, the lysed cells left in the plate were used for protein determination by the Bradford method (section 2.5.4). The KRBH samples were subsequently added to the pre-coated ELISA kit as described by the kit protocol. The absorbence of the bound substrates was read at Ex450 nm / Em570 & 630 nm using the SpectraMax i3 multimode plate reader. Concentrations of insulin secreted were extrapolated from the standard curve provided with the ELISA kit. The insulin concentrations used for the standard curve were 0.2, 0.5, 1.0, 2.0, 5.0, and 10 ng/ml. In order to ensure the ELISA was successful quality controls were used. Subsequently, the respective protein concentrations were used to normalise the insulin secretion and cellular content as determined by the ELISA kit.

2.5.3.   Amylin ELISA

2.5.3.1.   Amylin Content

The concentrations of cellular amylin content were determined, using the same stored samples (-20˚C) used to assess insulin content described earlier. Samples were brought to room temperature, where after a competitive ELISA assay was performed, where the IAPP in the samples competes with a set amount of IAPP bound to the plate for sites of the biotinylated detection antibody. Thereafter, advidin conjugated to horseradish peroxidase (HRP) was added to each well, followed by 30 minutes of incubation. After incubation, a 3,3',5,5'-tetramethylbenzidine (TMB) substrate was added and stopped after 15 minutes by the addition of sulphuric acid solution. The IAPP was then measured spectrophotometrically at 450 nm using the SpectraMax i3 multimode plate reader. Values used were extrapolated from the standard curve generated. Standard curve values were: 62.5, 125, 250, 500, 1000, 2000, and 4000 pg/ml.

2.5.3.2.   Amylin Secretion

The concentrations of IAPP secreted were determined, by using the same stored samples (-20˚C), used to assess the GSIS described earlier (section 2.5.2.1). Samples were brought to room temperature, where after an ELISA, described in section 2.5.3.1, was done. The IAPP was then measured spectrophotometrically at 450 nm using the SpectraMax i3 multimode plate reader. Values used were extrapolated from the standard curve generated. Subsequently, the respective protein concentrations were used to normalise the amylin secretion and cellular content as determined by the ELISA kit.

2.5.4.   Bradford Protein Quantification Assay

The Bradford assay was used in order to determine protein content (Bradford, 1976). As mentioned in the respective subsections (section 2.4.2, 2.5.2, and 2.5.3), this was done to compensate for relative cell numbers of the insulin and amylin assays. Briefly, a 5 µl sample of cell lysate from each well was transferred to a 96-well assay plate. Thereafter, 200 µl of the Bradford reagent was added to each well followed by 10 minutes of incubation at room temperature. After incubation, the absorbance was measured at 570 nm on a plate reader. Protein content values used were extrapolated from the standard curve generated. Protein values used for the standard curve were: 0.125, 0.25, 0.5, 0.75, 1, 1.5, and 2 mg.

2.5.5.   Proliferation Rate of Rat Insulinoma Cells

The rate of β-cell proliferation was assessed by measuring 5-bromo-2'-deoxyuridine (BrdU) incorporation into cellular DNA. The pyrimidine analogue gets incorporated into newly synthesised DNA instead of thymidine of proliferating cells and the extent of incorporation is quantifiable using an anti-BrdU antibody (Gratzner, 1982; Gratzner et al., 1975; Köhler and Milstein, 1975). Incubated with media containing BrdU, cells were co-treated for 24 hours with cytokine cocktail A and the different dosages of either Asp, PPAG, or GRT (Table 2.1). Thereafter, the media were removed, the cells fixed, and the DNA denatured in order to improve the accessibility of the incorporated BrdU to the detection antibody (mouse anti-BrdU body). The cells were incubated for 60 minutes with the primary antibody. Thereafter, binding of the primary antibody to the incorporated BrdU was detected with an anti-mouse IgG, HRP-linked antibody, after 30 minutes incubation at room temperature. To enhance the signal, a chemiluminescent reagent was added and the relative light units (RLU) measured using the SpectraMax i3 multimode plate reader. The RLU intensity in proportion to the amount of BrdU incorporated, is a direct indication of cell proliferation.

2.6. Oxidative Stress

2.6.1.   Reactive Oxygen Species – End-point Assay

Reactive oxygen species production in INS1 cells, as a measure of endogenous oxidative stress, was assessed by measuring dichlorofluorescein (DCF) fluorescence produced from the oxidised non-fluorescent fluorescein derivative (2'7'-dichlorofluorescein, DCFH). The fluorescence emitted by the conversion of DCFH to DCF by the free radicals is relative to the amount of ROS (Keston and Brandt, 1965; LeBel et al., 1992; Wang and Joseph, 1999).

To assess ROS production, INS1 cells were co-treated with the cytokine cocktail A and the different dosages of either Asp, PPAG, or GRT for 24 hours (Table 2.1). After 24 hours, the media were aspirated, and the cells washed with pre-warmed DPBS. Thereafter, 50 µl of DCFH (10 µM) was added to each well followed by 45 minutes of incubation under standard cell culture conditions. The DCFH was then aspirated and 50 µl of DPBS was added to each well. The DCF fluorescence signal was measured by using the SpectraMax i3 multimode plate reader at Ex485 nm / Em535 nm.

2.6.2.   Reactive Oxygen Species – Kinetic Assay

To assess oxidative stress, ROS production was measured kinetically over 24 hours. The INS1 cells were co-treated with cytokine cocktail A and the different dosages of either Asp, PPAG, or GRT (Table 2.1) with the addition of DCFH (10 µM) to each well of a black wall 96-well plate. The plate was placed into the SpectraMax i3 multimode plate reader to measure the fluorescence every hour for 24 hours. Temperature was maintained at 37°C with 5% CO_2. The fluorescence signal was measured at Ex/Em 485/535 nm. Fluorescent readings were normalised by a MTT assay.

2.6.3.   Nitric Oxide – End-point Assay

To further assess the effect of Asp, PPAG, and GRT, at different dosages (Table 2.1), on oxidative stress in INS1 pancreatic β-cells exposed to cytokine cocktail A, a colorimetric assay was done in order to measure the levels of NO_2- in an aqueous solution. Nitric oxide formation can be indirectly measured by assessing the number of NO_2- present. Nitrates are stable and non-volatile breakdown products of NO. The Griess assay uses sulfanilamide and *N*-1-napthylethylenediamine dihydrochloride (NED) under acidic (phosphoric acid) conditions to detect NO_2- levels (Green et al., 1982; Griess, 1879).

In order to perform the Griess assay the stored samples (section 2.4.2) were bought to room temperature. Thereafter 25 µl of the samples was transferred to a clean 96-well plate, and 25 µl of the Griess reagent added to each sample. Samples were incubated in the dark at room temperature for 15 minutes, and the absorbance was read at 520 nm, as well as 540 nm using the SpectraMax i3 multimode plate reader. The Griess reagent was made up according to the protocol of the manufacturer. Values used were extrapolated from the standard curve generated. Nitrite values used for the standard curve were: 1.56, 3.13, 6.25, 12.5, 25, 50, and 100 µM.

2.7. Beta Secreatse Inhibition in Rat Insulinoma Cells

In order to validate the effect seen in the purified BACE inhibition assay (section 2.1), BACE inhibition activity of GRT, PPAG, and Asp was assessed in the INS1 cells, using the same BACE activity detection kit described in section 2.1. The cells were exposed to the different dosages of either Asp, PPAG, or GRT and cytokine cocktail A in a black 96-well plate. The same BACE inhibitor, LY2886721 (section 2.1), was used at two different concentrations (A: 39 μM, and B: 3.9 μM) to serve as positive control as it is cell-permeable. Concentrations of Asp, PPAG, and GRT were the same concentrations indicated in Table 2.1. Thereafter, 24-hour kinetic readings were obtained at every 1 hour. The fluorescence signal was measure at 320 nm and 405 nm using the SpectraMax i3 multimode plate reader. Temperature was maintained at 37°C with 5% CO_2 for the duration of this assay.

2.8. Western Blots

2.8.1. Sample Collection

For western blot analysis, INS1 cells were cultured in 25 cm² flasks. Cells were seeded at a cell density of 7.9×10^5 cells/well followed by 4 days of incubation under standard cell culture conditions. Three 25 cm² flasks per treatment group were seeded on the same day to serve as technical replicates, this process was then performed again on two different days to serve as three biological repeats. Cells were co-treated and incubated for a period of 24 hours. The concentration of the cytokines in the cytokine cocktail was the same, while only one treatment concentration (100 μM Asp, 100 μM PPAG, 0.1 mg/ml GRT, as well as 39 μM of the LY2886721 BACE inhibitor) was selected. After 24 hours co-treatment, cells were lysed by adding 300 μl/flask of lysis buffer containing 10 μl/ml phenylmethylsulfonyl fluoride (PMSF). Thereafter the cells were scraped and mixed with the other two repeats and transferred into a 2 ml Eppendorf tube and frozen at -20°C for western blot analysis.

2.8.2. BCA Protein Determination

Stored samples (section 2.8.1) were thawed on ice. Thereafter the samples were homogenised at 25 Hertz (Hz) for 60 seconds, followed by 60 seconds on ice, repeated 5 times, using a tissue lyser. Samples were then centrifuged at 15 000 x g at 4°C for 15 minutes, where after the supernatant was transferred to a clean 2 ml Eppendorf tube for future analysis. Protein concentrations were determined using the bicinchoninic acid assay (BCA) assay (Smith et al., 1985). To determine the protein concentration, 5 μl of sample as well as

standards were added to a clean 96-well plate, followed by 25 μl of reagent A' (20 μl of reagent S to each 1 ml of reagent A), and the addition of 200 μl of reagent B to each well. The plate was then incubated for 15 minutes and the absorbance read at 630 nm and 750 nm using the SpectraMax i3 multimode plate reader. Values used were extrapolated from the standard curve generated.

2.8.3.   Running of SDS-PAGE Gels

After protein determination (section 2.8.2), loading volumes of samples were calculated to load 30 μg of protein per well. Previously stored samples were thawed on ice; where after 25 μl of each sample was mixed with 75 μl of 4X sample buffer (SB). The samples were then heated on a heating block at 95°C for 15 minutes to denature the proteins. Samples and markers of protein mass (precision plus protein™, WesternC™ and PageRuler™ Prestained Protein Ladder), used to help identify proteins of interest following chemiluminescent detection were loaded onto a 10% SDS-polyacrylamide gel electrophoresis (SDS-PAGE) precast gel. The gels were run at 150 V in a tetra cell tank filled with running buffer till the protein reached the bottom of the gel as indicated in Figure 2.4.
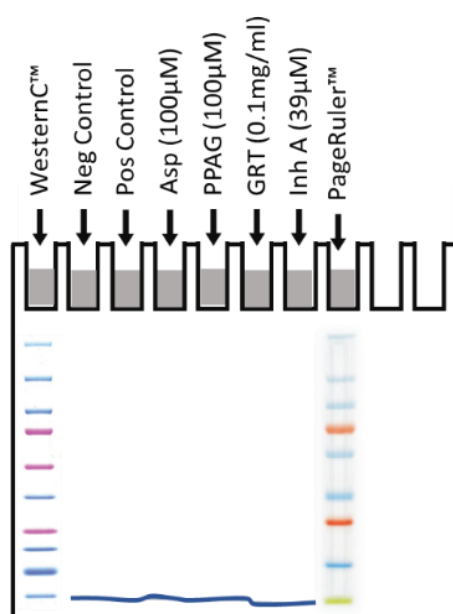
Figure 2.4: Western blot; loading of SDS-PAGE gels. Loading of markers and samples on a precast SDS-PAGE gel.

2.8.4. Transfer of Proteins to PVDF Membrane

The SDS-PAGE gels were transferred to an activated polyvinylidene difluoride (PVDF) membrane. Activation of the PVDF membrane is done by shaking the membrane in 100% methanol for 2 minutes. Thereafter, the PVDF membrane and stacks, provided with the transfer kit, were shaken in transfer buffer for 3 minutes. The stacks, membrane, and gel were then assembled in the cassette according to the protocol provided by the kit (Figure 2.5) and allowed 10 minutes of transfer. In order to ensure that the protein transferred from the gel onto the membrane, a Ponceau S stain was done on the PVDF membrane for 10 minutes on a shaker.

Cathode (-)

Filter Paper

SDS-PAGE Gel
PVDF Membrane
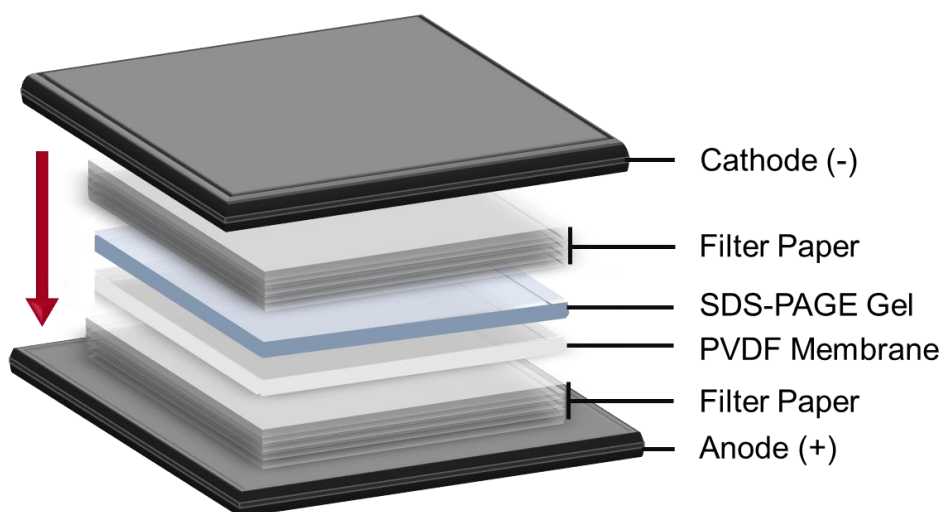
Filter Paper
Anode (+)

Figure 2.5: Western blot; PVDF membrane transfer. The transfer of the proteins from the SDS-PAGE gel to the PVDF membrane was assembled as follows: in order from the anode (+) to the cathode (-); filter paper; PVDF membrane; SDS-PAGE gel; and then filter paper. Transfer occurs from the cathode (-) to the anode (+), as indicated with the arrow direction.

2.8.5. Primary and Secondary Antibodies

The PVDF membrane was blocked in tris-buffered saline with tween 20 (TBST) containing 5% non-fat milk to minimise non-specific binding for 2 hours on the shaker, followed by 2 quick washes with TBST. Thereafter, primary antibodies diluted in TBST with 5% bovine serum albumin (BSA) according to product specifications (Table 2.2), were added to the membranes

and incubated at 4˚C on a shaker overnight. The following morning the membranes were washed in TBST for 10 minutes on the shaker, repeated 3 times. To detect antibody binding to the protein, the PVDF membrane was incubated with the corresponding secondary antibody (Table 2.2) at a 1:4000 dilution, with 2 µl of strepavidin in TBST containing 2.5% non-fat milk for 90 minutes on a shaker. Thereafter the membrane was washed with TBST for 10 minutes, three times. The housekeeping protein used was β-tubulin.

Table 2.2: Antibodies: western blots. Primary and secondary antibodies used for western blots.

Primary Antibody	Monoclonal / Polyclonal	Molecular Weight (kDA)	Primary Antibody Dilution	Secondary Antibody (1:4000)
Anti-Amylin	Monoclonal	± 10	1:500	Anti-Mouse
Anti-TMEM27	Monoclonal	± 38	1:1000	Anti-Rabbit
Anti-BACE2	Polyclonal	± 45	1:500	Anti-Rabbit
Anti-pNF-κB	Monoclonal	± 65	1:1000	Anti-Rabbit
Anti-NF-κB	Monoclonal	± 65	1:1000	Anti-Rabbit
Anti-β-Tubulin	Polyclonal	± 55	1:1000	Anti-Rabbit
Anti-COX2	Polyclonal	± 74	1:1000	Anti-Rabbit

2.8.6.   Chemiluminescent Detection

Labelled proteins were visualised using a chemiluminescent kit. The membrane was incubated for 5 minutes with enhanced chemiluminescent substrate (ECL), followed by imaging of the membrane on the Chemi Doc MP (BioRad). Image Lab Software was used to analyse images. For this study, all proteins were normalised to the housekeeping protein, β-tubulin in order to determine the relative expression of the specific protein.

2.9. Statistical Analysis

Statistical analyses were performed using the GraphPad Prism 5.0 Software. Blot analysis were done using the ImageLab software. All experiments were performed with three technical repeats of three independent experiments. The trapezoidal method (Figure 2.6) was used to calculate the area under the curve (AUC) of the kinetic assay results. One-way Analysis of

Variance (ANOVA) with the Tukey *post hoc* test for correction was conducted if $p<0.05$. A Man-Whitney test was also conducted where appropriate and as indicated. *p*-Values less than 0.05 were considered statistically significant. Data was expressed as mean ± standard error of the mean (SEM).

p-Values less than 0.1 were considered as a trend. As suggested in a review by Figueiredo Filho et al. (2013); although these trends are not statistically significant it may be of biological significance to note and will need to be further interogatted. A small effect seen may be exacerbated in a physiological system during a disease state, as factors such as stressors may exert synergestic effects on each other. The small sample size and associated SEM may potentially affect the statistical outcome of the data (Figueiredo Filho et al., 2013).
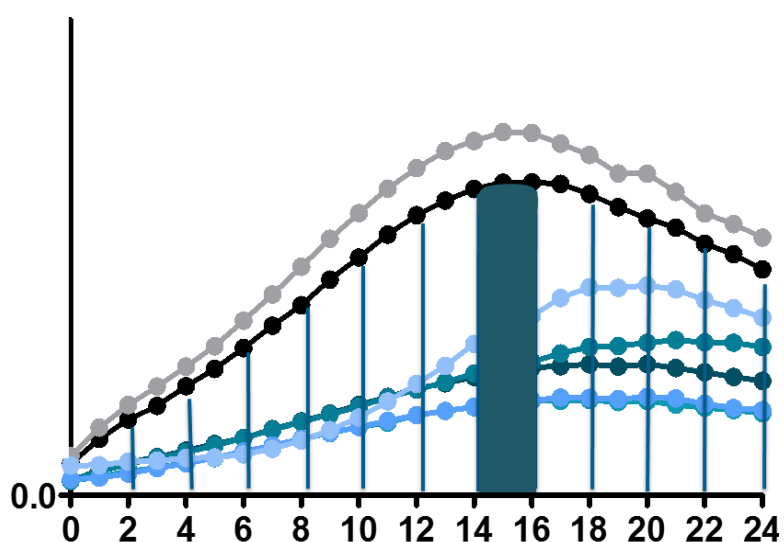
Figure 2.6: Trapezoidal method; area under the curve. Diagrammatic presentation of graphs generated from kinetic experiments, using the trapezoidal method to analyse data.

CHAPTER 3

Results

The effect(s) of GRT and two of its major bioactive polyphenols (Asp and PPAG), on BACE activity and pro-inflammatory effects in INS1 pancreatic β-cells was assessed. Cell viability was assessed by using MTT and ATP assays, together with an AV/PI as well as a caspase-3/7 activation assay. Cell function was assessed by measuring intracellular insulin and amylin content and secretion following glucose stimulation, as well as the rate of pancreatic β-cell proliferation. Oxidative stress was assessed by measuring ROS production and generation of nitrites from NO by using DCF and Griess assays, respectively. Beta secretase inhibition was assessed using a purified enzyme assay followed by a cell-based assay measuring BACE activity. Overall no change in mitochondrial dehydrogenase activity was observed, except at the highest concentrations of Asp (1000 µM) and GRT (1 mg/ml) where a decrease in activity was observed. A reduction in cellular ATP production was seen at 1000 µM of Asp and 1 mg/ml of GRT, while an increase in apoptosis/necrosis was seen at these concentrations of Asp and GRT. Insulin secretion increased after glucose stimulation, while no major effect was seen in insulin or amylin content. The proliferation rate of inflamed INS1 cells decreased at the highest concentrations of Asp (1000 µM), PPAG (1000 µM), and GRT (1 mg/ml). The end-point DCF assays showed a reduction in ROS production in the cells exposed to Asp, PPAG, or GRT relative to the pro-inflammatory cytokine cocktail A; except at the highest concentrations of Asp (1000 µM) and GRT (1 mg/ml) where an increase in ROS production was seen relative to the negative control. However, the kinetic DCF assays showed that Asp, PPAG, and GRT at high concentrations decreased ROS production. High concentrations of Asp (1000 µM) and GRT (1 mg/ml) seem to have BACE inhibitory activity as reduced BACE activity was observed.

Data presented is the mean (± SEM) of three independent biological repeats (n=3); with three technical repeats, relative to the negative control. The mean was calculated by averaging the 9 replicate values. The negative control refers to INS1 cells not exposed to any stressors or treatments, while the positive control was exposed to the pro-inflammatory cytokine cocktail A (section 2.3.1).

3.1. Cell Viability of Rat Insulinoma Cells

Rat insulinoma cell viability was assessed by using the MTT and ATP assays, together with an AV/PI assay as well as a caspase-3/7 activation assay.

3.1.1.   Inflammation in Rat Insulinoma Cells Exposed to Pro-Inflammatory Cytokines

In order to induce inflammation in INS1 cells, the cells were exposed to pro-inflammatory cytokines for 3, 6, and 24 hours, followed by MTT assays. The cytokines included different concentrations of TNF-α, IFN-γ, and IL-1β. The INS1 cells were also exposed to two different pro-inflammatory cytokine cocktails (A & B), containing the above-mentioned cytokines, but at different concentrations. The negative control, not exposed to cytokines, was set as 100% for statistical analysis and graphs.

Following 3 hours of exposure to the pro-inflammatory cytokines, no effect was observed in mitochondrial dehydrogenase activity for TNF-α or IFN-γ. Exposing the INS1 cells to IL-1β induced a slight significant increase in mitochondrial dehydrogenase activity at 0.01 and 1 ng/ml relative to the negative control (108.90% ± 1.69, p=0.042 and 109.00% ± 1.80, p=0.04 vs. 100% ± 1.33, respectively). Albeit not significant, 0.01 and 1 ng/ml of IL-1β showed a trend towards increased mitochondrial dehydrogenase activity relative to cytokine cocktail B (108.90% ± 1.69, p=0.071 and 109.00% ± 1.80, p=0.069 vs. 100.6% ± 2.62, respectively) (Figure 3.2 A).

After 6 hours of exposing the INS1 cells to TNF-α an increase in mitochondrial dehydrogenase activity was seen at 1.1 ng/ml relative to cytokine cocktail B (118.90% ± 4.22, p=0.028 vs. 97.32% ± 5.92), while relative to the negative control 1.1 ng/ml of TNF-α showed a trend towards increased activity (118.90% ± 4.22, p=0.081 vs. 100% ± 5.45), but not significantly. Albeit not significant, 25 ng/ml of TNF-α showed a trend towards increased mitochondrial dehydrogenase activity relative to cytokine cocktail B (116.50% ± 1.74, p=0.072 vs. 97.32% ± 5.92). The cells exposed to IFN-γ had no effect on mitochondrial dehydrogenase activity. Cells exposed to IL-1β showed no significant effect on mitochondrial dehydrogenase activity, but at 0.1 and 1 ng/ml a trend towards increased activity was observed relative to cytokine cocktail B (120.70% ± 5.70, p=0.062 and 119.60% ± 6.50, p=0.089 vs. 97.32% ± 5.92, respectively) (Figure 3.2 B).

Following 24 hours the INS1 cells exposed to cytokine cocktail B showed reduced mitochondrial dehydrogenase activity relative to the negative control (80.09 ± 5.89 p=0.031 vs. 100% ± 4.53) (Figure 3.2 C).

The cells exposed to 1.1 ng/ml of TNF-α, albeit not significant, showed a trend towards increased mitochondrial dehydrogenase activity after 24 hours when compared to both cytokine cocktail A (108.30% ± 5.48, p=0.066 vs. 90.56% ± 3.62) and cytokine cocktail B (108.30% ± 5.48, p=0.063 vs. 80.09% ± 5.89). However, 10 and 25 ng/ml of TNF-α indicated a significant increase in mitochondrial dehydrogenase activity relative to both cytokine cocktail A (110.30% ± 3.17, p=0.027 and 112.10% ± 4.75, p=0.011 vs. 90.56% ± 3.62) and cytokine cocktail B (110.30% ± 3.17, p=0.036 and 112.10% ± 4.75, p=0.021 vs. 80.09% ± 5.89) (Figure 3.2 C).

After 24 hours a significant increase in mitochondrial dehydrogenase activity was induced by IFN-γ at 1 ng/ml when compared to the negative control (121.10% ± 3.26, p=0.0055 vs. 100% ± 4.53). The cells exposed to 1, 10, and 100 ng/ml of IFN-γ showed a significant increase in mitochondrial dehydrogenase activity relative to both cytokine cocktail A (121.10% ± 3.26, p<0.001; 107.80% ± 3.61, p=0.038; and 107.50% ± 4.06, p=0.044 vs. 90.56% ± 3.62), respectively, and to cytokine cocktail B (121.10% ± 3.26, p=0.002; 107.80% ± 3.61, p=0.033; and 107.50% ± 4.06, p=0.036 vs. 80.09% ± 5.89) (Figure 3.2 C).

The cells exposed to 10 ng/ml of IL-1β for 24 hours showed a significant decrease in mitochondrial dehydrogenase activity relative to the negative control (77.10% ± 6.81, p=0.032 vs. 100% ± 4.53). Albeit not significant, 10 ng/ml of IL-1β showed a trend towards increased activity when compared to cytokine cocktail A (110.50% ± 5.55, p=0.083 vs. 90.56% ± 3.62) (Figure 3.2 C).

Thus, after the preliminary screening of the different individual pro-inflammatory cytokines as well as both cytokine cocktails it was indicated that cytokine cocktail A was not toxic to INS1 cells after 24 hours of exposure, while cytokine cocktail B showed a significant reduction in mitochondrial dehydrogenase activity. From these results it was decided to use cytokine cocktail A to induce an inflammatory state.
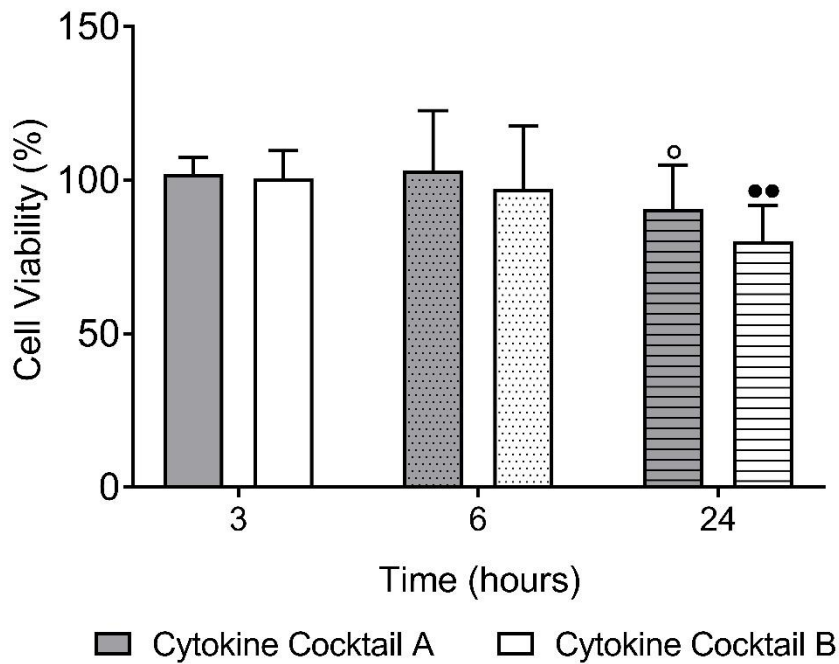
Figure 3.1: Effect of pro-inflammatory cytokine cocktails on cell viability. The effect of cytokine cocktail A and cytokine cocktail B on cell viability after 3, 6, and 24 hours of exposure under normal cell culture conditions. Cell viability was quantified by means of a MTT absorbance assay (570 nm). ☐: 3 hours; ☷: 6 hours; ☰: 24 hours

Data presented is the mean (± SEM) of three independent experiments (n=3). One-way ANOVA (Tukey post-hoc test); followed by a Man-Whitney test where appropriate; ^{o}=p<0.05 vs. cytokine cocktail A at 3 hours; ••=p<0.01 vs. cytokine cocktail B at 3 hours.
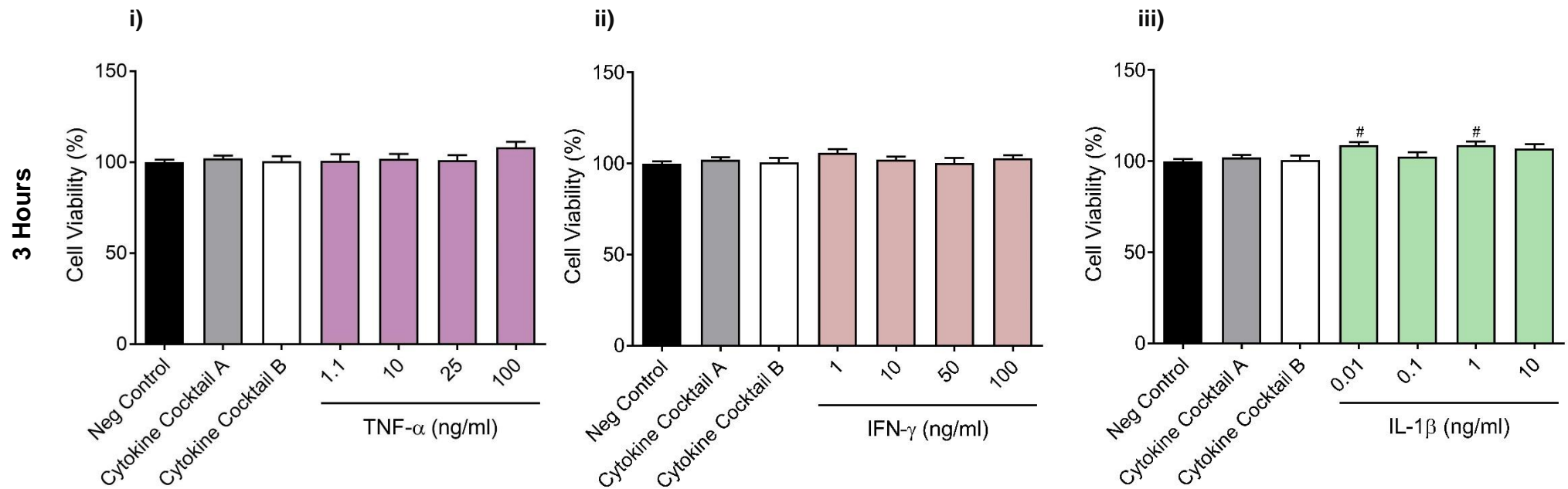
Figure 3.2 A: Effect of pro-inflammatory cytokines on INS1 cell viability. Effect of TNF-α (i), IFN-γ (ii), and IL-1β (iii), as well as two cytokine cocktails (A and B), on pancreatic β-cell viability 3 hours after exposure to the cytokines under normal cell culture conditions. Cell viability was quantified by means of a MTT absorbance assay (570 nm). Negative control: RPMI1640 medium.

Data presented is the mean (± SEM) of three independent experiments (n=3) relative to the negative control set at 100%. One-way ANOVA (Tukey post-hoc test); followed by a Man-Whitney test where appropriate; #=$p<0.05$ vs. negative control.
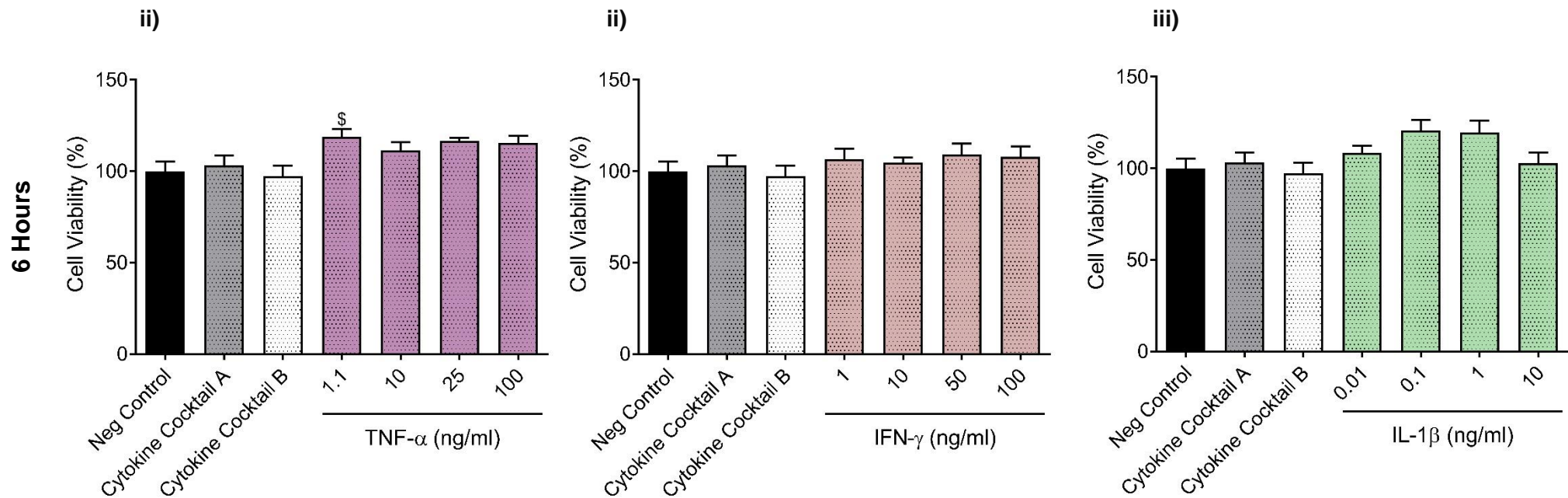
Figure 3.2 B: Effect of pro-inflammatory cytokines on INS1 cell viability. Effect of TNF-α (i), IFN-γ (ii), and IL-1β (iii), as well as two cytokine cocktails (A and B), on pancreatic β-cell viability 6 hours after exposure to the cytokines under normal cell culture conditions. Cell viability was quantified by means of a MTT absorbance assay (570 nm). Negative control: RPMI1640 medium.

Data presented is the mean (± SEM) of three independent experiments (n=3) relative to the negative control set at 100%. One-way ANOVA (Tukey post-hoc test); followed by a Man-Whitney test where appropriate; $^{\$}=p<0.05$ vs. cytokine cocktail B.
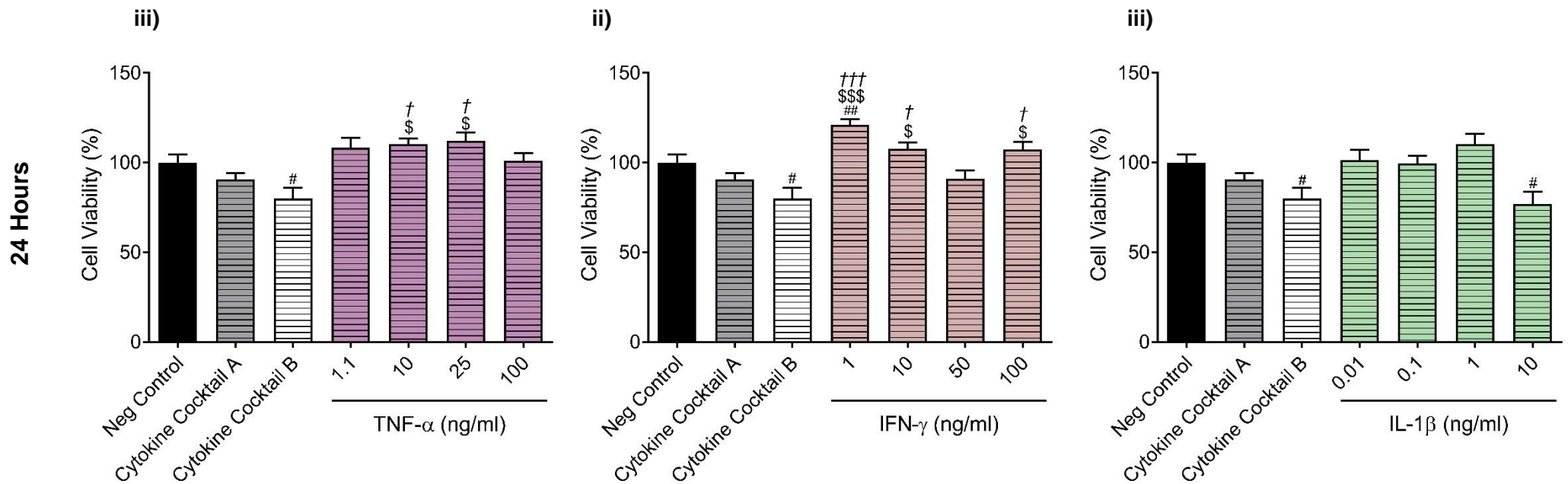
Figure 3.2 C: Effect of pro-inflammatory cytokines on INS1 cell viability. Effect of TNF-α (i), IFN-γ (ii), and IL-1β (iii), as well as two cytokine cocktails (A and B), on pancreatic β-cell viability 24 hours after exposure to the cytokines under normal cell culture conditions. Cell viability was quantified by means of a MTT absorbance assay (570 nm). Negative control: RPMI1640 medium.

Data presented is the mean (± SEM) of three independent experiments (n=3) relative to the negative control set at 100%. One-way ANOVA (Tukey post-hoc test); followed by a Man-Whitney test where appropriate; $^{\#}=p<0.05$, $^{\#\#}=p<0.01$ vs. negative control; $^{\dagger}=p<0.05$, $^{\dagger\dagger\dagger}=p<0.001$ vs. cytokine cocktail A; $^{\$}=p<0.05$, $^{\$\$\$}=p<0.001$ vs. cytokine cocktail B.

3.1.2. Effect of Asp, PPAG, and GRT on Rat Insulinoma Cell Viability –Toxicity

The effect of a range of concentrations of Asp, PPAG, and GRT on INS1 cells, in the absence of pro-inflammatory cytokines, was assessed by measuring cell viability with MTT assays. The negative control, not exposed to cytokine cocktail A or Asp, PPAG, or GRT, was set as 100% for statistical analysis and graphs.

After 24 hours of exposure of INS1 cells to Asp, no effect on mitochondrial dehydrogenase activity was observed when compared to the negative control. Albeit not significant, the lower concentrations of Asp (0.1, 1, 10, and 100 µM) showed a trend towards increased mitochondrial dehydrogenase activity relative to the pro-inflammatory cytokine cocktail A (108.00% ± 7.38, p=0.059; 106.40% ± 5.93, p=0.0503; 105.50% ± 6.75, p=0.094; and 101.70% ± 6.19, p=0.094 vs. 89.98% ± 4.08, respectively). In contrast to the lower concentrations, the highest concentration of Asp (1000 µM) showed a significant reduction in mitochondrial dehydrogenase activity relative to both the negative control as well as the pro-inflammatory cytokine cocktail A (46.06% ± 1.18, p<0.001 vs. 100% ± 5.73 and vs. 89.98% ± 4.08), respectively (Figure 3.3 A).

Rat insulinoma cells exposed to PPAG for 24 hours showed no measurable effect on mitochondrial dehydrogenase activity when compared to the negative control. However, 10 and 1000 µM of PPAG indicated a trend towards increased mitochondrial dehydrogenase activity relative to the pro-inflammatory cytokine cocktail A (106.00% ± 6.88, p=0.063 and 102.30% ± 4.77, p=0.094 vs. 89.98% ± 4.08, respectively), but not significantly (Figure 3.3 B).

Following a similar trend to Asp, INS1 cells exposed to GRT for 24 hours showed no effect on mitochondrial dehydrogenase activity, except for 0.1 mg/ml GRT where an increase in mitochondrial dehydrogenase activity was seen relative to the pro-inflammatory cytokine cocktail A (108.50% ± 5.01, p=0.03 vs. 89.98% ± 4.08); while 1 mg/ml of GRT significantly reduced mitochondrial dehydrogenase activity relative to both the negative control (69.83% ± 4.27, p=0.005 vs. 100% ± 5.73) as well as cytokine cocktail A (69.83% ± 4.27, p=0.008 vs. 89.98% ± 4.08) (Figure 3.3 C).
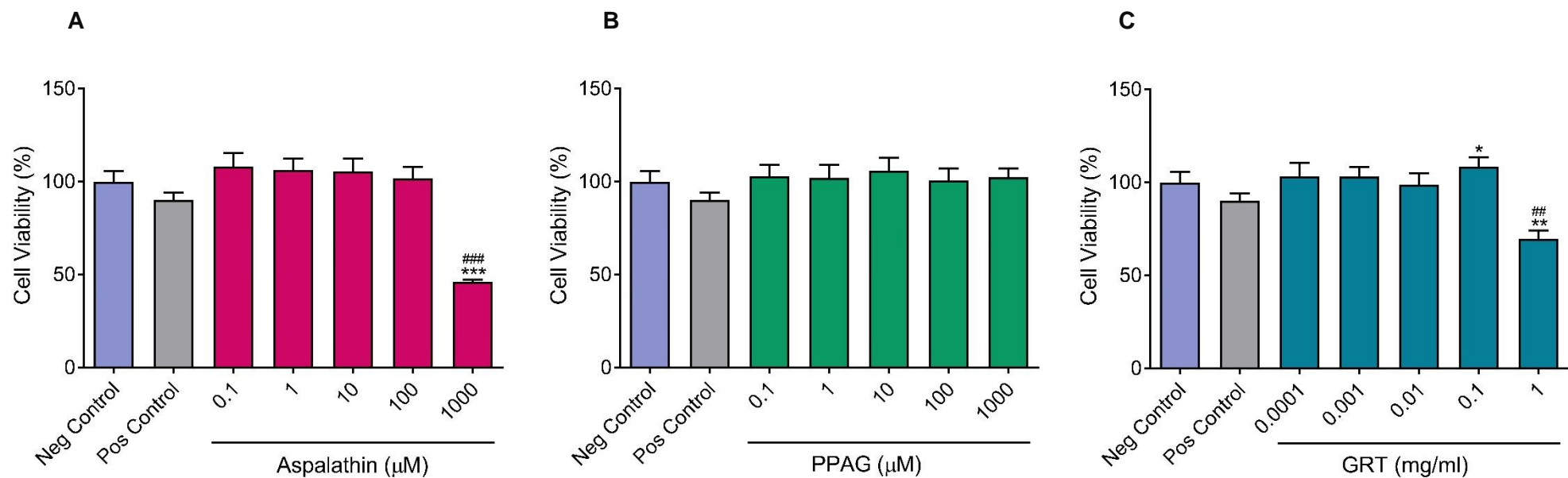
Figure 3.3: Effect of Asp, PPAG, and GRT on INS1 cell viability. Effect of Asp (A), PPAG (B), and GRT (C) exposure for 24 hours on pancreatic β-cell viability under normal cell culture conditions in the absence of a pro-inflammatory cytokine cocktail. Cell viability was quantified by means of a MTT absorbance assay (570 nm). Negative control: RPMI1640 medium; Positive control: Cytokine cocktail A.

Data presented is the mean (± SEM) of three independent experiments (n=3) relative to the negative control set at 100%. One-way ANOVA (Tukey post-hoc test); followed by a Man-Whitney test where appropriate; $^{\#\#}=p<0.01$; $^{\#\#\#}=p<0.001$ vs. negative control; $^{*}=p<0.05$; $^{**}=p<0.01$; $^{***}=p<0.001$ vs. positive control.

3.1.3. Effect of Asp PPAG, and GRT on Rat Insulinoma Cells Exposed to a Pro-Inflammatory Cytokine Cocktail

After exposing INS1 cells to cytokine cocktail A, as well as Asp, PPAG, and GRT the effect on cell viability was measured by performing MTT assays. The cells were exposed to the co-treatment for 24 hours. The negative control, not exposed to cytokine cocktail A or Asp, PPAG, or GRT, was set as 100% for statistical analysis and graphs.

The cells exposed to the pro-inflammatory cytokine cocktail A, although not statistical significant, showed reduced mitochondrial dehydrogenase activity relative to the negative control, and may be of biological significance to note (88.70% ± 4.17, p=0.077 vs. 100% ± 3.59) (Figure 3.4).

The INS1 cells co-treated with Asp and cytokine cocktail A showed no effect on mitochondrial dehydrogenase activity, except at the highest concentration of Asp (1000 µM) where a significant reduction was seen relative to both the negative control (19.02% ± 2.98, p<0.001 vs. 100% ± 3.59) and cytokine cocktail A (19.02% ± 2.98, p<0.001 vs. 88.70% ± 4.17) (Figure 3.4 A). The latter correspond with the effect seen when the INS1 cells were exposed to Asp in the absence of cytokines, just exacerbated indicative of a synergestic effect (section 3.1.2; Figure 3.3 A).

Cells co-treated with PPAG and the pro-inflammatory cytokine cocktail A showed no effect on mitochondrial dehydrogenase activity after 24 hours (Figure 3.4 B).

As was seen with Asp, cells exposed to cytokine cocktail A and GRT showed a significant reduction in mitochondrial dehydrogenase activity only at the highest concentration of 1 mg/ml relative to both the negative control (36.88% ± 1.53, p<0.001 vs. 100% ± 3.59) as well as cytokine cocktail A (36.88% ± 1.53, p<0.001 vs. 88.70% ± 4.17) (Figure 3.4 C). The significant decrease in mitochondrial dehydrogenase activity corresponds with the toxicity effect seen when the INS1 cells were only exposed to the GRT extract, in the absence of induced inflammation (section3.1.2; Figure 3.3 C).

Figure 3.4: Effect of Asp, PPAG, and GRT on INS1 cells exposed to pro-inflammatory cytokines. Effect of Asp (A), PPAG (B), and GRT (C) on the viability of pancreatic β-cells exposed to pro-inflammatory cytokine cocktail A for 24 hours under normal cell culture conditions. Cell viability quantified by means of a MTT absorbance assay (570 nm). Negative control: RPMI1640 medium; Positive control: Cytokine cocktail A.

Data presented is the mean (± SEM) of three independent experiments (n=3) relative to the negative control set at 100%. One-way ANOVA (Tukey post-hoc test); ###=p<0.001 vs. negative control; ***=p<0.001 vs. positive control.

3.1.4. Cellular ATP Content in Rat Insulinoma Cells

Intracellular ATP content in INS1 cells exposed to pro-inflammatory cytokines was also assessed after 24 hours of co-treatment. Luminescent signals were normalised to the protein values obtained by performing the Bradford assay. The negative control, not exposed to cytokine cocktail A or Asp, PPAG, or GRT, was set as 100% for statistical analysis and graphs.

The INS1 cells co-treated with Asp and cytokine cocktail A showed no effect on cellular ATP content, except at the highest concentration of Asp (1000 µM) where a decrease was seen relative to the negative control (79.11% ± 2.79, p=0.011 vs. 100% ± 6.62) and to cytokine cocktail A (79.11% ± 2.79, p=0.046 vs. 97.64% ± 8.46) (Figure 3.5 A).

The INS1 cells co-treated with PPAG and cytokine cocktail A showed no marked changes in cellular ATP content, except at the highest concentration of PPAG (1000 µM) where an increase relative to the negative control (129.70% ± 18.23, p=0.018 vs. 100% ± 6.62) and to cytokine cocktail A (129.70% ± 18.23, p=0.049 vs. 97.64% ± 8.46) was seen (Figure 3.5 B).

The INS1 cells exposed to cytokine cocktail A and GRT showed similar results to the results observed for the MTT assay, with decreased cellular ATP content at the highest concentration (1 mg/ml) relative to the negative control (46.96% ± 5.27, p=0.0004 vs. 100% ± 6.62) and to cytokine cocktail A (46.96% ± 5.27, p=0.0007 vs. 97.64% ± 8.46), respectively (Figure 3.5 C). Albeit not significant, 0.01 and 0.1 mg/ml of GRT showed a trend towards reduced ATP content when compared to the negative control (80.26% ± 7.93, p=0.094 and 81.59% ± 6.13, p=0.059 vs. 100% ± 6.62, respectively) (Figure 3.5 C).
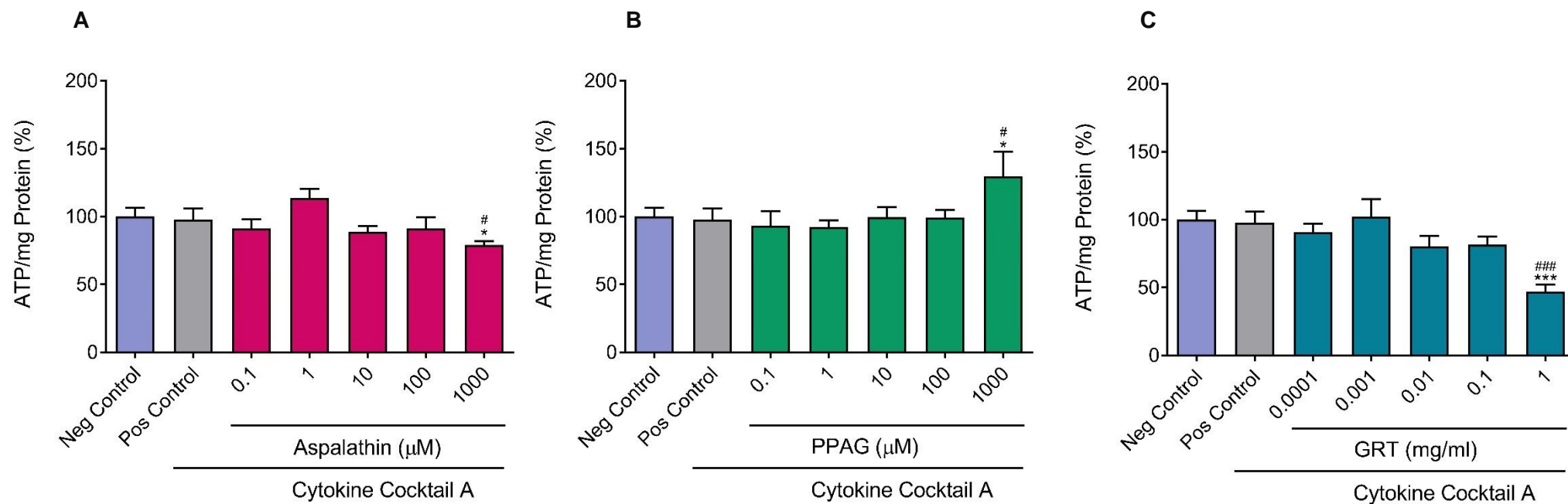
Figure 3.5: Effect of Asp, PPAG, and GRT on cellular ATP content in INS1 cells exposed to pro-inflammatory cytokines. Effect of Asp (A), PPAG (B), and GRT (C), on cellular ATP content in INS1 pancreatic β-cells exposed to pro-inflammatory cytokines for 24 hours after co-treatment under normal cell culture conditions. Luminescent quantification of cellular ATP content. Negative control: RPMI1640 medium; Positive control: Cytokine cocktail A.

Data presented is the mean (± SEM) of three independent experiments (n=3), relative to the negative control set at 100%. One-way ANOVA (Tukey post-hoc test); followed by a Man-Whitney test where appropriate; #=$p<0.05$, ###=$p<0.001$ vs. negative control; *=$p<0.05$, ***=$p<0.001$ vs. positive control.

3.1.5.   Apoptosis / Necrosis in Rat Insulinoma Cells

3.1.5.1.   Annexin-V / Propidium Iodide – Kinetic Assays

To assess the effect of Asp, PPAG, and GRT on INS1 cells exposed to pro-inflammatory cytokine cocktail A, cell survival and death of co-treated cells were assessed by kinetically determining early apoptosis as well as necrosis measuring AV/PI fluorescence hourly over a period of 24 hours. The AUC for each treatment was calculated over the 24 hours of co-treatment and expressed as an overall effect. The negative control, not exposed to cytokine cocktail A or Asp, PPAG, or GRT, was set as 100% for statistical analysis and graphs.
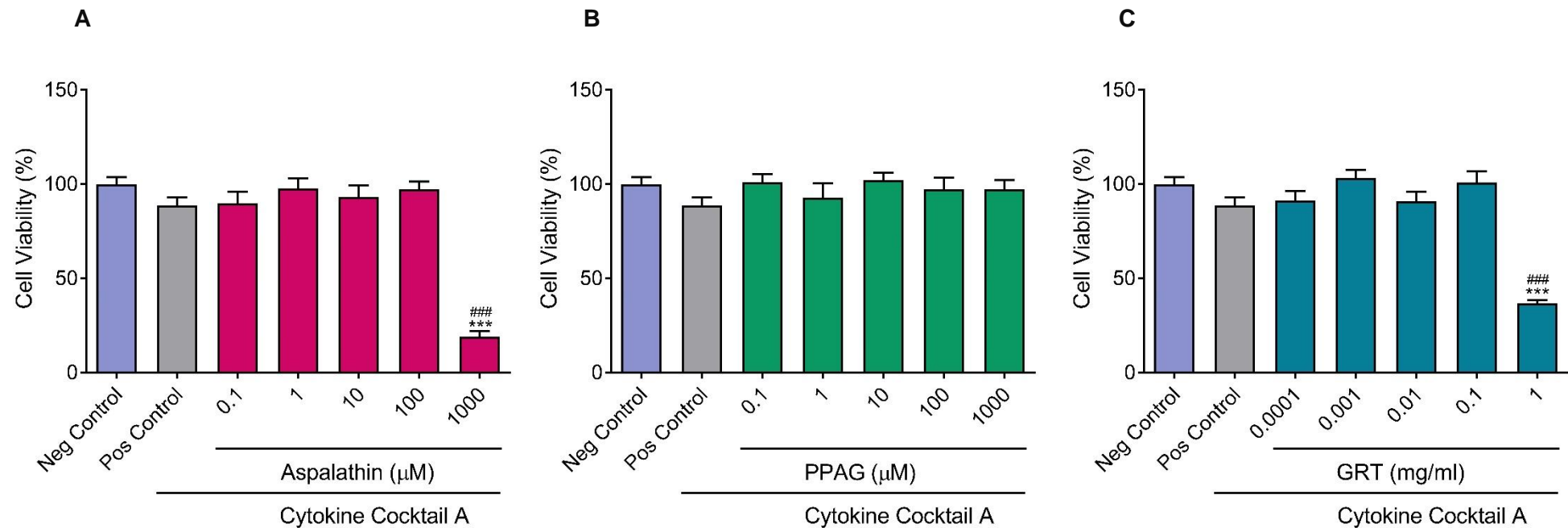
After 24 hours the cells exposed to pro-inflammatory cytokine cocktail A had no effect of the early apoptosis, but, although not significant, a trend towards increased necrosis relative to the negative control (143% ± 20.19, p=0.086 vs. 100% ± 12.06) was seen (Figure 3.6).

The INS1 cells co-treated with Asp only had an effect on the rate of early apoptosis at the highest concentration (1000 µM) that showed a significant increase in early apoptosis relative to both the negative control (287.10% ± 44.70, p<0.001 vs. 100% ± 12.41) and cytokine cocktail A (287.10% ± 44.70, p<0.001 vs. 119.40% ± 15.79), respectively. Exposure of INS1 cells to the pro-inflammatory cytokine cocktail A with Asp also showed a significant increase in necrosis at the highest concentration (1000 µM) when compared to both the negative control (673.70% ± 135.80, p<0.001 vs. 100% ± 12.06) as well as cytokine cocktail A (673.70% ± 135.80, p<0.001 vs. 143.00% ± 20.19), respectively (Figure 3.6 A). These findings verify the previous MTT results of cell viability seen (section 3.1.3).

Cells co-treated with PPAG showed a significant increase in early apoptosis only at the highest concentration (1000 µM) relative to the negative control (190.30% ± 22.69, p=0.003 vs. 100% ± 12.41) and cytokine cocktail A (190.30% ± 22.69, p=0.045 vs. 121.10% ± 15.00). However, PPAG co-treatment had no effect on necrosis in INS1 cells (Figure 3.6 B).

The INS1 cells co-treated with GRT showed a significant increase in early apoptosis at the highest concentration (1 mg/ml) relative to both the negative control (586.50% ± 70.81, p<0.001 vs. 100% ± 12.41) and cytokine cocktail A (586.50% ± 70.81, p<0.001 vs. 124.70% ± 13.97), respectively. Cells exposed to 0.1 mg/ml of GRT significantly increased necrosis relative to the negative control (196.90% ± 18.14, p=0.0002 vs. 100% ± 12.06), the highest concentration of GRT also significantly increased necrosis relative to both the negative control (1815.00% ± 270.60, p<0.001 vs. 100% ± 12.06) and cytokine cocktail A (1815.00% ± 270.60, p<0.001 vs. 143.00% ± 20.19), respectively (Figure 3.6 C). These effects seen verify the results seen in the MTT as well as ATP assays (section 3.1.3 and 3.1.4).
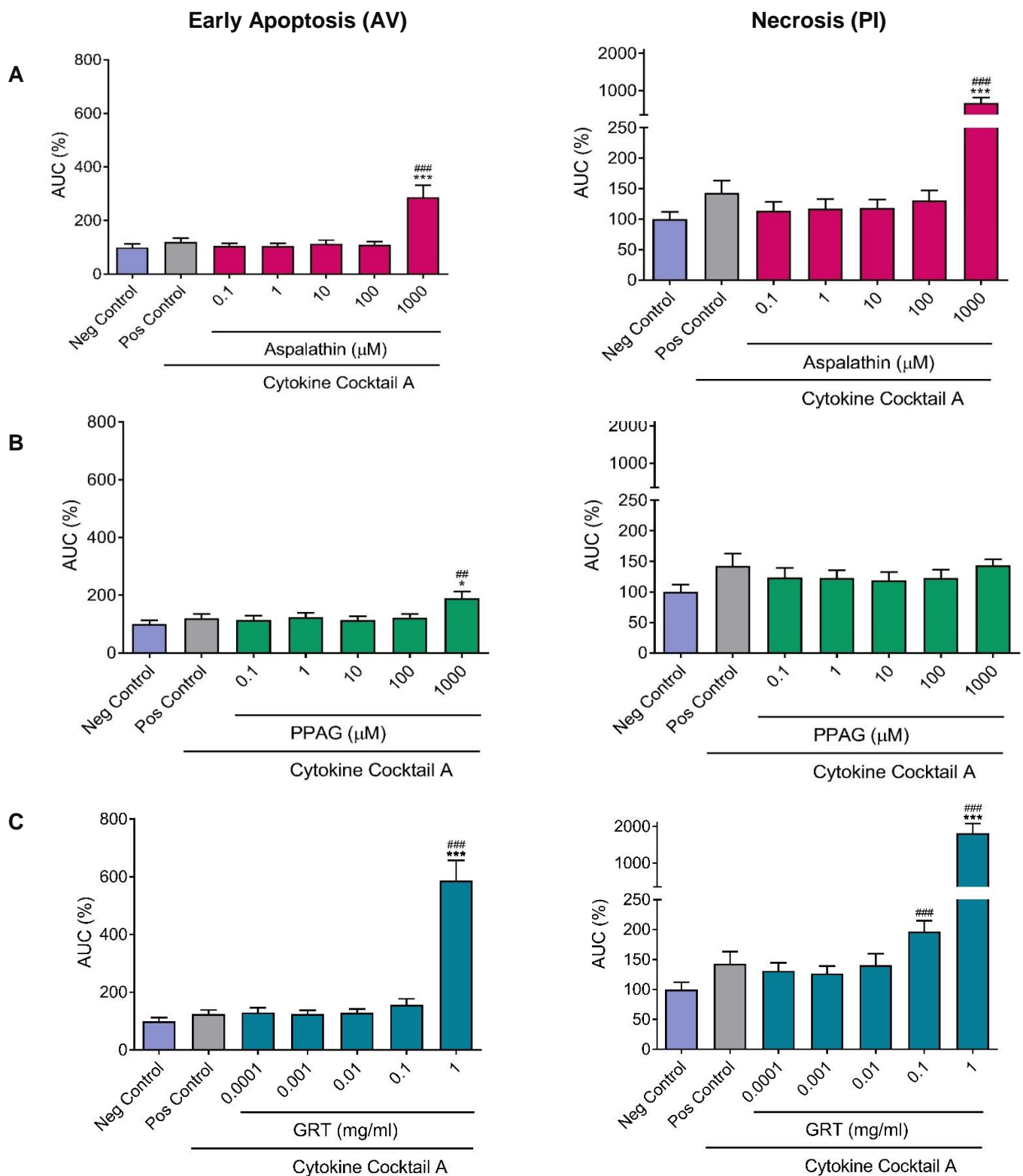
Figure 3.6: Early apoptosis and necrosis in INS1 cells exposed to pro-inflammatory cytokines. Effect of Asp (A), PPAG (B), and GRT (C) on INS1 pancreatic β-cell death was assessed kinetically over 24 hours, under normal cell culture conditions. Fluorescent quantification of early apoptosis and necrosis by means of an AV/PI assay using the SpectraMaxi3 (AV: Ex 485 nm/Em 535 nm; PI: Ex 535 nm/Em 617 nm). Negative control: RPMI1640 medium; Positive control: Cytokine cocktail A.

Data presented is the mean (± SEM) of three independent experiments (n=3), relative to the negative control set at 100%. One-way ANOVA (Tukey post-hoc test); followed by a Man-Whitney test where appropriate; $^{\#\#}=p<0.01$; $^{\#\#\#}=p<0.001$ vs. negative control; $^{*}=p<0.05$, $^{***}=p<0.001$ vs. positive control.

3.1.5.2.   Annexin-V / Propidium Iodide - Flow Cytometry

Survival and death of INS1 cells, 24 hours after exposure to co-treatments, was further assessed by measuring early apoptosis, late apoptosis, and necrosis by measuring the fluorescence of AV and PI using flow cytometry. The negative control not exposed to cytokine cocktail A or Asp, PPAG, or GRT, was used for statistical analysis and graphs.

In flow cytometry, the intensity of a distribution can be represented by the position of the "centre" of the distribution. The "centre" is usually represented mathematically by the mean, median or peak channel number. However, the data was not normally distributed; therefor the mean and median are not equal. It is necessassary to assess the mean and median of the data as change in one or the other may not be the same and may lead to misinterpretation of the data.

Flow cytometry analysis of univariate histograms used to assess the fluorescence intensity, as indicated by the treated population's mean fluorescence intensity, showed a significant increase in FL-1 AV intensity in the cells exposed to cytokine cocktail A (15450.00 RFU ± 1522.00, $p<0.001$ vs. 7749.00 RFU ± 491.20). The groups co-treated with Asp, PPAG, GRT, and inhibitor A showed a significant decrease in FL-1 intensity in comparison to cytokine cocktail A (9892.00 RFU ± 514.90, $p<0.001$; 7804.00 RFU ± 225.30, $p<0.001$; 10743.00 RFU ± 527.60, $p=0.0016$; and 8484.00 RFU ± 651.80, $p<0.001$ vs. 15455.00 RFU ± 1522.00) (Figure 3.7 and Figure 3.8 A). Cells co-treated with GRT showed a significant increase in FL-4 intensity when compared to both the negative control (1424.00 RFU ± 55.22, $p<0.001$ vs. 556.00 RFU ± 8.90) and cytokine cocktail A (1424.00 RFU ± 55.22, $p<0.001$ vs. 617.40 RFU ± 51.29) (Figure 3.7 and Figure 3.8 A). However, the fluorescence intensity measured by the treated population's median fluorescence intensity showed no significant change in FL-1 AV intensity; while cells co-treated with PPAG showed a significant decrease in FL-4 intensity relative to the negative control (373.40 RFU ± 5.64, $p=0.0188$ vs. 425.70 RFU ± 7.81) and cells co-treated with GRT a significant increase when compared to both the negative control (695.80 RFU ± 24.78, $p<0.001$ vs. 425.70 RFU ± 7.81) and to cytokine cocktail A (695.80 RFU ± 24.78, $p<0.001$ vs. 401.70 RFU ± 8.36) (Figure 3.7 and Figure 3.8 B). Results indicated in Figure 3.8 can also be seen in the representative images of peak shifts histograms seen in Figure 3.7.

In Figure 3.9 A, a theoretical representation of multivariate dot plot analysis for cell survival and death (apoptosis/necrosis) by flow cytometry using AV/PI. Increasing AV positivity (green fluorescence (FL1)) indicates early apoptosis, whilst increasing PI staining (orange/red fluorescence (FL-4)) indicates late apoptosis or necrosis. Representative flow cytometry dot

plot images used to quantify population shifts into demarcated quadrants with different treatments, indicating live (lower left quadrant), early apoptotic (lower right quadrant), late apoptotic (upper right quadrant) and necrotic (upper left quadrant) cells (Figure 3.9 B, C, D, E and F). Cells exposed to cytokine cocktail A showed a significant decrease in the live cell population (lower left quadrant) when compared to the negative control (75.85% ± 2.38, $p<0.001$ vs. 88.64% ± 1.71). A significant decrease in cell viability is also seen in the group co-treated with GRT in comparison to the negative control (76.08% ± 0.77, $p<0.001$ vs. 88.64% ± 1.71) as graphically illustrated in Figure 3.10. Cells exposed to Asp, PPAG, or inhibitor A showed a significant increase in cell viability when compared to cytokine cocktail A (83.55% ± 1.41, $p=0.011$; 88.70% ± 1.05, $p<0.001$; and 86.53% ± 1.32, $p=0.0002$ vs. 75.85% ± 2.38), respectively as graphically illustrated in Figure 3.10.

Cells exposed to cytokine cocktail A showed a significant increase in early apoptosis (lower right quadrant) in comparison to the negative control (19.15% ± 1.82, $p<0.001$ vs. 8.63% ± 1.44). Groups co-treated with Asp, PPAG, GRT, or inhibitor A showed a significant decrease in early apoptosis in comparison to cytokine cocktail A (11.85% ± 0.98, $p=0.0011$; 8.62% ± 0.84, $p<0.001$; 11.34% ± 0.73, $p=0.006$; and 9.58% ± 0.96, $p<0.001$ vs. 19.15% ± 1.82, respectively) (Figure 3.10).

After the 24 hours, the cells exposed to cytokine cocktail A and the cells co-treated with GRT showed a significant increase in late apoptosis (upper right quadrant) when compared to the negative control (3.26% ± 0.89, $p=0.02$ and 4.79% ± 0.30, $p<0.001$ vs. 0.98% ± 0.19, respectively) (Figure 3.10).

Interestingly, the cells co-treated with GRT showed a significant increase in necrosis (upper right quadrant) when compared to both the negative control and cytokine cocktail A (7.66% ± 0.32, $p<0.001$ vs. 1.74% ± 0.23 and 1.75% ± 0.59, respectively); while no effect was seen in the other groups (Figure 3.10).
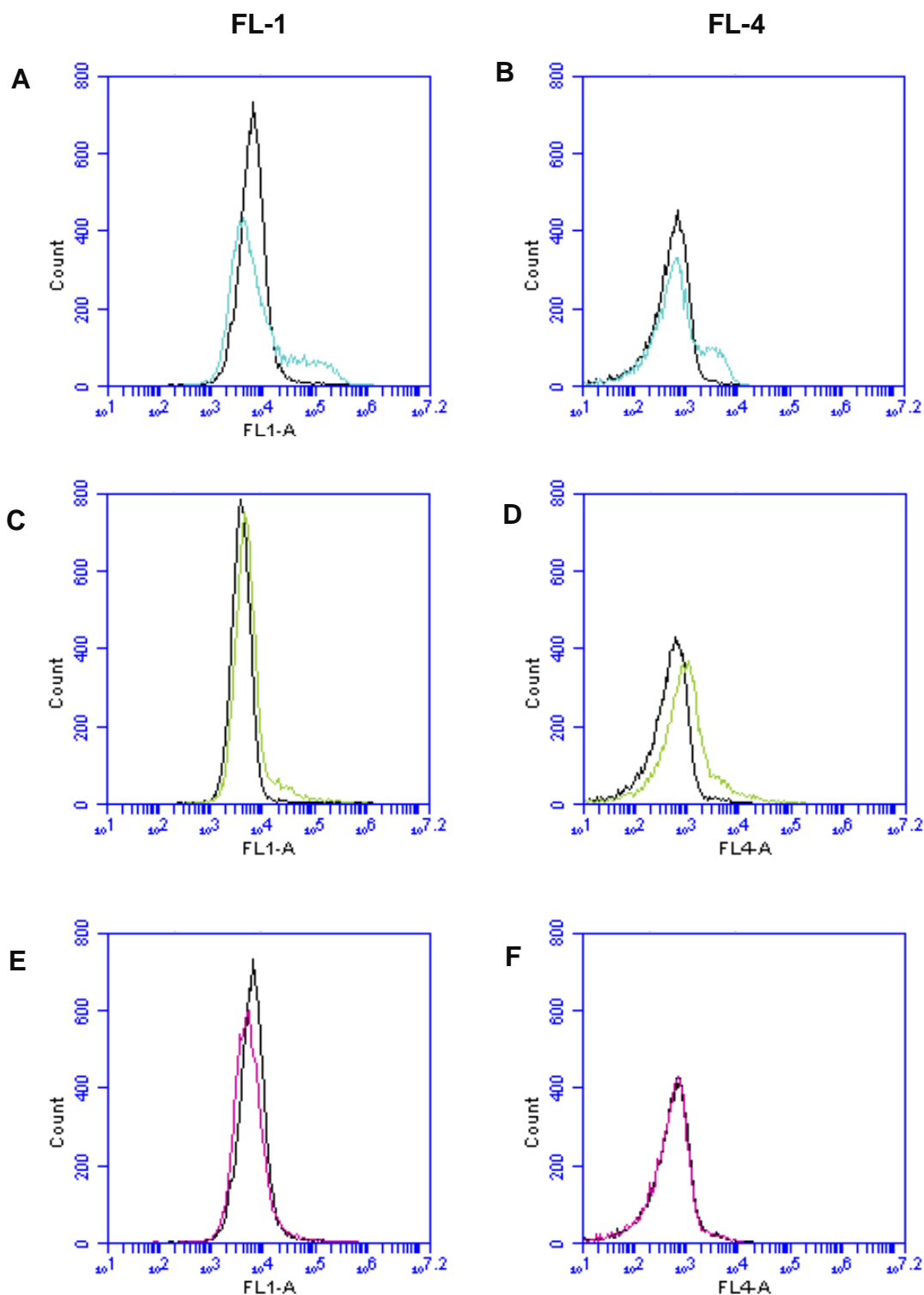
Figure 3.7: FL-4 / FL-1 histograms. Histograms indicating the shift in fluorescence measured by AV/PI, showing the shift in cell viability of INS1 cells assessed 24 hours after exposure to co-treatment under normal cell culture conditions. Fluorescent quantification of apoptosis and necrosis were assessed using an AV/PI assay by means of flow cytometry. Peak shift in FL-1 (A) and FL-4 (B) of the positive control to negative control; peak shift in FL-1 (C) and FL-4 (D) of the GRT (0.1 mg/ml) to negative control; peak shift in FL-1 (E) and FL- 4 (F) of the inhibitor A (39 µM) to negative control.
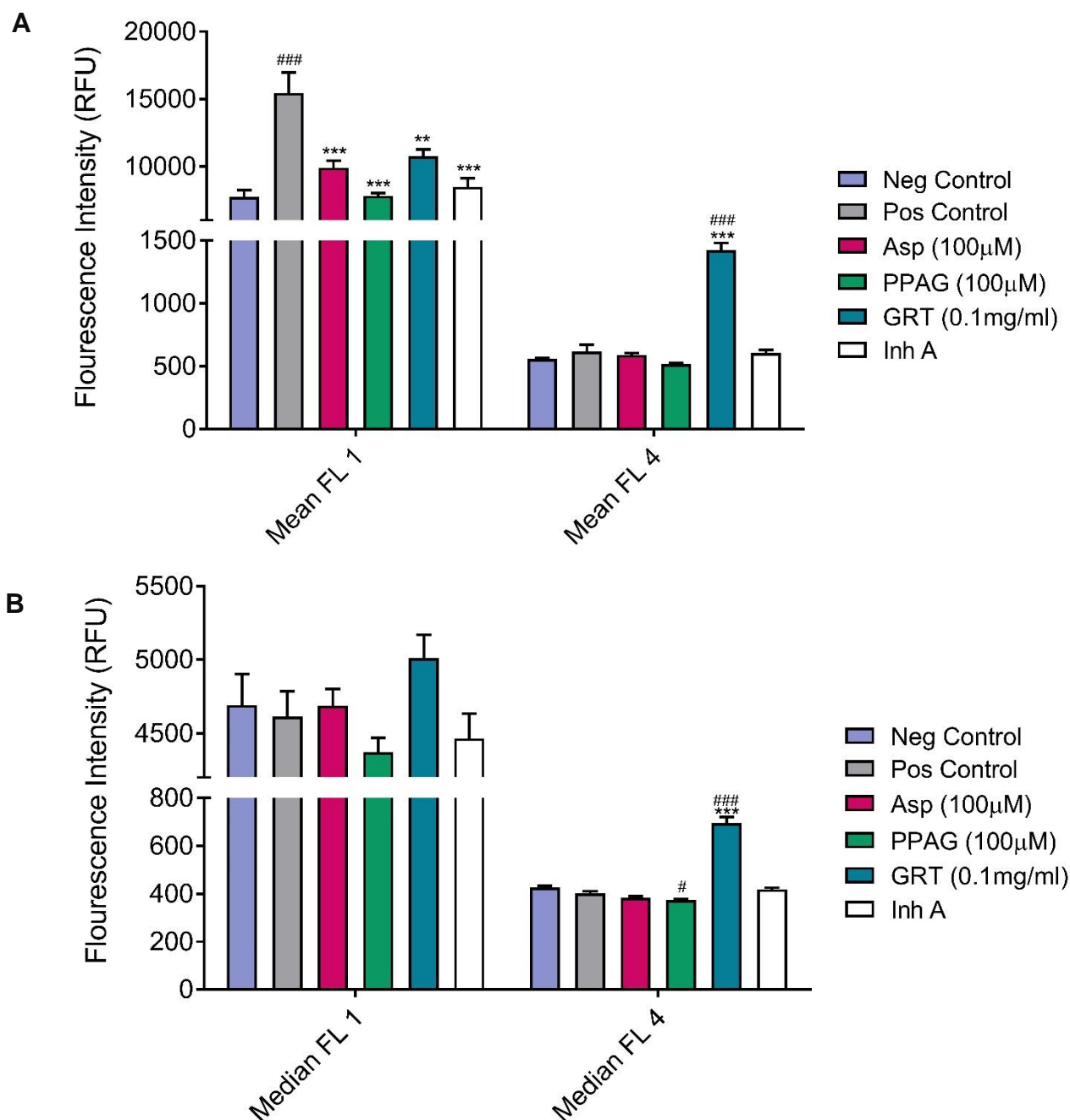
Figure 3.8: Apoptosis and necrosis in INS1 cells – Flow cytometry (AV/PI). Effect of Asp (100 μM), PPAG (100 μM), GRT (0.1 mg/ml), and inhibitor A (39μM) on inflamed pancreatic β-cell viability assessed 24 hours after exposure to co-treatment under normal cell culture conditions. Fluorescent quantification of apoptosis and necrosis were assessed using an AV/PI assay by means of flow cytometry. Fluorescent intensity measured by the mean of the treated population (A); fluorescent intensity measured by the median of the treated population (B). Negative control: RPMI1640 medium; Positive control: Cytokine cocktail A.

Data presented is the mean (± SEM) of three independent experiments (n=3), relative to the negative control. One-way ANOVA (Tukey post-hoc test); #=$p<0.05$; ###=$p<0.001$ vs. negative control; **=$p<0.01$, ***=$p<0.001$ vs. positive control.
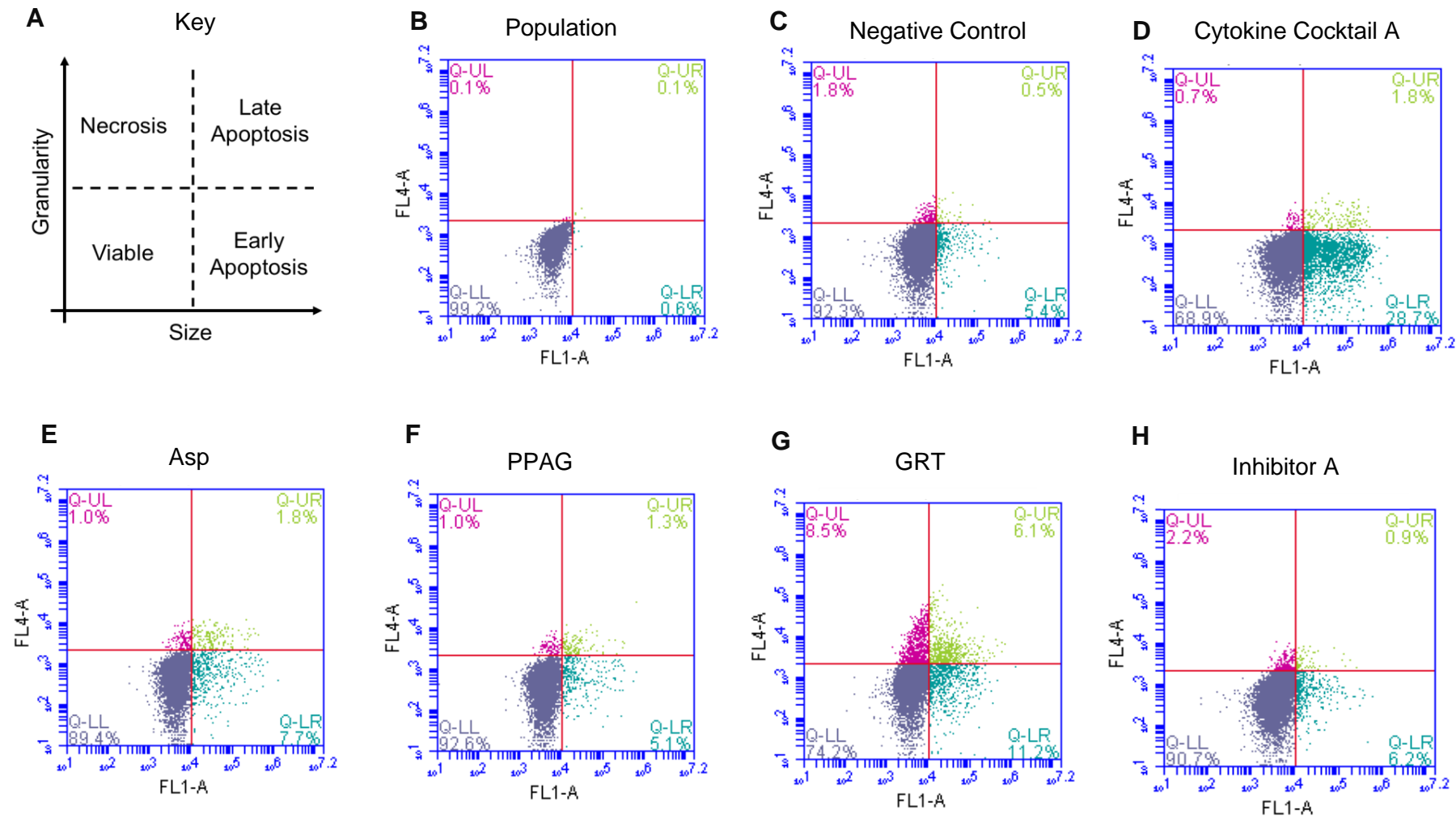
Figure 3.9: Effect of Asp, PPAG, and GRT on cell survival and death in INS1 cells exposed to pro-inflammatory cytokines. Flow cytometry analysis of AV/PI stained INS1 cells exposed to pro-inflammatory cytokines and co-treated with Asp, PPAG, or GRT for 24 hours. Diagrammatic presentation indicating the shift in cell viability as measured by AV/PI (A). Population of INS1 cells used for flow cytometry analysis (B). Negative control (C), pro-inflammatory cytokine cocktail A (D), Asp co-treatment (E), PPAG co-treatment (F), GRT co-treatment (G) and treatment with inhibitor A (39 µM) (H).
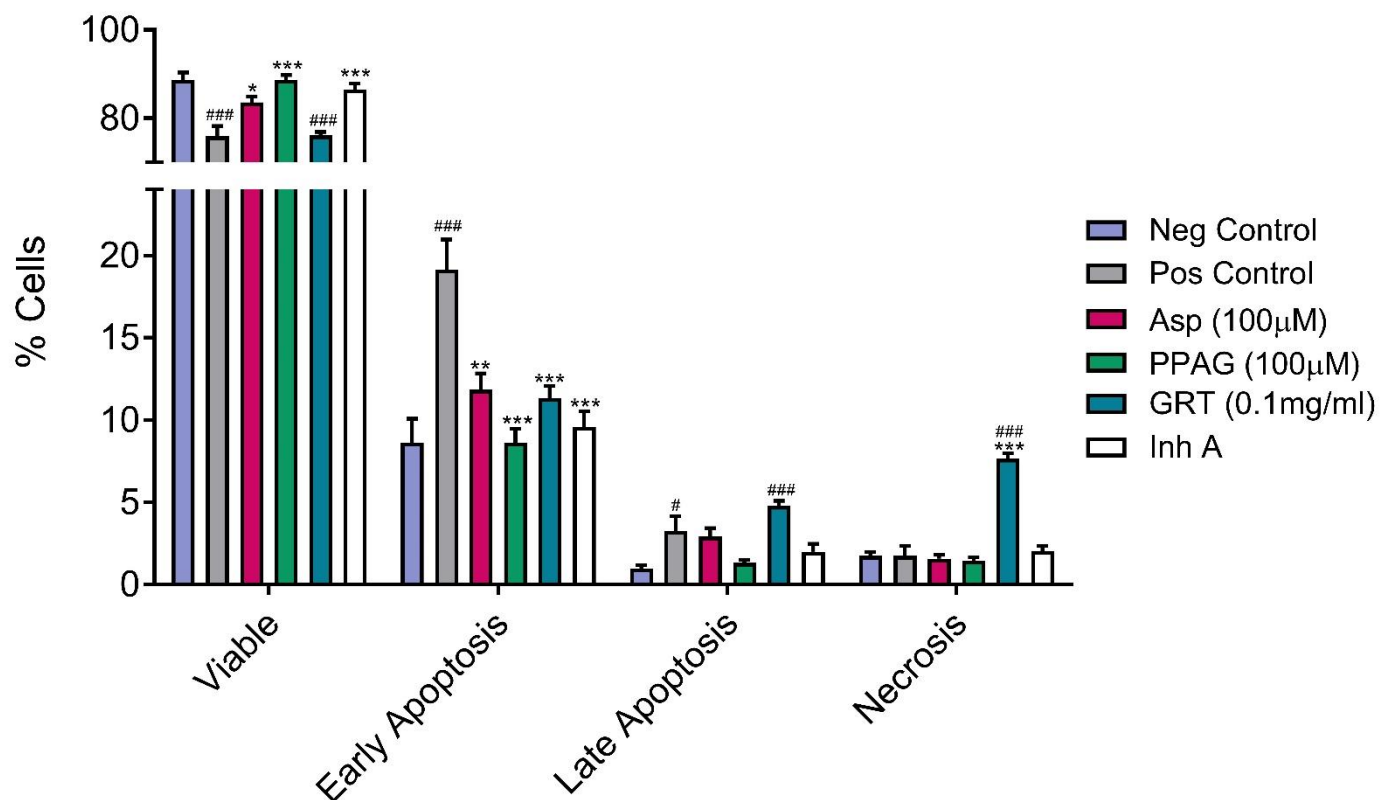
Figure 3.10: Effect of Asp, PPAG, and GRT on cell survival and death in INS1 cells exposed to pro-inflammatory cytokines. Graphical comparison of flow cytometry analysis of AV/PI stained INS1 cells exposed to pro-inflammatory cytokines and co-treated with Asp (100 μM), PPAG (100 μM), GRT (0.1 mg/ml), and inhibitor A (39 μM) for 24 hours under normal cell culture conditions. Negative control: RPMI1640 medium; Positive control: Cytokine cocktail A.

Data presented is the mean (± SEM) of three independent experiments (n=3), relative to the negative control. One-way ANOVA (Tukey post-hoc test); #=p<0.05, ###=p<0.001 vs. negative control; *=p<0.05, **=p<0.01, ***=p<0.001 vs. positive control.

Table 3.1: Cell viability as measured by AV/PI by using flow cytometry. Indication of the percentage of cells from the total number of cells (per treatment group) classified according to viability.

Treatment	Viable (%)	Early Stage Apoptosis (%)	Late Stage Apoptosis (%)	Necrosis (%)	Total (%)
Negative Control	88.64	8.63	0.98	1.76	100
Positive Control	75.80[a]	19.18[a]	3.20[b]	1.81	100
Asp	83.61[c]	11.80[d]	2.94	1.65	100
PPAG	88.64[e]	8.56[e]	1.32	1.47	100
GRT	76.05[a]	11.38[e]	4.82[a]	7.76[a, e]	100
Inhibitor A	86.52[e]	9.54[e]	1.97	1.97	100

[a]: #=p<0.05; [b]: ###= p<0.001 vs. negative control; [c]: *= p<0.05, [d]: **= p<0.01, [e]: ***= p<0.001 vs. positive control.

3.1.5.3.   Caspase-3/7 Activation in Rat Insulinoma Cells - Kinetic

Apoptosis of co-treated INS1 cells were assessed by hourly readings of caspase-3/7 activation over 24 hours. The AUC for each treatment was calculated over the 24 hours of co-treatment and expressed as an overall effect. The negative control not exposed to cytokine cocktail A or Asp, PPAG, or GRT was set as 100% for statistical analysis and graphs.

The cells exposed to the pro-inflammatory cytokine cocktail A showed a trend towards increased caspase-3/7 activation relative to the negative control (198.60% ± 53.30, p=0.084 vs. 100% ± 11.54), but not significantly (Figure 3.11). The fact that this change is not significant, while the change in the GRT co-treated group is significant, even if the mean value is lower than the cytokine cocktail's mean compared to the negative control, can be explained by the large SEM of the cytokine cocktail group.

Overall the INS1 co-treated with Asp showed no effect in apoptosis when compared to the negative control, except at the highest concentration of Asp (1000 µM) where an increase in apoptosis is seen relative to the negative control (303.40% ± 47.47, p=0.0006 vs. 100% ± 11.54) (Figure 3.11 A).

Cells co-treated with PPAG and the pro-inflammatory cytokine cocktail A had no effect on caspase-3/7 activation (Figure 3.11 B).

Co-treatment with GRT at the highest concentration (1 mg/ml) showed increased apoptosis when compared to the negative control (207% ± 19.26, p=0.005 vs. 100% ± 11.54) (Figure 3.11 C). The increase in late apoptosis of INS1 at the highest concentrations of both Asp and GRT verify the decrease observed cell viability in other experiments.
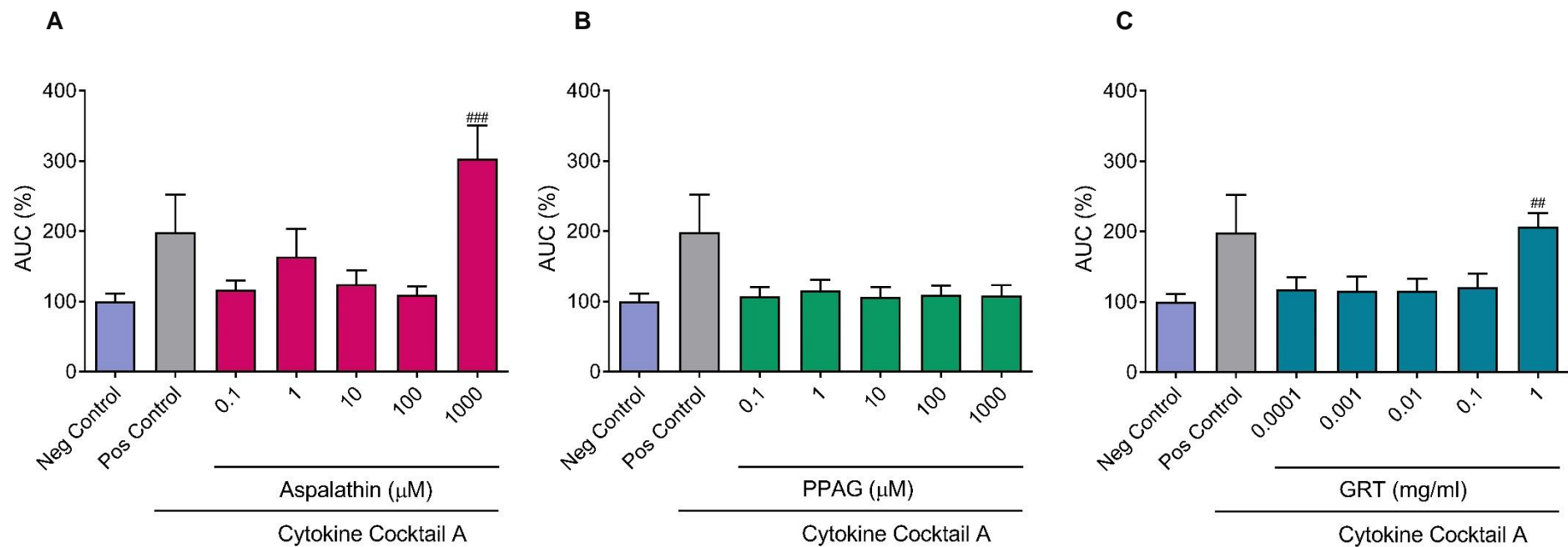
Figure 3.11: Effect of Asp, PPAG, and GRT on caspase-3/7 activation in INS1 cells exposed to pro-inflammatory cytokines. Kinetic caspase-3/7 activation assay over a 24-hour period presented as the area under the curve of the hourly measurements. Asp (A), PPAG (B) and GRT co-treatment (C). Caspase-3/7 activation was assessed hourly over 24 hours, under normal cell culture conditions using the SpectraMaxi3 (Ex 485 nm / Em 535 nm). Negative control: RPMI1640 medium; Positive control: Cytokine cocktail A.

Data presented is the mean (± SEM) of three independent experiments (n=3), relative to the negative control set at 100%. One-way ANOVA (Tukey post-hoc test); followed by a Man-Whitney test where appropriate; ##=p<0.01, ###=p<0.001 vs. negative control.

3.1.5.4. Caspase-3/7 Activation in Rat Insulinoma Cells – Fluorescence Imaging

Caspase-3/7 activation during the kinetic assay was visualised and quantified by fluorescent microscopy; as well as phase microscopy images of to assess cell morphology relating to cell viability. The fluorescent images were taken at the exact same area of the well as the phase microscopy images.   Caspase-3/7 positive cells are detected by their intense green fluorescent signal (Figure 3.12).

Under normal culture conditions healthy INS1 cells have a stellate or polyglonal shape and a clustering growth orientation, indicating good cell viability as the INS1 cell clusters are closely associated and are fixed to cell culture dish and the cytoplasm evenly spread (Figure 3.12 A; i) (Asfari et al., 1992; Fu et al., 2009; Hamid et al., 2002; Merglen et al., 2004).

Compared to the normal control INS1 cells exposed to cytokine cocktail A displayed a more multipolar spindle shape with larger open spaces between cells suggesting some retraction of cytoplasm volume, a decrease in cell size and loss of adhesion. The fluorescent images of the cells exposed to cytokine cocktail A demonstrate a slight increase in caspase-3/7 positive fluorescence cells (Figure 3.12 A; ii).

The INS1 cells co-treated with Asp (100 µM) and PPAG (100 µM) are morphologically similar to the stellate shaped cells and display a similar growth pattern as seen in the normal control cells, compared to cell exposed to the pro-inflammatory cytokine cocktail A where fewer caspase-3/7 positive cells were present (Figure 3.12 B; iii and iv).

Rat insulinoma cells co-treated with GRT (0.1 mg/ml) were morphologically similar to stellate shaped cells seen in the normal controls, however the cell growth pattern showed less clustering with larger spaces, suggesting loss of cells or cell volume compared to the normal control. The increase in caspase-3/7 positive cells compared to the normal control, albeit less than the pro-inflammatory control, supports increased apoptosis (Figure 3.12 B; v).
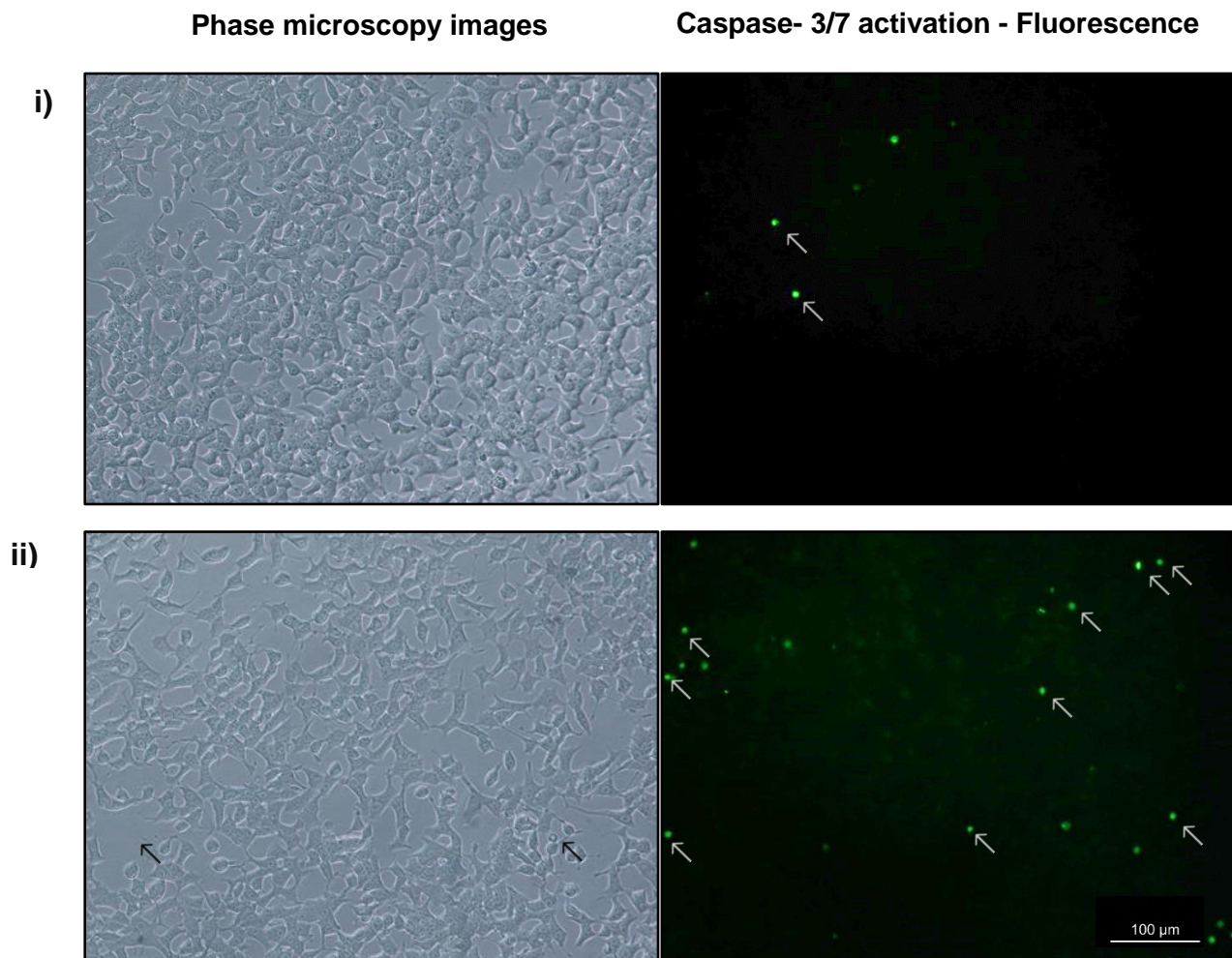
Figure 3.12 A: Effect of Asp, PPAG, and GRT on cell morphology and caspase-3/7 activation in INS1 cells exposed to pro-inflammatory cytokines. Representative light photomicrographs and fluorescent images of caspase-3/7 activation after 24 hours of co-treatment. Negative control (i) and cytokine cocktail A (ii). Images were taken on the Nikon inverted microscope at 20x objective; 200x magnification. Change in cell viability related to morphology and number of cells are indicated with black arrows. Fluorescent signal as result of caspase-3/7 activation is indicated with white arrows. Scale bar: 100 µm.

Phase microscopy images	Caspase- 3/7 activation - Fluorescence

iii)

iv)

v)
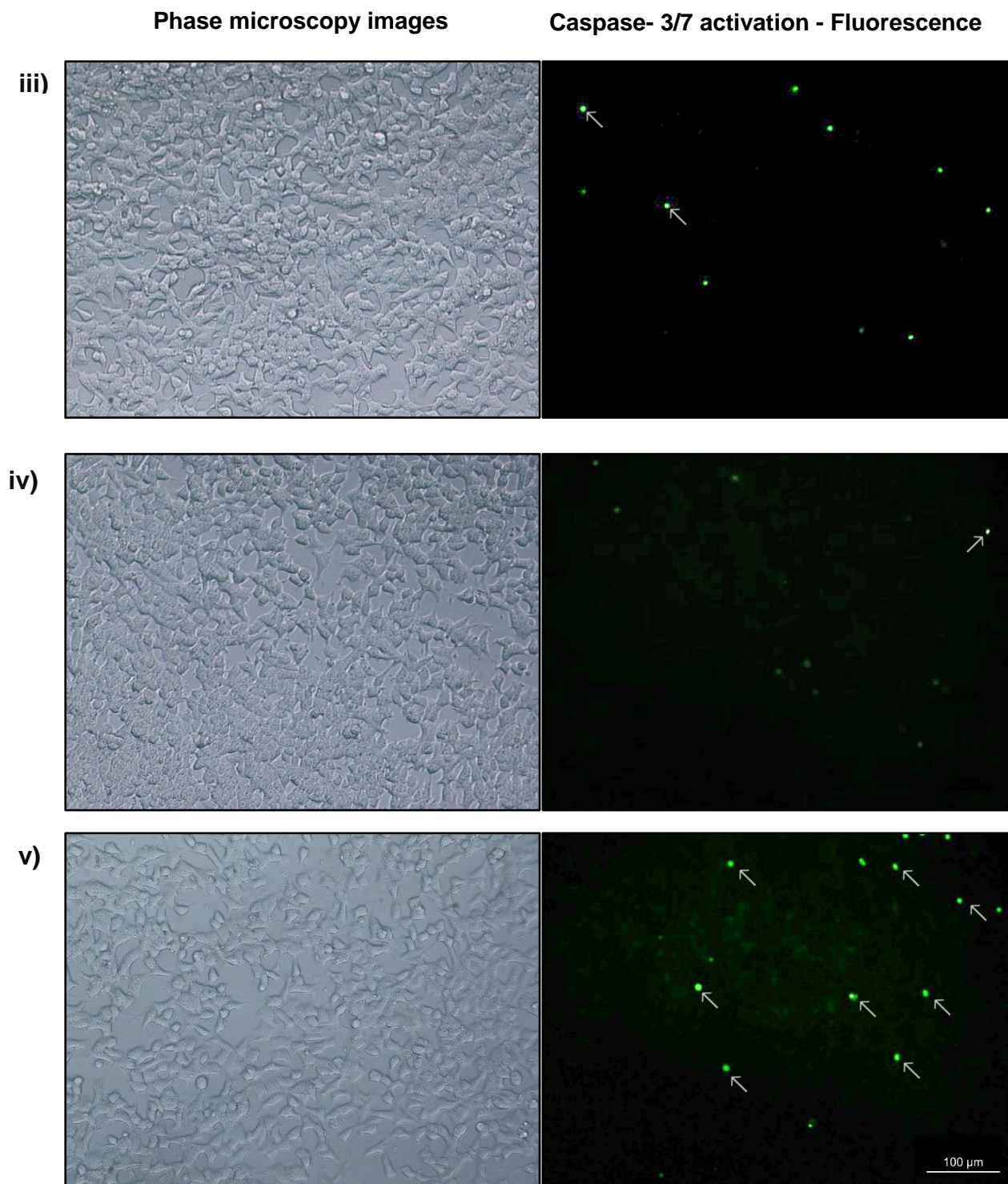
Figure 3.12 B: Effect of Asp, PPAG, and GRT on cell morphology and caspase-3/7 activation in INS1 cells exposed to pro-inflammatory cytokines. Representative light photomicrographs and fluorescent images of caspase-3/7 activation after 24 hours of co-treatment. Aspalathin (iii), PPAG (iv), and GRT (v). Images were taken on the Nikon inverted microscope at 20x objective; 200x magnification. Change in cell viability related to morphology and number of cells are indicated with black arrows. Fluorescent signal as result of caspase-3/7 activation is indicated with white arrows. Scale bar: 100 µm.

3.2. Rat Insulinoma Cell Function

Rat insulinoma cell function was assessed by GSIS and intracellular insulin content, followed by amylin content and secretion, as well as by measuring the rate of cell proliferation.

3.2.1. Glucose Stimulated Insulin Secretion in Rat Insulinoma Cells

Glucose stimulated insulin secretion was determined at basal as well as stimulated levels. For statistical analysis and graphs, the different treatment groups were compared to the amount of insulin secreted (ng/ml/mg protein) of the basal and glucose stimulated insulin secretion levels of the negative control.

The negative control showed an increase of 858.96% in insulin secretion after glucose stimulation when compared to the basal glucose levels of the negative control (72.19 ng/ml/mg ± 10.69, p=0.002 vs. 8.40 ng/ml/mg ± 1.66). Cytokine cocktail A showed an increase of 1039.19% in insulin secretion after glucose stimulation when compared to the basal levels of glucose (71.65 ng/ml/mg ± 6.80, p=0.002 vs. 6.89 ng/ml/mg ± 0.72) (Figure 3.13).

The INS1 cells exposed to co-treatment with Asp at the highest concentration (1000 µM) showed a significant increase in basal insulin secretion relative to negative control (15.93 ng/ml/mg ± 2.64, p=0.024 vs. 8.40 ng/ml/mg ± 1.66) and to cytokine cocktail A (15.93 ng/ml/mg ± 2.64, p=0.0038 vs. 6.89 ng/ml/mg ± 0.72) (Figure 3.13 A). However, after glucose stimulation Asp had no effect on insulin secretion.

The cells co-treated with PPAG had no significant effect on insulin secretion at basal levels or after glucose stimulation when compared to the negative control of the basal and stimulated levels, respectively (Figure 3.13 B).

After co-treatment with GRT, at basal levels, insulin secretion increased significantly at all concentrations used except the lowest concentration (0.0001 mg/ml) when compared to the negative control (27.06 ng/ml/mg ± 3.27, p=0.0011; 27.87 ng/ml/mg ± 3.49, p=0.0006; 28.67 ng/ml/mg ± 4.10, p=0.0003; and 28.43 ng/ml/mg ± 3.23, p=0.0004 vs. 8.40 ng/ml/mg ± 1.66, respectively) as well as cytokine cocktail A (27.06 ng/ml/mg ± 3.27, p=0.0004; 27.87 ng/ml/mg ± 3.49, p=0.0002; 28.67 ng/ml/mg ± 4.10, p=0.0001; and 28.43 ng/ml/mg ± 3.23, p=0.0001 vs. 6.89 ng/ml/mg ± 0.719, respectively). Although the cells maintained their ability to increase insulin secretion upon glucose stimulation the insulin secretion levels seemed to reduce in comparison to the negative control and cytokine cocktail A after glucose stimulation (Figure 3.13 C).

A

B

C
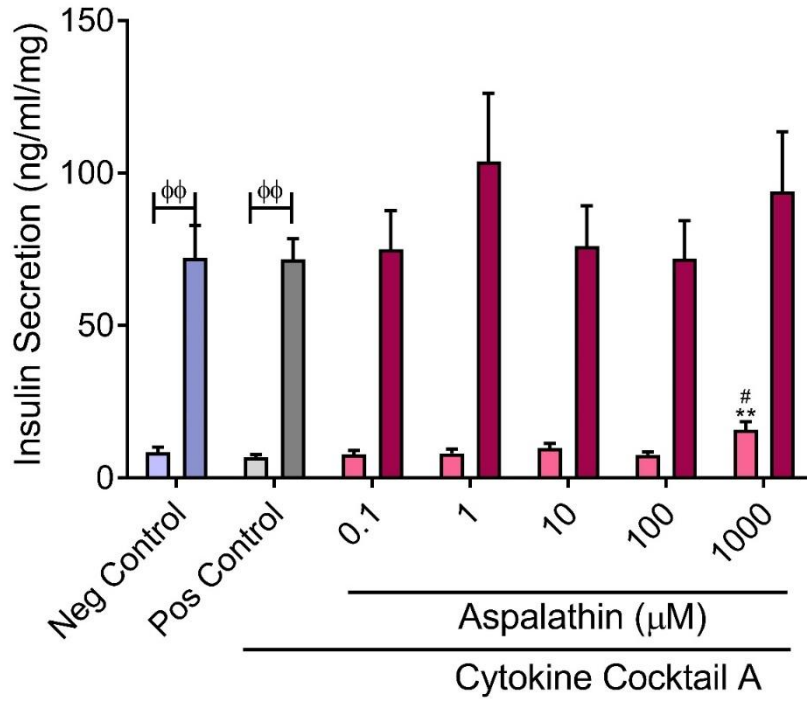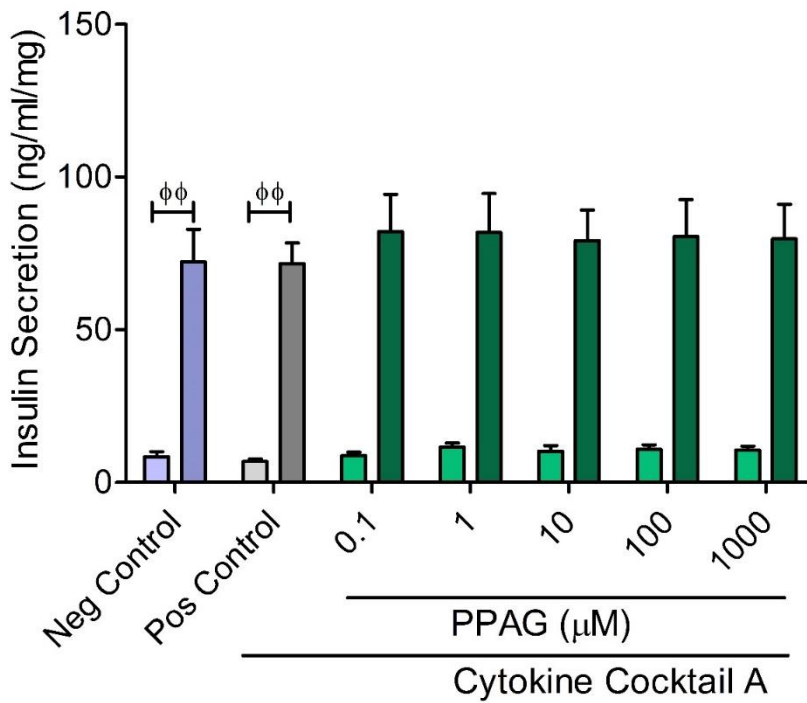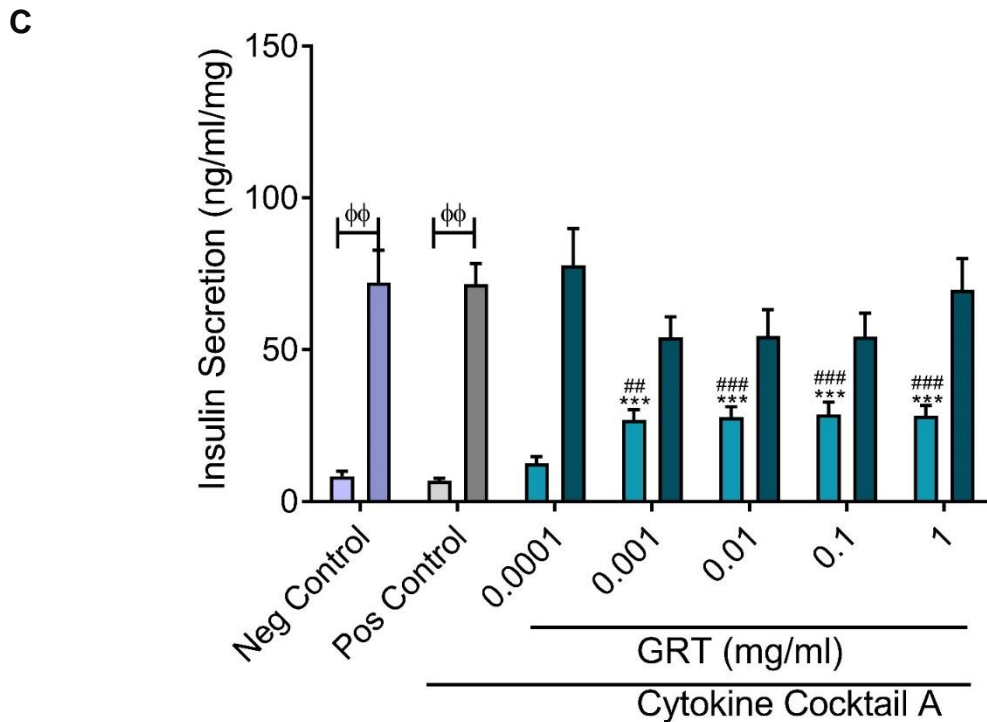
Figure 3.13: Glucose stimulated insulin secretion in INS1 cells exposed to pro-inflammatory cytokines. Effect of Asp (A), PPAG (B), and GRT (C) on basal (2.8 mM glucose) and glucose stimulated insulin secretion (16.7 mM glucose) in INS1 β-cells exposed to the pro-inflammatory cytokine cocktail A for 24 hours under normal cell culture conditions. The absorbence was measured using an ELISA (Ex 450 nm / Em 630 nm). Negative control: RPMI1640 medium; Positive control: Cytokine cocktail A. Basal glucose levels: ☐ Glucose stimulated levels: ■

Data presented is the mean (± SEM) of three independent experiments (n=3), relative to the negative control. One-way ANOVA (Tukey post-hoc test); followed by a Man-Whitney test where appropriate; $^{\Phi\Phi}= p<0.01$ stimulated vs. basal glucose levels; $^{\#}=p<0.05, ^{\#\#}=p<0.01, ^{\#\#\#}=p<0.001$ vs. negative control $^{**}=p<0.01, ^{***}=p<0.001$ vs. positive control.

3.2.2. Cellular Insulin Content in Rat Insulinoma Cells

To assess the residual intracellular insulin content as a measure of insulin synthesis and or dysfunction, stored insulin content from ruptured cells was determined by using an ELISA assay. The negative control was used to compare insulin secretion (ng/ml/mg) of the treatment groups to for statistical analysis and graphs.

Overall no significant effect on intracellular insulin content was seen after 24 hours of co-treatment (Figure 3.14).
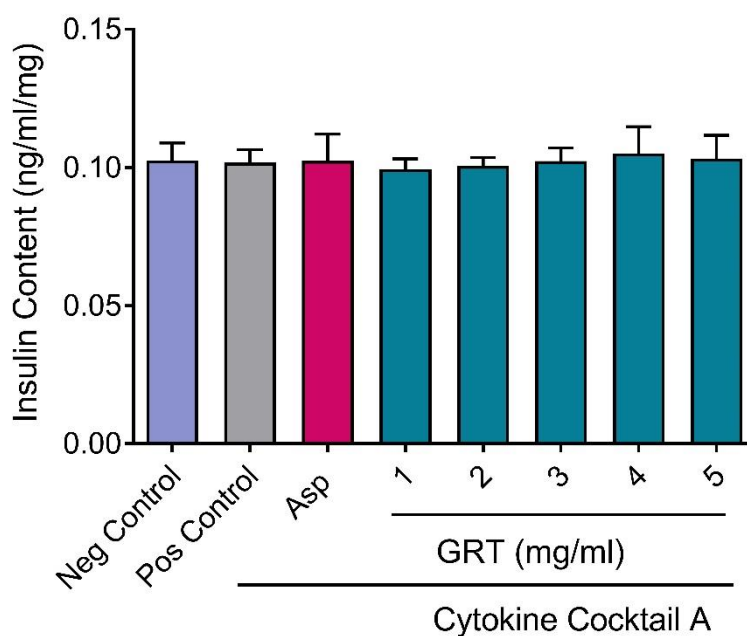
Figure 3.14: Cellular insulin content in INS1 cells exposed to pro-inflammatory cytokine cocktail A. Effect of Asp and GRT on cellular insulin content in INS1 β-cells, following the GSIS assay 24 hours after co-treatment under normal cell culture conditions. The absorbence was measured using an ELISA (Ex 450 nm / Em 630 nm). Negative control: RPMI1640 medium; Positive control: Cytokine cocktail A; Asp (µM): 1000; GRT (mg/ml) 1=0.0001; 2=0.001; 3=0.01; 4=0.1; and 5=1.

Data presented is the mean (± SEM) of three independent experiments (n=3), relative to the negative control. One-way ANOVA (Tukey post-hoc test).

3.2.3. Intracellular Amylin Content in Rat Insulinoma Cells

Intracellular amylin content in INS1 cells exposed to the pro-inflammatory cytokine cocktail A and to either Asp or GRT co-treatment for 24 hours was determined. The negative control was used as reference for statistical analysis and graphs. In comparison to negative control no significant effect of the treatment was observed in intracellular islet amylin content in the co-treated groups (Figure 3.15).
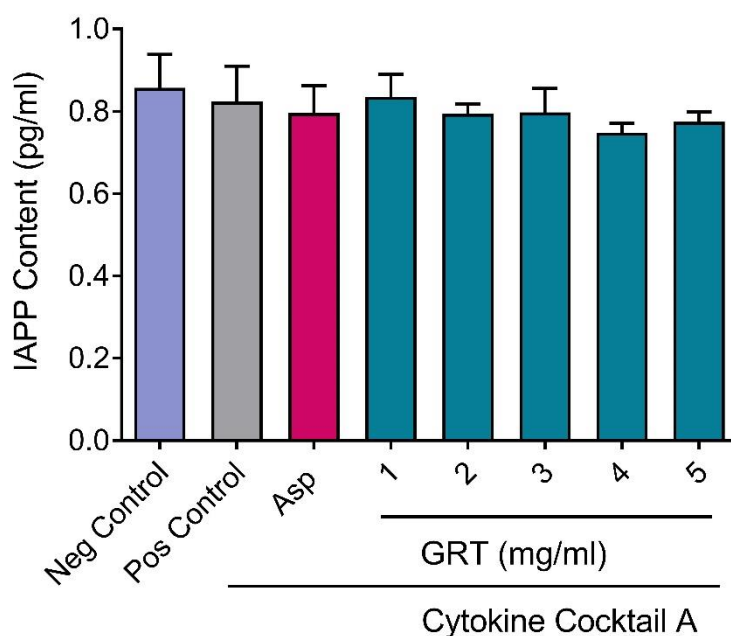
Figure 3.15: Cellular amylin content in INS1 cells exposed to pro-inflammatory cytokines. Effect of Asp and GRT on amylin content in INS1 β-cells, 24 hours after co-treatment under normal cell culture conditions. Amylin was quantified spectrophotometrically using an ELISA (450 nm). Negative control: RPMI1640 medium; Positive control: Cytokine cocktail A; Asp (μM): 1000; GRT (mg/ml) 1=0.0001; 2=0.001; 3=0.01; 4=0.1; and 5=1.

Data presented is the mean (± SEM) of three independent experiments (n=3), relative to the negative control. One-way ANOVA (Tukey post-hoc test).

3.2.4. Amylin Secretion in Rat Insulinoma Cells

Amylin secretion of INS1 cells after 24 hours of exposure to pro-inflammatory cytokines and to either Asp or GRT co-treatment was determined. The negative control was used as reference or statistical analysis and graphs. After 24 hours of co-treatment no effect was seen in IAPP secretion (Figure 3.16).
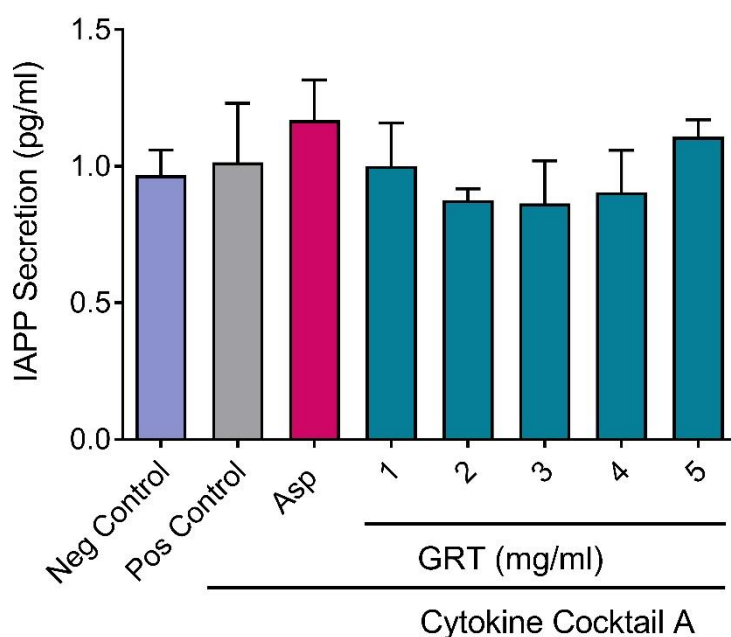
Figure 3.16: Amylin secretion in INS1 cells. Effect of Asp and GRT on amylin secretion in INS1 β-cells exposed to pro-inflammatory cytokines, 24 hours after co-treatment under normal cell culture conditions. Amylin was quantified spectrophotometrically using an ELISA (450 nm). Negative control: RPMI1640 medium; Positive control: Cytokine cocktail A; Asp (µM): 1000; GRT (mg/ml) 1=0.0001; 2=0.001; 3=0.01; 4=0.1; and 5=1.

Data presented is the mean (± SEM) of three independent experiments (n=3), relative to the negative control. One-way ANOVA (Tukey post-hoc test).

3.2.5.   Insulin to Amylin Secretion Ratio

The ratio of insulin to amylin secretion was calculated after 24 hours of co-treatment. No significant changes were seen (Figure 3.17).
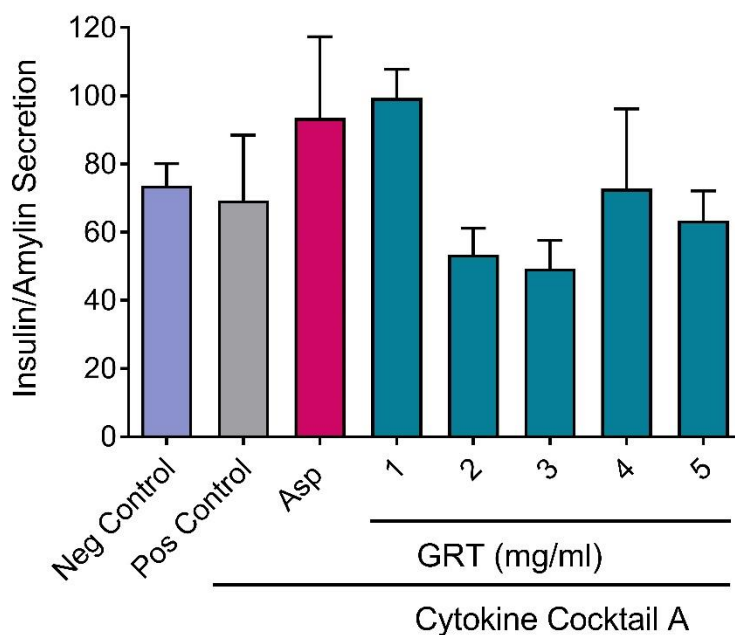
Figure 3.17: Insulin to amylin secretion ratio. Ratio of insulin to amylin secretion in INS1 pancreatic β-cells exposed to pro-inflammatory cytokines, 24 hours after co-treatment with Asp or GRT under normal cell culture conditions. Negative control: RPMI1640 medium; Positive control: Cytokine cocktail A; Asp (µM): 1000; GRT (mg/ml) 1=0.0001; 2=0.001; 3=0.01; 4=0.1; and 5=1.

Data presented is the mean (± SEM) of three independent experiments (n=3), relative to the negative control. One-way ANOVA (Tukey post-hoc test).

3.2.6.   Proliferation Rate of Rat Insulinoma Cells

The proliferation rate of INS1 cells exposed to the pro-inflammatory cytokine cocktail A with either Asp, PPAG, or GRT was assessed after 24 hours. The negative control, not exposed to cytokine cocktail A or Asp, PPAG, or GRT, was set as 100% for statistical analysis and graphs.

The INS1 cells exposed to the pro-inflammatory cytokine cocktail A showed a significant decrease in the rate of proliferation when compared to the negative control (80.21% ± 3.08, p=0.021 vs. 100% ± 3.27) (Figure 3.18).

The cells exposed to the lowest concentration of Asp (0.1 µM) showed a significant increase in the rate of cell proliferation relative to cytokine cocktail A (105.90% ± 4.68, p=0.0085 vs. 80.21% ± 3.08). In contrast, the highest concentration of Asp (1000 µM) showed a significant decrease in the rate of cell proliferation relative to the negative control (71.66% ± 6.92, p=0.0025 vs. 100% ± 3.27) (Figure 3.18 A), corresponding with the previous cell viability findings. Albeit not significant, 100 µM of Asp showed a trend towards a decreased rate of proliferation relative to the negative control (80.38% ± 3.73, p=0.092 vs. 100% ± 3.27).

The rate of cell proliferation in the INS1 cells was not affected by PPAG, except at the highest concentration (1000 µM) where a significant decrease in the rate of proliferation was seen in comparison to the negative control (79.70% ± 4.90, p=0.036 vs. 100% ± 3.27), while 10 µM of PPAG, although not significant, showed a trend towards a reduction in the rate of cell proliferation relative to the negative control (80.77% ± 3.74, p=0.056 vs. 100% ± 3.27) (Figure 3.18 B).

Co-treatment with 0.001, 0.01, and 1 mg/ml of GRT decreased the rate of cell proliferation significantly relative to the negative control (76.90% ± 4.58, p=0.0036; 60.39% ± 4.67, p<0.001; and 13.18% ± 1.80, p<0.001 vs. 100% ± 3.27); while only 0.01, and 1 mg/ml of GRT showed a decrease relative to cytokine cocktail A (60.39% ± 4.67, p=0.02 and 13.18% ± 1.80, p<0.001 vs. 80.21 % ± 3.08) (Figure 3.18 C). The decrease in the rate of cell proliferation, at the highest concentration, verifies the effects seen in the other cell viability results, while the decrease in the rate of proliferation at 0.1 mg/ml of GRT does not correspond with the cell viability results.
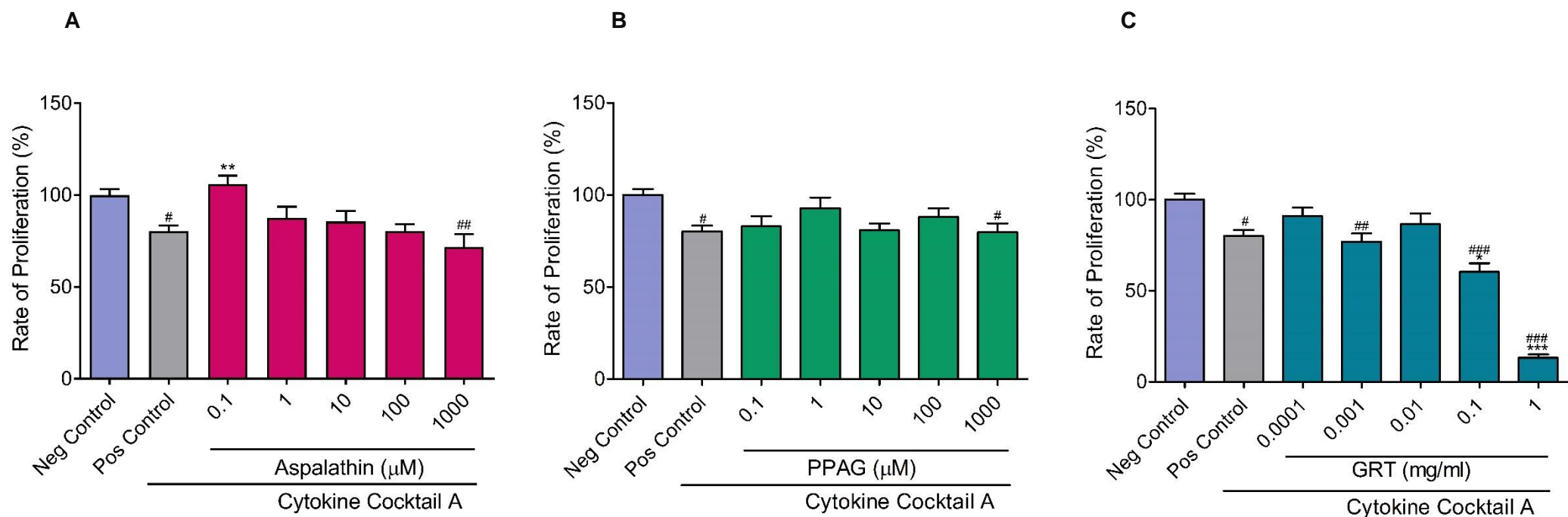
Figure 3.18: Proliferation rate of INS1 cells exposed to pro-inflammatory cytokines. Effect of Asp (A), PPAG (B), and GRT (C), on the proliferation rate of inflamed INS1 β-cells, 24 hours after co-treatment with Asp, PPAG, and GRT under normal cell culture conditions. Fluorescent quantification of the proliferation rate was assessed by measuring BrdU incorporation into INS1 cells (425 nm). Negative control: RPMI1640 medium; Positive control: Cytokine cocktail A.

Data presented is the mean (± SEM) of three independent experiments (n=3), relative to the negative control set at 100%. One-way ANOVA (Tukey post-hoc test); #=p<0.05, ##=p<0.01, ###=p<0.001 vs. negative control; *=p<0.05, **=p<0.01, ***=p<0.001 vs. positive control.

3.3. Oxidative Stress in Rat Insulinoma Cells

Oxidative stress in INS1 cells was assessed, first, by the DCF assay measuring ROS, and thereafter by the Griess assay measuring nitrites formed from NO. The negative control, not exposed to cytokine cocktail A or Asp, PPAG, or GRT, was set as 100% for statistical analysis and graphs.

3.3.1. Reactive Oxygen Species Production in Rat Insulinoma Cells - End-point Assay

Oxidative stress in INS1 cells exposed to pro-inflammatory cytokines, was assessed by measuring ROS production using an end-point DCF assay 24 hours after co-treatment. After 24 hours, the pro-inflammatory cytokine cocktail A significantly increased ROS production (133.10% ± 5.09, p=0.0014 vs. 100% ± 3.72) (Figure 3.19).

More specifically, 100 and 1000 µM of Asp showed a significant increase in ROS production in comparison to the negative control (139.10% ± 7.99, p=0.0013 and 153.90% ± 14.04, p<0.001 vs. 100% ± 3.72, respectively), while 0.1 and 10 µM of Asp showed a significant reduction in ROS production in comparison to cytokine cocktail A (97.66% ± 3.75, p=0.0098 and 96.67% ± 2.24, p=0.0072 vs. 133.10% ± 5.09, respectively) (Figure 3.19 A).

Cells co-treated with PPAG showed a significant decrease in ROS production at all concentrations in comparison to cytokine cocktail A (101.80% ± 3.77, p=0.0030; 103.20% ± 4.70, p=0.0053; 95.54% ± 5.61, p=0.0002; 107.30% ± 8.04, p=0.024; and 90.53% ± 3.93, p<0.001 vs. 133.10% ± 5.09, respectively) (Figure 3.19 B).

Co-treatment of INS1 cells with GRT indicated a significant decrease in ROS at all concentrations when compared to cytokine cocktail A (103.30% ± 6.15, p=0.008; 96.80% ± 3.67, p=0.0006; 102.30% ± 4.60, p=0.0053; and 86.05% ± 7.02, p<0.001 vs. 133.10% ± 5.09, respectively). However, the highest concentration of GRT (1 mg/ml) significantly increased ROS production in comparison to the negative control (130.80% ± 7.18, p=0.006 vs. 100% ± 3.72) (Figure 3.19 C).
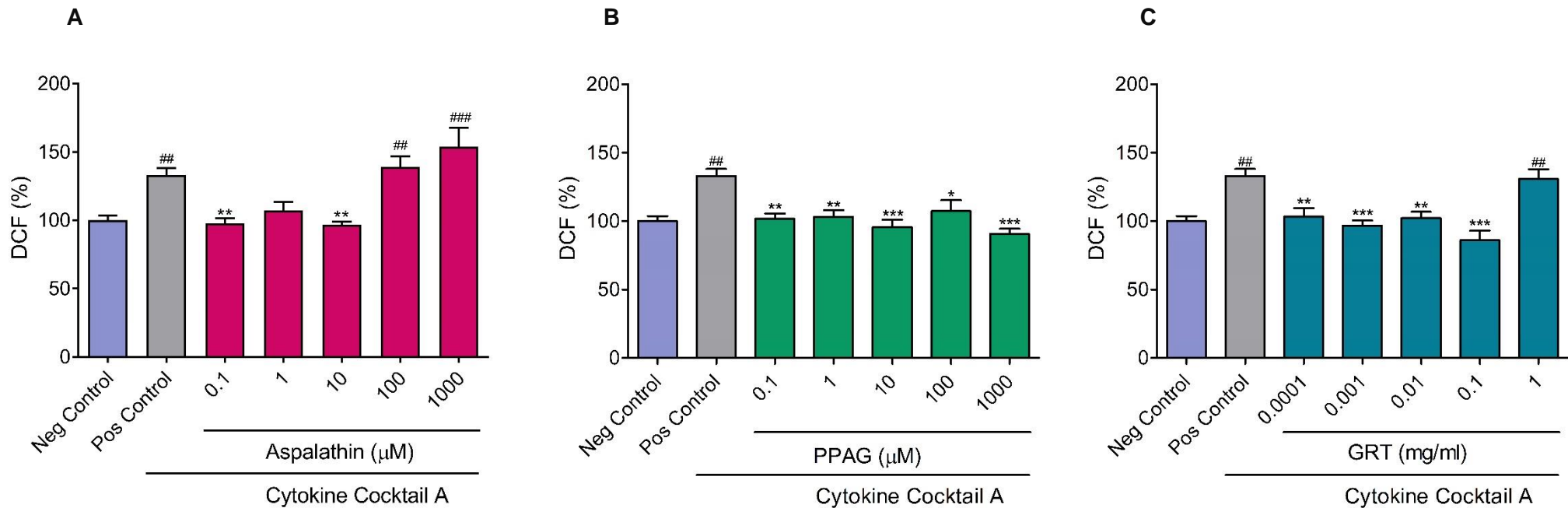
Figure 3.19: Oxidative stress; reactive oxygen species in INS1 cells – End-point. Effect of Asp (A), PPAG (B), and GRT (C), on ROS generation in inflamed pancreatic β-cells, assessed 24 hours after co-treatment under normal cell conditions. Fluorescent quantification of ROS was measured by using the DCF (Ex 485 nm / Ex 535 nm). Negative control: RPMI1640 medium; Positive control: Cytokine cocktail A.

Data presented is the mean (± SEM) of three independent experiments (n=3), relative to the negative control set at 100%. One-way ANOVA (Tukey post-hoc test); #=p<0.05, ##=p<0.01, ###=p<0.001 vs. negative control; *=p<0.05, **=p<0.01, ***=p<0.001 vs. positive control.

3.3.2. Reactive Oxygen Species Production in Rat Insulinoma Cells - Kinetic

Oxidative stress in INS1 cells was also kinetically assessed by measuring ROS production at 1-hour intervals over 24 hours. The AUC for each treatment was calculated over the 24 hours of co-treatment and expressed as an overall effect. The negative control, not exposed to cytokine cocktail A or Asp, PPAG, or GRT, was set as 100% for statistical analysis and graphs.

The INS1 cells co-treated with Asp at 1, 100, and 1000 μM significantly reduced ROS production over 24 hours compared to the negative control ($22.06\% \pm 3.04$, $p=0.0065$; $21.67\% \pm 5.21$, $p=0.0061$; and $22.21\% \pm 4.05$, $p=0.007$ vs. $100\% \pm 17.23$, respectively) as well as cytokine cocktail A ($22.06\% \pm 3.04$, $p=0.047$; $21.67\% \pm 5.21$, $p=0.044$; and $22.21\% \pm 4.05$, $p=0.047$ vs. $85.53\% \pm 16.60$, respectively) (Figure 3.20 A).

Co-treatment with PPAG showed a significant decrease in ROS production at 0.1, 10, and 1000 μM in comparison to the negative control ($19.03\% \pm 2.64$, $p=0.0039$; $19.94\% \pm 3.23$, $p=0.0044$; and $14.25\% \pm 0.91$, $p=0.0018$ vs. $100\% \pm 17.23$, respectively) and to cytokine cocktail A ($19.03\% \pm 2.64$, $p=0.03$; $19.94\% \pm 3.23$, $p=0.034$; and $14.25\% \pm 0.91$, $p=0.016$ vs. $85.53\% \pm 16.60$, respectively) (Figure 3.20 B).

In a similar trend to Asp, co-treatment with GRT showed a significant decrease in ROS production over 24 hours at 0.001, 0.1, and 1 mg/ml in comparison to the negative control ($16.83\% \pm 2.21$, $p=0.0007$; $13.94\% \pm 3.42$, $p=0.0004$; and $20.83\% \pm 4.43$, $p=0.0014$ vs. $100\% \pm 17.23$, respectively) as well as cytokine cocktail A ($16.83\% \pm 2.21$, $p=0.0083$; $13.94\% \pm 3.42$, $p=0.0052$; and $20.83\% \pm 4.43$, $p=0.016$ vs. $85.53\% \pm 16.60$, respectively) (Figure 3.20 C).
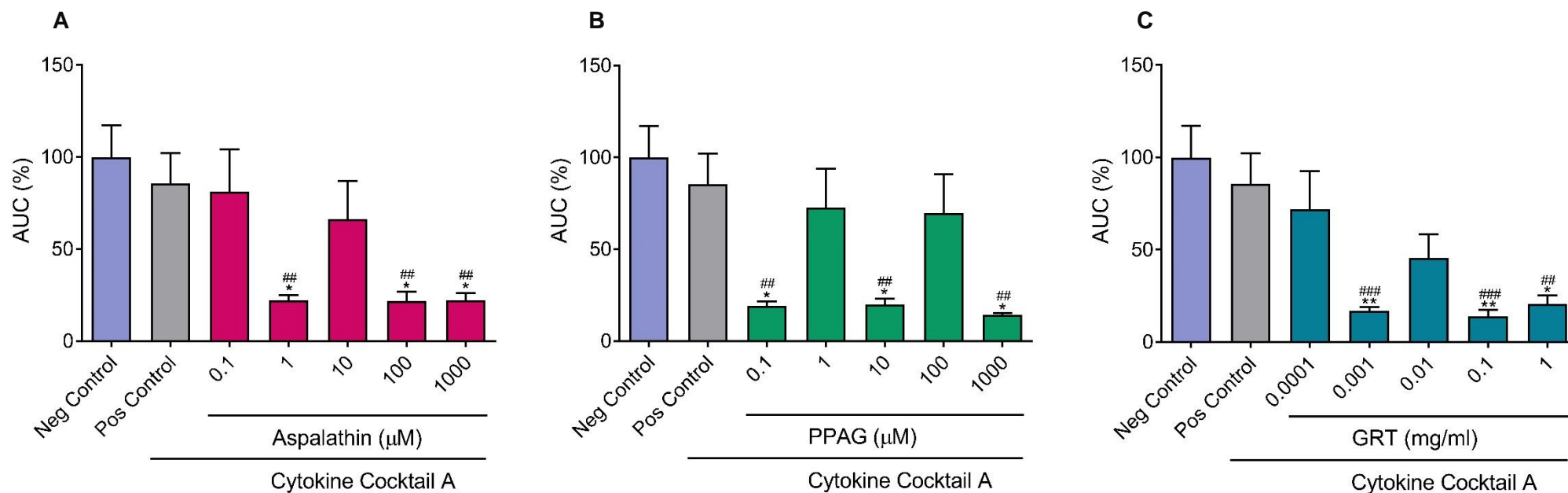
Figure 3.20: Oxidative stress; reactive oxygen species in INS1 cells exposed to pro-inflammatory cytokines. Effect of Asp (A), PPAG (B), and GRT (C), on ROS generation INS1 pancreatic β-cells, exposed to pro-inflammatory cytokines was assessed kinetically for 24 hours under normal cell culture conditions. Fluorescent quantification of ROS was measured by using the DCF (Ex 485 nm / Ex 535 nm). Negative control: RPMI1640 medium; Positive control: Cytokine cocktail A.

Data presented is the mean (± SEM) of three independent experiments (n=3), relative to the negative control set at 100%. One-way ANOVA (Tukey post-hoc test); ##=p<0.01, ###=p<0.001 vs. negative control; *=p<0.05, **=p<0.01 vs. positive control.

3.3.3. Nitric Oxide Production in Rat Insulinoma Cells

Oxidative stress was further assessed by the amount of nitrates as an indirect measure of NO production in INS1 cells exposed to the pro-inflammatory cytokine cocktail A with either Asp, PPAG, or GRT for 24 hours. The negative control, not exposed to cytokine cocktail A or Asp, PPAG, or GRT, was used as reference for statistical analysis and graphs.

Overall there was no significant effect seen between the treated groups and the negative control or pro-inflammatory cytokine cocktail A after 24 hours of exposure (Figure 3.21).

A Without Cytokine Cocktail A

B With Cytokine Cocktail A
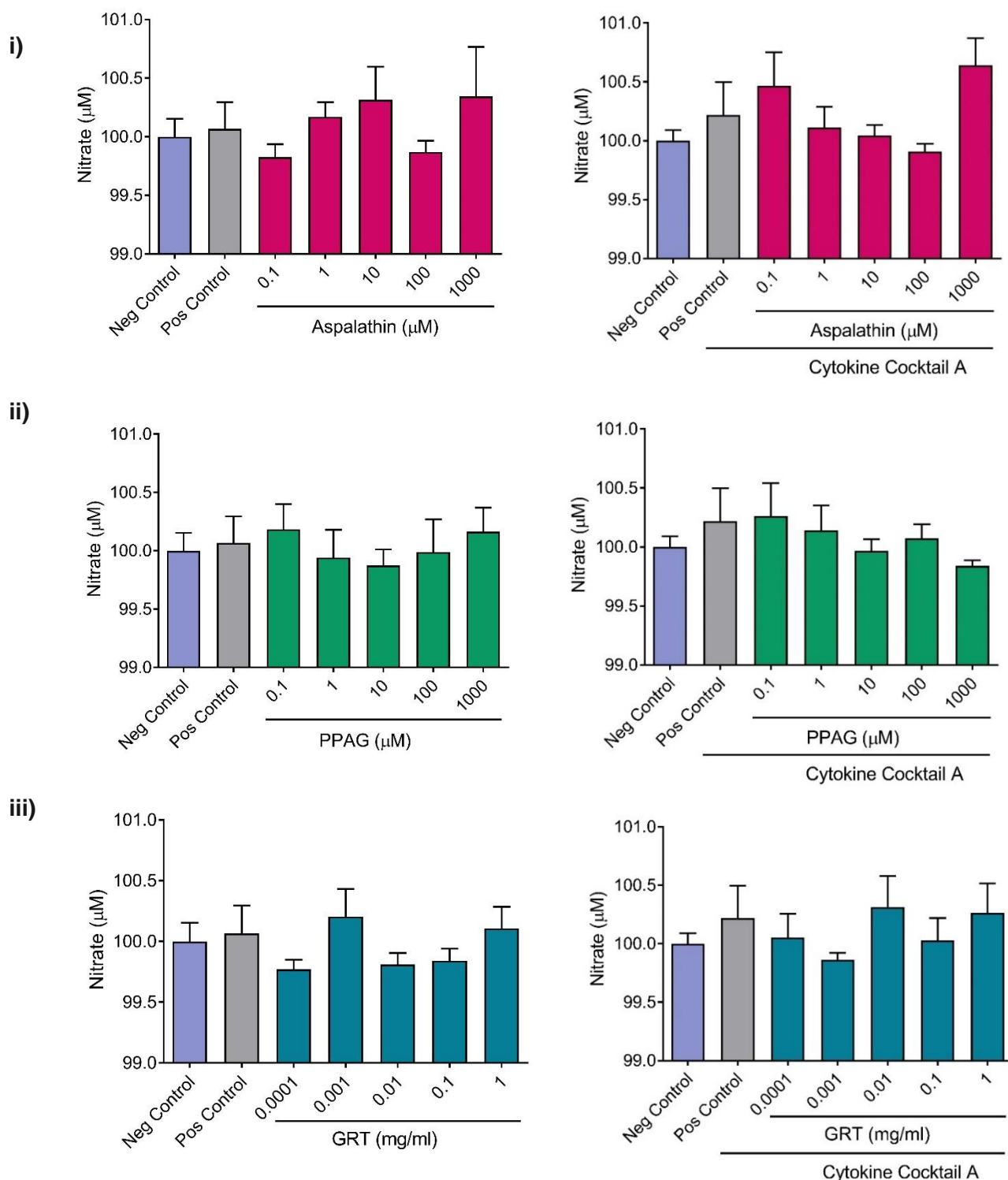
Figure 3.21: Oxidative stress; nitrate generation in INS1 cells. Effect of Asp (i), PPAG (ii), and GRT (iii), on NO in INS1 pancreatic β-cells in without cytokine cocktail A (A) and with cytokine cocktail A (B) for 24 hours. Fluorescent quantification of nitrites was measured by using the Griess assay (540 nm). Negative control: RPMI1640 medium; Positive control: Cytokine cocktail A.

Data presented is the mean (± SEM) of three independent experiments (n=3), relative to the negative control. One-way ANOVA (Tukey post-hoc test).

3.4. Beta Secretase Inhibition in Rat Insulinoma Cells

Beta secretase inhibition activity of Asp, PPAG, and GRT in INS1 cells was assessed by a purified BACE enzyme assay, followed by a BACE assay *in vitro*.

3.4.1. Beta Secretase Inhibition - Purified-enzyme Assay

Beta secretase inhibition activity of Asp, PPAG, and GRT was compared to that specific treatment's lowest concentration used. The BACE inhibition assay indicates a concentration dependent response after 2 hours of incubation with the known BACE inhibitor, as an enhancement in fluorescence is seen, indicating that the substrate is cleaved by BACE. After 2 hours, the two highest concentrations of the known inhibitor (LY2886721); 3.9 and 39 µM, reduced BACE activity significantly when compared to the lowest concentration used (0.0039 µM), ($71.89\% \pm 6.44$, $p=0.0010$; $23.44\% \pm 5.88$, $p<0.001$, vs. $103.50\% \pm 0.73$, respectively). Aspalathin and PPAG showed no significant effect after the 2 hours of incubation, while GRT, more specifically the highest concentration (1 mg/ml), showed a significant effect on BACE activity as a decrease in BACE activity was observed ($83.37\% \pm 3.40$, $p<0.001$ vs. $102\% \pm 1.75$) (Figure 3.22).
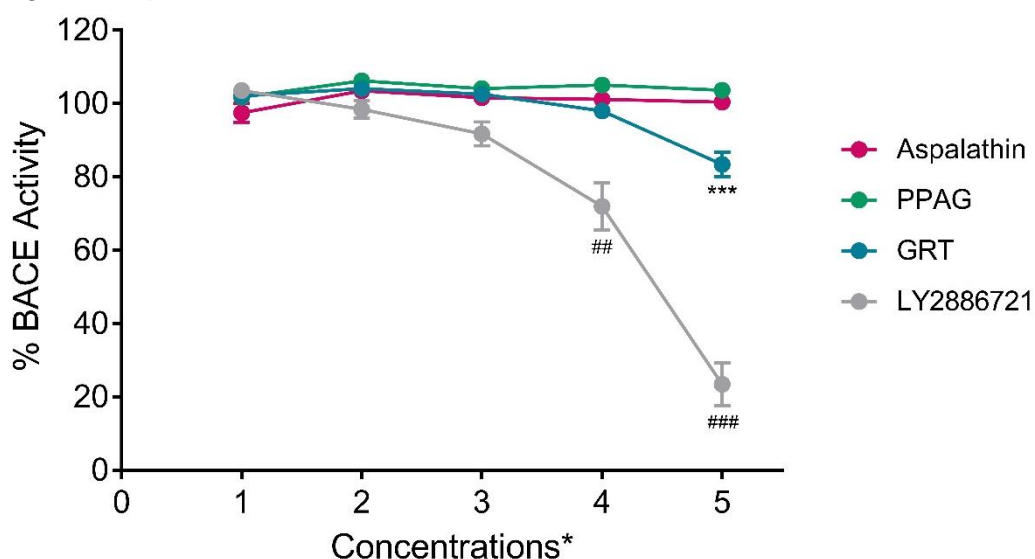
Figure 3.22: Beta secretase inhibition by Asp, PPAG, and GRT. Beta secretase inhibition activity of Asp, PPAG, and GRT was compared to a known inhibitor (LY2886721) using a purified BACE enzyme assay. Beta secretase activity assessed 2 hours after incubation at room temperature (Ex 320 nm / Ex 405 nm). *Concentrations: LY2886721 (mM): 1=0.0039, 2=0.039, 3=0.39, 4=3.9, 5=39; Asp and PPAG (µM): 1=0.1, 2=1, 3=10, 4=100, 5=1000; GRT (mg/ml): 1=0.0001, 2=0.001, 3=0.01, 4=0.1, 5=1.

Data presented is the mean ($\pm$ SEM) of three independent experiments (n=3), relative to that specific treatment's lowest concentration used; ##=$p<0.05$, ###=$p<0.001$ vs. control of LY2886721; ***=$p<0.001$ vs. control of GRT.

3.4.2.   Beta Secretase Inhibition by Asp, PPAG, and GRT - Cell Based Assay

Beta secretase inhibition by Asp, PPAG, and GRT was assessed kinetically over 24 hours measuring the fluorescence, which is enhanced when BACE cleaves the substrate. A known BACE inhibitor was used as second control at two different concentrations; A: 39 µM, and B: 3.9 µM. The negative control, not exposed to cytokine cocktail A or Asp, PPAG, or GRT, was set as 100% for statistical analysis and graphs.

Inhibitor A (39 µM) showed a significant decrease in BACE activity when compared to the negative control (61.56% ± 10.55, $p<0.001$ vs. 100% ± 2.84) as well as cytokine cocktail A (61.56% ± 10.55, $p<0.001$ vs. 96.23% ± 2.51) (Figure 3.23).

The INS1 cells co-treated with Asp showed a significant decrease in BACE activity at 100 and 1000 µM in comparison to the negative control (77.42% ± 1.73, $p=0.0073$ and 56.20% ± 2.05, $p<0.001$ vs. 100% ± 2.84, respectively) and to cytokine cocktail A (77.42% ± 1.73, $p=0.048$ and 56.20% ± 2.05, $p<0.001$ vs. 96.23% ± 2.51, respectively) (Figure 3.23 A).

In contrast to Asp, cells co-treated with PPAG showed no effect on BACE activity except at the highest concentration (1000 µM) where a significant increase in BACE activity was observed over 24 hours in comparison to the negative control (235.80% ± 15.78, $p<0.001$ vs. 100% ± 2.84) and cytokine cocktail A (235.80% ± 15.78, $p<0.001$ vs. 96.23% ± 2.51) (Figure 3.23 B).

Following a similar trend to Asp, cells co-treated with GRT showed a significant decrease in BACE activity at 0.1 and 1 mg/ml when compared to the negative control (67.47% ± 1.20, $p<0.001$ and 39.80% ± 0.55, $p<0.001$ vs. 100% ± 2.84, respectively) as well as cytokine cocktail A (67.47% ± 1.20, $p=0.0002$ and 39.80% ± 0.55, $p<0.001$ vs. 96.23% ± 2.51), (Figure 3.23 C).
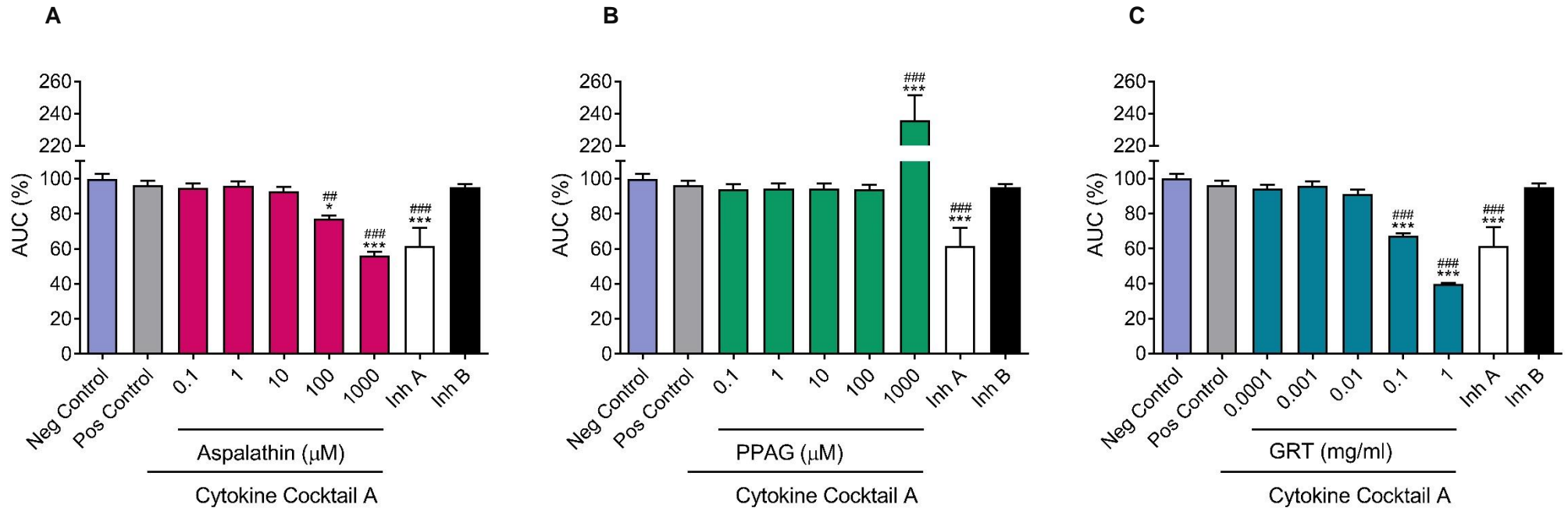
Figure 3.23: Beta secretase inhibition by Asp, PPAG, and GRT. Effect of Asp (A), PPAG (B), and GRT (C), on BACE activity in INS1 pancreatic β-cells exposed to the pro-inflammatory cytokines, was assessed kinetically for 24 hours, under normal cell culture conditions. Fluorescent quantification of BACE activity was assessed using the BACE assay (Ex 320 nm / Ex 405 nm). Negative control: RPMI1640 medium; Positive control: Cytokine cocktail A.

Data presented is the mean (± SEM) of three independent experiments (n=3), relative to the negative control set at 100%. One-way ANOVA (Tukey post-hoc test); ##=p<0.01, ###=p<0.001 vs. negative control; *=p<0.05, ***=p<0.001 vs. positive control.

3.4.3. Protein Expression in Rat Insulinoma Cells Exposed to Pro-Inflammatory Cytokines

The effect of Asp, PPAG, and GRT on protein expression was assessed in INS1 cells exposed to the pro-inflammatory cytokine cocktail A by Western blots.

3.4.3.1. Western blots

Western blot analysis, also known as the protein immunoblot, was used to assess molecular markers of interest and the potential signalling pathways that are altered in INS1 cells by pro-inflammatory cytokines. Proteins of interest include amylin, TMEM27, BACE2, NF-κB, and COX2, relating to cell viability, cell function, oxidative stress, and autophagy. Chemiluminescent images of PVDF membranes were taken (Figure 3.24) where after the images were quantified as the intensity of protein expressed. Values obtained were normalised to β-tubulin which served as the house keeping protein. The negative control was used as reference for statistical analysis and graphs.

3.4.3.1.1. Amylin Expression

Although not significant, the cells co-treated with GRT (0.1 mg/ml) for 24 hours had the largest fold decrease (0.5 X fold change) in amylin expression in comparison to the negative control (0.51 ± 0.04 vs. 1.0 ± 0.25) (Figure 3.25).

3.4.3.1.2. TMEM27 Expression

Although no significant changes were seen in TMEM27 expression after 24 hours of co-treatment, cytokine cocktail A had the most extensive fold decrease (0.5 X fold change) in TMEM27 expression (0.59 ± 0.13 vs. 1.0 ± 0.21) , followed by PPAG (100 μM) and GRT (0.1 mg/ml) (Figure 3.26).

3.4.3.1.3. BACE2 Expression

Rat Insulinoma cells showed no significant change in BACE2 expression. The cells co-treated with Asp (100 μM) showed the largest fold increase in BACE2 expression compare to the negative control (1.30 ± 0.36 vs. 1.0 ± 0.40), however it is not significant (Figure 3.27).

3.4.3.1.4.   COX2 Expression

Rat Insulinoma cells showed no significant change in COX2 expression after 24 hours of co-treatment. However, cytokine cocktail A showed the largest fold increase in COX2 expression (1.5 X fold change) when compared to the negative control (1.61 ± 0.53 vs. 1.0 ± 0.34), however it is not significant (Figure 3.28).

3.4.3.1.5.   Phosphorylated NF- κB to Total NF- κB Expression

The ratio of pNF-κB to NF-κB was determined to assess phosphorylation of NF- κB. After 24 hours of co-treatment no significant change was observed. However, the cells exposed to cytokine cocktail A and the group co-treated with GRT (0.1 mg/ml) showed a fold increase (1.5 X fold change, respectively) in the ratio of pNF-κB to NF-κB in comparison to the negative control (1.39 ± 0.57 vs. 1.0 ± 0.36 and 1.33 ± 0.58 vs. 1.0 ± 0.36, respectively) (Figure 3.29).
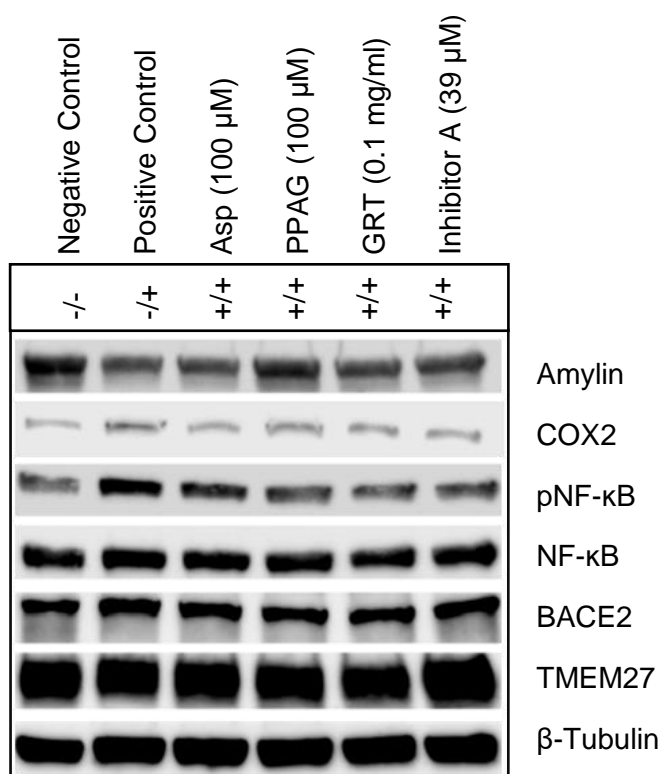
Figure 3.24: Western blot images of protein expression in INS1 cells exposed to inflammatory cytokines. Representative images of PVDF membranes after incubation with the primary antibodies overnight, followed with their specific secondary antibodies for 1.5 hours. After incubation, the membranes were exposed to ECL for 5 minutes where after the ChemiDoc was used to take chemiluminescent images. (-): without cytokine cocktail A and treatment; (+): with cytokine cocktail A and Asp, PPAG, or GRT.
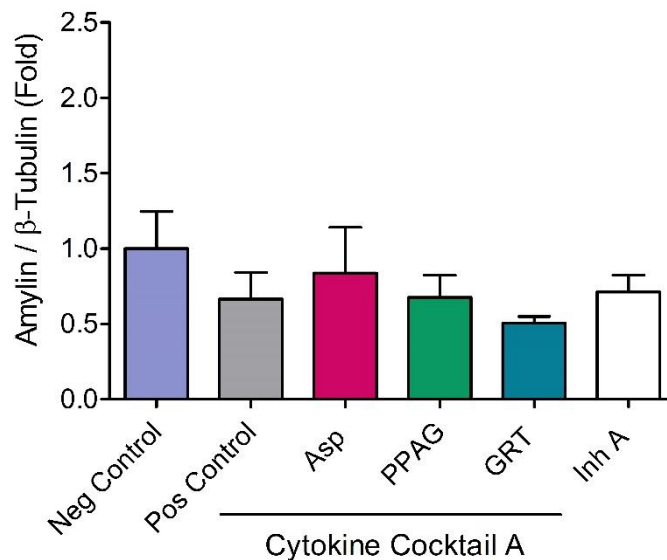
Figure 3.25: Amylin expression in INS1 cells exposed to pro-inflammatory cytokines.
Amylin expression in INS1 cells 24 hours after co-treatment with cytokine cocktail A and 100 µM of Asp, 100 µM of PPAG, 0.1 mg/ml of GRT, and 39 µM of Inhibitor A. Chemiluminescent images were obtained on the ChemiDoc to quantify protein expression. Negative control: RPMI1640 medium; Positive control: Cytokine cocktail A.

Data presented is the mean (± SEM) of three independent experiments (n=3), relative to the negative control; One-way ANOVA (Tukey post-hoc test).
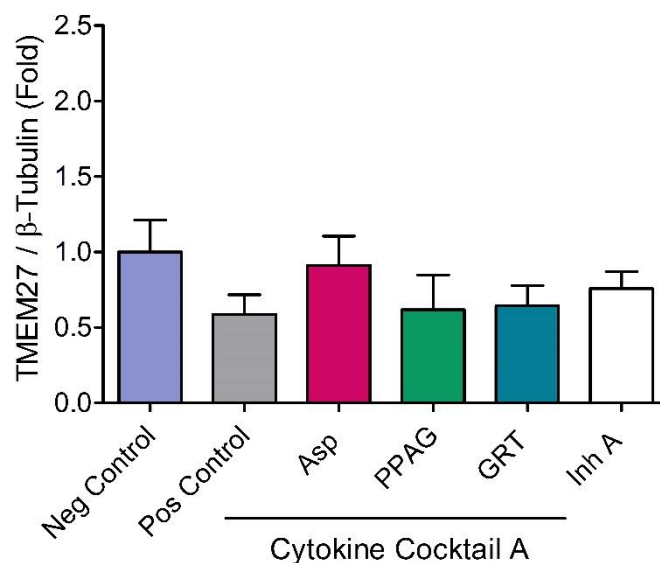
Figure 3.26: TMEM27 expression in INS1 cells exposed to pro-inflammatory cytokines.
TMEM27 expression in INS1 cells 24 hours after co-treatment with cytokine cocktail A and 100 µM of Asp, 100 µM of PPAG, 0.1 mg/ml of GRT, and 39 µM of Inhibitor A. Chemiluminescent images were obtained on the ChemiDoc to quantify protein expression. Negative control: RPMI1640 medium; Positive control: Cytokine cocktail A.

Data presented is the mean (± SEM) of three independent experiments (n=3), relative to the negative control; One-way ANOVA (Tukey post-hoc test).
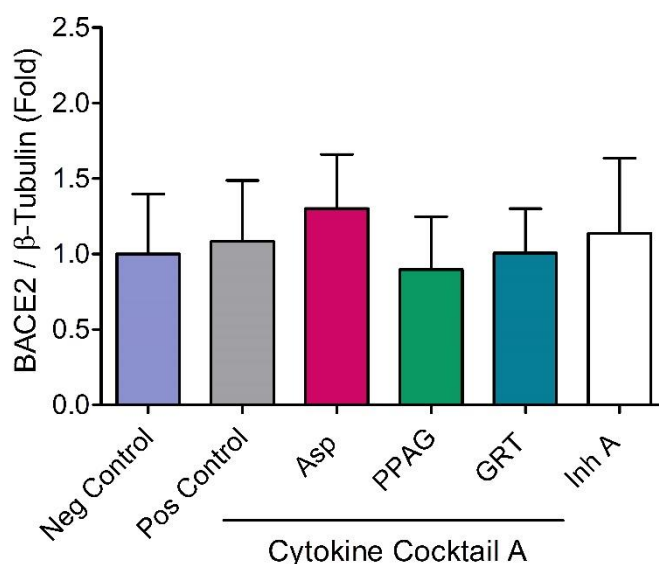
Figure 3.27: BACE2 expression in INS1 cells exposed to pro-inflammatory cytokines.
BACE2 expression in INS1 cells 24 hours after co-treatment with cytokine cocktail A and 100
µM of Asp, 100 µM of PPAG, 0.1 mg/ml of GRT, and 39 µM of Inhibitor A. Chemiluminescent
images were obtained on the ChemiDoc to quantify protein expression.   Negative control:
RPMI1640 medium; Positive control: Cytokine cocktail A.

Data presented is the mean (± SEM) of three independent experiments (n=3), relative to the negative
control; One-way ANOVA (Tukey post-hoc test).
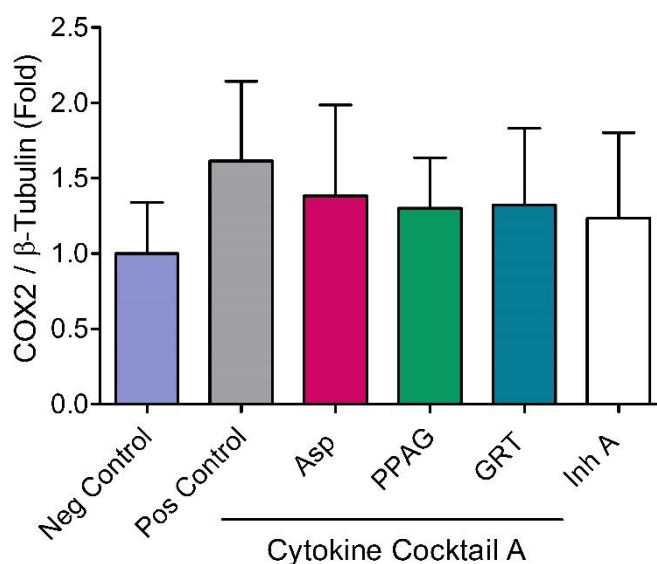
Figure 3.28: COX2 expression in INS1 cells exposed to pro-inflammatory cytokines.
COX2 expression in INS1 cells 24 hours after co-treatment with cytokine cocktail A and 100
µM of Asp, 100 µM of PPAG, 0.1 mg/ml of GRT, and 39 µM of Inhibitor A. Chemiluminescent
images were obtained on the ChemiDoc to quantify protein expression.   Negative control:
RPMI1640 medium; Positive control: Cytokine cocktail A.

Data presented is the mean (± SEM) of three independent experiments (n=3), relative to the negative
control; One-way ANOVA (Tukey post-hoc test).
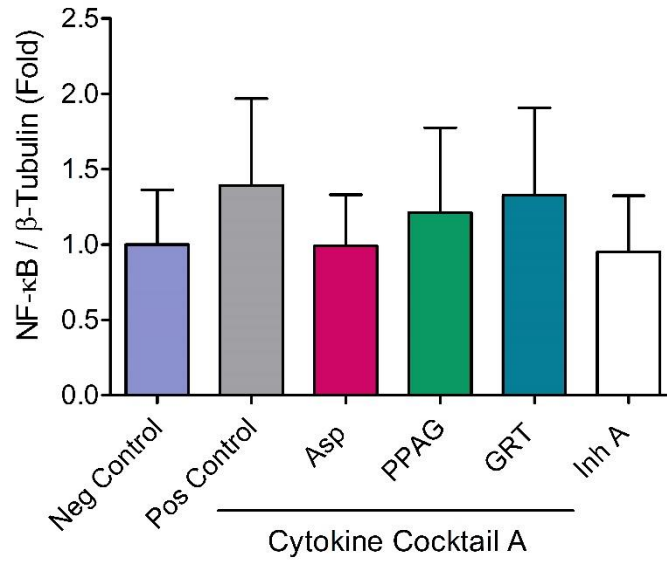
Figure 3.29: NF-κB expression in INS1 cells exposed to pro-inflammatory cytokines. NF-κB expression in INS1 cells 24 hours after co-treatment with cytokine cocktail A and 100 µM of Asp, 100 µM of PPAG, 0.1 mg/ml of GRT, and 39 µM of Inhibitor A. Chemiluminescent images were obtained on the ChemiDoc to quantify protein expression. Negative control: RPMI1640 medium; Positive control: Cytokine cocktail A.

Data presented is the mean (± SEM) of three independent experiments (n=3), relative to the negative control; One-way ANOVA (Tukey post-hoc test).

3.5. Summary of Results

Table 3.2: Summary of Results. Summary of the effect of Asp, PPAG, and GRT on cell viability, cell function, oxidative stress, and BACE activity in inflamed INS1 cells.

	Asp	PPAG	GRT
Cell Viability *Arrows indicate a decrease in cell viability not a decrease in the measurement.*			
-MTT	↓ at high [ ]	No effect	↓ at high [ ]
-Cellular ATP Content	↓ at high [ ]	↑ at high [ ]	↓ at high [ ]
-Early Apoptosis/Necrosis	↓ at high [ ]	↓ at high [ ], but no effect on necrosis	↓ at high [ ]
-Late Apoptosis	↓ at high [ ]	No effect	↓ at high [ ]
Cell Function			
-Insulin Secretion	Increased at basal glucose levels at only the highest [ ]	No effect	Only increased at basal glucose levels at higher [ ]
-Insulin Content	No effect	– – –	No effect
-Amylin Content	No effect	– – –	No effect
-Amylin Secretion	No effect	– – –	No effect
-Proliferation Rate	↓ at high [ ]	↓ at high [ ]	↓ at high [ ]
Oxidative Stress			
-ROS (End-point)	↓ at lower [ ]	↓ Overall	↓ at lower [ ]
-ROS (Kinetic)	↓ at low and high [ ]	↓ at low and high [ ]	↓ at low and high [ ]
-NO (End-point)	No significant effect	No significant effect	No significant effect

	Asp	PPAG	GRT
BACE Inhibition			
-Purified Enzyme Assay	No effect	No effect	BACE Inhibition at high [ ]
-Cell Based (Kinetic)	BACE Inhibition at high [ ]	Increase BACE activity at highest [ ]	BACE Inhibition at high [ ]
Western Blots			
-Amylin	No effect	No effect	No effect
-TMEM27	No effect	No effect	No effect
-BACE2	No effect	No effect	No effect
-COX2	No effect	No effect	No effect
-pNf-κB / Nf-κB	No effect	No effect	No effect

*↑: Increase; ↓ : Decrease; ---- : Was not tested in that particular experimental technique.

CHAPTER 4

Discussion

Exposure of pancreatic β-cells to perpetual damage linked to chronic low-grade inflammation and stressors such as gluco- and lipotoxicity lead to the progression of T2D. These stressors negatively influence pancreatic β-cell function via several mechanistic and signalling pathways involved in inflammation, as well as oxidative stress culminating in IR (Abedini and Schmidt, 2013; Harding and Ron, 2002; Hull et al., 2004; Prentki and Nolan, 2006; Robertson et al., 2004; Weir and Bonner-Weir, 2004). At first, pancreatic β-cells maintain homeostasis by activating anti-inflammatory pathways and increasing insulin secretion to compensate for IR. The chronic exposure of pancreatic β-cells to excessive glucose levels leads to β-cell dysfunction and hyperglycemia. Insulin resistance and hyperglycemia in turn exacerbate the inflammatory pathway and ultimately results in the loss of pancreatic β-cell functional mass due to an imbalance between cell death and proliferation of β-cells (Kahn, 1998; Larsson and Ahrén, 1996; Maedler et al., 2002; Perley and Kipnis, 1967; Polonsky et al., 1988).

Pancreatic β-cell inflammation also results from elevated levels of toxic IAPP due to misfolding and aggregation of toxic amyloid fibril depositions. Amylin is co-secreted with insulin after glucose stimulation. Increased levels of amylin are observed in T2D individuals and positively correlate with BACE2 levels (Figure 4.1) (Alcarraz-Vizán et al., 2017, 2015, Clark et al., 1996a, 1996b; Gasa et al., 2001; Hou et al., 1999; Kahn et al., 1999). High levels of BACE2 are expressed in pancreatic β-cells, however, there are speculations regarding the role of BACE2 in the pancreas and its role in the progression of T2D. Beta secretase 2 is seen to both benefit and damage pancreatic β-cells by regulating insulin secretion through the cleavage of TMEM27, and by increasing IAAP deposition, respectively (Figure 4.1) (Abedini and Schmidt, 2013; Alcarraz-Vizán et al., 2017, 2015; Esterházy et al., 2011; Southan and Hancock, 2013; Stützer et al., 2013; Vassar, 2014). Therefore, investigating the interaction between inflammation, BACE activity and amyloid deposition may provide insights into the role(s) thereof in pancreatic β-cell impairment and may reveal an opportunity for the development of novel therapeutic targets to protect and preserve pancreatic β-cells, such as specifically targeting the activities of BACE2.

Aspalathin and PPAG, both polyphenolic components of Rooibos, have strong antioxidant properties, the ability to increase glucose uptake in muscle cells and increase insulin secretion from β-cells (Beltrán-Debón et al., 2011; Bramati et al., 2002; Joubert et al., 2008; Joubert and de Beer, 2011; Kawano et al., 2009; Ku et al., 2015; McKay and Blumberg, 2007). In addition

to antioxidant properties, several studies have indicated that polyphenols exert a protective effect against Aβ formation and aggregation by acting as BACE1 inhibitors (Shimmyo et al., 2008). Elevated BACE1 expression is seen to increase Aβ levels via NF-κB, indicating that BACE1 interplays with inflammatory pathways (Figure 4.1) (Buggia-Prevot et al., 2008; Fu et al., 2014). In the pancreatic islets BACE2 is highly expressed and its inhibition has been associated with increased β-cell mass and improved hyperglycemia as a result of increased insulin secretion and glucose uptake. In this study, the GRT Rooibos extract, rich in Asp and PPAG, was assessed as a potential novel therapeutic agent that directly targets BACE2 activity and consequently protects β-cell mass, decreases β-cell inflammation and the progression of T2D. Furthermore, the Rooibos extract may remediate inflammation-induced cellular damages, thereby indirectly reducing the deleterious effects of BACE. Thus far, neither the BACE inhibitory effect, nor the anti-inflammatory effect of Rooibos in pancreatic β-cells has been reported on.

In this study, pro-inflammatory cytokines were used to mimic a state of moderate inflammation, associated with IAPP and T2D, *in vitro* using INS1 cells. An Aspalathin-rich Rooibos extract, and two of its major bioactive phenolic compounds, Asp and PPAG, were assessed for their protective effect(s) on INS1 cells exposed to a pro-inflammatory cytokine cocktail over 24 hours. Furthermore, their ability to inhibit BACE activity and thereby reduce the risk for developing T2D, was assessed by studying cell function and viability, as well as its effect on oxidative stress via several mechanistic and signalling pathways.
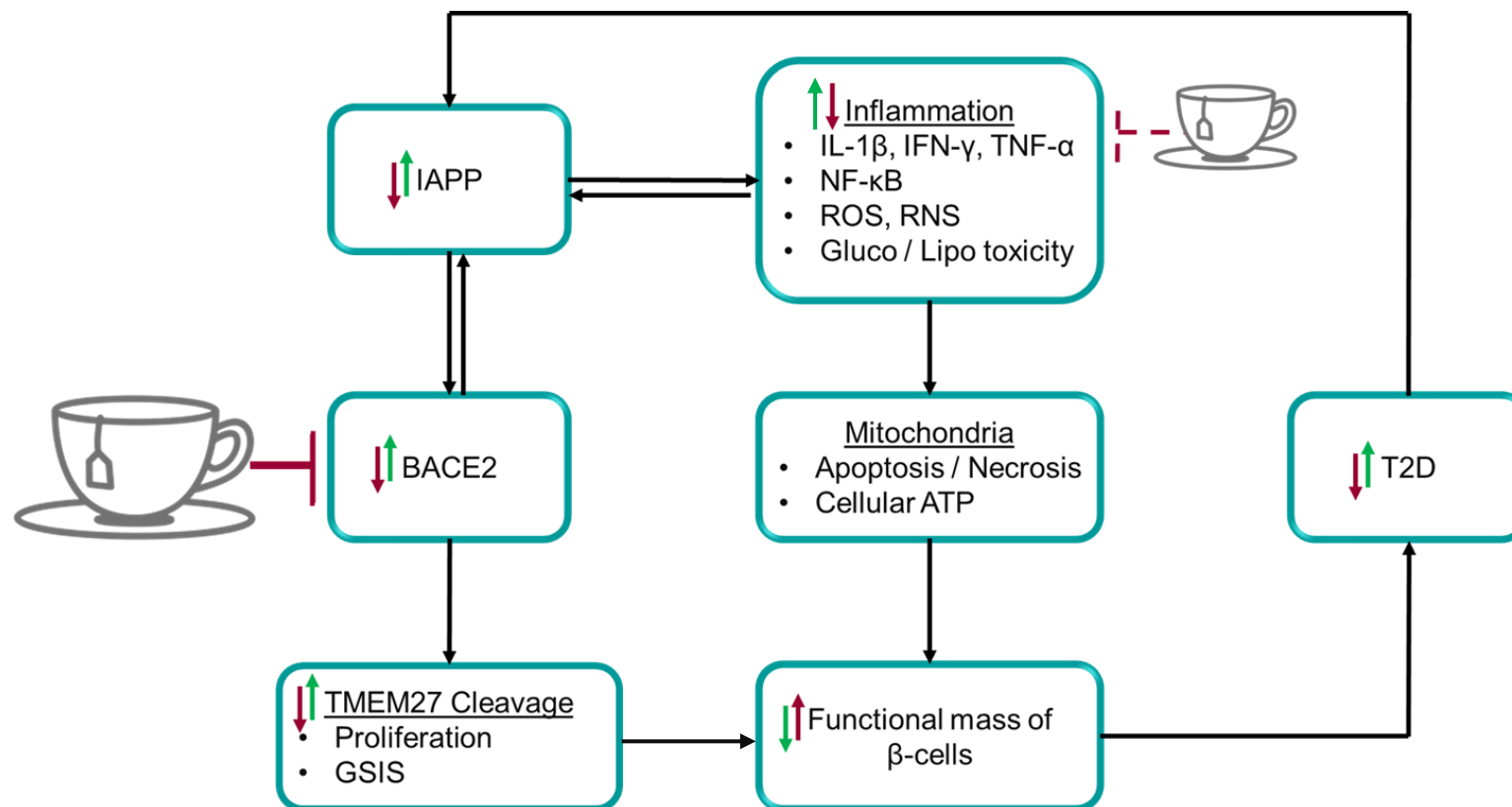
Figure 4.1: Proposed mechanisms involved in beta secretase 2 inhibition in pancreatic beta-cells. Type 2 diabetes is associated with a loss of pancreatic β-cell functional mass. In T2D subject, amylin levels are elevated and are associated with increased BACE2 expression. Beta secretase 2 modulates amylin expression. Amylin-induced inflammation in conjunction with other stressors such as glucotoxicity, lipotoxicity, and oxidative stress leads to β-cell dysfunction by decreasing ATP production as well as cell death. The latter can be compensated for by increasing the rate of proliferation. However, the increased levels of BACE2, seen in T2D, decreases the rate of proliferation and negatively influences insulin signalling, exacerbating β-cell dysfunction and the progression of T2D. Plant polyphenols may inhibit BACE activity as well as directly target inflammatory responses.

4.1. Establishing a Non-Lethal Pro-Inflammatory State in Rat Insulinoma Cells

The first part of the aim of the study was to determine whether GRT, Asp, and PPAG can reduce a state of moderate inflammation in INS1 cells. Therefore, the first objective of the aim was to establish a pro-inflammatory model using the INS1 cells and a non-lethal combination of pro-inflammatory cytokines.   In a disease state, elevated levels of glucose would be present and will further induce inflammation. However, for the purpose of this study co-exposure with high glucose levels, apart from the cytokine cocktail, was excluded as the cytokine cocktail directly stimulates inflammation.   A cytokine cocktail of three different pro-inflammatory cytokines were used to establish the inflammatory condition in rat insulinoma INS1 cells, representative of the T2D disease state. A range of literature-based concentrations of TNF-α, IL-1β, and IFN-γ acting as inducers of moderate inflammation were assessed in INS1 cells (Chellan, 2014; Dai et al., 2013; Kacheva et al., 2011; Yang et al., 2015; Yang and Johnson, 2013).   In addition to assessing the effect of the individual cytokines at different concentrations, two previously published pro-inflammatory cytokine cocktails, A and B, were used to assess the combined effects of the cytokines, characteristic of T2D pathophysiology. The two pro-inflammatory cytokine cocktails provide more insights into the effect(s) these cytokines might exert; such as a synergistic or antagonistic effect on each other. Cell viability of INS1 cells was assessed after 3, 6, and 24 hours of exposure to these cytokines. After 3 and 6 hours, no measurable effect was seen in the cells exposed to TNF-α or IFN-γ (Figure 3.2 A and B).   However, the cells exposed to IL-1β showed a significant increase in mitochondrial dehydrogenase activity at two concentrations (0.01 and 1 ng/ml) after 3 hours (Figure 3.2 A). The increased mitochondrial activity could reflect a pro-inflammatory mediated superoxide flash response whereby increased ROS functions to scavenge NO and thereby attenuate the cytokine-induced NO response (Broniowska et al., 2015). It has been proposed that IL-1β and IL-6 simulate the production and secretion of each other (Cahill and Rogers, 2008) and IL-6 has previously been shown to exert both pro- and anti-inflammatory effects (Kamimura et al., 2003; Starkie et al., 2003; Steensberg et al., 2003; Z. Xing et al., 1998). A study by Choi et al. (2004), showed that IL-6 protects pancreatic β-cells from pro-inflammatory cytokine-induced cell death and functional impairment *in vitro* and *in vivo.* After 24 hours of exposure, TNF-α had no measurable effect on mitochondrial dehydrogenase activity, while IFN-γ exposure induced a significant increase at 1 ng/ml relative to the negative control (Figure 3.2 C). Although TNF-α is one of the most important death effector molecules, most cells are not susceptible to apoptosis by TNF-α alone due to the concomitant activation of the anti-apoptotic process by TNF-α (Beg and Baltimore, 1996; Van Antwerp et al., 1996). Nuclear factor-kappa B has been implicated as an important molecule in the protection of cells against

TNF-α induced apoptosis (Chu et al., 1997), while other studies reported increased cell death in pancreatic islet cells through NF-κB activation (Han et al., 2001; Heimberg et al., 2001), indicating a complex interplay between cytokines and TFs, which may be different according the modes of cell death. Chang et al. (2003), found evidence supporting the role of NF-κB in the protection of pancreatic β-cells against TNF-α induced apoptosis, which may explain why our study indicated that TNF-α had no effect on mitochondrial dehydrogenase activity (cell death). After 24 hours of exposure, IL-1β was the only cytokine to significantly reduced mitochondrial dehydrogenase activity, but only at the highest concentration used (10 ng/ml) (Figure 3.2 C). Interleukin 1-beta has previously been proposed to be the master switch of inflammation. In comparison to 3 and 6 hours of exposure, 24 hours of exposure to cytokine cocktail A and B induced the largest reduction in mitochondrial activity (Figure 3.1). Previously it has been reported that TNF-α, IL-1β, and IFN-γ exert a synergistic effect on the production of IL-12 in β-cells (Taylor-Fishwick et al., 2013), which may explain our findings showing that the cytokines in the cocktails exert a synergistic effect, resulting in decreased cell viability in comparison to the cytokines individually. Another study by Rabinovitch et al. (1990) showed that IL-1β and TNF-α, as individual stressors, are cytotoxic to islet cells and that this cytotoxicity may be amplified by combining IL-1β and TNF-α and/or adding IFN-γ. Furthermore, a study by Chang et al. (2003) used an IFN-γ/TNF-α in a synergistic model to study the role of NF-κB activation in pancreatic cell death, linking the effects of the cytokine cocktails to the induction of a pro-inflammatory state. It is important to reflect on the complexity of the pathogenesis of different disease states and the various roles of each cytokine during the different stages of disease progression. Although only cytokine cocktail B induced a significant decrease in mitochondrial dehydrogenase activity after 24 hours (Figure 3.2 C), cytokine cocktail A was selected to induce inflammation in our study, as a state of moderate inflammation was needed to represent the T2D disease state, without inducing premature and large scale INS1 cell death. Furthermore, Chellan (2014) used a similar cytokine cocktail as cytokine cocktail A, in cells derived from mice, where cell viability was significantly reduced after 24 hours of exposure. In contrast to our results, the same combination of cytokines at similar concentrations to cytokine cocktail B did not induce cell death after 24 hours. However, this contradiction may possibly be explained by the fact that our cells are derived from rats while Yang and Johnson (2003) used cells derived from mice. It should be considered that the initial point of the pro-inflammatory state might have been missed and might have started before 24 hours as the previous time point was at 6 hours. It was also decided to use 24 hours as the standard period for exposure since we sought to induce a chronic state of inflammation and this was the longest feasible period within which to maintain this immortalised cell population.

Although cytokine cocktail A showed no significant change in the MTT results, it did show some apoptosis inducing effects, as measured by means of flow cytometry using the AV/PI assay. Beta-cell apoptosis in T2D has been reported in only a few studies (Butler et al., 2003; Kaneto et al., 1999), presumably owing to low probability of detecting ongoing β-cell apoptosis in given pancreatic sections of slowly progressive T2D. Therefore, by assessing cell death kinetically, as in this study, the probability of missing the point of cell death is reduced. The kinetic assays of cell death, although not statistically significant, showed a trend towards increased necrosis in the cells exposed to cytokine cocktail A, which may be of biological significance. In addition to elevated insulin levels, recent studies have described elevated circulating levels of IL-1β, TNF-α, and/or AGEs (Donath and Shoelson, 2011), which could potentially induce β-cell dysfunction or apoptosis in the long term. However, in this study no measurable effect was seen when comparing the insulin secretion of the negative control to cytokine cocktail A (Figure 3.13). The 1.5X fold change seen in protein expression of COX2 (Figure 3.28) and NF-κB (Figure 3.29), verified the inflammatory state induced by the cytokines, as both these proteins are involved in related inflammatory pathways. However, a study by Poligone and Baldwin (2001) demonstrated that COX2 expression may inhibit nuclear translocation of NF-κB and that the cyclopentenone prostaglandins inhibit NF-κB. They also indicated that prostaglandin E_2 strongly synergizes with the inflammatory cytokine TNF-α to promote NF-κB-dependent transcription and gene expression. Furthermore, cytokine cocktail A, although not significantly, negatively influenced insulin signalling through TMEM27 cleavage as a 0.5X fold change in TMEM27 (Figure 3.26) as well as amylin (Figure 3.25) expression was observed; both of these proteins are associated with insulin signalling. The latter verifies the findings of previous studies that have shown that BACE2 cleaves TMEM27 and can negatively influence insulin production (Alcarraz-Vizán et al., 2015; Esterházy et al., 2011; Stützer et al., 2013). A study by Zhang and Kim, 1995 showed that TNF-α inhibits GSIS in INS1 cells. Furthermore, Kiely et al., 2007 showed that the addition of IL-1β, TNF-α, and IFN-γ (at concentrations that did not induce apoptosis) inhibited chronic and acute stimulated levels of insulin secretion while increasing cellular glucose uptake. However, more time points need to be assessed to determine the effect of these stressors in a more chronic state of moderate inflammation, and levels of IL-6 will need to be assessed to determine if INS1 cells first initiate an anti-inflammatory state before exerting a pro-inflammatory state. It is also important to consider that this study only assessed the treatment effects of Asp, PPAG, or GRT by performing co-treatments, while in a physiological state representative of T2D an inflammation state will already be present and glucose levels would be elevated. Therefore, it will be vital to assess the treatment effect of Asp, PPAG, or GRT by doing pre-treatment with these cytokines to induce a chronic low-grade inflammatory state prior to treatment.

Furthermore, it should also be considered to pre-treat the INS1 cells with Asp, PPAG, and GRT to determine if these extracts will prevent damage induced by inflammation in INS1 cells.

4.2. Effect of Asp, PPAG, and GRT on Rat Insulinoma Cells in a Pro-Inflammatory State

4.2.1. Rat Insulinoma Cell Viability

The first objective to the first aim was also to determine the potential protective effect of Asp, PPAG, and GRT on inflamed INS1 cells. This was done by assessing the effect of Asp, PPAG, and GRT on INS1 cells with experimentally induced moderate inflammation after 24 hours of co-treatment with cytokine cocktail A. After 24 hours, no change was observed in mitochondrial dehydrogenase activity, except at the highest concentrations of Asp (1000 µM) and GRT (1 mg/ml) used, both inducing a significant reduction in mitochondrial dehydrogenase activity (Figure 3.4 A and C). A study done by Bae et al., 2015 showed that pre-treatment with either kazinol C or isokazinol D abolished cytokine-induced toxicity in both RINm5F cells and pancreatic islets by inhibiting NF-κB signalling, however, our results showed no change in NF-κB expression after co-treatment (Figure 3.29). To determine if the toxic effects seen at these concentrations of Asp and GRT were the result of the induced inflammation state in conjunction with Asp and GRT or if it is just a result of its toxicity, INS1 cells were exposed for 24 hours in the absence of the cytokine cocktail A with the same range of concentrations of Asp, PPAG, and GRT used in the inflamed cells. This showed that Asp and GRT seem to exhibit a positive effect on INS1 cells, although not statistically significant, by showing a trend towards increased mitochondrial dehydrogenase activity at lower concentrations (Figure 3.3 A and C) and may be biological significant. However, it is important to note that the highest concentrations of Asp and GRT reduced the mitochondrial dehydrogenase activity of the cells, while PPAG had no measurable effect (Figure 3.3 B). This may be due to the higher content of Asp than PPAG in the GRT extract. Therefore, it can be proposed that the highest concentrations of Asp and GRT exerted prooxidative effects (Joubert et al., 2005), and that an induced inflammation state in INS1 cells exacerbates the toxic effect. However, it has previously been stated that plant polyphenols could negatively influence MTT results as these plant polyphenols interact with the MTT (Bruggisser et al., 2002; Piwen Wang et al., 2010), therefore an ATP assay was done to verify MTT cell viability results. Overall no measurable effect was seen on cellular ATP production except at the highest concentration of Asp and GRT, which indicated a significant reduction in cellular ATP production (Figure 3.5 A and C) and can be associated with the decreased mitochondrial dehydrogenase activity seen. In contrast to our findings, Li et al., 2006 reported that green tea polyphenols increase insulin secretion and ATP production. Interestingly, PPAG at the

highest concentration assessed in this study showed an increase in cellular ATP production, indicative of increased mitochondrial activity (Figure 3.5 B). A similar effect of PPAG, at the highest concentration, was seen when assessing oxidative stress, where a significant reduction in ROS production was seen both after 24 hours (Figure 3.19 B), relative to cytokine cocktail A, and kinetically over 24 hours (Figure 3.20 B), relative to both the negative control and cytokine cocktail A. The GRT extract showed a significant increase in insulin secretion at basal levels, while only the highest concentration of Asp showed an increase (Figure 3.13 A and C). It has previously been proposed that ATP production correlates positively with insulin secretion where increased mitochondrial ATP production, in response to hyperglycemia, closes the ATP sensitive K^+ channels, leading to membrane depolarization, opening of voltage-sensitive Ca^{2+} channels, Ca^{2+} ion influx and insulin granule exocytosis (Chatterjee et al., 2012).

All the aforementioned assays only assessed cell viability after 24 hours of co-treatment which is only indicative of the viability of the cells at that specific moment, giving a snapshot of what is happening in the INS1 cells. Therefore, cell viability was further assessed, by measuring early and late apoptosis and necrosis kinetically. As previously mentioned, Bae et al., 2015 showed that pre-treatment with either kazinol C or isokazinol D abolished cytokine-induced toxicity in both RINm5F cells and islets by inhibiting NF-κB signalling pathways, thus inhibiting apoptotic cell death and defects in insulin secretion. This effect is verified in our study as the lower concentrations of Asp, PPAG, and GRT decreased cell death measured by AV/PI (Figure 3.6 A,B, and C) and caspase-3/7 (Figure 3.11 A, B, and C) kinetically, as well as increased basal insulin secretion in INS1 cells were observed after GRT exposure (Figure 3.13 C). The higher concentrations of Asp, and, in particular, GRT, did not have this protective effect on the INS1 cells. This was observed as a reduction in mitochondrial dehydrogenase activity (Figure 3.4 A and C), decreased ATP production (Figure 3.5 A and C), and increased early apoptosis and necrosis were seen after 24 hours of co-treatment with Asp and GRT at its highest concentrations (Figure 3.6 A and C), as well as increased caspase-3/7 activation (Figure 3.11 A and C) with Asp exposure, as seen in the kinetic assay. These results were verified by means of flow cytometry as this affords assessment of each cell individually and a clear distinction can be made between early and late apoptosis, as well as necrosis. The flow cytometry results showed that the higher concentrations of Asp and GRT reduce cell viability as increased fluorescence of AV and PI were measured, with GRT showing a significant increase especially in necrosis and Asp in early apoptosis (Figure 3.10).

Fluorescent and phase microscopy images were taken after 24 hours of co-treatment. The phase microscopy images indicate a change in cell morphology in the GRT-exposed cells as more areas void of cells were seen. In addition, there was a change in the morphology and

size of the cells, from stellate to a smaller and more circular shape, with the cytoplasm unevenly spread. These cells were also less adhesive and had poor cluster orientation. Furthermore, the GRT-exposed cells had increased fluorescence, indicative of cell death (Figure 3.12 B; x).

It is important to note that the highest concentrations of Asp and GRT that showed decreased cell viability. Interestingly, as was confirmed by Joubert et al., (2005), Rooibos and Asp have been shown to exhibit both antioxidant and prooxidant effects depending on the dose used. It is also important to realise that cell culture does not account for bioavailability of the extracts the and compounds, and therefore the concentrations used are more representative of the plasma concentrations. The concentrations of GRT, Asp, and PPAG where toxic effects were observed were extremely high and thus not physiologically relevant if it were to be extrapolated to any form of sentient model, particularly in light of most polyphenolic compounds, including Asp, having low bioavailability (Bowles et al., 2017; Breiter et al., 2011; Stalmach et al., 2009).

4.2.2.   Rat Insulinoma Cell Function

The main function of pancreatic β-cells is to secrete insulin in response to plasma glucose concentrations, therefore a GSIS assay was done to measure insulin secretion. At basal glucose levels, only the highest concentrations of Asp induced a significant increase in insulin secretion, while PPAG had no measurable effect. In the presence of cytokine cocktail A, the INS1 cells exposed to GRT significantly increased insulin secretion overall (Figure 3.13 C), correlating with the suggested trend towards increased cell activity at the lower concentrations of GRT. Glucose stimulated insulin secretion indicated an overall increase in insulin secretion after glucose stimulation in the cells treated with Asp, PPAG, and GRT (Figure 3.13 A, B, and C). Interestingly, the stimulatory effect of GRT seen at basal levels seems to be lost after glucose stimulation (Figure 3.13 C). This may be explained by the possibility that the insulin stores are depleted at basal levels and thus there was insufficient stored insulin to adequately respond to glucose stimulation. However, cellular insulin content of the INS1 cells was also determined, but no measurable changes were seen (Figure 3.14). In contrast to our findings, it has previously been shown that Asp and PPAG increase insulin secretion from several β-cell lines which were not exposed to stressors (Bramati et al., 2002; Kawano et al., 2009; Ku et al., 2015; McKay and Blumberg, 2007).

Insulin and amylin are co-secreted from β-cells; thus, amylin is also indicative of cell function. No measurable effect was seen in both glucose stimulated amylin secretion and cellular content (Figure 3.15 and Figure 3.16). It is important to note that amylin content was measured from the same samples used to measure GSIS. It is possible that amylin levels

may already be depleted at basal levels as seen in the insulin secretion results. In addition, the insulin:amylin secretion ratio in INS1 cells is yet to be published. For further studies, amylin secretion at basal levels needs to be measured. Cell function was also assessed by measuring the proliferation rate of INS1 cells. After 24 of co-treatment with the highest concentration of Asp and the two highest concentrations of GRT a significant decrease in the rate of INS1 cell proliferation was seen (Figure 3.18 A and C), verifying the reduction in cell viability in previous experiments. These results show that the second highest concentration of GRT, as previously mentioned, might decrease both cell viability and function by increasing cell death and reducing cell proliferation.

In contrast to our findings, genistein, an isoflavone first isolated from Genista tinctoria, is seen to increase insulin secretion and cell proliferation rate in β-cells (Fu et al., 2010). Amylin was expressed at approximately 65 kDa in our Western blot analysis. In contrast to our finding, most studies showed amylin expression at 4-6 kDa (Cai et al., 2011). Trikha and Jeremic, 2013, showed amylin expression in RIN-m5F cells, with induced human amylin, at 6 kDa. A study done by Despa et al., 2012, showed that amylin trimers in diabetic heart tissue vary from 10 to 50 kDa depending on the type of trimer. However, it has been seen in studies that have probed for the amyloid precursor protein that the expression was between 95 – 130 kDa (Kulas et al., 2017), indicative of a bigger molecule. This finding suggests that amylin polymerization, an indication of a toxic environment, has not occurred. Furthermore, the INS1 cells used in this study were derived from rats, which are reported to not have the capacity to polymerize amylin to form amyloid fibrils (Betsholtz et al., 1989). This further supports the notion that amylin polymerization did not occur and corresponds with our previous findings (Gilead and Gazit, 2008).

4.2.3.   Oxidative Stress in Rat Insulinoma Cells

Cell viability and function are closely related to oxidative stress. The interplay between oxidative stress and inflammatory states directly affects cell function and viability; with an escalation in either state exacerbating the other. Therefore, the reduction in cell viability seen at the highest concentration of Asp may be explained by the significant increase in ROS production after 24 hours of treatment. The lower concentrations of Asp as well PPAG and GRT show an overall decrease in ROS production. Polyphenols, including Asp exhibit both antioxidant, and at high concentrations pro-oxidant activities that deplete the intrinsic antioxidant systems resulting in increased ROS (Joubert et al., 2005) as was observed in this study. However, when ROS were monitored kinetically Asp, PPAG, and GRT reduced ROS production, but not in a dose dependent manner. This contradiction can be explained by the fact that the end-point DCF assay readings were only taken at one specific moment and that

by making use of the DCF assay kinetically, an overall observation can be measured. The kinetic data was collected hourly for the 24 hours, whereafter the AUC was calculated which was an indication of what the overall effect was during the 24 hours and not what happened at each time point. For future analysis it may help to assess the effects at each time point to look at kinetic patterns which will also indicate when in the 24-hour period effects was induced.

In pancreatic β-cells two types of cellular responses can be distinguished depending on the level of NO production. Stressors, such as inflammation, lipotoxicity or hyperglycaemia lead to elevated levels of NO, and are due to the activation of iNOS, which promotes cell death (Lee et al., 2010; Meidute Abaraviciene et al., 2008). However, during homeostasis, low levels of NO is produced by endothelial NO synthase (eNOS) and promotes cell survival (Bachar et al., 2010; Cahuana et al., 2008). NO mediates cellular responses induced by cytokines. Several cytokines, including mixed cocktail of cytokines, IL-1β, IFN-γ, TNF-α, IL-177 and IL-6,8 increase NO production by inducing iNOS expression through activation of NF-κB (Darville and Eizirik, 1998; Ortis et al., 2008). Cytokine cocktail A contained similar cytokines and therefore NO production was assessed. Nitric oxide is unstable and is converted to nitrates, which were measured by means of a Griess assay. Aspalathin, PPAG, and GRT had no measurable effect on nitrate production (Figure 3.21 A, B, and C). A study by Chang et al., 2003 indicated that NO does not play a significant role in β-cell death in the presence of TNF-α, and in fact, at physiological levels, plays a vital role in normal cellular signalling (Chan et al., 2011). Quercetin, a flavonol derived from *Quercus,* and naringenin, a flavanone found in citrus fruits, are seen to induce pAkt activation and participate in β-cell protection from cytokine-induced apoptosis, possibly by a NO-independent mechanism and are proposed to be potent agents to benefit β-cell mass preservation (Lin et al., 2012). It is important to consider that the type of oxidative stress influences the antioxidant properties of polyphenols, as seen in RINm5F cells. The latter showed that ROS levels generated via different oxidative stresses were variable and that drug screening (or, in this case, Asp, PPAG, and GRT) using a single type of stress can create bias when assessing antioxidant properties of a compound. Therefore, a combination of several stresses with several cellular and molecular approaches would provide a more accurate experimental outcome in determining the efficacy of the antioxidant (Auberval et al., 2015).

4.3. Inhibition of Beta Secretase Activity with Asp, PPAG, and GRT in Rat Insulinoma Cells

The second part of the aim was to determine if Asp, PPAG, and GRT can inhibit the activity of BACE. Beta secretase is involved in both insulin signalling through TMEM27 cleavage and

amyloid deposition. In the purified BACE enzyme assay, the highest concentration of GRT seems to have BACE inhibition activity, while PPAG and Asp had no measurable effect (Figure 3.22). However, the effect seen in the purified assay is not indicative of what happens in vitro. Therefore, an in vitro BACE inhibition assay was optimised, as this assay has not been previously described, using INS1 cells. Two concentrations (a high and a low concentration) of a known BACE inhibitor were used as positive controls. As all the other experiments were done either after 24 hours or over a 24-hour period, this in vitro assay was also performed after 24 hours of co-treatment. As seen in the purified assay, the highest concentration of the known inhibitor significantly reduced BACE activity, while the lower concentration of the inhibitor had no measurable effect on BACE activity (Figure 3.23). Similar to the purified assay, GRT seems to reduce BACE activity in a dose-dependent manner with the two highest concentrations significantly reducing BACE activity in INS1 cells (Figure 3.22 C). In contrast to the purified assay, Asp also seems to reduce BACE activity in a dose-dependent manner as the two highest concentrations used reduced BACE activity significantly (Figure 3.23 A).

A study done by Jeon et al (2003) showed that the methanolic extract of commercial green tea has the ability to inhibit BACE1. Catechin, a phenol derived from *Senegalia catechu*, has also been seen to inhibit BACE1 in a dose dependent and non-competitive manner. A study done by Shimmyo et al. 2008 showed that four flavonols, quercetin, kaempherol, myricetin, and morin, and one flavone, apigenin, directly inhibited BACE1 activity in both a cell-free system and neuronal cells (Shimmyo et al., 2008). However, therapeutic BACE1 inhibition to block Aβ production and associated toxicity needs to be balanced as negative effects might arise from diminishing other physiological functions of BACE1, such as processing of substrates involved in neuronal function of the brain and periphery (Koelsch, 2017). The latter also needs to be considered as the inhibition of BACE2 might have negative effects on other systems.

It is proposed that the BACE1 promoter contains NF-κB binding elements (Bourne et al., 2007) and therefore elevated BACE1 expression may elevate Aβ levels in a NF-κB-dependent manner (Buggia-Prevot et al., 2008). Chronic treatment with luteolin, a flavone derived from *Lamiaceae*, and also present in Rooibos, was shown to inhibit BACE1 activity and reduce Aβ levels in the brain (Zheng et al., 2015), therefore more research is needed on chronic exposure of Asp, PPAG, and GRT on β-cells as this study only assessed BACE inhibition over 24 hours. The different effects seen in the two assays may be explained by the fact that by using the purified BACE assay, no other cellular processes were considered. Further, the molecule size, its half-life, and the time of inhibition may play a role. Although a decrease in BACE activity is seen in the *in vitro* assay, protein expression in the Western blot assay did not show a decrease in the expression of BACE2 (Figure 3.27). This can be said to be an advantage

as BACE2 also plays a role in other physiological processes, making it crucial that there is reduction in BACE enzyme activity without diminishing its expression.

CHAPTER 5

Conclusion

By investigating the correlation between inflammation and BACE modulation in pancreatic β-cells, our INS1 cytokine-induced inflammatory cell model revealed two divergent effects of GRT and Asp. At high concentrations GRT and Asp increased ROS, activated caspase-3/7, and decreased cell viability, suggesting that at high concentrations GRT and Asp could induce pro-oxidative effects, a well described phenomenon in polyphenols purported to have strong antioxidant effects. However, at lower concentrations GRT, Asp, and PPAG ameliorate oxidative stress. This is a key finding since a strong correlation between inflammation and oxidative stress exists in many chronic diseases of lifestyle including T2D. Thus, ameliorating oxidative stress may have profound effects on vulnerable pancreatic β-cells, which are well described as having reduced antioxidative capacity. Since BACE regulation indirectly affects islet inflammation, the BACE inhibitory capacity of GRT and Asp is also an important finding of this study and the link between this inhibition and the regulation of oxidative stress warrants further investigation. In addition to improving cell viability at lower concentrations, Asp and GRT also modulated cell function by increasing basal insulin secretion; the potential benefit of this effect still needs to be explored.

Taken together, the lower concentrations of Asp and GRT tested in this study show promise in the amelioration of inflammation-induced oxidative stress and pancreatic β-cell damage.

CHAPTER 6

Study Limitations and Future Work

This study presents with some limitations, however, with more time and resources it is possible to overcome many of these obstacles. As seen in many studies, factors such as the treatment period, acute or chronic, the mode of treatment and treatment dosages, as well as the model influence the outcome.

This study only assessed the effect of Asp, PPAG, and GRT for a period of 24 hours. More investigation is needed to assess the effect of these compounds over a longer period as T2D is a chronic disease state. Furthermore, INS1 cells were co-treated to assess the effect of Asp, PPAG, and GRT on cell viability and function in the setting of inflammation. Thus, it is necessary to assess the effect(s) of these compounds when the cells are pre-treated with the cytokine cocktail to first induce the inflammatory state and then with the compounds to serve as treatment. This will be more representative of a chronic, progressive disease state. Moreover, the effect(s) of the compounds should also be tested by pre-treating INS1 cells with these compounds followed by the induction of an inflammatory state. The latter may provide insights into the preventative/prophylactic effect(s) of these compounds on inflammation in pancreatic β-cells. Further investigation into the effect(s) of cytokine cocktail B on cell viability (i.e. mitochondrial dehydrogenase activity and ATP production) and function (i.e. proliferation) could have been done before excluding it from these experiments. The latter will unsure that the most appropriate cytokine cocktail is used to induce a state of moderate inflammation.

Postive controls for the probes (i.e. DCF) were not included in our experiments. Including positive controls in future studies will ensure that the measuremnts are indeed indicative of what should be measured and not due other factors. It will also be important to include the BACE inhibitor in all the cell viability and function assays to help elucidate its effect.

The INS1 cell line was chosen for this study, as these cells possesses key physiological properties of human pancreatic β-cells; such as physiological responses to glucose as well as presenting with a moderate amount of insulin and amylin content. However, INS1 cells are derived from rat insulinomas. Rodents, and in this case rats, are shown to be unable to form amyloid fibrils from the secreted amylin. This limits this study to fully elucidate the role of the compounds on amyloid-induced inflammation, and moreso directly on toxic amyloid formation and/or breakdown. Transfections with hIAPP may be useful to overcome this obstacle. Moreover, non-cell based amyloid fibril formation inhibition assays may help to elucidate the

mechanistic and signalling pathways involved in amyloid formation and associated inflammation that are altered/regulated by novel therapeutic targets. The purity of the INS1 cells were not assessed. For future studies it will be nessesasry to assess the purity of the cells by measuring the response of the INS1 cells to glucose and compare the response to other pancreatic β-cell lines.

Importantly, the development and progression of T2D is a result of multiple stressors including; glucotoxicity, lipotoxicity, oxidative stress, and inflammation. It is necessary to induce the disease state with these stressors respectively, as well as in combination, as this study only assessed cytokine-induced inflammation. More insights into the interplay between the mechanistic and signalling pathways altered by these different stressors may reveal novel therapeutic targets to protect and preserve vulnerable β-cells.

This study showed limited changes in protein expression in the proteins tested for. It is necessary to assess the effect of Asp, PPAG, and GRT on proteins further downstream in the signalling pathways to see the effect of these compounds. Gene expression assays can help to further assess the effect of Asp, PPAG, and GRT on gene regulation of the genes of interest. This will also provide more insights into the mechanisms involved by indicating if any change in gene expression corresponds with protein expression; revealing if these compounds just effect protein expression or if they change the genes itself.

Due to limited time and resources, a small sample size was assessed (n=3). The latter may have had a negative effect on the statistical power of the results, as poor signicance was observed in most of the experiments. A larger sample size will help to unsure that the effect(s) observed are not / are significant and not just coincidence.   The kinetic data was analysed using a One-way ANOVA and are therefore not a complete indication of results as time and treatments are involved. To fully interrogate our kinetic assay data a statistician will be consulted, and a Two-way ANOVA will be performed.

Importantly, the results in this study are only representative of a specific cell line, thus one minor part of an organ, and moreso, biological system. It is vital to assess the effect(s) of these compounds in more physiological accurate models such as co-culturing with different cell lines (e.g. 3D cultures or transwell co-cultures) and/or animal models. Nevertheless, the results from this study provide an excellent starting point as it helps to complete the picture of interactions between an organisms' cellular components and environment, which ultimately determines its functionality.

CHAPTER 7

References

Abdul-Hay, S.O., Sahara, T., McBride, M., Kang, D., Leissring, M.A., 2012. Identification of BACE2 as an avid ß-amyloid-degrading protease. Mol. Neurodegener. 7, 46. https://doi.org/10.1186/1750-1326-7-46

Abedini, A., Schmidt, A.M., 2013. Mechanisms of islet amyloidosis toxicity in type 2 diabetes. FEBS Lett. 587, 1119–1127. https://doi.org/10.1016/j.febslet.2013.01.017

Ailhaud, G., Fukamizu, A., Massiera, F., Negrel, R., Saint-Marc, P., Teboul, M., 2000. Angiotensinogen, angiotensin II and adipose tissue development. Int. J. Obes. Relat. Metab. Disord. J. Int. Assoc. Study Obes. 24 Suppl 4, S33-35.

Akesson, B., Panagiotidis, G., Westermark, P., Lundquist, I., 2003. Islet amyloid polypeptide inhibits glucagon release and exerts a dual action on insulin release from isolated islets. Regul. Pept. 111, 55–60.

Akpinar, P., Kuwajima, S., Krützfeldt, J., Stoffel, M., 2005. Tmem27: a cleaved and shed plasma membrane protein that stimulates pancreatic beta cell proliferation. Cell Metab. 2, 385–397. https://doi.org/10.1016/j.cmet.2005.11.001

Alam, A., Moonga, B., Bevis, P., Huang, C., Zaidi, M., 1993. Amylin inhibits bone resorption by a direct effect on the motility of rat osteoclasts. Exp. Physiol. 78, 183–196. https://doi.org/10.1113/expphysiol.1993.sp003679

Alcarraz-Vizán, G., Casini, P., Cadavez, L., Visa, M., Montane, J., Servitja, J.-M., Novials, A., 2015. Inhibition of BACE2 counteracts hIAPP-induced insulin secretory defects in pancreatic β-cells. FASEB J. Off. Publ. Fed. Am. Soc. Exp. Biol. 29, 95–104. https://doi.org/10.1096/fj.14-255489

Alcarraz-Vizán, G., Castaño, C., Visa, M., Montane, J., Servitja, J.-M., Novials, A., 2017. BACE2 suppression promotes β-cell survival and function in a model of type 2 diabetes induced by human islet amyloid polypeptide overexpression. Cell. Mol. Life Sci. CMLS 74, 2827–2838. https://doi.org/10.1007/s00018-017-2505-1

Alonso-Castro, A.J., Zapata-Bustos, R., Gómez-Espinoza, G., Salazar-Olivo, L.A., 2012. Isoorientin Reverts TNF-α-Induced Insulin Resistance in Adipocytes Activating the

Insulin Signaling Pathway. Endocrinology 153, 5222–5230. https://doi.org/10.1210/en.2012-1290

Altirriba, J., Gasa, R., Casas, S., Ramírez-Bajo, M.J., Ros, S., Gutierrez-Dalmau, A., Ruiz de Villa, M.C., Barbera, A., Gomis, R., 2010. The role of transmembrane protein 27 (TMEM27) in islet physiology and its potential use as a beta cell mass biomarker. Diabetologia 53, 1406–1414. https://doi.org/10.1007/s00125-010-1728-6

Andreozzi, F., Laratta, E., Sciacqua, A., Perticone, F., Sesti, G., 2004. Angiotensin II impairs the insulin signaling pathway promoting production of nitric oxide by inducing phosphorylation of insulin receptor substrate-1 on Ser312 and Ser616 in human umbilical vein endothelial cells. Circ. Res. 94, 1211–1218. https://doi.org/10.1161/01.RES.0000126501.34994.96

Arita, Y., Kihara, S., Ouchi, N., Takahashi, M., Maeda, K., Miyagawa, J., Hotta, K., Shimomura, I., Nakamura, T., Miyaoka, K., Kuriyama, H., Nishida, M., Yamashita, S., Okubo, K., Matsubara, K., Muraguchi, M., Ohmoto, Y., Funahashi, T., Matsuzawa, Y., 1999. Paradoxical decrease of an adipose-specific protein, adiponectin, in obesity. Biochem. Biophys. Res. Commun. 257, 79–83.

Arnush, M., Heitmeier, M.R., Scarim, A.L., Marino, M.H., Manning, P.T., Corbett, J.A., 1998. IL-1 produced and released endogenously within human islets inhibits beta cell function. J. Clin. Invest. 102, 516–526.

Asfari, M., Janjic, D., Meda, P., Li, G., Halban, P.A., Wollheim, C.B., 1992. Establishment of 2-mercaptoethanol-dependent differentiated insulin-secreting cell lines. Endocrinology 130, 167–178. https://doi.org/10.1210/endo.130.1.1370150

Ashcroft, F.M., Rorsman, P., 1989. Electrophysiology of the pancreatic beta-cell. Prog. Biophys. Mol. Biol. 54, 87–143.

Auberval, N., Dal, S., Bietiger, W., Seyfritz, E., Peluso, J., Muller, C., Zhao, M., Marchioni, E., Pinget, M., Jeandidier, N., Maillard, E., Schini-Kerth, V., Sigrist, S., 2015. Oxidative Stress Type Influences the Properties of Antioxidants Containing Polyphenols in RINm5F Beta Cells [WWW Document]. Evid. Based Complement. Alternat. Med. URL https://www.hindawi.com/journals/ecam/2015/859048/ (accessed 6.7.18).

Ayeleso, A., Brooks, N., Oguntibeju, O., 2014. Modulation of antioxidant status in streptozotocin-induced diabetic male Wistar rats following intake of red palm oil and/or

rooibos. Asian Pac. J. Trop. Med. 7, 536–544. https://doi.org/10.1016/S1995-7645(14)60090-0

Bachar, E., Ariav, Y., Cerasi, E., Kaiser, N., Leibowitz, G., 2010. Neuronal nitric oxide synthase protects the pancreatic beta cell from glucolipotoxicity-induced endoplasmic reticulum stress and apoptosis. Diabetologia 53, 2177–2187. https://doi.org/10.1007/s00125-010-1833-6

Badman, M.K., Shennan, K.I., Jermany, J.L., Docherty, K., Clark, A., 1996. Processing of pro-islet amyloid polypeptide (proIAPP) by the prohormone convertase PC2. FEBS Lett. 378, 227–231.

Bae, U.-J., Jang, H.-Y., Lim, J.M., Hua, L., Ryu, J.-H., Park, B.-H., 2015. Polyphenols isolated from Broussonetia kazinoki prevent cytokine-induced β-cell damage and the development of type 1 diabetes. Exp. Mol. Med. 47, e160. https://doi.org/10.1038/emm.2015.16

Bailyes, E.M., Shennan, K.I., Seal, A.J., Smeekens, S.P., Steiner, D.F., Hutton, J.C., Docherty, K., 1992. A member of the eukaryotic subtilisin family (PC3) has the enzymic properties of the type 1 proinsulin-converting endopeptidase. Biochem. J. 285, 391–394.

Baldwin, A.S., 1996. The NF-kappa B and I kappa B proteins: new discoveries and insights. Annu. Rev. Immunol. 14, 649–683. https://doi.org/10.1146/annurev.immunol.14.1.649

Balfour, J.A., Plosker, G.L., 1999. Rosiglitazone. Drugs 57, 921-930-932.

Bansal, A.K., Bilaspuri, G.S., 2011. Impacts of Oxidative Stress and Antioxidants on Semen Functions [WWW Document]. Vet. Med. Int. URL https://www.hindawi.com/journals/vmi/2011/686137/abs/ (accessed 5.1.18).

Barnes, K.M., Miner, J.L., 2009. Role of resistin in insulin sensitivity in rodents and humans. Curr. Protein Pept. Sci. 10, 96–107.

Bastard, J.P., Jardel, C., Bruckert, E., Blondy, P., Capeau, J., Laville, M., Vidal, H., Hainque, B., 2000. Elevated levels of interleukin 6 are reduced in serum and subcutaneous adipose tissue of obese women after weight loss. J. Clin. Endocrinol. Metab. 85, 3338–3342. https://doi.org/10.1210/jcem.85.9.6839

Bastard, J.-P., Maachi, M., Van Nhieu, J.T., Jardel, C., Bruckert, E., Grimaldi, A., Robert, J.-J., Capeau, J., Hainque, B., 2002. Adipose tissue IL-6 content correlates with

resistance to insulin activation of glucose uptake both in vivo and in vitro. J. Clin. Endocrinol. Metab. 87, 2084–2089. https://doi.org/10.1210/jcem.87.5.8450

Bates, S.H., Myers, M.G., 2003. The role of leptin receptor signaling in feeding and neuroendocrine function. Trends Endocrinol. Metab. TEM 14, 447–452.

Beg, A.A., Baltimore, D., 1996. An essential role for NF-kappaB in preventing TNF-alpha-induced cell death. Science 274, 782–784.

Beltrán-Debón, R., Rull, A., Rodríguez-Sanabria, F., Iswaldi, I., Herranz-López, M., Aragonès, G., Camps, J., Alonso-Villaverde, C., Menéndez, J.A., Micol, V., Segura-Carretero, A., Joven, J., 2011. Continuous administration of polyphenols from aqueous rooibos (Aspalathus linearis) extract ameliorates dietary-induced metabolic disturbances in hyperlipidemic mice. Phytomedicine Int. J. Phytother. Phytopharm. 18, 414–424. https://doi.org/10.1016/j.phymed.2010.11.008

Benditt, E. p., Eriksen, N., Hermodson, M. a., Ericsson, L. h., 1971. The major proteins of human and monkey amyloid substance: Common properties including unusual N-terminal amino acid sequences. FEBS Lett. 19, 169–173. https://doi.org/10.1016/0014-5793(71)80506-9

Bennett, B.D., Babu-Khan, S., Loeloff, R., Louis, J.-C., Curran, E., Citron, M., Vassar, R., 2000. Expression Analysis of BACE2 in Brain and Peripheral Tissues. J. Biol. Chem. 275, 20647–20651. https://doi.org/10.1074/jbc.M002688200

Benson, S.C., Pershadsingh, H.A., Ho, C.I., Chittiboyina, A., Desai, P., Pravenec, M., Qi, N., Wang, J., Avery, M.A., Kurtz, T.W., 2004. Identification of telmisartan as a unique angiotensin II receptor antagonist with selective PPARgamma-modulating activity. Hypertens. Dallas Tex 1979 43, 993–1002. https://doi.org/10.1161/01.HYP.0000123072.34629.57

Berg, A.H., Scherer, P.E., 2005. Adipose tissue, inflammation, and cardiovascular disease. Circ. Res. 96, 939–949. https://doi.org/10.1161/01.RES.0000163635.62927.34

Bestermann, W., Houston, M.C., Basile, J., Egan, B., Ferrario, C.M., Lackland, D., Hawkins, R.G., Reed, J., Rogers, P., Wise, D., Moore, M.A., 2005. Addressing the global cardiovascular risk of hypertension, dyslipidemia, diabetes mellitus, and the metabolic syndrome in the southeastern United States, part II: treatment recommendations for management of the global cardiovascular risk of hypertension, dyslipidemia, diabetes mellitus, and the metabolic syndrome. Am. J. Med. Sci. 329, 292–305.

Betsholtz, C., Christmansson, L., Engström, U., Rorsman, F., Svensson, V., Johnson, K.H., Westermark, P., 1989. Sequence divergence in a specific region of islet amyloid polypeptide (IAPP) explains differences in islet amyloid formation between species. FEBS Lett. 251, 261–264. https://doi.org/10.1016/0014-5793(89)81467-X

Binder, H., Köhler, G., Arnold, K., Zschörnig, O., 2000. pH and Ca 2+ dependent interaction of Annexin V with phospholipid membranes: a combined study using fluorescence techniques, microelectrophoresis and infrared spectroscopy. Phys. Chem. Chem. Phys. 2, 4615–4623. https://doi.org/10.1039/b003033n

Boghossian, S., Dube, M.G., Torto, R., Kalra, P.S., Kalra, S.P., 2006. Hypothalamic clamp on insulin release by leptin-transgene expression. Peptides 27, 3245–3254. https://doi.org/10.1016/j.peptides.2006.07.022

Bokarewa, M., Nagaev, I., Dahlberg, L., Smith, U., Tarkowski, A., 2005. Resistin, an Adipokine with Potent Proinflammatory Properties. J. Immunol. 174, 5789–5795. https://doi.org/10.4049/jimmunol.174.9.5789

Bonora, E., Zavaroni, I., Coscelli, C., Butturini, U., 1983. Decreased hepatic insulin extraction in subjects with mild glucose intolerance. Metabolism. 32, 438–446.

Bourlier, V., Zakaroff-Girard, A., Miranville, A., De Barros, S., Maumus, M., Sengenes, C., Galitzky, J., Lafontan, M., Karpe, F., Frayn, K.N., Bouloumié, A., 2008. Remodeling phenotype of human subcutaneous adipose tissue macrophages. Circulation 117, 806–815. https://doi.org/10.1161/CIRCULATIONAHA.107.724096

Bourne, K.Z., Ferrari, D.C., Lange-Dohna, C., Rossner, S., Wood, T.G., Perez-Polo, J.R., 2007. Differential regulation of BACE1 promoter activity by nuclear factor-kappaB in neurons and glia upon exposure to beta-amyloid peptides. J. Neurosci. Res. 85, 1194–1204. https://doi.org/10.1002/jnr.21252

Bowles, S., Joubert, E., de Beer, D., Louw, J., Brunschwig, C., Njoroge, M., Lawrence, N., Wiesner, L., Chibale, K., Muller, C., 2017. Intestinal Transport Characteristics and Metabolism of C-Glucosyl Dihydrochalcone, Aspalathin. Mol. Basel Switz. 22. https://doi.org/10.3390/molecules22040554

Bradford, M.M., 1976. A rapid and sensitive method for the quantitation of microgram quantities of protein utilizing the principle of protein-dye binding. Anal. Biochem. 72, 248–254. https://doi.org/10.1016/0003-2697(76)90527-3

Brain, S.D., Wimalawansa, S., MacIntyre, I., Williams, T.J., 1990. The demonstration of vasodilator activity of pancreatic amylin amide in the rabbit. Am. J. Pathol. 136, 487–490.

Bramati, L., Minoggio, M., Gardana, C., Simonetti, P., Mauri, P., Pietta, P., 2002. Quantitative characterization of flavonoid compounds in Rooibos tea (Aspalathus linearis) by LC-UV/DAD. J. Agric. Food Chem. 50, 5513–5519.

Breiter, T., Laue, C., Kressel, G., Gröll, S., Engelhardt, U.H., Hahn, A., 2011. Bioavailability and antioxidant potential of rooibos flavonoids in humans following the consumption of different rooibos formulations. Food Chem. 128, 338–347. https://doi.org/10.1016/j.foodchem.2011.03.029

Briaud, I., Harmon, J.S., Kelpe, C.L., Segu, V.B., Poitout, V., 2001. Lipotoxicity of the pancreatic beta-cell is associated with glucose-dependent esterification of fatty acids into neutral lipids. Diabetes 50, 315–321.

Broniowska, K.A., Oleson, B.J., McGraw, J., Naatz, A., Mathews, C.E., Corbett, J.A., 2015. How the Location of Superoxide Generation Influences the β-Cell Response to Nitric Oxide. J. Biol. Chem. 290, 7952–7960. https://doi.org/10.1074/jbc.M114.627869

Bruggisser, R., von Daeniken, K., Jundt, G., Schaffner, W., Tullberg-Reinert, H., 2002. Interference of plant extracts, phytoestrogens and antioxidants with the MTT tetrazolium assay. Planta Med. 68, 445–448. https://doi.org/10.1055/s-2002-32073

Bruun, J.M., Lihn, A.S., Pedersen, S.B., Richelsen, B., 2005. Monocyte chemoattractant protein-1 release is higher in visceral than subcutaneous human adipose tissue (AT): implication of macrophages resident in the AT. J. Clin. Endocrinol. Metab. 90, 2282–2289. https://doi.org/10.1210/jc.2004-1696

Buggia-Prevot, V., Sevalle, J., Rossner, S., Checler, F., 2008. NFkappaB-dependent control of BACE1 promoter transactivation by Abeta42. J. Biol. Chem. 283, 10037–10047. https://doi.org/10.1074/jbc.M706579200

Burks, D.J., White, M.F., 2001. IRS proteins and beta-cell function. Diabetes 50, S140. https://doi.org/10.2337/diabetes.50.2007.S140

Butcher, M.J., Hallinger, D., Garcia, E., Machida, Y., Chakrabarti, S., Nadler, J., Galkina, E.V., Imai, Y., 2014. Association of proinflammatory cytokines and islet resident leucocytes

with islet dysfunction in type 2 diabetes. Diabetologia 57, 491–501. https://doi.org/10.1007/s00125-013-3116-5

Butler, A.E., Janson, J., Bonner-Weir, S., Ritzel, R., Rizza, R.A., Butler, P.C., 2003. Beta-cell deficit and increased beta-cell apoptosis in humans with type 2 diabetes. Diabetes 52, 102–110.

Cahill, C.M., Rogers, J.T., 2008. Interleukin (IL) 1β Induction of IL-6 Is Mediated by a Novel Phosphatidylinositol 3-Kinase-dependent AKT/IκB Kinase α Pathway Targeting Activator Protein-1. J. Biol. Chem. 283, 25900–25912. https://doi.org/10.1074/jbc.M707692200

Cahuana, G.M., Tejedo, J.R., Hmadcha, A., Ramírez, R., Cuesta, A.L., Soria, B., Martin, F., Bedoya, F.J., 2008. Nitric oxide mediates the survival action of IGF-1 and insulin in pancreatic β cells. Cell. Signal. 20, 301–310. https://doi.org/10.1016/j.cellsig.2007.10.001

Cai, K., Qi, D., Hou, X., Wang, O., Chen, J., Deng, B., Qian, L., Liu, X., Le, Y., 2011. MCP-1 Upregulates Amylin Expression in Murine Pancreatic β Cells through ERK/JNK-AP1 and NF-κB Related Signaling Pathways Independent of CCR2. PLOS ONE 6, e19559. https://doi.org/10.1371/journal.pone.0019559

Carlsson, P.O., Berne, C., Jansson, L., 1998. Angiotensin II and the endocrine pancreas: effects on islet blood flow and insulin secretion in rats. Diabetologia 41, 127–133. https://doi.org/10.1007/s001250050880

Casas, S., Casini, P., Piquer, S., Altirriba, J., Soty, M., Cadavez, L., Gomis, R., Novials, A., 2010. BACE2 plays a role in the insulin receptor trafficking in pancreatic β-cells. Am. J. Physiol. - Endocrinol. Metab. 299, E1087–E1095. https://doi.org/10.1152/ajpendo.00420.2010

Cassis, L.A., 2000. Fat cell metabolism: insulin, fatty acids, and renin. Curr. Hypertens. Rep. 2, 132–138.

Chan, J.Y., Cooney, G.J., Biden, T.J., Laybutt, D.R., 2011. Differential regulation of adaptive and apoptotic unfolded protein response signalling by cytokine-induced nitric oxide production in mouse pancreatic beta cells. Diabetologia 54, 1766–1776. https://doi.org/10.1007/s00125-011-2139-z

Chang, H.Y., Yang, X., 2000. Proteases for Cell Suicide: Functions and Regulation of Caspases. Microbiol. Mol. Biol. Rev. 64, 821–846.

Chang, I., Kim, S., Kim, J.Y., Cho, N., Kim, Y.-H., Kim, H.S., Lee, M.-K., Kim, K.-W., Lee, M.-S., 2003. Nuclear factor kappaB protects pancreatic beta-cells from tumor necrosis factor-alpha-mediated apoptosis. Diabetes 52, 1169–1175.

Chargé, S.B., de Koning, E.J., Clark, A., 1995. Effect of pH and insulin on fibrillogenesis of islet amyloid polypeptide in vitro. Biochemistry (Mosc.) 34, 14588–14593.

Chatterjee, S., Browning, E.A., Hong, N., DeBolt, K., Sorokina, E.M., Liu, W., Birnbaum, M.J., Fisher, A.B., 2012. Membrane depolarization is the trigger for PI3K/Akt activation and leads to the generation of ROS. Am. J. Physiol. Heart Circ. Physiol. 302, H105-114. https://doi.org/10.1152/ajpheart.00298.2011

Chellan, N., 2014. The effect of Cyclopia maculata extract on β-cell function, protection against oxidative stress and cell survival (Thesis). Stellenbosch: Stellenbosch University.

Chen, W., Sudji, I.R., Wang, E., Joubert, E., van Wyk, B.-E., Wink, M., 2013. Ameliorative effect of aspalathin from rooibos (Aspalathus linearis) on acute oxidative stress in Caenorhabditis elegans. Phytomedicine Int. J. Phytother. Phytopharm. 20, 380–386. https://doi.org/10.1016/j.phymed.2012.10.006

Chin, S.Y., Hall, J.M., Brain, S.D., Morton, I.K., 1994. Vasodilator responses to calcitonin gene-related peptide (CGRP) and amylin in the rat isolated perfused kidney are mediated via CGRP1 receptors. J. Pharmacol. Exp. Ther. 269, 989–992.

Cho, K.-H., Wolkenhauer, O., 2003. Analysis and modelling of signal transduction pathways in systems biology. Biochem. Soc. Trans. 31, 1503–1509. https://doi.org/10.1042/bst0311503

Choi, J.S., Islam, M.N., Ali, M.Y., Kim, E.J., Kim, Y.M., Jung, H.A., 2014. Effects of C-glycosylation on anti-diabetic, anti-Alzheimer's disease and anti-inflammatory potential of apigenin. Food Chem. Toxicol. Int. J. Publ. Br. Ind. Biol. Res. Assoc. 64, 27–33. https://doi.org/10.1016/j.fct.2013.11.020

Choi, S.-E., Choi, K.-M., Yoon, I.-H., Shin, J.-Y., Kim, J.-S., Park, W.-Y., Han, D.-J., Kim, S.-C., Ahn, C., Kim, J.-Y., Hwang, E.-S., Cha, C.-Y., Szot, G.L., Yoon, K.-H., Park, C.-G., 2004. IL-6 protects pancreatic islet beta cells from pro-inflammatory cytokines-induced

cell death and functional impairment in vitro and in vivo. Transpl. Immunol. 13, 43–53. https://doi.org/10.1016/j.trim.2004.04.001

Christiansen, T., Richelsen, B., Bruun, J.M., 2005. Monocyte chemoattractant protein-1 is produced in isolated adipocytes, associated with adiposity and reduced after weight loss in morbid obese subjects. Int. J. Obes. 2005 29, 146–150. https://doi.org/10.1038/sj.ijo.0802839

Chu, Z.L., McKinsey, T.A., Liu, L., Gentry, J.J., Malim, M.H., Ballard, D.W., 1997. Suppression of tumor necrosis factor-induced cell death by inhibitor of apoptosis c-IAP2 is under NF-kappaB control. Proc. Natl. Acad. Sci. U. S. A. 94, 10057–10062.

Clark, A., Chargé, S.B., Badman, M.K., de Koning, E.J., 1996a. Islet amyloid in type 2 (non-insulin-dependent) diabetes. APMIS Acta Pathol. Microbiol. Immunol. Scand. 104, 12–18.

Clark, A., Charge, S.B., Badman, M.K., MacArthur, D.A., de Koning, E.J., 1996b. Islet amyloid polypeptide: actions and role in the pathogenesis of diabetes. Biochem. Soc. Trans. 24, 594–599.

Clark, A., Nilsson, M.R., 2004. Islet amyloid: a complication of islet dysfunction or an aetiological factor in Type 2 diabetes? Diabetologia 47, 157–169. https://doi.org/10.1007/s00125-003-1304-4

Cohen, A.S., Calkins, E., 1959. Electron microscopic observations on a fibrous component in amyloid of diverse origins. Nature 183, 1202–1203.

Collier, J.J., Fueger, P.T., Hohmeier, H.E., Newgard, C.B., 2006. Pro- and antiapoptotic proteins regulate apoptosis but do not protect against cytokine-mediated cytotoxicity in rat islets and beta-cell lines. Diabetes 55, 1398–1406.

Cooper, G.J., Willis, A.C., Clark, A., Turner, R.C., Sim, R.B., Reid, K.B., 1987. Purification and characterization of a peptide from amyloid-rich pancreases of type 2 diabetic patients. Proc. Natl. Acad. Sci. U. S. A. 84, 8628–8632.

Corbett, J.A., Sweetland, M.A., Wang, J.L., Lancaster, J.R., McDaniel, M.L., 1993. Nitric oxide mediates cytokine-induced inhibition of insulin secretion by human islets of Langerhans. Proc. Natl. Acad. Sci. U. S. A. 90, 1731–1735.

Corbett, J.A., Wang, J.L., Sweetland, M.A., Lancaster, J.R., McDaniel, M.L., 1992. Interleukin 1 beta induces the formation of nitric oxide by beta-cells purified from rodent islets of Langerhans. Evidence for the beta-cell as a source and site of action of nitric oxide. J. Clin. Invest. 90, 2384–2391. https://doi.org/10.1172/JCI116129

Crouch, S.P., Kozlowski, R., Slater, K.J., Fletcher, J., 1993. The use of ATP bioluminescence as a measure of cell proliferation and cytotoxicity. J. Immunol. Methods 160, 81–88.

Cybulska, B., Kłosiewicz-Latoszek, L., 2018. How do we know that statins are diabetogenic, and why? Is it an important issue in the clinical practice? Kardiologia Pol. Pol. Heart J. 76, 1217–1223. https://doi.org/10.5603/KP.a2018.0150

Dahlman, I., Kaaman, M., Olsson, T., Tan, G.D., Bickerton, A.S.T., Wåhlén, K., Andersson, J., Nordström, E.A., Blomqvist, L., Sjögren, A., Forsgren, M., Attersand, A., Arner, P., 2005. A unique role of monocyte chemoattractant protein 1 among chemokines in adipose tissue of obese subjects. J. Clin. Endocrinol. Metab. 90, 5834–5840. https://doi.org/10.1210/jc.2005-0369

Dai, X., Ding, Y., Zhang, Z., Cai, X., Li, Y., 2013. Quercetin and quercitrin protect against cytokine-induced injuries in RINm5F β-cells via the mitochondrial pathway and NF-κB signaling. Int. J. Mol. Med. 31, 265–271. https://doi.org/10.3892/ijmm.2012.1177

Dandona, P., Aljada, A., Bandyopadhyay, A., 2004. Inflammation: the link between insulin resistance, obesity and diabetes. Trends Immunol. 25, 4–7.

Darville, M.I., Eizirik, D.L., 1998. Regulation by cytokines of the inducible nitric oxide synthase promoter in insulin-producing cells. Diabetologia 41, 1101–1108. https://doi.org/10.1007/s001250051036

Davis, J.E., Gabler, N.K., Walker-Daniels, J., Spurlock, M.E., 2008. Tlr-4 Deficiency Selectively Protects Against Obesity Induced by Diets High in Saturated Fat. Obesity 16, 1248–1255. https://doi.org/10.1038/oby.2008.210

de Luca, C., Olefsky, J.M., 2008. Inflammation and Insulin Resistance. FEBS Lett. 582, 97–105. https://doi.org/10.1016/j.febslet.2007.11.057

Dean, P.M., Matthews, E.K., 1970. Glucose-induced electrical activity in pancreatic islet cells. J. Physiol. 210, 255–264.

DeFronzo, R.A., 2004. Dysfunctional fat cells, lipotoxicity and type 2 diabetes. Int. J. Clin. Pract. Suppl. 9–21.

Delaunay, F., Khan, A., Cintra, A., Davani, B., Ling, Z.C., Andersson, A., Ostenson, C.G., Gustafsson, J., Efendic, S., Okret, S., 1997. Pancreatic beta cells are important targets for the diabetogenic effects of glucocorticoids. J. Clin. Invest. 100, 2094–2098. https://doi.org/10.1172/JCI119743

Despa, S., Margulies, K.B., Chen, L., Knowlton, A.A., Havel, P.J., Taegtmeyer, H., Bers, D.M., Despa, F., 2012. Hyperamylinemia contributes to cardiac dysfunction in obesity and diabetes - a study in humans and rats. Circ. Res. 110, 598–608. https://doi.org/10.1161/CIRCRESAHA.111.258285

Dludla, P.V., Muller, C.J.F., Louw, J., Joubert, E., Salie, R., Opoku, A.R., Johnson, R., 2014. The cardioprotective effect of an aqueous extract of fermented rooibos (Aspalathus linearis) on cultured cardiomyocytes derived from diabetic rats. Phytomedicine Int. J. Phytother. Phytopharm. 21, 595–601. https://doi.org/10.1016/j.phymed.2013.10.029

Domitrović, R., Jakovac, H., Vasiljev Marchesi, V., Vladimir-Knežević, S., Cvijanović, O., Tadić, Z., Romić, Z., Rahelić, D., 2012. Differential hepatoprotective mechanisms of rutin and quercetin in CCl(4)-intoxicated BALB/cN mice. Acta Pharmacol. Sin. 33, 1260–1270. https://doi.org/10.1038/aps.2012.62

Donath, M.Y., 2014. Targeting inflammation in the treatment of type 2 diabetes: time to start. Nat. Rev. Drug Discov. 13, 465–476. https://doi.org/10.1038/nrd4275

Donath, M.Y., Ehses, J.A., Maedler, K., Schumann, D.M., Ellingsgaard, H., Eppler, E., Reinecke, M., 2005. Mechanisms of β-Cell Death in Type 2 Diabetes. Diabetes 54, S108–S113. https://doi.org/10.2337/diabetes.54.suppl_2.S108

Donath, M.Y., Shoelson, S.E., 2011. Type 2 diabetes as an inflammatory disease. Nat. Rev. Immunol. 11, 98–107. https://doi.org/10.1038/nri2925

Donath, M.Y., Størling, J., Berchtold, L.A., Billestrup, N., Mandrup-Poulsen, T., 2008. Cytokines and β-Cell Biology: from Concept to Clinical Translation. Endocr. Rev. 29, 334–350. https://doi.org/10.1210/er.2007-0033

Donath, M.Y., Størling, J., Maedler, K., Mandrup-Poulsen, T., 2003. Inflammatory mediators and islet beta-cell failure: a link between type 1 and type 2 diabetes. J. Mol. Med. Berl. Ger. 81, 455–470. https://doi.org/10.1007/s00109-003-0450-y

Duncan, B.B., Schmidt, M.I., Pankow, J.S., Ballantyne, C.M., Couper, D., Vigo, A., Hoogeveen, R., Folsom, A.R., Heiss, G., Atherosclerosis Risk in Communities Study, 2003. Low-grade systemic inflammation and the development of type 2 diabetes: the atherosclerosis risk in communities study. Diabetes 52, 1799–1805.

Efrat, S., 2004. Regulation of insulin secretion: insights from engineered beta-cell lines. Ann. N. Y. Acad. Sci. 1014, 88–96.

Efrat, S., Linde, S., Kofod, H., Spector, D., Delannoy, M., Grant, S., Hanahan, D., Baekkeskov, S., 1988. Beta-cell lines derived from transgenic mice expressing a hybrid insulin gene-oncogene. Proc. Natl. Acad. Sci. U. S. A. 85, 9037–9041.

Ehses, J.A., Böni-Schnetzler, M., Faulenbach, M., Donath, M.Y., 2008. Macrophages, cytokines and β-cell death in Type 2 diabetes. Biochem. Soc. Trans. 36, 340–342. https://doi.org/10.1042/BST0360340

Ehses, J.A., Ellingsgaard, H., Böni-Schnetzler, M., Donath, M.Y., 2009. Pancreatic islet inflammation in type 2 diabetes: from alpha and beta cell compensation to dysfunction. Arch. Physiol. Biochem. 115, 240–247. https://doi.org/10.1080/13813450903025879

Ehses, J.A., Perren, A., Eppler, E., Ribaux, P., Pospisilik, J.A., Maor-Cahn, R., Gueripel, X., Ellingsgaard, H., Schneider, M.K.J., Biollaz, G., Fontana, A., Reinecke, M., Homo-Delarche, F., Donath, M.Y., 2007. Increased number of islet-associated macrophages in type 2 diabetes. Diabetes 56, 2356–2370. https://doi.org/10.2337/db06-1650

Eizirik, D.L., Mandrup-Poulsen, T., 2001. A choice of death--the signal-transduction of immune-mediated beta-cell apoptosis. Diabetologia 44, 2115–2133. https://doi.org/10.1007/s001250100021

Elayat, A.A., el-Naggar, M.M., Tahir, M., 1995. An immunocytochemical and morphometric study of the rat pancreatic islets. J. Anat. 186, 629–637.

End, D.W., Smets, G., Todd, A.V., Applegate, T.L., Fuery, C.J., Angibaud, P., Venet, M., Sanz, G., Poignet, H., Skrzat, S., Devine, A., Wouters, W., Bowden, C., 2001. Characterization of the antitumor effects of the selective farnesyl protein transferase inhibitor R115777 in vivo and in vitro. Cancer Res. 61, 131–137.

Eriksson, K.F., Lindgärde, F., 1991. Prevention of type 2 (non-insulin-dependent) diabetes mellitus by diet and physical exercise. The 6-year Malmö feasibility study. Diabetologia 34, 891–898.

Esterházy, D., Stützer, I., Wang, H., Rechsteiner, M.P., Beauchamp, J., Döbeli, H., Hilpert, H., Matile, H., Prummer, M., Schmidt, A., Lieske, N., Boehm, B., Marselli, L., Bosco, D., Kerr-Conte, J., Aebersold, R., Spinas, G.A., Moch, H., Migliorini, C., Stoffel, M., 2011. Bace2 is a β cell-enriched protease that regulates pancreatic β cell function and mass. Cell Metab. 14, 365–377. https://doi.org/10.1016/j.cmet.2011.06.018

Evans, J.L., Goldfine, I.D., Maddux, B.A., Grodsky, G.M., 2003. Are oxidative stress-activated signaling pathways mediators of insulin resistance and beta-cell dysfunction? Diabetes 52, 1–8.

Ezenwaka, C.E., Nwagbara, E., Seales, D., Okali, F., Sell, H., Eckel, J., 2009. Insulin resistance, leptin and monocyte chemotactic protein-1 levels in diabetic and non-diabetic Afro-Caribbean subjects. Arch. Physiol. Biochem. 115, 22–27. https://doi.org/10.1080/13813450802676343

Fain, J.N., Madan, A.K., Hiler, M.L., Cheema, P., Bahouth, S.W., 2004. Comparison of the release of adipokines by adipose tissue, adipose tissue matrix, and adipocytes from visceral and subcutaneous abdominal adipose tissues of obese humans. Endocrinology 145, 2273–2282. https://doi.org/10.1210/en.2003-1336

Figueiredo Filho, D.B., Paranhos, R., Rocha, E.C. da, Batista, M., Silva Jr., J.A. da, Santos, M.L.W.D., Marino, J.G., 2013. When is statistical significance not significant? Braz. Polit. Sci. Rev. 7, 31–55. https://doi.org/10.1590/S1981-38212013000100002

Ford, E.S., 2003. The metabolic syndrome and C-reactive protein, fibrinogen, and leukocyte count: findings from the Third National Health and Nutrition Examination Survey. Atherosclerosis 168, 351–358.

Freeman, D.J., Norrie, J., Sattar, N., Neely, R.D., Cobbe, S.M., Ford, I., Isles, C., Lorimer, A.R., Macfarlane, P.W., McKillop, J.H., Packard, C.J., Shepherd, J., Gaw, A., 2001. Pravastatin and the development of diabetes mellitus: evidence for a protective treatment effect in the West of Scotland Coronary Prevention Study. Circulation 103, 357–362.

Fried, S.K., Bunkin, D.A., Greenberg, A.S., 1998. Omental and subcutaneous adipose tissues of obese subjects release interleukin-6: depot difference and regulation by glucocorticoid. J. Clin. Endocrinol. Metab. 83, 847–850. https://doi.org/10.1210/jcem.83.3.4660

Fu, X., Zhang, J., Guo, L., Xu, Y., Sun, L., Wang, S., Feng, Y., Gou, L., Zhang, L., Liu, Y., 2014. Protective role of luteolin against cognitive dysfunction induced by chronic cerebral hypoperfusion in rats. Pharmacol. Biochem. Behav. 126, 122–130. https://doi.org/10.1016/j.pbb.2014.09.005

Fu, Y., Tian, W., Pratt, E.B., Dirling, L.B., Shyng, S.-L., Meshul, C.K., Cohen, D.M., 2009. Down-Regulation of ZnT8 Expression in INS-1 Rat Pancreatic Beta Cells Reduces Insulin Content and Glucose-Inducible Insulin Secretion. PLoS ONE 4, e5679. https://doi.org/10.1371/journal.pone.0005679

Fu, Z., Zhang, W., Zhen, W., Lum, H., Nadler, J., Bassaganya-Riera, J., Jia, Z., Wang, Y., Misra, H., Liu, D., 2010. Genistein induces pancreatic beta-cell proliferation through activation of multiple signaling pathways and prevents insulin-deficient diabetes in mice. Endocrinology 151, 3026–3037. https://doi.org/10.1210/en.2009-1294

Gasa, R., Gomis, R., Casamitjana, R., Novials, A., 2001. High glucose concentration favors the selective secretion of islet amyloid polypeptide through a constitutive secretory pathway in human pancreatic islets. Pancreas 22, 307–310.

Gedulin, B.R., Rink, T.J., Young, A.A., 1997. Dose-response for glucagonostatic effect of amylin in rats. Metabolism. 46, 67–70.

Ghanim, H., Aljada, A., Hofmeyer, D., Syed, T., Mohanty, P., Dandona, P., 2004. Circulating mononuclear cells in the obese are in a proinflammatory state. Circulation 110, 1564–1571. https://doi.org/10.1161/01.CIR.0000142055.53122.FA

Gilbey, S.G., Ghatei, M.A., Bretherton-Watt, D., Zaidi, M., Jones, P.M., Perera, T., Beacham, J., Girgis, S., Bloom, S.R., 1991. Islet amyloid polypeptide: production by an osteoblast cell line and possible role as a paracrine regulator of osteoclast function in man. Clin. Sci. Lond. Engl. 1979 81, 803–808.

Gilead, S., Gazit, E., 2008. The Role of the 14–20 Domain of the Islet Amyloid Polypeptide in Amyloid Formation. Exp. Diabetes Res. 2008. https://doi.org/10.1155/2008/256954

Golstein, P., Kroemer, G., 2007. Cell death by necrosis: towards a molecular definition. Trends Biochem. Sci. 32, 37–43. https://doi.org/10.1016/j.tibs.2006.11.001

Goossens, G.H., 2008. The role of adipose tissue dysfunction in the pathogenesis of obesity-related insulin resistance. Physiol. Behav. 94, 206–218. https://doi.org/10.1016/j.physbeh.2007.10.010

Gratzner, H.G., 1982. Monoclonal antibody to 5-bromo- and 5-iododeoxyuridine: A new reagent for detection of DNA replication. Science 218, 474–475. https://doi.org/10.1126/science.7123245

Gratzner, H.G., Leif, R.C., Ingram, D.J., Castro, A., 1975. The use of antibody specific for bromodeoxyuridine for the immunofluorescent determination of DNA replication in single cells and chromosomes. Exp. Cell Res. 95, 88–94.

Green, L.C., Wagner, D.A., Glogowski, J., Skipper, P.L., Wishnok, J.S., Tannenbaum, S.R., 1982. Analysis of nitrate, nitrite, and [15N]nitrate in biological fluids. Anal. Biochem. 126, 131–138. https://doi.org/10.1016/0003-2697(82)90118-X

Greenberg, A.S., McDaniel, M.L., 2002. Identifying the links between obesity, insulin resistance and β-cell function: potential role of adipocyte-derived cytokines in the pathogenesis of type 2 diabetes. Eur. J. Clin. Invest. 32, 24–34. https://doi.org/10.1046/j.1365-2362.32.s3.4.x

Griess, P., n.d. Bemerkungen zu der Abhandlung der HH. Weselsky und Benedikt „Ueber einige Azoverbindungen". Berichte Dtsch. Chem. Ges. 12, 426–428. https://doi.org/10.1002/cber.187901201117

Grunnet, L.G., Aikin, R., Tonnesen, M.F., Paraskevas, S., Blaabjerg, L., Størling, J., Rosenberg, L., Billestrup, N., Maysinger, D., Mandrup-Poulsen, T., 2009. Proinflammatory cytokines activate the intrinsic apoptotic pathway in beta-cells. Diabetes 58, 1807–1815. https://doi.org/10.2337/db08-0178

Guilherme, A., Virbasius, J.V., Puri, V., Czech, M.P., 2008. Adipocyte dysfunctions linking obesity to insulin resistance and type 2 diabetes. Nat. Rev. Mol. Cell Biol. 9, 367–377. https://doi.org/10.1038/nrm2391

Guo, J.H., Chen, H., Ruan, Y.C., Zhang, X.L., Zhang, X.H., Fok, K.L., Tsang, L.L., Yu, M.K., Huang, W.Q., Sun, X., Chung, Y.W., Jiang, X., Sohma, Y., Chan, H.C., 2014. Glucose-induced electrical activities and insulin secretion in pancreatic islet β-cells are modulated by CFTR. Nat. Commun. 5, 4420. https://doi.org/10.1038/ncomms5420

Gurzov, E.N., Germano, C.M., Cunha, D.A., Ortis, F., Vanderwinden, J.-M., Marchetti, P., Zhang, L., Eizirik, D.L., 2010. p53 up-regulated modulator of apoptosis (PUMA) activation contributes to pancreatic beta-cell apoptosis induced by proinflammatory cytokines and endoplasmic reticulum stress. J. Biol. Chem. 285, 19910–19920. https://doi.org/10.1074/jbc.M110.122374

Halban, P.A., Praz, G.A., Wollheim, C.B., 1983. Abnormal glucose metabolism accompanies failure of glucose to stimulate insulin release from a rat pancreatic cell line (RINm5F). Biochem. J. 212, 439–443.

Hamid, M., McCluskey, J.T., McClenaghan, N.H., Flatt, P.R., 2002. COMPARISON OF THE SECRETORY PROPERTIES OF FOUR INSULIN-SECRETING CELL LINES. Endocr. Res. 28, 35–47. https://doi.org/10.1081/ERC-120004536

Han, X., Sun, Y., Scott, S., Bleich, D., 2001. Tissue inhibitor of metalloproteinase-1 prevents cytokine-mediated dysfunction and cytotoxicity in pancreatic islets and beta-cells. Diabetes 50, 1047–1055.

Hanabusa, T., Kubo, K., Oki, C., Nakano, Y., Okai, K., Sanke, T., Nanjo, K., 1992. Islet amyloid polypeptide (IAPP) secretion from islet cells and its plasma concentration in patients with non-insulin-dependent diabetes mellitus. Diabetes Res. Clin. Pract. 15, 89–96.

Harding, H.P., Ron, D., 2002. Endoplasmic reticulum stress and the development of diabetes: a review. Diabetes 51 Suppl 3, S455-461.

Hardy, J., Selkoe, D.J., 2002. The amyloid hypothesis of Alzheimer's disease: progress and problems on the road to therapeutics. Science 297, 353–356. https://doi.org/10.1126/science.1072994

Harris, P.J., Cooper, M.E., Hiranyachattada, S., Berka, J.L., Kelly, D.J., Nobes, M., Wookey, P.J., 1997. Amylin stimulates proximal tubular sodium transport and cell proliferation in the rat kidney. Am. J. Physiol. 272, F13-21. https://doi.org/10.1152/ajprenal.1997.272.1.F13

Hattori, Y., Suzuki, K., Hattori, S., Kasai, K., 2006. Metformin inhibits cytokine-induced nuclear factor kappaB activation via AMP-activated protein kinase activation in vascular endothelial cells. Hypertens. Dallas Tex 1979 47, 1183–1188. https://doi.org/10.1161/01.HYP.0000221429.94591.72

Heimberg, H., Heremans, Y., Jobin, C., Leemans, R., Cardozo, A.K., Darville, M., Eizirik, D.L., 2001. Inhibition of cytokine-induced NF-kappaB activation by adenovirus-mediated expression of a NF-kappaB super-repressor prevents beta-cell apoptosis. Diabetes 50, 2219–2224.

Henegar, C., Tordjman, J., Achard, V., Lacasa, D., Cremer, I., Guerre-Millo, M., Poitou, C., Basdevant, A., Stich, V., Viguerie, N., Langin, D., Bedossa, P., Zucker, J.-D., Clement,

K., 2008. Adipose tissue transcriptomic signature highlights the pathological relevance of extracellular matrix in human obesity. Genome Biol. 9, R14. https://doi.org/10.1186/gb-2008-9-1-r14

Henriksen, E.J., Jacob, S., Kinnick, T.R., Youngblood, E.B., Schmit, M.B., Dietze, G.J., 1999. ACE inhibition and glucose transport in insulinresistant muscle: roles of bradykinin and nitric oxide. Am. J. Physiol. 277, R332-336.

Herder, C., Müller-Scholze, S., Rating, P., Koenig, W., Thorand, B., Haastert, B., Holle, R., Illig, T., Rathmann, W., Seissler, J., Wichmann, H.-E., Kolb, H., 2006. Systemic monocyte chemoattractant protein-1 concentrations are independent of type 2 diabetes or parameters of obesity: results from the Cooperative Health Research in the Region of Augsburg Survey S4 (KORA S4). Eur. J. Endocrinol. 154, 311–317. https://doi.org/10.1530/eje.1.02090

Hess, D., Li, L., Martin, M., Sakano, S., Hill, D., Strutt, B., Thyssen, S., Gray, D.A., Bhatia, M., 2003. Bone marrow-derived stem cells initiate pancreatic regeneration. Nat. Biotechnol. 21, 763–770. https://doi.org/10.1038/nbt841

Higham, C.E., Hull, R.L., Lawrie, L., Shennan, K.I., Morris, J.F., Birch, N.P., Docherty, K., Clark, A., 2000. Processing of synthetic pro-islet amyloid polypeptide (proIAPP) "amylin" by recombinant prohormone convertase enzymes, PC2 and PC3, in vitro. Eur. J. Biochem. 267, 4998–5004.

Hoekstra, D., Buist-Arkema, R., Klappe, K., Reutelingsperger, C.P., 1993. Interaction of annexins with membranes: the N-terminus as a governing parameter as revealed with a chimeric annexin. Biochemistry (Mosc.) 32, 14194–14202.

Höppener, J.W., Verbeek, J.S., de Koning, E.J., Oosterwijk, C., van Hulst, K.L., Visser-Vernooy, H.J., Hofhuis, F.M., van Gaalen, S., Berends, M.J., Hackeng, W.H., 1993. Chronic overproduction of islet amyloid polypeptide/amylin in transgenic mice: lysosomal localization of human islet amyloid polypeptide and lack of marked hyperglycaemia or hyperinsulinaemia. Diabetologia 36, 1258–1265.

Höppener, J.W.M., Oosterwijk, C., Nieuwenhuis, M.G., Posthuma, G., Thijssen, J.H.H., Vroom, T.M., Ahrén, B., Lips, C.J.M., 1999. Extensive islet amyloid formation is induced by development of Type II diabetes mellitus and contributes to its progression: pathogenesis of diabetes in a mouse model. Diabetologia 42, 427–434. https://doi.org/10.1007/s001250051175

Hotamisligil, G.S., Erbay, E., 2008. Nutrient sensing and inflammation in metabolic diseases. Nat. Rev. Immunol. 8, 923–934. https://doi.org/10.1038/nri2449

Hotamisligil, G.S., Shargill, N.S., Spiegelman, B.M., 1993. Adipose expression of tumor necrosis factor-alpha: direct role in obesity-linked insulin resistance. Science 259, 87–91.

Hou, X., Ling, Z., Quartier, E., Foriers, A., Schuit, F., Pipeleers, D., Van Schravendijk, C., 1999. Prolonged exposure of pancreatic beta cells to raised glucose concentrations results in increased cellular content of islet amyloid polypeptide precursors. Diabetologia 42, 188–194. https://doi.org/10.1007/s001250051138

Huang, G., Shi, L.Z., Chi, H., 2009. Regulation of JNK and p38 MAPK in the immune system: Signal integration, propagation and termination. Cytokine 48, 161–169. https://doi.org/10.1016/j.cyto.2009.08.002

Hug, C., Wang, J., Ahmad, N.S., Bogan, J.S., Tsao, T.-S., Lodish, H.F., 2004. T-cadherin is a receptor for hexameric and high-molecular-weight forms of Acrp30/adiponectin. Proc. Natl. Acad. Sci. U. S. A. 101, 10308–10313. https://doi.org/10.1073/pnas.0403382101

Hull, R.L., Westermark, G.T., Westermark, P., Kahn, S.E., 2004. Islet Amyloid: A Critical Entity in the Pathogenesis of Type 2 Diabetes. J. Clin. Endocrinol. Metab. 89, 3629–3643. https://doi.org/10.1210/jc.2004-0405

Jaikaran, E.T., Clark, A., 2001. Islet amyloid and type 2 diabetes: from molecular misfolding to islet pathophysiology. Biochim. Biophys. Acta 1537, 179–203.

James, J.H., Wagner, K.R., King, J.K., Leffler, R.E., Upputuri, R.K., Balasubramaniam, A., Friend, L.A., Shelly, D.A., Paul, R.J., Fischer, J.E., 1999. Stimulation of both aerobic glycolysis and Na(+)-K(+)-ATPase activity in skeletal muscle by epinephrine or amylin. Am. J. Physiol. 277, E176-186.

Janciauskiene, S., Ahrén, B., 2000. Fibrillar islet amyloid polypeptide differentially affects oxidative mechanisms and lipoprotein uptake in correlation with cytotoxicity in two insulin-producing cell lines. Biochem. Biophys. Res. Commun. 267, 619–625. https://doi.org/10.1006/bbrc.1999.1989

Janson, J., Ashley, R.H., Harrison, D., McIntyre, S., Butler, P.C., 1999. The mechanism of islet amyloid polypeptide toxicity is membrane disruption by intermediate-sized toxic amyloid particles. Diabetes 48, 491–498.

Jares-Erijman, E.A., Jovin, T.M., 2003. FRET imaging. Nat. Biotechnol. 21, 1387–1395. https://doi.org/10.1038/nbt896

Jeon, S.-Y., Bae, K., Seong, Y.-H., Song, K.-S., 2003. Green tea catechins as a BACE1 (beta-secretase) inhibitor. Bioorg. Med. Chem. Lett. 13, 3905–3908.

Jeong, H.R., An, S.S.A., 2015. Causative factors for formation of toxic islet amyloid polypeptide oligomer in type 2 diabetes mellitus. Clin. Interv. Aging 10, 1873–1879. https://doi.org/10.2147/CIA.S95297

Johnson, A.R., Milner, J.J., Makowski, L., 2012. The inflammation highway: metabolism accelerates inflammatory traffic in obesity. Immunol. Rev. 249, 218–238. https://doi.org/10.1111/j.1600-065X.2012.01151.x

Johnson, K.H., O'Brien, T.D., Hayden, D.W., Jordan, K., Ghobrial, H.K., Mahoney, W.C., Westermark, P., 1988. Immunolocalization of islet amyloid polypeptide (IAPP) in pancreatic beta cells by means of peroxidase-antiperoxidase (PAP) and protein A-gold techniques. Am. J. Pathol. 130, 1–8.

Jones, T.H., Kennedy, R.L., 1993. Cytokines and hypothalamic-pituitary function. Cytokine 5, 531–538.

Joubert, E., de Beer, D., 2011. Rooibos (Aspalathus linearis) beyond the farm gate: From herbal tea to potential phytopharmaceutical. South Afr. J. Bot., Special issue on Economic Botany 77, 869–886. https://doi.org/10.1016/j.sajb.2011.07.004

Joubert, E., Gelderblom, W.C.A., Louw, A., de Beer, D., 2008. South African herbal teas: Aspalathus linearis, Cyclopia spp. and Athrixia phylicoides--a review. J. Ethnopharmacol. 119, 376–412. https://doi.org/10.1016/j.jep.2008.06.014

Joubert, E., Winterton, P., Britz, T.J., Gelderblom, W.C.A., 2005. Antioxidant and pro-oxidant activities of aqueous extracts and crude polyphenolic fractions of rooibos (Aspalathus linearis). J. Agric. Food Chem. 53, 10260–10267. https://doi.org/10.1021/jf051355a

Jourdan, T., Godlewski, G., Cinar, R., Bertola, A., Szanda, G., Liu, J., Tam, J., Han, T., Mukhopadhyay, B., Skarulis, M.C., Ju, C., Aouadi, M., Czech, M.P., Kunos, G., 2013. Activation of the Nlrp3 inflammasome in infiltrating macrophages by endocannabinoids mediates beta cell loss in type 2 diabetes. Nat. Med. 19, 1132–1140. https://doi.org/10.1038/nm.3265

Kacheva, S., Lenzen, S., Gurgul-Convey, E., 2011. Differential effects of proinflammatory cytokines on cell death and ER stress in insulin-secreting INS1E cells and the involvement of nitric oxide. Cytokine 55, 195–201. https://doi.org/10.1016/j.cyto.2011.04.002

Kahn, B.B., 1998. Type 2 diabetes: when insulin secretion fails to compensate for insulin resistance. Cell 92, 593–596.

Kahn, S.E., Andrikopoulos, S., Verchere, C.B., 1999. Islet amyloid: a long-recognized but underappreciated pathological feature of type 2 diabetes. Diabetes 48, 241–253.

Kahn, S.E., D'Alessio, D.A., Schwartz, M.W., Fujimoto, W.Y., Ensinck, J.W., Taborsky, G.J., Porte, D., 1990. Evidence of cosecretion of islet amyloid polypeptide and insulin by beta-cells. Diabetes 39, 634–638.

Kahn, S.E., Fujimoto, W.Y., D'Alessio, D.A., Ensinck, J.W., Porte, D., 1991. Glucose stimulates and potentiates islet amyloid polypeptide secretion by the B-cell. Horm. Metab. Res. Horm. Stoffwechselforschung Horm. Metab. 23, 577–580. https://doi.org/10.1055/s-2007-1003759

Kahn, S.E., Haffner, S.M., Heise, M.A., Herman, W.H., Holman, R.R., Jones, N.P., Kravitz, B.G., Lachin, J.M., O'Neill, M.C., Zinman, B., Viberti, G., ADOPT Study Group, 2006. Glycemic durability of rosiglitazone, metformin, or glyburide monotherapy. N. Engl. J. Med. 355, 2427–2443. https://doi.org/10.1056/NEJMoa066224

Kahn, S.E., Verchere, C.B., Andrikopoulos, S., Asberry, P.J., Leonetti, D.L., Wahl, P.W., Boyko, E.J., Schwartz, R.S., Newell-Morris, L., Fujimoto, W.Y., 1998. Reduced amylin release is a characteristic of impaired glucose tolerance and type 2 diabetes in Japanese Americans. Diabetes 47, 640–645.

Kamei, N., Tobe, K., Suzuki, R., Ohsugi, M., Watanabe, T., Kubota, N., Ohtsuka-Kowatari, N., Kumagai, K., Sakamoto, K., Kobayashi, M., Yamauchi, T., Ueki, K., Oishi, Y., Nishimura, S., Manabe, I., Hashimoto, H., Ohnishi, Y., Ogata, H., Tokuyama, K., Tsunoda, M., Ide, T., Murakami, K., Nagai, R., Kadowaki, T., 2006. Overexpression of monocyte chemoattractant protein-1 in adipose tissues causes macrophage recruitment and insulin resistance. J. Biol. Chem. 281, 26602–26614. https://doi.org/10.1074/jbc.M601284200

Kamimura, D., Ishihara, K., Hirano, T., 2003. IL-6 signal transduction and its physiological roles: the signal orchestration model. Rev. Physiol. Biochem. Pharmacol. 149, 1–38. https://doi.org/10.1007/s10254-003-0012-2

Kaneto, H., Kajimoto, Y., Miyagawa, J., Matsuoka, T., Fujitani, Y., Umayahara, Y., Hanafusa, T., Matsuzawa, Y., Yamasaki, Y., Hori, M., 1999. Beneficial effects of antioxidants in diabetes: possible protection of pancreatic beta-cells against glucose toxicity. Diabetes 48, 2398–2406.

Kang, C.-H., Choi, Y.H., Moon, S.-K., Kim, W.-J., Kim, G.-Y., 2013. Quercetin inhibits lipopolysaccharide-induced nitric oxide production in BV2 microglial cells by suppressing the NF-κB pathway and activating the Nrf2-dependent HO-1 pathway. Int. Immunopharmacol. 17, 808–813. https://doi.org/10.1016/j.intimp.2013.09.009

Kang, Y.E., Kim, J.M., Joung, K.H., Lee, J.H., You, B.R., Choi, M.J., Ryu, M.J., Ko, Y.B., Lee, M.A., Lee, J., Ku, B.J., Shong, M., Lee, K.H., Kim, H.J., 2016. The Roles of Adipokines, Proinflammatory Cytokines, and Adipose Tissue Macrophages in Obesity-Associated Insulin Resistance in Modest Obesity and Early Metabolic Dysfunction. PLoS ONE 11. https://doi.org/10.1371/journal.pone.0154003

Kao, T.-K., Ou, Y.-C., Lin, S.-Y., Pan, H.-C., Song, P.-J., Raung, S.-L., Lai, C.-Y., Liao, S.-L., Lu, H.-C., Chen, C.-J., 2011. Luteolin inhibits cytokine expression in endotoxin/cytokine-stimulated microglia. J. Nutr. Biochem. 22, 612–624. https://doi.org/10.1016/j.jnutbio.2010.01.011

Kautzky-Willer, A., Thomaseth, K., Pacini, G., Clodi, M., Ludvik, B., Streli, C., Waldhäusl, W., Prager, R., 1994. Role of islet amyloid polypeptide secretion in insulin-resistant humans. Diabetologia 37, 188–194.

Kawano, A., Nakamura, H., Hata, S., Minakawa, M., Miura, Y., Yagasaki, K., 2009. Hypoglycemic effect of aspalathin, a rooibos tea component from Aspalathus linearis, in type 2 diabetic model db/db mice. Phytomedicine 16, 437–443. https://doi.org/10.1016/j.phymed.2008.11.009

Kayed, R., Head, E., Thompson, J.L., McIntire, T.M., Milton, S.C., Cotman, C.W., Glabe, C.G., 2003. Common structure of soluble amyloid oligomers implies common mechanism of pathogenesis. Science 300, 486–489. https://doi.org/10.1126/science.1079469

Kern, P.A., Ranganathan, S., Li, C., Wood, L., Ranganathan, G., 2001. Adipose tissue tumor necrosis factor and interleukin-6 expression in human obesity and insulin resistance.

Am. J. Physiol. Endocrinol. Metab. 280, E745-751. https://doi.org/10.1152/ajpendo.2001.280.5.E745

Kerr, J.F., Wyllie, A.H., Currie, A.R., 1972. Apoptosis: a basic biological phenomenon with wide-ranging implications in tissue kinetics. Br. J. Cancer 26, 239–257.

Kershaw, E.E., Flier, J.S., 2004. Adipose tissue as an endocrine organ. J. Clin. Endocrinol. Metab. 89, 2548–2556. https://doi.org/10.1210/jc.2004-0395

Keston, A.S., Brandt, R., 1965. The fluorometric analysis of ultramicro quantities of hydrogen peroxide. Anal. Biochem. 11, 1–5. https://doi.org/10.1016/0003-2697(65)90034-5

Kiely, A., McClenaghan, N.H., Flatt, P.R., Newsholme, P., 2007. Pro-inflammatory cytokines increase glucose, alanine and triacylglycerol utilization but inhibit insulin secretion in a clonal pancreatic beta-cell line. J. Endocrinol. 195, 113–123. https://doi.org/10.1677/JOE-07-0306

Kim, C.-S., Park, H.-S., Kawada, T., Kim, J.-H., Lim, D., Hubbard, N.E., Kwon, B.-S., Erickson, K.L., Yu, R., 2006. Circulating levels of MCP-1 and IL-8 are elevated in human obese subjects and associated with obesity-related parameters. Int. J. Obes. 2005 30, 1347–1355. https://doi.org/10.1038/sj.ijo.0803259

Kimoto, K., Suzuki, K., Kizaki, T., Hitomi, Y., Ishida, H., Katsuta, H., Itoh, E., Ookawara, T., Suzuki, K., Honke, K., Ohno, H., 2003. Gliclazide protects pancreatic beta-cells from damage by hydrogen peroxide. Biochem. Biophys. Res. Commun. 303, 112–119.

Klover, P.J., Zimmers, T.A., Koniaris, L.G., Mooney, R.A., 2003. Chronic exposure to interleukin-6 causes hepatic insulin resistance in mice. Diabetes 52, 2784–2789.

Ko, F.N., Chu, C.C., Lin, C.N., Chang, C.C., Teng, C.M., 1998. Isoorientin-6"-O-glucoside, a water-soluble antioxidant isolated from Gentiana arisanensis. Biochim. Biophys. Acta 1389, 81–90.

Koelsch, G., 2017. BACE1 Function and Inhibition: Implications of Intervention in the Amyloid Pathway of Alzheimer's Disease Pathology. Mol. Basel Switz. 22. https://doi.org/10.3390/molecules22101723

Köhler, G., Milstein, C., 1975. Continuous cultures of fused cells secreting antibody of predefined specificity. Nature 256, 495–497.

Kong, M.F., King, P., Macdonald, I.A., Stubbs, T.A., Perkins, A.C., Blackshaw, P.E., Moyses, C., Tattersall, R.B., 1997. Infusion of pramlintide, a human amylin analogue, delays gastric emptying in men with IDDM. Diabetologia 40, 82–88. https://doi.org/10.1007/s001250050646

Ku, S.-K., Kwak, S., Kim, Y., Bae, J.-S., 2015. Aspalathin and Nothofagin from Rooibos (Aspalathus linearis) Inhibits High Glucose-Induced Inflammation In Vitro and In Vivo. Inflammation 38, 445–455. https://doi.org/10.1007/s10753-014-0049-1

Kulas, J.A., Puig, K.L., Combs, C.K., 2017. Amyloid precursor protein in pancreatic islets. J. Endocrinol. 235, 49–67. https://doi.org/10.1530/JOE-17-0122

Kulkarni, R.N., Winnay, J.N., Daniels, M., Brüning, J.C., Flier, S.N., Hanahan, D., Kahn, C.R., 1999. Altered function of insulin receptor substrate-1–deficient mouse islets and cultured β-cell lines. J. Clin. Invest. 104, R69–R75.

Kumarappan, C.T., Mandal, S.C., 2008. Polyphenolic extract of Ichnocarpus frutescens attenuates diabetic complications in streptozotocin-treated diabetic rats. Ren. Fail. 30, 307–322. https://doi.org/10.1080/08860220701857449

Kusminski, C.M., Shetty, S., Orci, L., Unger, R.H., Scherer, P.E., 2009. Diabetes and apoptosis: lipotoxicity. Apoptosis Int. J. Program. Cell Death 14, 1484–1495. https://doi.org/10.1007/s10495-009-0352-8

Laaksonen, D.E., Lindström, J., Lakka, T.A., Eriksson, J.G., Niskanen, L., Wikström, K., Aunola, S., Keinänen-Kiukaanniemi, S., Laakso, M., Valle, T.T., Ilanne-Parikka, P., Louheranta, A., Hämäläinen, H., Rastas, M., Salminen, V., Cepaitis, Z., Hakumäki, M., Kaikkonen, H., Härkönen, P., Sundvall, J., Tuomilehto, J., Uusitupa, M., Finnish diabetes prevention study, 2005. Physical activity in the prevention of type 2 diabetes: the Finnish diabetes prevention study. Diabetes 54, 158–165.

Lajtha, A., Perez-Polo, R., Roßner, S., 2008. Handbook of Neurochemistry and Molecular Neurobiology: Development and Aging Changes in the Nervous System. Springer Science & Business Media.

Larsson, H., Ahrén, B., 1996. Failure to adequately adapt reduced insulin sensitivity with increased insulin secretion in women with impaired glucose tolerance. Diabetologia 39, 1099–1107.

LeBel, C.P., Ischiropoulos, H., Bondy, S.C., 1992. Evaluation of the probe 2',7'-dichlorofluorescin as an indicator of reactive oxygen species formation and oxidative stress. Chem. Res. Toxicol. 5, 227–231.

Lebovitz, H.E., 2001. Insulin resistance: definition and consequences. Exp. Clin. Endocrinol. Diabetes Off. J. Ger. Soc. Endocrinol. Ger. Diabetes Assoc. 109 Suppl 2, S135-148. https://doi.org/10.1055/s-2001-18576

Leckström, A., Björklund, K., Permert, J., Larsson, R., Westermark, P., 1997. Renal elimination of islet amyloid polypeptide. Biochem. Biophys. Res. Commun. 239, 265–268. https://doi.org/10.1006/bbrc.1997.7465

Lee, J.W., Kim, W.H., Yeo, J., Jung, M.H., 2010. ER stress is implicated in mitochondrial dysfunction-induced apoptosis of pancreatic beta cells. Mol. Cells 30, 545–549. https://doi.org/10.1007/s10059-010-0161-5

Leighton, B., Cooper, G.J., 1988. Pancreatic amylin and calcitonin gene-related peptide cause resistance to insulin in skeletal muscle in vitro. Nature 335, 632–635. https://doi.org/10.1038/335632a0

Lerner, A.G., Upton, J.-P., Praveen, P.V.K., Ghosh, R., Nakagawa, Y., Igbaria, A., Shen, S., Nguyen, V., Backes, B.J., Heiman, M., Heintz, N., Greengard, P., Hui, S., Tang, Q., Trusina, A., Oakes, S.A., Papa, F.R., 2012. IRE1α induces thioredoxin-interacting protein to activate the NLRP3 inflammasome and promote programmed cell death under irremediable ER stress. Cell Metab. 16, 250–264. https://doi.org/10.1016/j.cmet.2012.07.007

Li, C., Allen, A., Kwagh, J., Doliba, N.M., Qin, W., Najafi, H., Collins, H.W., Matschinsky, F.M., Stanley, C.A., Smith, T.J., 2006. Green Tea Polyphenols Modulate Insulin Secretion by Inhibiting Glutamate Dehydrogenase. J. Biol. Chem. 281, 10214–10221. https://doi.org/10.1074/jbc.M512792200

Li, X.-L., Chen, T., Wong, Y.-S., Xu, G., Fan, R.-R., Zhao, H.-L., Chan, J.C.N., 2011. Involvement of mitochondrial dysfunction in human islet amyloid polypeptide-induced apoptosis in INS-1E pancreatic beta cells: An effect attenuated by phycocyanin. Int. J. Biochem. Cell Biol. 43, 525–534. https://doi.org/10.1016/j.biocel.2010.12.008

Liao, J.K., Laufs, U., 2005. PLEIOTROPIC EFFECTS OF STATINS. Annu. Rev. Pharmacol. Toxicol. 45, 89–118. https://doi.org/10.1146/annurev.pharmtox.45.120403.095748

Lin, C.-Y., Ni, C.-C., Yin, M.-C., Lii, C.-K., 2012. Flavonoids protect pancreatic beta-cells from cytokines mediated apoptosis through the activation of PI3-kinase pathway. Cytokine 59, 65–71. https://doi.org/10.1016/j.cyto.2012.04.011

Lipinski, B., 2001. Pathophysiology of oxidative stress in diabetes mellitus. J. Diabetes Complications 15, 203–210. https://doi.org/10.1016/S1056-8727(01)00143-X

Llanos, P., Contreras-Ferrat, A., Barrientos, G., Valencia, M., Mears, D., Hidalgo, C., 2015. Glucose-Dependent Insulin Secretion in Pancreatic β-Cell Islets from Male Rats Requires Ca2+ Release via ROS-Stimulated Ryanodine Receptors. PLoS ONE 10. https://doi.org/10.1371/journal.pone.0129238

López-Lázaro, M., 2009. Distribution and biological activities of the flavonoid luteolin. Mini Rev. Med. Chem. 9, 31–59.

Lubet, R.A., Christov, K., You, M., Yao, R., Steele, V.E., End, D.W., Juliana, M.M., Grubbs, C.J., 2006. Effects of the farnesyl transferase inhibitor R115777 (Zarnestra) on mammary carcinogenesis: prevention, therapy, and role of HaRas mutations. Mol. Cancer Ther. 5, 1073–1078. https://doi.org/10.1158/1535-7163.MCT-05-0398

Ludvik, B., Clodi, M., Kautzky-Willer, A., Schuller, M., Graf, H., Hartter, E., Pacini, G., Prager, R., 1994. Increased levels of circulating islet amyloid polypeptide in patients with chronic renal failure have no effect on insulin secretion. J. Clin. Invest. 94, 2045–2050.

Lumeng, C.N., DelProposto, J.B., Westcott, D.J., Saltiel, A.R., 2008. Phenotypic switching of adipose tissue macrophages with obesity is generated by spatiotemporal differences in macrophage subtypes. Diabetes 57, 3239–3246. https://doi.org/10.2337/db08-0872

Lumeng, C.N., Saltiel, A.R., 2011. Inflammatory links between obesity and metabolic disease. J. Clin. Invest. 121, 2111–2117. https://doi.org/10.1172/JCI57132

Lupi, R., Del Guerra, S., Bugliani, M., Boggi, U., Mosca, F., Torri, S., Del Prato, S., Marchetti, P., 2006. The direct effects of the angiotensin-converting enzyme inhibitors, zofenoprilat and enalaprilat, on isolated human pancreatic islets. Eur. J. Endocrinol. 154, 355–361. https://doi.org/10.1530/eje.1.02086

Lupi, R., Del Guerra, S., Marselli, L., Bugliani, M., Boggi, U., Mosca, F., Marchetti, P., Del Prato, S., 2004. Rosiglitazone prevents the impairment of human islet function induced by fatty acids: evidence for a role of PPARgamma2 in the modulation of insulin

secretion. Am. J. Physiol. Endocrinol. Metab. 286, E560-567. https://doi.org/10.1152/ajpendo.00561.2002

Lupi, R., Dotta, F., Marselli, L., Del Guerra, S., Masini, M., Santangelo, C., Patané, G., Boggi, U., Piro, S., Anello, M., Bergamini, E., Mosca, F., Di Mario, U., Del Prato, S., Marchetti, P., 2002. Prolonged exposure to free fatty acids has cytostatic and pro-apoptotic effects on human pancreatic islets: evidence that beta-cell death is caspase mediated, partially dependent on ceramide pathway, and Bcl-2 regulated. Diabetes 51, 1437–1442.

Lyngsø, D., Simonsen, L., Bülow, J., 2002. Metabolic effects of interleukin-6 in human splanchnic and adipose tissue. J. Physiol. 543, 379–386.

Maassen, J.A., Romijn, J.A., Heine, R.J., 2007. Fatty acid-induced mitochondrial uncoupling in adipocytes as a key protective factor against insulin resistance and beta cell dysfunction: a new concept in the pathogenesis of obesity-associated type 2 diabetes mellitus. Diabetologia 50, 2036–2041. https://doi.org/10.1007/s00125-007-0776-z

MacDonald, C., 1990. Development of new cell lines for animal cell biotechnology. Crit. Rev. Biotechnol. 10, 155–178. https://doi.org/10.3109/07388559009068265

Maedler, K., Carr, R.D., Bosco, D., Zuellig, R.A., Berney, T., Donath, M.Y., 2005. Sulfonylurea induced beta-cell apoptosis in cultured human islets. J. Clin. Endocrinol. Metab. 90, 501–506. https://doi.org/10.1210/jc.2004-0699

Maedler, K., Sergeev, P., Ris, F., Oberholzer, J., Joller-Jemelka, H.I., Spinas, G.A., Kaiser, N., Halban, P.A., Donath, M.Y., 2002. Glucose-induced beta cell production of IL-1beta contributes to glucotoxicity in human pancreatic islets. J. Clin. Invest. 110, 851–860. https://doi.org/10.1172/JCI15318

Malmgren, S., Nicholls, D.G., Taneera, J., Bacos, K., Koeck, T., Tamaddon, A., Wibom, R., Groop, L., Ling, C., Mulder, H., Sharoyko, V.V., 2009. Tight Coupling between Glucose and Mitochondrial Metabolism in Clonal β-Cells Is Required for Robust Insulin Secretion. J. Biol. Chem. 284, 32395–32404. https://doi.org/10.1074/jbc.M109.026708

Marais, C., Steenkamp, J.A., Ferreira, D., 1996. The occurrence of phenylpyruvic acid in woody plants: Biosynthetic significance. Tetrahedron Lett. 37, 5763–5764. https://doi.org/10.1016/0040-4039(96)01178-1

Marchetti, P., Del Guerra, S., Marselli, L., Lupi, R., Masini, M., Pollera, M., Bugliani, M., Boggi, U., Vistoli, F., Mosca, F., Del Prato, S., 2004. Pancreatic islets from type 2 diabetic patients have functional defects and increased apoptosis that are ameliorated by metformin. J. Clin. Endocrinol. Metab. 89, 5535–5541. https://doi.org/10.1210/jc.2004-0150

Marchetti, P., Lupi, R., Federici, M., Marselli, L., Masini, M., Boggi, U., Del Guerra, S., Patanè, G., Piro, S., Anello, M., Bergamini, E., Purrello, F., Lauro, R., Mosca, F., Sesti, G., Del Prato, S., 2002. Insulin secretory function is impaired in isolated human islets carrying the Gly(972)-->Arg IRS-1 polymorphism. Diabetes 51, 1419–1424.

Maritim, A.C., Sanders, R.A., Watkins, J.B., 2003. Diabetes, oxidative stress, and antioxidants: a review. J. Biochem. Mol. Toxicol. 17, 24–38. https://doi.org/10.1002/jbt.10058

Marselli, L., Dotta, F., Piro, S., Santangelo, C., Masini, M., Lupi, R., Realacci, M., del Guerra, S., Mosca, F., Boggi, U., Purrello, F., Navalesi, R., Marchetti, P., 2001. Th2 Cytokines Have a Partial, Direct Protective Effect on the Function and Survival of Isolated Human Islets Exposed to Combined Proinflammatory and Th1 Cytokines. J. Clin. Endocrinol. Metab. 86, 4974–4978. https://doi.org/10.1210/jcem.86.10.7938

Martín-Aragón, S., Jiménez-Aliaga, K.L., Benedí, J., Bermejo-Bescós, P., 2016. Neurohormetic responses of quercetin and rutin in a cell line over-expressing the amyloid precursor protein (APPswe cells). Phytomedicine Int. J. Phytother. Phytopharm. 23, 1285–1294. https://doi.org/10.1016/j.phymed.2016.07.007

März, P., Gadient, R.A., Otten, U., 1996. Expression of interleukin-6 receptor (IL-6R) and gp130 mRNA in PC12 cells and sympathetic neurons: modulation by tumor necrosis factor alpha (TNF-alpha). Brain Res. 706, 71–79.

Marzban, L., Trigo-Gonzalez, G., Verchere, C.B., 2005. Processing of pro-islet amyloid polypeptide in the constitutive and regulated secretory pathways of beta cells. Mol. Endocrinol. Baltim. Md 19, 2154–2163. https://doi.org/10.1210/me.2004-0407

Masters, B.R., 2014. Paths to Förster's resonance energy transfer (FRET) theory. Eur. Phys. J. H 39, 87–139. https://doi.org/10.1140/epjh/e2013-40007-9

Masters, S.L., Dunne, A., Subramanian, S.L., Hull, R.L., Tannahill, G.M., Sharp, F.A., Becker, C., Franchi, L., Yoshihara, E., Chen, Z., Mullooly, N., Mielke, L.A., Harris, J., Coll, R.C., Mills, K.H.G., Mok, K.H., Newsholme, P., Nuñez, G., Yodoi, J., Kahn, S.E., Lavelle,

E.C., O'Neill, L.A.J., 2010. Activation of the Nlrp3 inflammasome by islet amyloid polypeptide provides a mechanism for enhanced IL-1β in type 2 diabetes. Nat. Immunol. 11, 897–904. https://doi.org/10.1038/ni.1935

Maury, E., Noël, L., Detry, R., Brichard, S.M., 2009. In vitro hyperresponsiveness to tumor necrosis factor-alpha contributes to adipokine dysregulation in omental adipocytes of obese subjects. J. Clin. Endocrinol. Metab. 94, 1393–1400. https://doi.org/10.1210/jc.2008-2196

McKay, D.L., Blumberg, J.B., 2007. A review of the bioactivity of south African herbal teas: rooibos (Aspalathus linearis) and honeybush (Cyclopia intermedia). Phytother. Res. 21, 1–16. https://doi.org/10.1002/ptr.1992

Meidute Abaraviciene, S., Lundquist, I., Galvanovskis, J., Flodgren, E., Olde, B., Salehi, A., 2008. Palmitate-Induced β-Cell Dysfunction Is Associated with Excessive NO Production and Is Reversed by Thiazolidinedione-Mediated Inhibition of GPR40 Transduction Mechanisms. PLoS ONE 3. https://doi.org/10.1371/journal.pone.0002182

Merglen, A., Theander, S., Rubi, B., Chaffard, G., Wollheim, C.B., Maechler, P., 2004. Glucose Sensitivity and Metabolism-Secretion Coupling Studied during Two-Year Continuous Culture in INS-1E Insulinoma Cells. Endocrinology 145, 667–678. https://doi.org/10.1210/en.2003-1099

Minokoshi, Y., Kim, Y.-B., Peroni, O.D., Fryer, L.G.D., Müller, C., Carling, D., Kahn, B.B., 2002. Leptin stimulates fatty-acid oxidation by activating AMP-activated protein kinase. Nature 415, 339. https://doi.org/10.1038/415339a

Mirsafian, H., Mat Ripen, A., Merican, A.F., Bin Mohamad, S., 2014. Amino acid sequence and structural comparison of BACE1 and BACE2 using evolutionary trace method. ScientificWorldJournal 2014, 482463. https://doi.org/10.1155/2014/482463

Miyazaki, J., Araki, K., Yamato, E., Ikegami, H., Asano, T., Shibasaki, Y., Oka, Y., Yamamura, K., 1990. Establishment of a pancreatic beta cell line that retains glucose-inducible insulin secretion: special reference to expression of glucose transporter isoforms. Endocrinology 127, 126–132. https://doi.org/10.1210/endo-127-1-126

Miyazaki, Y., Matsuda, M., DeFronzo, R.A., 2002. Dose-response effect of pioglitazone on insulin sensitivity and insulin secretion in type 2 diabetes. Diabetes Care 25, 517–523.

Mohamed-Ali, V., Goodrick, S., Rawesh, A., Katz, D.R., Miles, J.M., Yudkin, J.S., Klein, S., Coppack, S.W., 1997. Subcutaneous adipose tissue releases interleukin-6, but not tumor necrosis factor-alpha, in vivo. J. Clin. Endocrinol. Metab. 82, 4196–4200. https://doi.org/10.1210/jcem.82.12.4450

Morioka, T., Asilmaz, E., Hu, J., Dishinger, J.F., Kurpad, A.J., Elias, C.F., Li, H., Elmquist, J.K., Kennedy, R.T., Kulkarni, R.N., 2007. Disruption of leptin receptor expression in the pancreas directly affects β cell growth and function in mice. J. Clin. Invest. 117, 2860–2868. https://doi.org/10.1172/JCI30910

Mosmann, T., 1983. Rapid colorimetric assay for cellular growth and survival: application to proliferation and cytotoxicity assays. J. Immunol. Methods 65, 55–63.

Mulder, H., Ahrén, B., Sundler, F., 1996. Islet amyloid polypeptide and insulin gene expression are regulated in parallel by glucose in vivo in rats. Am. J. Physiol. 271, E1008-1014.

Muller, C.J.F., Joubert, E., de Beer, D., Sanderson, M., Malherbe, C.J., Fey, S.J., Louw, J., 2012. Acute assessment of an aspalathin-enriched green rooibos (Aspalathus linearis) extract with hypoglycemic potential. Phytomedicine 20, 32–39. https://doi.org/10.1016/j.phymed.2012.09.010

Muller, C.J.F., Joubert, E., Pheiffer, C., Ghoor, S., Sanderson, M., Chellan, N., Fey, S.J., Louw, J., 2013. Z-2-(β-d-glucopyranosyloxy)-3-phenylpropenoic acid, an α-hydroxy acid from rooibos (Aspalathus linearis) with hypoglycemic activity. Mol. Nutr. Food Res. 57, 2216–2222. https://doi.org/10.1002/mnfr.201300294

Murano, I., Barbatelli, G., Parisani, V., Latini, C., Muzzonigro, G., Castellucci, M., Cinti, S., 2008. Dead adipocytes, detected as crown-like structures, are prevalent in visceral fat depots of genetically obese mice. J. Lipid Res. 49, 1562–1568. https://doi.org/10.1194/jlr.M800019-JLR200

Nagaev, I., Bokarewa, M., Tarkowski, A., Smith, U., 2006. Human Resistin Is a Systemic Immune-Derived Proinflammatory Cytokine Targeting both Leukocytes and Adipocytes. PLoS ONE 1. https://doi.org/10.1371/journal.pone.0000031

Nakayama, M., Inoguchi, T., Sonta, T., Maeda, Y., Sasaki, S., Sawada, F., Tsubouchi, H., Sonoda, N., Kobayashi, K., Sumimoto, H., Nawata, H., 2005. Increased expression of NAD(P)H oxidase in islets of animal models of Type 2 diabetes and its improvement by an AT1 receptor antagonist. Biochem. Biophys. Res. Commun. 332, 927–933. https://doi.org/10.1016/j.bbrc.2005.05.065

Nicoletti, I., Migliorati, G., Pagliacci, M.C., Grignani, F., Riccardi, C., 1991. A rapid and simple method for measuring thymocyte apoptosis by propidium iodide staining and flow cytometry. J. Immunol. Methods 139, 271–279. https://doi.org/10.1016/0022-1759(91)90198-O

Nijveldt, R.J., van Nood, E., van Hoorn, D.E., Boelens, P.G., van Norren, K., van Leeuwen, P.A., 2001. Flavonoids: a review of probable mechanisms of action and potential applications. Am. J. Clin. Nutr. 74, 418–425.

Nomura, S., Shouzu, A., Omoto, S., Nishikawa, M., Fukuhara, S., 2000. Significance of chemokines and activated platelets in patients with diabetes. Clin. Exp. Immunol. 121, 437–443.

Oh, Y.S., Lee, Y.-J., Park, E.Y., Jun, H.-S., 2011. Interleukin-6 treatment induces beta-cell apoptosis via STAT-3-mediated nitric oxide production. Diabetes Metab. Res. Rev. 27, 813–819. https://doi.org/10.1002/dmrr.1233

Ortis, F., Pirot, P., Naamane, N., Kreins, A.Y., Rasschaert, J., Moore, F., Théâtre, E., Verhaeghe, C., Magnusson, N.E., Chariot, A., Ørntoft, T.F., Eizirik, D.L., 2008. Induction of nuclear factor-κB and its downstream genes by TNF-α and IL-1β has a pro-apoptotic role in pancreatic beta cells. Diabetologia 51, 1213–1225. https://doi.org/10.1007/s00125-008-0999-7

Orzel, J., Daszykowski, M., Kazura, M., de Beer, D., Joubert, E., Schulze, A.E., Beelders, T., de Villiers, A., Malherbe, C.J., Walczak, B., 2014. Modeling of the total antioxidant capacity of rooibos (Aspalathus linearis) tea infusions from chromatographic fingerprints and identification of potential antioxidant markers. J. Chromatogr. A 1366, 101–109. https://doi.org/10.1016/j.chroma.2014.09.030

Oslowski, C.M., Hara, T., O'Sullivan-Murphy, B., Kanekura, K., Lu, S., Hara, M., Ishigaki, S., Zhu, L.J., Hayashi, E., Hui, S.T., Greiner, D., Kaufman, R.J., Bortell, R., Urano, F., 2012. Thioredoxin-interacting protein mediates ER stress-induced β cell death through initiation of the inflammasome. Cell Metab. 16, 265–273. https://doi.org/10.1016/j.cmet.2012.07.005

Pan, P.-H., Lin, S.-Y., Wang, Y.-Y., Chen, W.-Y., Chuang, Y.-H., Wu, C.-C., Chen, C.-J., 2014. Protective effects of rutin on liver injury induced by biliary obstruction in rats. Free Radic. Biol. Med. 73, 106–116. https://doi.org/10.1016/j.freeradbiomed.2014.05.001

Pan, X.-R., Li, G.-W., Hu, Y.-H., Wang, J.-X., Yang, W.-Y., An, Z.-X., Hu, Z.-X., Juan-Lin, Xiao, J.-Z., Cao, H.-B., Liu, P.-A., Jiang, X.-G., Jiang, Y.-Y., Wang, J.-P., Zheng, H., Zhang, H., Bennett, P.H., Howard, B.V., 1997. Effects of Diet and Exercise in Preventing NIDDM in People With Impaired Glucose Tolerance: The Da Qing IGT and Diabetes Study. Diabetes Care 20, 537–544. https://doi.org/10.2337/diacare.20.4.537

Papanicolaou, D.A., Wilder, R.L., Manolagas, S.C., Chrousos, G.P., 1998. The pathophysiologic roles of interleukin-6 in human disease. Ann. Intern. Med. 128, 127–137.

Parulkar, A.A., Pendergrass, M.L., Granda-Ayala, R., Lee, T.R., Fonseca, V.A., 2001. Nonhypoglycemic effects of thiazolidinediones. Ann. Intern. Med. 134, 61–71.

Paulsson, J.F., Ludvigsson, J., Carlsson, A., Casas, R., Forsander, G., Ivarsson, S.A., Kockum, I., Lernmark, Å., Marcus, C., Lindblad, B., Westermark, G.T., 2014. High plasma levels of islet amyloid polypeptide in young with new-onset of type 1 diabetes mellitus. PloS One 9, e93053. https://doi.org/10.1371/journal.pone.0093053

Pereverzev, A., Vajna, R., Pfitzer, G., Hescheler, J., Klockner, U., Schneider, T., 2002. Reduction of insulin secretion in the insulinoma cell line INS-1 by overexpression of a Ca(v)2.3 (alpha1E) calcium channel antisense cassette. Eur. J. Endocrinol. 146, 881–889. https://doi.org/10.1530/eje.0.1460881

Perley, M.J., Kipnis, D.M., 1967. Plasma insulin responses to oral and intravenous glucose: studies in normal and diabetic sujbjects. J. Clin. Invest. 46, 1954–1962. https://doi.org/10.1172/JCI105685

Petersen, E.W., Carey, A.L., Sacchetti, M., Steinberg, G.R., Macaulay, S.L., Febbraio, M.A., Pedersen, B.K., 2005. Acute IL-6 treatment increases fatty acid turnover in elderly humans in vivo and in tissue culture in vitro. Am. J. Physiol. Endocrinol. Metab. 288, E155-162. https://doi.org/10.1152/ajpendo.00257.2004

Pham-Huy, L.A., He, H., Pham-Huy, C., 2008. Free Radicals, Antioxidants in Disease and Health. Int. J. Biomed. Sci. IJBS 4, 89–96.

Pickup, J.C., 2004. Inflammation and activated innate immunity in the pathogenesis of type 2 diabetes. Diabetes Care 27, 813–823.

Piwen Wang, Henning, S.M., Heber, D., 2010. Limitations of MTT and MTS-Based Assays for Measurement of Antiproliferative Activity of Green Tea Polyphenols. PLoS ONE 5, 1–10. https://doi.org/10.1371/journal.pone.0010202

Poggi, M., Bastelica, D., Gual, P., Iglesias, M.A., Gremeaux, T., Knauf, C., Peiretti, F., Verdier, M., Juhan-Vague, I., Tanti, J.F., Burcelin, R., Alessi, M.C., 2007. C3H/HeJ mice carrying a toll-like receptor 4 mutation are protected against the development of insulin resistance in white adipose tissue in response to a high-fat diet. Diabetologia 50, 1267–1276. https://doi.org/10.1007/s00125-007-0654-8

Poitout, V., Robertson, R.P., 2002. Minireview: Secondary beta-cell failure in type 2 diabetes--a convergence of glucotoxicity and lipotoxicity. Endocrinology 143, 339–342. https://doi.org/10.1210/endo.143.2.8623

Poligone, B., Baldwin, A.S., 2001. Positive and Negative Regulation of NF-κB by COX-2 ROLES OF DIFFERENT PROSTAGLANDINS. J. Biol. Chem. 276, 38658–38664. https://doi.org/10.1074/jbc.M106599200

Polonsky, K.S., Given, B.D., Hirsch, L.J., Tillil, H., Shapiro, E.T., Beebe, C., Frank, B.H., Galloway, J.A., Van Cauter, E., 1988. Abnormal patterns of insulin secretion in non-insulin-dependent diabetes mellitus. N. Engl. J. Med. 318, 1231–1239. https://doi.org/10.1056/NEJM198805123181903

Porat, Y., Kolusheva, S., Jelinek, R., Gazit, E., 2003. The human islet amyloid polypeptide forms transient membrane-active prefibrillar assemblies. Biochemistry (Mosc.) 42, 10971–10977. https://doi.org/10.1021/bi034889i

Pradhan, A.D., Manson, J.E., Rifai, N., Buring, J.E., Ridker, P.M., 2001. C-Reactive Protein, Interleukin 6, and Risk of Developing Type 2 Diabetes Mellitus. JAMA 286, 327–334. https://doi.org/10.1001/jama.286.3.327

Prentki, M., Nolan, C.J., 2006. Islet beta cell failure in type 2 diabetes. J. Clin. Invest. 116, 1802–1812. https://doi.org/10.1172/JCI29103

Qatanani, M., Lazar, M.A., 2007. Mechanisms of obesity-associated insulin resistance: many choices on the menu. Genes Dev. 21, 1443–1455. https://doi.org/10.1101/gad.1550907

Qing, H., Zhou, W., Christensen, M.A., Sun, X., Tong, Y., Song, W., 2004. Degradation of BACE by the ubiquitin-proteasome pathway. FASEB J. Off. Publ. Fed. Am. Soc. Exp. Biol. 18, 1571–1573. https://doi.org/10.1096/fj.04-1994fje

Rabinovitch, A., Sumoski, W., Rajotte, R.V., Warnock, G.L., 1990. Cytotoxic effects of cytokines on human pancreatic islet cells in monolayer culture. J. Clin. Endocrinol. Metab. 71, 152–156. https://doi.org/10.1210/jcem-71-1-152

Renehan, A.G., Booth, C., Potten, C.S., 2001. What is apoptosis, and why is it important? BMJ 322, 1536–1538.

Richardson, S.J., Willcox, A., Bone, A.J., Foulis, A.K., Morgan, N.G., 2009. Islet-associated macrophages in type 2 diabetes. Diabetologia 52, 1686–1688. https://doi.org/10.1007/s00125-009-1410-z

Riss, T.L., Moravec, R.A., Niles, A.L., Duellman, S., Benink, H.A., Worzella, T.J., Minor, L., 2004. Cell Viability Assays, in: Sittampalam, G.S., Coussens, N.P., Brimacombe, K., Grossman, A., Arkin, M., Auld, D., Austin, C., Baell, J., Bejcek, B., Chung, T.D.Y., Dahlin, J.L., Devanaryan, V., Foley, T.L., Glicksman, M., Hall, M.D., Hass, J.V., Inglese, J., Iversen, P.W., Kahl, S.D., Kales, S.C., Lal-Nag, M., Li, Z., McGee, J., McManus, O., Riss, T., Trask, O.J., Weidner, J.R., Xia, M., Xu, X. (Eds.), Assay Guidance Manual. Eli Lilly & Company and the National Center for Advancing Translational Sciences, Bethesda (MD).

Roberts, A.N., Leighton, B., Todd, J.A., Cockburn, D., Schofield, P.N., Sutton, R., Holt, S., Boyd, Y., Day, A.J., Foot, E.A., 1989. Molecular and functional characterization of amylin, a peptide associated with type 2 diabetes mellitus. Proc. Natl. Acad. Sci. U. S. A. 86, 9662–9666.

Robertson, R.P., Harmon, J., Tran, P.O., Tanaka, Y., Takahashi, H., 2003. Glucose Toxicity in β-Cells: Type 2 Diabetes, Good Radicals Gone Bad, and the Glutathione Connection. Diabetes 52, 581–587. https://doi.org/10.2337/diabetes.52.3.581

Robertson, R.P., Harmon, J., Tran, P.O.T., Poitout, V., 2004. Beta-cell glucose toxicity, lipotoxicity, and chronic oxidative stress in type 2 diabetes. Diabetes 53 Suppl 1, S119-124.

Roche, H.M., 2004. Dietary lipids and gene expression. Biochem. Soc. Trans. 32, 999–1002. https://doi.org/10.1042/BST0320999

Rossetti, L., Giaccari, A., DeFronzo, R.A., 1990. Glucose toxicity. Diabetes Care 13, 610–630.

Rotter, V., Nagaev, I., Smith, U., 2003. Interleukin-6 (IL-6) induces insulin resistance in 3T3-L1 adipocytes and is, like IL-8 and tumor necrosis factor-alpha, overexpressed in human fat cells from insulin-resistant subjects. J. Biol. Chem. 278, 45777–45784. https://doi.org/10.1074/jbc.M301977200

Russell, M.A., Cooper, A.C., Dhayal, S., Morgan, N.G., 2013. Differential effects of interleukin-13 and interleukin-6 on Jak/STAT signaling and cell viability in pancreatic β-cells. Islets 5, 95–105. https://doi.org/10.4161/isl.24249

Russell, M.A., Morgan, N.G., 2014. The impact of anti-inflammatory cytokines on the pancreatic β-cell. Islets 6, e950547. https://doi.org/10.4161/19382014.2014.950547

Sabio, G., Das, M., Mora, A., Zhang, Z., Jun, J.Y., Ko, H.J., Barrett, T., Kim, J.K., Davis, R.J., 2008. A stress signaling pathway in adipose tissue regulates hepatic insulin resistance. Science 322, 1539–1543. https://doi.org/10.1126/science.1160794

Sakagashira, S., Hiddinga, H.J., Tateishi, K., Sanke, T., Hanabusa, T., Nanjo, K., Eberhardt, N.L., 2000. S20G Mutant Amylin Exhibits Increased in Vitro Amyloidogenicity and Increased Intracellular Cytotoxicity Compared to Wild-Type Amylin. Am. J. Pathol. 157, 2101–2109.

Saltiel, A.R., 2000. Series Introduction: The molecular and physiological basis of insulin resistance: emerging implications for metabolic and cardiovascular diseases. J. Clin. Invest. 106, 163–164.

Salvesen, G.S., 2002. Caspases: opening the boxes and interpreting the arrows. Cell Death Differ. 9, 3–5. https://doi.org/10.1038/sj.cdd.4400963

Sánchez-Solana, B., Laborda, J., Baladrón, V., 2012. Mouse Resistin Modulates Adipogenesis and Glucose Uptake in 3T3-L1 Preadipocytes Through the ROR1 Receptor. Mol. Endocrinol. 26, 110–127. https://doi.org/10.1210/me.2011-1027

Sandovici, I., Hammerle, C.M., Cooper, W.N., Smith, N.H., Tarry-Adkins, J.L., Dunmore, B.J., Bauer, J., Andrews, S.R., Yeo, G.S.H., Ozanne, S.E., Constância, M., 2016. Ageing is associated with molecular signatures of inflammation and type 2 diabetes in rat pancreatic islets. Diabetologia 59, 502–511. https://doi.org/10.1007/s00125-015-3837-8

Sanke, T., Bell, G.I., Sample, C., Rubenstein, A.H., Steiner, D.F., 1988. An islet amyloid peptide is derived from an 89-amino acid precursor by proteolytic processing. J. Biol. Chem. 263, 17243–17246.

Santerre, R.F., Cook, R.A., Crisel, R.M., Sharp, J.D., Schmidt, R.J., Williams, D.C., Wilson, C.P., 1981. Insulin synthesis in a clonal cell line of simian virus 40-transformed hamster pancreatic beta cells. Proc. Natl. Acad. Sci. U. S. A. 78, 4339–4343.

Saraiva, M.J., Birken, S., Costa, P.P., Goodman, D.S., 1984. Amyloid fibril protein in familial amyloidotic polyneuropathy, Portuguese type. Definition of molecular abnormality in transthyretin (prealbumin). J. Clin. Invest. 74, 104–119.

Sartipy, P., Loskutoff, D.J., 2003. Monocyte chemoattractant protein 1 in obesity and insulin resistance. Proc. Natl. Acad. Sci. U. S. A. 100, 7265–7270. https://doi.org/10.1073/pnas.1133870100

Schultze, S.M., Hemmings, B.A., Niessen, M., Tschopp, O., 2012. PI3K/AKT, MAPK and AMPK signalling: protein kinases in glucose homeostasis. Expert Rev. Mol. Med. 14, e1. https://doi.org/10.1017/S1462399411002109

Sekine, N., Ishikawa, T., Okazaki, T., Hayashi, M., Wollheim, C.B., Fujita, T., n.d. Synergistic activation of NF-κb and inducible isoform of nitric oxide synthase induction by interferon-γ and tumor necrosis factor-α in INS-1 cells. J. Cell. Physiol. 184, 46–57. https://doi.org/10.1002/(SICI)1097-4652(200007)184:1<46::AID-JCP5>3.0.CO;2-L

Sell, H., Dietze-Schroeder, D., Kaiser, U., Eckel, J., 2006. Monocyte chemotactic protein-1 is a potential player in the negative cross-talk between adipose tissue and skeletal muscle. Endocrinology 147, 2458–2467. https://doi.org/10.1210/en.2005-0969

Senn, J.J., Klover, P.J., Nowak, I.A., Mooney, R.A., 2002. Interleukin-6 induces cellular insulin resistance in hepatocytes. Diabetes 51, 3391–3399.

Sharma, A.M., Janke, J., Gorzelniak, K., Engeli, S., Luft, F.C., 2002. Angiotensin blockade prevents type 2 diabetes by formation of fat cells. Hypertens. Dallas Tex 1979 40, 609–611.

Shay, J.W., Wright, W.E., 2000. Hayflick, his limit, and cellular ageing. Nat. Rev. Mol. Cell Biol. 1, 72–76. https://doi.org/10.1038/35036093

Shen, S.-W., Reaven, G.M., Farquhar, J.W., 1970. Comparison of impedance to insulin-mediated glucose uptake in normal subjects and in subjects with latent diabetes. J. Clin. Invest. 49, 2151–2160.

Shi, Y., Liang, X., Zhang, H., Wu, Q., Qu, L., Sun, Q., 2013. Quercetin protects rat dorsal root ganglion neurons against high glucose-induced injury in vitro through Nrf-2/HO-1 activation and NF-κB inhibition. Acta Pharmacol. Sin. 34, 1140–1148. https://doi.org/10.1038/aps.2013.59

Shimmyo, Y., Kihara, T., Akaike, A., Niidome, T., Sugimoto, H., 2008. Flavonols and flavones as BACE-1 inhibitors: structure-activity relationship in cell-free, cell-based and in silico studies reveal novel pharmacophore features. Biochim. Biophys. Acta 1780, 819–825. https://doi.org/10.1016/j.bbagen.2008.01.017

Shirahama, T., Cohen, A.S., 1967. HIGH-RESOLUTION ELECTRON MICROSCOPIC ANALYSIS OF THE AMYLOID FIBRIL. J. Cell Biol. 33, 679–708.

Shiuchi, T., Iwai, M., Li, H.-S., Wu, L., Min, L.-J., Li, J.-M., Okumura, M., Cui, T.-X., Horiuchi, M., 2004. Angiotensin II type-1 receptor blocker valsartan enhances insulin sensitivity in skeletal muscles of diabetic mice. Hypertens. Dallas Tex 1979 43, 1003–1010. https://doi.org/10.1161/01.HYP.0000125142.41703.64

Shoelson, S.E., Lee, J., Goldfine, A.B., 2006. Inflammation and insulin resistance. J. Clin. Invest. 116, 1793–1801. https://doi.org/10.1172/JCI29069

Sies, H., 1997. Oxidative stress: oxidants and antioxidants. Exp. Physiol. 82, 291–295. https://doi.org/10.1113/expphysiol.1997.sp004024

Skelin, M., Rupnik, M., Cencic, A., 2010. Pancreatic beta cell lines and their applications in diabetes mellitus research. ALTEX 27, 105–113.

Skurk, T., Alberti-Huber, C., Herder, C., Hauner, H., 2007. Relationship between adipocyte size and adipokine expression and secretion. J. Clin. Endocrinol. Metab. 92, 1023–1033. https://doi.org/10.1210/jc.2006-1055

Slater, T.F., Sawyer, B., Straeuli, U., 1963. STUDIES ON SUCCINATE-TETRAZOLIUM REDUCTASE SYSTEMS. III. POINTS OF COUPLING OF FOUR DIFFERENT TETRAZOLIUM SALTS. Biochim. Biophys. Acta 77, 383–393.

Smith, P.K., Krohn, R.I., Hermanson, G.T., Mallia, A.K., Gartner, F.H., Provenzano, M.D., Fujimoto, E.K., Goeke, N.M., Olson, B.J., Klenk, D.C., 1985. Measurement of protein using bicinchoninic acid. Anal. Biochem. 150, 76–85.

Song, M.J., Kim, K.H., Yoon, J.M., Kim, J.B., 2006. Activation of Toll-like receptor 4 is associated with insulin resistance in adipocytes. Biochem. Biophys. Res. Commun. 346, 739–745. https://doi.org/10.1016/j.bbrc.2006.05.170

Sopasakis, V.R., Sandqvist, M., Gustafson, B., Hammarstedt, A., Schmelz, M., Yang, X., Jansson, P.-A., Smith, U., 2004. High local concentrations and effects on differentiation implicate interleukin-6 as a paracrine regulator. Obes. Res. 12, 454–460. https://doi.org/10.1038/oby.2004.51

Southan, C., Hancock, J.M., 2013. A tale of two drug targets: the evolutionary history of BACE1 and BACE2. Front. Genet. 4, 293. https://doi.org/10.3389/fgene.2013.00293

Souza, S.C., Palmer, H.J., Kang, Y.H., Yamamoto, M.T., Muliro, K.V., Paulson, K.E., Greenberg, A.S., 2003. TNF-alpha induction of lipolysis is mediated through activation of the extracellular signal related kinase pathway in 3T3-L1 adipocytes. J. Cell. Biochem. 89, 1077–1086. https://doi.org/10.1002/jcb.10565

Sowa, R., Sanke, T., Hirayama, J., Tabata, H., Furuta, H., Nishimura, S., Nanjo, K., 1990. Islet amyloid polypeptide amide causes peripheral insulin resistance in vivo in dogs. Diabetologia 33, 118–120. https://doi.org/10.1007/BF00401051

Stalmach, A., Mullen, W., Pecorari, M., Serafini, M., Crozier, A., 2009. Bioavailability of C-linked dihydrochalcone and flavanone glucosides in humans following ingestion of unfermented and fermented rooibos teas. J. Agric. Food Chem. 57, 7104–7111. https://doi.org/10.1021/jf9011642

Starkie, R., Ostrowski, S.R., Jauffred, S., Febbraio, M., Pedersen, B.K., 2003. Exercise and IL-6 infusion inhibit endotoxin-induced TNF-alpha production in humans. FASEB J. Off. Publ. Fed. Am. Soc. Exp. Biol. 17, 884–886. https://doi.org/10.1096/fj.02-0670fje

Steensberg, A., Fischer, C.P., Keller, C., Møller, K., Pedersen, B.K., 2003. IL-6 enhances plasma IL-1ra, IL-10, and cortisol in humans. Am. J. Physiol. Endocrinol. Metab. 285, E433-437. https://doi.org/10.1152/ajpendo.00074.2003

Steer, S.A., Scarim, A.L., Chambers, K.T., Corbett, J.A., 2005. Interleukin-1 Stimulates β-Cell Necrosis and Release of the Immunological Adjuvant HMGB1. PLOS Med. 3, e17. https://doi.org/10.1371/journal.pmed.0030017

Stephens, J.M., Pekala, P.H., 1991. Transcriptional repression of the GLUT4 and C/EBP genes in 3T3-L1 adipocytes by tumor necrosis factor-alpha. J. Biol. Chem. 266, 21839–21845.

Steppan, C.M., Wang, J., Whiteman, E.L., Birnbaum, M.J., Lazar, M.A., 2005. Activation of SOCS-3 by resistin. Mol. Cell. Biol. 25, 1569–1575. https://doi.org/10.1128/MCB.25.4.1569-1575.2005

Stützer, I., Selevsek, N., Esterházy, D., Schmidt, A., Aebersold, R., Stoffel, M., 2013. Systematic proteomic analysis identifies β-site amyloid precursor protein cleaving enzyme 2 and 1 (BACE2 and BACE1) substrates in pancreatic β-cells. J. Biol. Chem. 288, 10536–10547. https://doi.org/10.1074/jbc.M112.444703

Suganami, T., Mieda, T., Itoh, M., Shimoda, Y., Kamei, Y., Ogawa, Y., 2007a. Attenuation of obesity-induced adipose tissue inflammation in C3H/HeJ mice carrying a Toll-like receptor 4 mutation. Biochem. Biophys. Res. Commun. 354, 45–49. https://doi.org/10.1016/j.bbrc.2006.12.190

Suganami, T., Tanimoto-Koyama, K., Nishida, J., Itoh, M., Yuan, X., Mizuarai, S., Kotani, H., Yamaoka, S., Miyake, K., Aoe, S., Kamei, Y., Ogawa, Y., 2007b. Role of the Toll-like receptor 4/NF-kappaB pathway in saturated fatty acid-induced inflammatory changes in the interaction between adipocytes and macrophages. Arterioscler. Thromb. Vasc. Biol. 27, 84–91. https://doi.org/10.1161/01.ATV.0000251608.09329.9a

Suzuki, T., Fujikura, K., Higashiyama, T., Takata, K., 1997. DNA Staining for Fluorescence and Laser Confocal Microscopy. J. Histochem. Cytochem. 45, 49–53. https://doi.org/10.1177/002215549704500107

Tak, P.P., Firestein, G.S., 2001. NF-kappaB: a key role in inflammatory diseases. J. Clin. Invest. 107, 7–11. https://doi.org/10.1172/JCI11830

Takahashi, H.K., Cambiaghi, T.D., Luchessi, A.D., Hirabara, S.M., Vinolo, M.A.R., Newsholme, P., Curi, R., 2012. Activation of survival and apoptotic signaling pathways in lymphocytes exposed to palmitic acid. J. Cell. Physiol. 227, 339–350. https://doi.org/10.1002/jcp.22740

Tanaka, Y., Gleason, C.E., Tran, P.O.T., Harmon, J.S., Robertson, R.P., 1999. Prevention of glucose toxicity in HIT-T15 cells and Zucker diabetic fatty rats by antioxidants. Proc. Natl. Acad. Sci. U. S. A. 96, 10857–10862.

Tarkowski, A., Bjersing, J., Shestakov, A., Bokarewa, M.I., 2010. Resistin competes with lipopolysaccharide for binding to toll-like receptor 4. J. Cell. Mol. Med. 14, 1419–1431. https://doi.org/10.1111/j.1582-4934.2009.00899.x

Taylor, R.C., Cullen, S.P., Martin, S.J., 2008. Apoptosis: controlled demolition at the cellular level. Nat. Rev. Mol. Cell Biol. 9, 231–241. https://doi.org/10.1038/nrm2312

Taylor-Fishwick, D.A., Weaver, J.R., Grzesik, W., Chakrabarti, S., Green-Mitchell, S., Imai, Y., Kuhn, N., Nadler, J.L., 2013. Production and function of IL-12 in islets and beta cells. Diabetologia 56, 126–135. https://doi.org/10.1007/s00125-012-2732-9

Thomaseth, K., Kautzky-Willer, A., Ludvik, B., Prager, R., Pacini, G., 1996. Integrated mathematical model to assess beta-cell activity during the oral glucose test. Am. J. Physiol. 270, E522-531. https://doi.org/10.1152/ajpendo.1996.270.3.E522

Thompson, R.G., Peterson, J., Gottlieb, A., Mullane, J., 1997. Effects of pramlintide, an analog of human amylin, on plasma glucose profiles in patients with IDDM: results of a multicenter trial. Diabetes 46, 632–636.

Tikellis, C., Wookey, P.J., Candido, R., Andrikopoulos, S., Thomas, M.C., Cooper, M.E., 2004. Improved islet morphology after blockade of the renin- angiotensin system in the ZDF rat. Diabetes 53, 989–997.

Torgerson, J.S., Hauptman, J., Boldrin, M.N., Sjöström, L., 2004. XENical in the prevention of diabetes in obese subjects (XENDOS) study: a randomized study of orlistat as an adjunct to lifestyle changes for the prevention of type 2 diabetes in obese patients. Diabetes Care 27, 155–161.

Torres-Leal, F.L., Fonseca-Alaniz, M.H., Oliveira, A.C. de, Alonso-Vale, M.I.C., 2012. Adipose Tissue Inflammation and Insulin Resistance. https://doi.org/10.5772/53974

Trikha, S., Jeremic, A.M., 2013. Distinct Internalization Pathways of Human Amylin Monomers and Its Cytotoxic Oligomers in Pancreatic Cells. PLoS ONE 8. https://doi.org/10.1371/journal.pone.0073080

Trujillo, M.E., Sullivan, S., Harten, I., Schneider, S.H., Greenberg, A.S., Fried, S.K., 2004. Interleukin-6 regulates human adipose tissue lipid metabolism and leptin production in vitro. J. Clin. Endocrinol. Metab. 89, 5577–5582. https://doi.org/10.1210/jc.2004-0603

Tsigos, C., Papanicolaou, D.A., Kyrou, I., Defensor, R., Mitsiadis, C.S., Chrousos, G.P., 1997. Dose-dependent effects of recombinant human interleukin-6 on glucose regulation. J. Clin. Endocrinol. Metab. 82, 4167–4170. https://doi.org/10.1210/jcem.82.12.4422

Tuomilehto, J., Lindström, J., Eriksson, J.G., Valle, T.T., Hämäläinen, H., Ilanne-Parikka, P., Keinänen-Kiukaanniemi, S., Laakso, M., Louheranta, A., Rastas, M., Salminen, V., Uusitupa, M., Finnish Diabetes Prevention Study Group, 2001. Prevention of type 2 diabetes mellitus by changes in lifestyle among subjects with impaired glucose tolerance. N. Engl. J. Med. 344, 1343–1350. https://doi.org/10.1056/NEJM200105033441801

Turk, V., Stoka, V., Vasiljeva, O., Renko, M., Sun, T., Turk, B., Turk, D., 2012. Cysteine cathepsins: from structure, function and regulation to new frontiers. Biochim. Biophys. Acta 1824, 68–88. https://doi.org/10.1016/j.bbapap.2011.10.002

Unger, R.H., Zhou, Y.T., 2001. Lipotoxicity of beta-cells in obesity and in other causes of fatty acid spillover. Diabetes 50 Suppl 1, S118-121.

Van Antwerp, D.J., Martin, S.J., Kafri, T., Green, D.R., Verma, I.M., 1996. Suppression of TNF-alpha-induced apoptosis by NF-kappaB. Science 274, 787–789.

van Hall, G., Steensberg, A., Sacchetti, M., Fischer, C., Keller, C., Schjerling, P., Hiscock, N., Møller, K., Saltin, B., Febbraio, M.A., Pedersen, B.K., 2003. Interleukin-6 stimulates lipolysis and fat oxidation in humans. J. Clin. Endocrinol. Metab. 88, 3005–3010. https://doi.org/10.1210/jc.2002-021687

Vanden Berghe, W., Vermeulen, L., De Wilde, G., De Bosscher, K., Boone, E., Haegeman, G., 2000. Signal transduction by tumor necrosis factor and gene regulation of the inflammatory cytokine interleukin-6. Biochem. Pharmacol. 60, 1185–1195.

Vankoningsloo, S., Piens, M., Lecocq, C., Gilson, A., De Pauw, A., Renard, P., Demazy, C., Houbion, A., Raes, M., Arnould, T., 2005. Mitochondrial dysfunction induces triglyceride accumulation in 3T3-L1 cells: role of fatty acid beta-oxidation and glucose. J. Lipid Res. 46, 1133–1149. https://doi.org/10.1194/jlr.M400464-JLR200

Vassar, R., 2014. BACE1 inhibitor drugs in clinical trials for Alzheimer's disease. Alzheimers Res. Ther. 6, 89. https://doi.org/10.1186/s13195-014-0089-7

Venugopal, C., Demos, C.M., Rao, K.S.J., Pappolla, M.A., Sambamurti, K., 2008. Beta-secretase: structure, function, and evolution. CNS Neurol. Disord. Drug Targets 7, 278–294.

Vermes, I., Haanen, C., Steffens-Nakken, H., Reutelingsperger, C., 1995. A novel assay for apoptosis. Flow cytometric detection of phosphatidylserine expression on early apoptotic cells using fluorescein labelled Annexin V. J. Immunol. Methods 184, 39–51.

Vlassara, H., 1997. Recent Progress in Advanced Glycation End Products and Diabetic Complications. Diabetes 46, S19–S25. https://doi.org/10.2337/diab.46.2.S19

Vozarova, B., Weyer, C., Lindsay, R.S., Pratley, R.E., Bogardus, C., Tataranni, P.A., 2002. High white blood cell count is associated with a worsening of insulin sensitivity and predicts the development of type 2 diabetes. Diabetes 51, 455–461.

Waisundara, V.Y., Hoon, L.Y., 2015. Free radical scavenging ability of Aspalathus linearis in two in vitro models of diabetes and cancer. J. Tradit. Complement. Med. 5, 174–178. https://doi.org/10.1016/j.jtcme.2014.11.009

Wang, C., Youle, R.J., 2009. The role of mitochondria in apoptosis*. Annu. Rev. Genet. 43, 95–118. https://doi.org/10.1146/annurev-genet-102108-134850

Wang, H., Joseph, J.A., 1999. Quantifying cellular oxidative stress by dichlorofluorescein assay using microplate reader. Free Radic. Biol. Med. 27, 612–616.

Ward, W.K., Bolgiano, D.C., McKnight, B., Halter, J.B., Porte, D., 1984. Diminished B cell secretory capacity in patients with noninsulin-dependent diabetes mellitus. J. Clin. Invest. 74, 1318–1328. https://doi.org/10.1172/JCI111542

Weir, G.C., Bonner-Weir, S., 2004. Five stages of evolving beta-cell dysfunction during progression to diabetes. Diabetes 53 Suppl 3, S16-21.

Weisberg, S.P., Hunter, D., Huber, R., Lemieux, J., Slaymaker, S., Vaddi, K., Charo, I., Leibel, R.L., Ferrante, A.W., 2006. CCR2 modulates inflammatory and metabolic effects of high-fat feeding. J. Clin. Invest. 116, 115–124. https://doi.org/10.1172/JCI24335

Weisberg, S.P., McCann, D., Desai, M., Rosenbaum, M., Leibel, R.L., Ferrante, A.W., 2003. Obesity is associated with macrophage accumulation in adipose tissue. J. Clin. Invest. 112, 1796–1808. https://doi.org/10.1172/JCI19246

Weksler-Zangen, S., Raz, I., Lenzen, S., Jörns, A., Ehrenfeld, S., Amir, G., Oprescu, A., Yagil, Y., Yagil, C., Zangen, D.H., Kaiser, N., 2008. Impaired glucose-stimulated insulin secretion is coupled with exocrine pancreatic lesions in the Cohen diabetic rat. Diabetes 57, 279–287. https://doi.org/10.2337/db07-0520

Westermark, P., Engström, U., Johnson, K.H., Westermark, G.T., Betsholtz, C., 1990. Islet amyloid polypeptide: pinpointing amino acid residues linked to amyloid fibril formation. Proc. Natl. Acad. Sci. U. S. A. 87, 5036–5040.

Westermark, P., Sletten, K., Johansson, B., Cornwell, G.G., 1990. Fibril in senile systemic amyloidosis is derived from normal transthyretin. Proc. Natl. Acad. Sci. U. S. A. 87, 2843–2845.

Westermark, P., Wernstedt, C., Wilander, E., Sletten, K., 1986. A novel peptide in the calcitonin gene related peptide family as an amyloid fibril protein in the endocrine pancreas. Biochem. Biophys. Res. Commun. 140, 827–831.

Westermark, P., Wilander, E., Westermark, G.T., Johnson, K.H., 1987. Islet amyloid polypeptide-like immunoreactivity in the islet B cells of Type 2 (non-insulin-dependent) diabetic and non-diabetic individuals. Diabetologia 30, 887–892. https://doi.org/10.1007/BF00274799

Westwell-Roper, C.Y., Ehses, J.A., Verchere, C.B., 2014. Resident Macrophages Mediate Islet Amyloid Polypeptide–Induced Islet IL-1β Production and β-Cell Dysfunction. Diabetes 63, 1698–1711. https://doi.org/10.2337/db13-0863

Weyer, C., Bogardus, C., Pratley, R.E., 1999. Metabolic characteristics of individuals with impaired fasting glucose and/or impaired glucose tolerance. Diabetes 48, 2197–2203.

Weyer, C., Funahashi, T., Tanaka, S., Hotta, K., Matsuzawa, Y., Pratley, R.E., Tataranni, P.A., 2001. Hypoadiponectinemia in obesity and type 2 diabetes: close association with insulin resistance and hyperinsulinemia. J. Clin. Endocrinol. Metab. 86, 1930–1935. https://doi.org/10.1210/jcem.86.5.7463

Wieser, V., Moschen, A.R., Tilg, H., 2013. Inflammation, cytokines and insulin resistance: a clinical perspective. Arch. Immunol. Ther. Exp. (Warsz.) 61, 119–125. https://doi.org/10.1007/s00005-012-0210-1

Woerle, H.J., Albrecht, M., Linke, R., Zschau, S., Neumann, C., Nicolaus, M., Gerich, J.E., Göke, B., Schirra, J., 2008. Impaired Hyperglycemia-Induced Delay in Gastric Emptying in Patients With Type 1 Diabetes Deficient for Islet Amyloid Polypeptide. Diabetes Care 31, 2325–2331. https://doi.org/10.2337/dc07-2446

Wookey, P.J., Cao, Z., Cooper, M.E., 1998. Interaction of the renal amylin and renin-angiotensin systems in animal models of diabetes and hypertension. Miner. Electrolyte Metab. 24, 389–399. https://doi.org/57400

Wookey, P.J., Tikellis, C., Du, H.C., Qin, H.F., Sexton, P.M., Cooper, M.E., 1996. Amylin binding in rat renal cortex, stimulation of adenylyl cyclase, and activation of plasma renin. Am. J. Physiol. 270, F289-294. https://doi.org/10.1152/ajprenal.1996.270.2.F289

Xing, Z., Gauldie, J., Cox, G., Baumann, H., Jordana, M., Lei, X.F., Achong, M.K., 1998. IL-6 is an antiinflammatory cytokine required for controlling local or systemic acute inflammatory responses. J. Clin. Invest. 101, 311–320.

Xu, F.-P., Chen, M.-S., Wang, Y.-Z., Yi, Q., Lin, S.-B., Chen, A.F., Luo, J.-D., 2004. Leptin induces hypertrophy via endothelin-1-reactive oxygen species pathway in cultured neonatal rat cardiomyocytes. Circulation 110, 1269–1275. https://doi.org/10.1161/01.CIR.0000140766.52771.6D

Xu, H., Barnes, G.T., Yang, Q., Tan, G., Yang, D., Chou, C.J., Sole, J., Nichols, A., Ross, J.S., Tartaglia, L.A., Chen, H., 2003. Chronic inflammation in fat plays a crucial role in the development of obesity-related insulin resistance. J. Clin. Invest. 112, 1821–1830. https://doi.org/10.1172/JCI200319451

Yalow, R.S., Berson, S.A., 1960. Plasma insulin concentrations in nondiabetic and early diabetic subjects. Determinations by a new sensitive immuno-assay technic. Diabetes 9, 254–260.

Yang, Y.H.C., Johnson, J.D., 2013. Multi-parameter single-cell kinetic analysis reveals multiple modes of cell death in primary pancreatic β-cells. J Cell Sci 126, 4286–4295. https://doi.org/10.1242/jcs.133017

Yang, Y.H.C., Wills, Q.F., Johnson, J.D., 2015. A live-cell, high-content imaging survey of 206 endogenous factors across five stress conditions reveals context-dependent survival effects in mouse primary beta cells. Diabetologia 58, 1239–1249. https://doi.org/10.1007/s00125-015-3552-5

Yao, Y., Wang, S.-X., Zhang, Y.-K., Qu, Z., Liu, G., Zou, W.-Z., 2013. A clinicopathological analysis in a large cohort of Chinese patients with renal amyloid light-chain amyloidosis. Nephrol. Dial. Transplant. Off. Publ. Eur. Dial. Transpl. Assoc. - Eur. Ren. Assoc. 28, 689–697. https://doi.org/10.1093/ndt/gfs501

Yudkin, J.S., Stehouwer, C.D., Emeis, J.J., Coppack, S.W., 1999. C-reactive protein in healthy subjects: associations with obesity, insulin resistance, and endothelial dysfunction: a potential role for cytokines originating from adipose tissue? Arterioscler. Thromb. Vasc. Biol. 19, 972–978.

Zang, M., Xu, S., Maitland-Toolan, K.A., Zuccollo, A., Hou, X., Jiang, B., Wierzbicki, M., Verbeuren, T.J., Cohen, R.A., 2006. Polyphenols stimulate AMP-activated protein kinase, lower lipids, and inhibit accelerated atherosclerosis in diabetic LDL receptor-deficient mice. Diabetes 55, 2180–2191. https://doi.org/10.2337/db05-1188

Zeyda, M., Stulnig, T.M., 2009. Obesity, inflammation, and insulin resistance--a mini-review. Gerontology 55, 379–386. https://doi.org/10.1159/000212758

Zhang, D., Liu, Z.-X., Choi, C.S., Tian, L., Kibbey, R., Dong, J., Cline, G.W., Wood, P.A., Shulman, G.I., 2007. Mitochondrial dysfunction due to long-chain Acyl-CoA dehydrogenase deficiency causes hepatic steatosis and hepatic insulin resistance. Proc. Natl. Acad. Sci. U. S. A. 104, 17075–17080. https://doi.org/10.1073/pnas.0707060104

Zhang, S., Kim, K.H., 1995. TNF-alpha inhibits glucose-induced insulin secretion in a pancreatic beta-cell line (INS-1). FEBS Lett. 377, 237–239.

Zhang, X.-X., Pan, Y.-H., Huang, Y.-M., Zhao, H.-L., 2016. Neuroendocrine hormone amylin in diabetes. World J. Diabetes 7, 189–197. https://doi.org/10.4239/wjd.v7.i9.189

Zhang, Y., Proenca, R., Maffei, M., Barone, M., Leopold, L., Friedman, J.M., 1994. Positional cloning of the mouse obese gene and its human homologue. Nature 372, 425–432. https://doi.org/10.1038/372425a0

Zhao, H.-L., Lai, F.M.M., Tong, P.C.Y., Zhong, D.-R., Yang, D., Tomlinson, B., Chan, J.C.N., 2003. Prevalence and clinicopathological characteristics of islet amyloid in chinese patients with type 2 diabetes. Diabetes 52, 2759–2766.

Zhao, H.-L., Sui, Y., Guan, J., He, L., Gu, X.-M., Wong, H.K., Baum, L., Lai, F.M.M., Tong, P.C.Y., Chan, J.C.N., 2009. Amyloid oligomers in diabetic and nondiabetic human pancreas. Transl. Res. J. Lab. Clin. Med. 153, 24–32. https://doi.org/10.1016/j.trsl.2008.10.009

Zheng, N., Yuan, P., Li, C., Wu, J., Huang, J., 2015. Luteolin Reduces BACE1 Expression through NF-κB and through Estrogen Receptor Mediated Pathways in HEK293 and SH-SY5Y Cells. J. Alzheimers Dis. JAD 45, 659–671. https://doi.org/10.3233/JAD-142517

Zhou, R., Tardivel, A., Thorens, B., Choi, I., Tschopp, J., 2010. Thioredoxin-interacting protein links oxidative stress to inflammasome activation. Nat. Immunol. 11, 136–140. https://doi.org/10.1038/ni.1831

CHAPTER 8

Addendum A: Aseptic Tecniques

Effective and efficient cell culture procedures depend on keeping the cells free from micro-organisms such as bacteria, fungi, and viruses which lead to contamination. Aseptic techniques are designed to serve as a barrier between the micro-organisms in the environment and sterile cell culture, reducing the risk of contamination. The essentials of working aseptically are a sterile work area, sterile reagents, and sterile handling. Sterile work areas include the use of a cell culture hood, running at all times. For the purposes of this study a biosafety level 2 cell culture hood was used. The work area should be organized with only the items necessary for the specific procedure and should be cleaned with 70% ethanol (EtOH) before and after use. Everything that enters the hood, such as flasks, reagents, and pipettes, should be sprayed down with 70% EtOH. A Bunsen burner was used to sterilize glass pipettes. Protective wear, such as shoe covers, gloves, lab coats, and face masks were worn at all times, to reduce the risk of contamination as well as protect the user from chemicals that might spill. Spillage should be reported and cleaned according to the specific standard operating procedure (SOP: TC B1-V03).

Addendum B: Assay Protocols

Table 8.1: Purified BACE enzyme assay. Protocol steps as provided with assay kit.

Reaction Number	1	2	3	4	5	6	7	8
Assay Description	Negative Control: No enzyme (µl)	Positive Control: Enzyme (µl)	Inhibition (µl)	Test Samples (µl)	Standard Curve (µl)			
Fluorescent Assay Buffer	80	78	78-X	80-Y	79	78	77	75
BACE1 Substrate Solution (50 µM)	20	20	20	20	20	20	20	20
BACE1 Enzyme Solution (0.3 units / µl)		2	2					
Inhibitor Solution			X					
Sample Enzyme				Y				
Assay Standard Solution (100 µM)					1	2	3	5
Total	100	100	100	100	100	100	100	100
*X: Amount (µl) of inhibitor added; Y: Amount (µl) of test samples added								

ATP Assay

1. Prepare 96 multi-well plates with INS1 cells in complete growth medium, 75 µl per well for 96-well plates.
2. Prepare control wells containing medium without cells to obtain a value for background
3. luminescence.
4. Add extracts compound to experimental wells and incubate according to culture protocol (24 hours of incubation).
5. Add 75 µl of CellTiter-Glo® Reagent to each well after the 24 hours of treatment incubation.
6. Incubate for 30 minutes under normal cell culture conditions (Mix contents every 10 minutes to induce cell lysis)
7. Record luminescence.
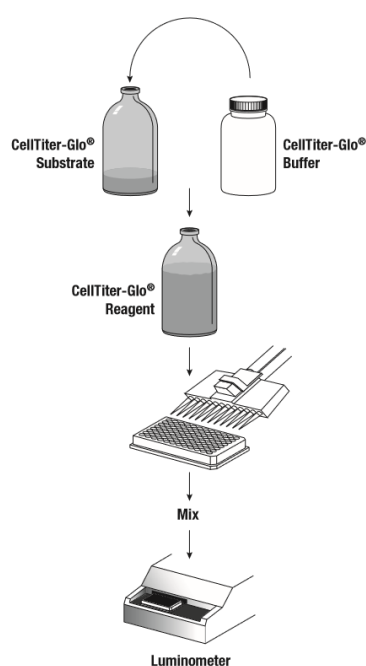
Figure 8.1: Diagrammatic presentation of ATP assay steps. Add CellTiter-Glo® buffer to CellTiter-Glo® substrate to get the CellTiter-Glo® reagent. Add 75 µl of CellTiter-Glo® reagent to each well after treatment incubation. Incubate for 30 minutes, under normal cell culture conditions. Record luminescence.

Griess Assay

1. Mix equal volumes of 1× Griess Reagent and sample.
2. Incubate for 15 minutes in the dark.
3. Read the absorbance at 540 nm.

Cell Proliferation Rate

A: Reagent Preparation

1. Prepare 1X wash buffer by diluting 20X wash buffer (included in each BrdU ELISA kit) in purified water.
2. Prepare 1X detection antibody solution by diluting BrdU detection antibody 1:100 with detection antibody diluent (green).
3. Prepare 1X HRP-conjugated secondary antibody solution by diluting antimouse IgG, HRP-linked antibody 1:100 with HRP-linked antibody diluent (red).
4. Prepare 10X BrdU solution by diluting BrdU 1:100 with cell culture medium.

B: BrdU Incorporation

1. Plate cells in 96-well plate and incubate with extracts substance.
2. Add prepared 10X BrdU solution to plate wells, for a final 1X concentration. (Example: for 100 µl medium in the plate, add 10 µl of 10X BrdU solution per well).
3. Place cells in incubator for 24 hours.
4. Remove medium.

C: BrdU Assay

1. Add 100 µl / well of the fixing / denaturing solution, keep the plate at room temperature for 30 min. Remove solution.
2. Add 100 µl / well prepared 1X detection antibody solution, keep plate at room temperature for 1 hour. Remove solution and wash plate 3 times with 1X wash buffer.
3. Add 100 µl / well prepared 1X HRP-conjugated secondary antibody solution, keep plate at room temperature for 30 min. Remove the solution and wash plate 3 times with 1X wash buffer.
4. Prepare working solution by mixing equal parts luminol / enhancer solution and stable peroxide buffer.
5. Add 100 µl of the working solution to each well. Use a plate-based luminometer to measure relative light units (RLU) at 425 nm within 1-10 min following addition of the substrate. Optimal signal intensity is achieved when read within 10 min.

Table 8.2: Steps of insulin ELISA kit.

Well #	Step 1	Step 2	Step 3-4 Assay Buffer	Step 5-7 Standards/ Controls/ Samples	Step 8 Detection Ab	Step 8-10	Step 11 Enzyme Solution	Step 11-13	Step 14 Substrate	Step 14	Step 15 Stop Solution	Step 15
A1, B1	Dilute each bottle 10X Wash Buffer with 450mL Deionized Water.	Wash plate 3X with 300 µL Wash Buffer. Remove residual buffer by tapping smartly on absorbent towels	20 µL	--------------	80 µL	Seal, Agitate, Incubate 2 hours at Room Temperature. Wash 3X with 300 µL Wash Buffer	100 µL	Seal, Agitate, Incubate 30 minutes at Room Temperature. Wash 6X with 300 µL Wash Buffer	100 µL	Seal, Agitate, Incubate 15 minutes at Room Temperature.	100 µL	Read Absorbance at 450 nm and 590 nm.
C1, D1			10 µL	10 µL of 0.2 ng/mL Standard	80 µL		100 µL		100 µL		100 µL	
E1, F1			10 µL	10 µL of 0.5 ng/mL Standard	80 µL		100 µL		100 µL		100 µL	
G1, H1			10 µL	10 µL of 1 ng/mL Standard	80 µL		100 µL		100 µL		100 µL	
A2, B2			10 µL	10 µL of 2 ng/mL Standard	80 µL		100 µL		100 µL		100 µL	
C2, D2			10 µL	10 µL of 5 ng/mL Standard	80 µL		100 µL		100 µL		100 µL	
E2, F2			10 µL	10 µL of 10 ng/mL Standard	80 µL		100 µL		100 µL		100 µL	
G2, H2			10 µL	10 µL of QC I	80 µL		100 µL		100 µL		100 µL	
A3, B3			10 µL	10 µL of QC II	80 µL		100 µL		100 µL		100 µL	
C3, D3 ↓			10 µL	10 µL of Sample	80 µL		100 µL		100 µL		100 µL	

ELISA – IAPP Secretion / Content
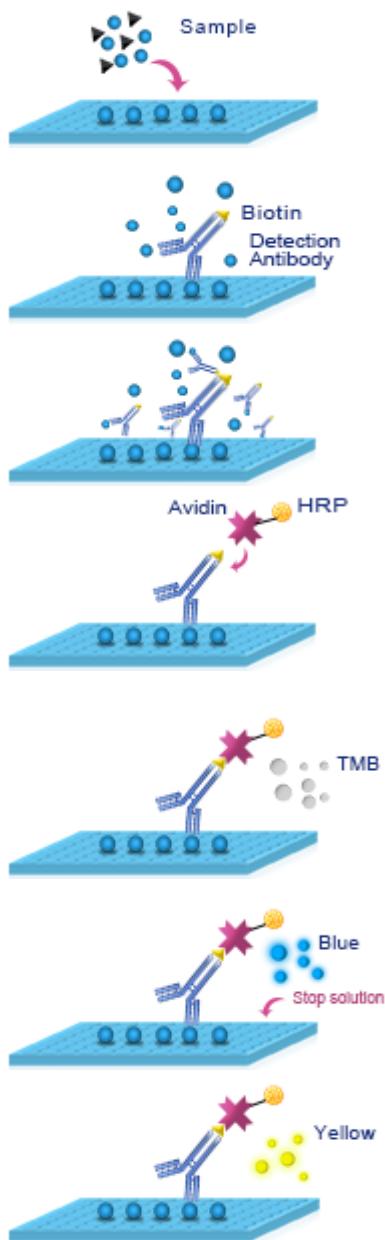
1. Add 50 µL of standard or sample to each well.

2. Immediately add 50 µL of biotinylated detection antibody to each well.

3. Incubate for 45 min at 37℃. Aspirate and wash 3 times.

4. Add 100 µl of HRP conjugate to each well. Incubate for 30 min at 37℃. Aspirate and wash 5 times.

5. Add 90 µL of substrate reagent. Incubate for 15 min at 37°C.

6. Add 50 µL of stop solution.

7. Read the OD at 450 nm immediately. Calculation of the results.

Figure 8.2: Diagrammatic presentation of IAPP ELISA steps. Add samples to each well, followed by the addition of the biotinylated detection antibody. After 45 minutes of incubation at 37°C, add HRP conjugate and incubate for 30 minutes. Wash 5 times then add the substrate reagent and incubate for 15 minutes. After incubation add stop solution and read the OD at 450nm.

Addendum C: Solutions

Krebs's-Ringer Bicarbonate HEPES Buffer

Table 8.3: Krebs's-Ringer Bicarbonate HEPES Buffer components.

Component	mM	MW	In 125 ml
NaCl	119	58.44	0.87 g
NaCHO$_3$	25	84.01	0.26 g
KCl	4.74	74.01	0.045 g
MgCl$_2$	1.19	95.21	0.014 g
CaCl$_2$	2.54	110.98	0.035 g
2% BSA	2%	100	2.5 g
10 nM Hepes10 mM	10 nM	238.3	1.25 ml
		+ Sterile water to 125 ml	

Glucose

- Stock: 500 mM (180.16 MW) into 10 ml of KRHB
- Basal: 2.8 mM: 252 µl into 45 ml of KRHB
- Stimulated: 16.7 mM: 1.503 ml into 45 ml of KRHB

Ethanol-acid Solution

- 37.5 ml of EtOH (molecular graded) + 644 µl of conc HCl + 11.85 ml cell culture tested H$_2$O.

Sorensen's Glycine Buffer

- 0.751 g glycine (0.1M) + 0.584 g NaCl (0.1 M) in 100 ml cell culture tested H$_2$O.

MTT

- 90 mg (2 mg/ml) + 45 ml DPBS

BSA Assay

- Dye: methanol and phosphoric acid
- Standards (BSA): 2, 1.5, 1, 0.75, 0.5, 0.25, 0.125 mg/ml

BCA Assay

- Reagent S: surfactant solution
- Reagent A: sodium carbonate, sodium bicarbonate, bicinchoninic acid and sodium tartrate in 0.1 M sodium hydroxide
- Reagent B: 4% cupric sulphate
- Standards (BSA): 2, 1.5, 1, 0.75, 0.5, 0.25, 0.125 mg/ml

Sample Buffer 4X (SB)

- 100 µl (β- Mercaptoethanol) + 900 µl (Laemli sample buffer)

10X TBS (pH = 7.6):

Table 8.4: Components of 10X TBS.

Reagent	1 l	2 l
200 mM Tris	24.22 g	48.44 g
1.37 M NaCl [MW=58.44]	80.06 g	160.12 g
		+ Make up to 1 l with ddH$_2$O

1X TBST

- Dilute 100 ml of 10X TBS to 900 ml dH$_2$O and add 1 ml Tween-20

Lysis Buffer

Table 8.5: Components of lysis buffer used to lyse cells for protein determination.

	Stock	Final Conc.	50 ml
Tris	1 M	50 mM	2.5 g
DTT	-	1 mM	0.008 g
NaF	-	50 mM	0.104 g
Na_3VO_4	10 mM	100 µM	500 µl
NP40	-	1%	500 µl
Triton X 114	-	1%	500 µl
RNase	10 mg/ml	25 µg/ml	125 µl
Protease inhibitor tablets			2 Tablets
Phospho inhibiting tablets			5 Tablets
			+ Sterile water to 50 ml

Add PMSF before using (10 µl/300 µl of lysis buffer)

Addendum D: Extract Treatments

Treatment with extract in the absence of the cytokine cocktail.

*All stocks dissolved in RPMI 1640 cell culture medium.

Asp

- Stock concentrations: 1000 µM
- 452.41 mM = 0.45 mg/ml

PPAG

- Stock concentration: 1000 µM
- 320.25 mM = 0.32 mg/ml

GRT

- Stock concentration: 1000 µg/ml
- 1 mg/ml

Table 8.6: Concentrations used for extract treatment in the absence of the cytokine cocktail.

Asp (µM)	PPAG (µM)	GRT (mg/ml)
1000	1000	1
100	100	0.1
10	10	0.01
1	1	0.001
0.1	0.1	0.0001

Co-treatment of extracts with cytokine cocktails.

*All stocks dissolved in RPMI 1640.

Asp

- Stock concentrations: 2000 µM
- 452.41 mM = 0.90 mg/ml

PPAG

- Stock concentration: 2000 μM
- 320.25 mM = 0.64 mg/ml

GRT

- Stock concentration: 2000 μg/ml
- 2 mg/ml

Table 8.7: Concentrations used for co-treatment. *Concentrations of stocks are doubled since co-treatment was done in a 1:1 ratio.*

Asp (μM)	PPAG (μM)	GRT (mg/ml)
2000	2000	2
200	200	0.2
20	20	0.02
2	2	0.002
0.2	0.2	0.0002

Addendum E: Cytokines and Cytokine Cocktails

Individual cytokine treatments

- TNF-α: Stock: 10 000 ng/ml
- IFN-γ: Stock: 100 000 ng/ml
- IL-1β: Stock: 10 000 ng/ml

Table 8.8: Concentrations used for treatment.

TNF-α (ng/ml)	IFN-γ (ng/ml)	IL-1β (ng/ml)
100	100	10
25	50	1
10	10	0.1
1.1	1	0.01

Cytokine cocktails

Cocktail A

- 1.1 ng/ml (TNF-α)
- 1 ng/ml (IFN-γ)
- 0.1 ng/ml (IL-1β)

Cocktail B

- 25 ng/ml (TNF-α)
- 10 ng/ml (IFN-γ)
- 10 ng/ml (IL-1β)

Co-treatment of extracts with cytokine cocktails.

Cytokine cocktail A

*Concentrations of stocks are doubled since co-treatment was done in a 1:1 ratio

- 2.2 ng/ml (TNF-α)
- 2 ng/ml (IFN-γ)
- 0.2 ng/ml (IL-1β)

Addendum F: Catalogue Numbers

Equipment

Description	Manufacturer
Absorbance microplate reader (ELX800)	Bio-Tek Instruments; Friedrichshall, Germany
Benchtop centrifuge (SL 16R)	Thermo Fisher Scientific
Benchtop microfuge (5415 R)	Eppendorf; Hamburg, Germany
Benchtop microfuge (5810 R)	Eppendorf
Biohazard safety cabinet, class II	Airvolution; Johannesburg, South Africa
Bunsen burner	INTEGRA Biosciences AG; Landquart, Switzerland
ChemiDoc	Bio-Rad
Cylinders (50, 100, 500, 1000, 2000 ml)	Lasec; Cape Town, South Africa
Fine Balance scale	United Scientific
Flow Cytometer BD Accuri ™ C6	BioSciences, Johannesburg, South Africa
Haemocytometer Bright-Line™	Hausser Scientific Company; Horsham, PA, USA
Heating block	Labnet International Inc.; NJ, US
Homogenising Beads	Qiagen; Hilden, Germany

Description	Manufacturer
Incubator (Galaxy R)	RS Biotech; West Lothian, United Kingdom
Inverted microscope (CKX 41)	Olympus; NY, USA
Magnetic Stirrer	Lasec
Mini Protean Tetra Cell	Bio-Rad
Multichannel Pipette	Eppendorf
Nikon Inverted fluorescence microscope	Nikon; NY, USA
Orbital shaker	Stoval life Science
pH meter	Lasec
Pipette boy	Labnet International; Edison, NJ, USA
Pipettes (10 ,20, 100, 200, 300, 1000 µl)	Eppendorf
PowerPac HC	Bio-Rad
Scale	United Scientific
Glass bottles (100, 200, 1000 2000, 5000 ml)	Lasec; Cape Town, South Africa
SpectraMax i3	Molecular Devices, California, United States
Tissue Lyser	Qiagen
Trans-Blot® Turbo™	Bio-Rad
Waterbath	Memmert; Heilbronn, German

Reagents

Description	Manufacturer	Catalogue Number
10X Tris / Glycine / SDS Buffer (Running Buffer)	Bio-Rad	161-0772
4X Laemmli sample buffer	Bio-Rad	161-0747
Annexin- V	Sigma-Aldrich	A9210
Anti-Amylin	Abcam	115766
Anti-BACE2	Abcam	Ab5670
Anti-Mouse IgG	Santa Cruz Biotechnology	sc-2318
Anti-Rabbit IgG	Santa Cruz Biotechnology	sc-2357
Anti-TMEM27	Abcam	200664
Asp	High Force Research Ltd; Durham, England	batch: SZ1-356-54
BACE Inhibition Assay	Sigma-Aldrich	CS0010
BACE Inhibitor	BioVision	2299-5, 25
Bovine serum albumin (BSA)	Roche	A4919 03117332001
BrdU proliferation assay kit	Cell Signalling	5492
$CaCl_2$	Sigma-Aldrich	C5670
Carbon dioxide (Co_2)	Air Products; Centurion, Cape Town, SA	N/A
Caspase – 3 / 7	Invitrogen™, ThermoFisher	C10732

Description	Manufacturer	Catalogue Number
CellTiter-Glo® Luminescent Cell Viability Assay	Promegra	G7571
Clarity™ Western ECL Substrate	Bio-Rad	170-5061
COX2	Abcam	Ab52237
DCF	Sigma-Aldrich	35848
DC™ Protein Assay Reagent A	Bio-Rad	500-0113
DC™ Protein Assay Reagent B	Bio-Rad	500-0114
DC™ Protein Assay Reagent S	Bio-Rad	500-0115
Dimethyl sulfoxide (DMSO)	Sigma-Aldrich	D4540
DTT	Sigma-Aldrich	43815
Dulbecco's phosphate buffered saline (DPBS)	Lonza	BE17-513F
Ethanol	Sigma-Aldrich	32221
Fetal bovine serum (FBS) - Gibco	Thermo Fisher Scientific	SH3007903HI
Glucose	Sigma-Aldrich	G7021
Glycine	Sigma-Aldrich	G7126
Griess reagent	Sigma-Aldrich	G4410
GRT	Afriplex (Pty) Ltd., Paarl, South Africa	N/A
HCl	Sigma-Aldrich	H1758

Description	Manufacturer	Catalogue Number
Hepes	Lonza	BE17-737E
INS1 rat insulinoma cells	Gift from Vrije Universiteit, Brussels, Belgium	
Instant Skimmed Powder Milk	SPAR	-
Interferon gamma (IFN-γ)	Sigma-Aldrich	I3275
Interleukin-1 beta (IL-1β)	Sigma-Aldrich	I2393
KCl	Sigma-Aldrich	P5405
Liquid Nitrogen	Air Products; Centurion, Cape Town, SA	N/A
Methanol	Sigma-Aldrich	67-56-1
$MgCl_2$	Sigma-Aldrich	M4880
Mini-Protean® TGX Stain-Free™ Gels	Bio-Rad	456-8044
Molecular graded EtOH	Sigma-Aldrich	34870
MTT (3-(4,5-dimethylthiazol-2-yl)-2,5-diphenyltetrazoluim)	Sigma-Aldrich	M5655
Na_3VO_4	Sigma-Aldrich	S6508
$NaCHO_3$	Sigma-Aldrich	S3817
NaCl	Sigma-Aldrich	S5886
NaF	Sigma-Aldrich	S7920
NF-κB Phospho	Cell Signalling	3033

Description	Manufacturer	Catalogue Number
NF-κB Total	Cell Signalling	8242
Nitrate	Sigma-Aldrich	74246
NP40	Sigma-Aldrich	CA-630 (1-3021)
PageRuler™ Prestained Protein Ladder	Thermo Fisher Scientific	26619
Phosphor inhibiting tablet	Roche	4906837001
PMSF	Sigma-Aldrich	78830
Ponceau S Stain	Sigma-Aldrich	P23295
PPAG	High Force Research Ltd; Durham, England	N/A
Precision plus protein™, WesternC™	Bio-Rad	1610399
Precision Protein™ StrepTactin-HRP Conjugate	Bio-Rad	161-0381
Propidium iodide	Sigma-Aldrich	P4170
Protease inhibiting cocktail	Roche	5892953001
Quick Start™ Bradford Protein Assay Kit	Bio-Rad	500-0203
Rat IAPP ELISA Kit	Elabscience	E-EL-R2448
Rat/Mouse Insulin ELISA Kit	Merck	EZRMI-13K
Restore™ PLUS Western Blot Stripping Buffer	Thermo Fisher Scientific	46430
RNase	Sigma-Aldrich	R6513

Description	Manufacturer	Catalogue Number
Rosswell Park Memorial Institute 1640 (RPMI 1640)	Lonza	BE12-115F
Sterile water	Sigma-Aldrich	W3500
Transblot® Turbo™ RTA Transfer Kit, LF PVDF	Bio-Rad	170-4274
Tris	Sigma-Aldrich	93352
Triton X114	Sigma-Aldrich	93422
Tryphan Blue	Invitrogen™, ThermoFisher	T10282
Tumor necrosis factor alpha (TNF-α)	Sigma-Aldrich	PMC3014
Tween-20	Sigma-Aldrich	58980C
β- Mercaptoethanol	Sigma-Aldrich	60-24-2
β-Tubulin	Cell Signalling	2146

Software

Description	Manufacturer
ChemiDoc™ Touch Imaging System	BioRad; California, USA
Gen5 software (version 1.05)	Bio-Tek Instruments
GraphPad Prism 7	Graphpad Software; CA, USA
ImageLab	BioRad; California, USA

Description	Manufacturer
Leica Qwin Software	Leica Microsystems; Nussloch, German
Microsoft: Excel / Word / PowerPoint	Microsoft Corporation; WA, USA
NIS-Elements - Microscope Imaging Software	Nikon; NY, USA
SoftMax® Pro	Molecular Devices; CA, USA
Software, Accuri c6	BioSciences, Johannesburg, South Africa

Consumables

Description	Manufacturer	Catalogue Number
Cell culture flask 25 cm^2	Whitehead, Nest	707003
Cell culture flask 75 cm^2	Whitehead, Nest	708003
Cell culture plate (black, 96 well)	Lasec	P1PLA045K-000096ST
Cell culture plate (clear, 6 well)	Lasec	P1PLA044C-000006
Cell culture plate (clear, 96 well)	Whitehead, Nest	701001
Cell culture plate (white, 96 well)	Lasec	P1pLA045W-000096ST
Cell scrapers	Whitehead, Nest	710001
Cryogenic vial (2 ml)	Greiner	PGRE122279

Description	Manufacturer	Catalogue Number
Eppendorf tube (2 ml)	Eppendorf, Hamburg, Germany	22363344
Filters (500 ml)	Corning	CR/430769
Filters (syringes)	Merck	SLGP033RS
Gel loading tips	Whitehead	010-1-200µl
Glass Pasteur pipet tips (aspirate)	Lasec	GLASP20M150
Glass Tips (10, 25, 50 ml) (Pippeteboy)	Lasec	PLAS1PI033
Pipette tips (10 ,20, 100, 200, 300, 1000 µl)	Scientific group	AX/TF-300-L-R-S/S
Reservoirs	Scientific group	CR/4870
Sterile falcon tube 15 ml	Whitehead, Nest	601001
Sterile falcon tube 50 ml	Whitehead, Nest	602072
Syringe-driven filters	Merck Millipore	SLGP033RS

Addendum F: Outputs from Study

<u>Conferences / symposiums</u>

<u>Poster Presentations</u>

- Stellenbosch University, Faculty of Medicine and Health Sciences Annual Academic Day (30 August 2017):
  J. Burger, C.J.F. Muller, N. Chellan, J. Lopes; Beta secretase regulation and inflammation in pancreatic beta cells: the potential role of Rooibos.

- Stellenbosch University, Faculty of Medicine and Health Sciences Annual Academic Day (29 August 2018):
  J. Burger, C.J.F. Muller, N. Chellan, J. Lopes; Beta secretase regulation and inflammation in pancreatic beta cells: the potential role of Rooibos.

<u>Oral Presentations</u>

- BRIP Research Symposium (16 October 2017):
  J. Burger, C.J.F. Muller, N. Chellan, J. Lopes; Beta secretase regulation and inflammation in pancreatic beta cells: the potential role of Rooibos.

- European Association for the Study of Diabetes Scientist Training Course, Barcelona, Spain November 2017.
  N. Chellan, J. Burger, J-L Jansen van Vuuren, C. Muller, A novel assessment of the role of beta secretase in pancreatic beta

- CoBNeST (PSSA) Conference (7- 10 October 2018):
  J. Burger, C.J.F. Muller, N. Chellan, J. Lopes; The effect of Rooibos phenolic compounds on inflammation in pancreatic β-cells.

- BRIP Research Symposium (16 October 2018):
  J. Burger, C.J.F. Muller, N. Chellan, J. Lopes; Beta secretase regulation and inflammation in pancreatic β-cells: the potential role of Rooibos.

Addendum G: Electronic Copy